

**A novel genetic system
for the functional analysis of essential
proteins of the human malaria parasite
*Plasmodium falciparum***

**Dissertation with the aim of achieving a doctoral degree at the
Faculty of Mathematics, Informatics and Natural Sciences
Department of Biology
Universität Hamburg**

**submitted by
Jakob Birnbaum**

Hamburg, 2017

Vorsitz der Prüfungskommission: Prof. Julia Kehr

1. Gutachter der Dissertation: Prof. Tim Gilberger

2. Gutachter der Dissertation: Dr. Tobias Spielmann

Dissertationsdatum: 28.07.2017

Eidesstattliche Versicherung

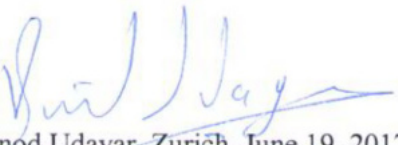
Hiermit erkläre ich an Eides statt, dass ich die vorliegende Dissertationsschrift selbst verfasst und keine anderen als die angegebenen Quellen und Hilfsmittel benutzt habe.

Hamburg, den 25.06.2017

Jakob Birnbaum

Language certificate

I am a native speaker, have read the present PhD thesis and hereby confirm that it complies with the rules of the English language.



Vinod Udayar, Zurich, June 19, 2017

Summary

The causative agent of the severest form of malaria in humans is the protozoan parasite *Plasmodium falciparum* that is transmitted by female *Anopheles* mosquitos. The pathology of this disease is solely caused by the asexual replication of the parasite in erythrocytes. Despite recent progress in reducing the global impact of malaria, the disease remains a major health burden in tropical and subtropical areas. In addition, the rapid spread of resistance to the most used and most effective anti-malaria drug artemisinin jeopardizes the progress made in the last years.

The highly specialized life cycle of the parasite led to profound adaptations to support the survival in the intracellular environment of the erythrocyte. Of approximately 5600 genes encoded in the *P. falciparum* genome more than one third is annotated as ‘unknown function’ in PlasmoDB (the *Plasmodium* genome database). This indicates that a large part of the parasites’ biology remains unknown. As many of these unknown genes are restricted to *Apicomplexa* or the genus *Plasmodium*, they are fundamental to understand the specific biology of this parasite. Moreover, due to the absence of homologs of these genes in the host, they are best suited as targets for therapeutic interventions. However, the lack of homology does not provide hints of their function. Thus, studies of these genes, especially essential ones, are often hampered by limitations of current methods for gene function studies in this parasite. As a consequence, the identification and analysis of these parasite specific genes were commonly restricted to selected single genes per study and often unsuccessful.

Most functional methods require integration of episomal plasmid DNA into the genome of the parasite. This proved to be a slow and rate limiting process. In order to elucidate more of the specific biology of *P. falciparum* parasites, a method that permits rapid genomic modifications was developed in this thesis. For this method, a targeting region was fused to a tag of choice and an additional selection marker that was expressed upon fusion to the target gene by single homologous recombination-based integrated into the genome. Thus, the gene fused to the tag was expressed under the endogenous promoter. The tag of choice and the additional selection marker were separated by a skip peptide, leading to the translation of two independent peptides from a single RNA. Hence, the resistance marker is not attached to the tagged gene product. Addition of the selection drug, corresponding to the additional resistance marker, only permits the survival of parasites carrying the integration. This system for rapid genomic modifications was termed selection linked integration (SLI). In this thesis the method was used to successfully target 29 genes and create an overall of 54 knock-in cell lines. The average time to integration was 15.2 (± 4.8) days. Therefore SLI dramatically increased the success rate and speed to obtain modified genes compared to the previously used conventional passive drug cycling method. In addition, the method was shown to be versatile, permitting C-terminal and N-terminal tagging of genes, selectable disruption of genes, as well as the knock-in of a gene copy with a point mutation that rendered the parasites less susceptible to the drug artemisinin.

In order to allow the functional analysis of proteins in *P. falciparum* SLI was combined with conditional gene and protein inactivation techniques used in other organisms. To do this and to localize the endogenous target

in the parasite, SLI was carried out with a 2xFKBP-GFP tag. The FKBP domain is part of an inducible FKBP-FRB heterodimerization system under the control of a small ligand. This system can be harnessed for a method known as knock sideways (KS) that allows the conditional depletion of the target protein from its site of action into an unrelated cellular compartment. For this a second construct with an FRB domain and a strong targeting signal is used. Constructs for the mislocalization of target proteins to two sites were established in this thesis: the nucleus (for non-nuclear proteins) and the plasma membrane (for nuclear proteins). Appropriate mislocalizer constructs were then episomally expressed in the knock-in cell line of the target protein. Thus, upon addition of a small molecule (rapalog), the FKBP and FRB domains dimerized and the protein was 'mislocalized'. If the target protein is important for the asexual development of the parasite the mislocalization will have detrimental effects. In total 28 proteins were localized in this study whereof 18 were found in the cytosol of the parasite, 9 showed a nuclear distribution and one candidate was exported. Knock sideways showed an efficient mislocalization for 19 out of 22 proteins tested in this thesis. These results were confirmed on genetic level using selectable gene disruptions of the candidates by SLI (SLI-TGD). For all 8 essential proteins that were identified by KS no targeted gene disruption cell line was obtained. In contrast, for 11 proteins that were found not to be essential in the KS screen, the targeted gene disruption cell lines were obtained and thus complemented the knock sideways data.

To further test the newly established system, the gene associated with reduced susceptibility to the currently most important drug artemisinin, named *kelch13*, was targeted. The protein was shown to be localized to a novel compartment in the parasite and proved to be important for transition from ring to trophozoite stage using knock sideways. Excision of the functional gene by the inducible Cre recombinase system (diCre) resulted in a similar phenotype. Moreover, the mutation that confers artemisinin resistance was knocked-in and shown to mediate reduced artemisinin susceptibility of parasites, in a so called ring stage survival assay. This work localized this important protein for the first time and conditionally inactivated it.

In order to identify potential interaction partners of Kelch13 and proteins that reside in the same compartment, the proximity dependent biotin identification (BioID) method was combined with the FKBP-FRB heterodimerization system in an approach that we termed DIQ-BioID (dimerization induced quantitative BioID). The biotin ligase BirA* was fused to an FRB domain and episomally expressed in the Kelch13 knock-in cell line. Addition of rapalog led to dimerization with Kelch13 and proteins in close proximity were biotinylated. The DIQ-BioID screen identified 20 significantly enriched proteins. Eleven potential interaction partners were tagged by SLI and all candidates were shown to co-localize with Kelch13, highlighting the specificity of the approach.

Overall, the here presented systems of SLI, KS and DIQ-BioID will streamline identification and analysis of essential genes in *P. falciparum* asexual blood stages. In addition, it will facilitate the identification of interaction partners. SLI permitted rapid genomic changes and proved to be very robust. It can be used as platform for the KS system and the localization of endogenous proteins but will also aid many other systems. Finally, the here provided tools for the study of Kelch13 will be instrumental to elucidate its cellular function and to gain insight into the artemisinin resistance mechanism.

Zusammenfassung

Die schwerwiegendste Form der Malaria für den Menschen wird durch Parasiten der Art *Plasmodium falciparum* ausgelöst, welcher durch weibliche *Anopheles* Mücken übertragen wird. Das Krankheitsbild wird dabei ausschließlich durch die asexuelle Vermehrung des Erregers in den roten Blutkörperchen verursacht. Trotz der jüngsten Erfolge die globalen Auswirkungen von Malaria einzudämmen bleibt die Erkrankung eine große gesundheitliche Belastung in tropischen und subtropischen Gebieten. Darüber hinaus gefährdet die schnelle Verbreitung der Resistenz gegen das am häufigsten angewendete und wirksamste Anti-Malaria Medikament Artemisinin den Fortschritt der letzten Jahre.

Der hochspezialisierte Lebenszyklus des Parasiten innerhalb der Erythrozyten führte zu tiefgreifenden Veränderungen, um in dieser Umgebung erfolgreich zu überleben. Von den schätzungsweise 5600 Genen die im Genom von *P. falciparum* codiert sind ist mehr als ein Drittel als „Gene unbekannter Funktion“ in PlasmoDB (der *Plasmodium* Genom Datenbank) annotiert. Dies verdeutlicht, dass ein großer Teil der Biologie des Erregers unbekannt ist. Da viele dieser unbekannt Genen auf *Apicomplexa* oder die Gattung *Plasmodium* beschränkt sind, ist es von zentraler Bedeutung, die spezifische Biologie des Parasiten zu verstehen. Darüber hinaus sind sie auf Grund der fehlenden Homologie zu Genen im menschlichen Wirt bestens geeignet als Ziel therapeutischer Interventionen. Allerdings gibt es durch fehlende Homologien auch keine Hinweise auf die Funktion dieser Gene und die Analyse, insbesondere der essentiellen Gene, wird weiterhin durch Limitierungen in den derzeit zur Verfügung stehenden Methoden zur funktionellen Analyse beeinträchtigt. Infolgedessen wurde die Identifizierung und Analyse dieser für den Parasiten spezifischen Gene auf einzelne, ausgewählte Gene pro Studie beschränkt und waren oftmals nicht erfolgreich.

Die meisten Methoden zur funktionellen Analyse erfordern die genomische Integration eines episomalen Plasmides, welches sehr zeitaufwändig ist und oftmals den limitierenden Schritt der Analyse darstellt. Um mehr über die spezifische Biologie von *P. falciparum* in Erfahrung zu bringen wurde im Rahmen dieser Arbeit eine Methode entwickelt die rapide Modifikationen am Genom des Erregers zulässt. Dabei wurde eine Zielregion, welche für die auf einfach homologer Rekombination basierenden Integration ins Genom benötigt wird, mit einem beliebigen Marker fusioniert sowie einem zusätzlichen Resistenzmarker. Dieses Konstrukt wird nur nach Integration ins Genom unter dem endogenen Promoter des Zielgenes exprimiert. Der Resistenzmarker und der beliebige Marker wurden dabei von einem „skip peptid“ getrennt, auf Grund dessen bei der Translation von einer mRNA zwei unabhängige Produkte entstehen. Der Resistenzmarker ist somit nicht an das Zielprotein angehängt. Bei anschließender Selektion mittels der zum Resistenzmarker komplementären Droge werden nur Parasiten überleben welche die Integration tragen. Dieses System für rapide genomische Modifikationen wurde selektions-gekoppelte Integration (*engl.* selection linked integration – SLI) genannt. Die Technik wurde im Rahmen dieser Arbeit genutzt um 29 Gene gezielt zu modifizieren infolgedessen 54 „knock-in“ Zelllinien entstanden sind. Die durchschnittliche Zeit zur Integration ins Genom betrug dabei 15.2 (± 4.8) Tage. Dies stellt erheblich gesteigerte Erfolgsrate dar und vermindert die Zeit, welche zum Erlangen genetisch modifizierte Parasiten benötigt wird, im Vergleich mit der bisher verwendeten passiven Selektionsmethode. Darüber hinaus wurde in dieser Arbeit gezeigt, dass die Methode auf vielfältige Weise eingesetzt werden kann da sie C- oder N-terminale Fusion an Gene ermöglichte, das Unterbrechen von

Genen zuließ (*engl.* targeted gene disruptions - TGD), was die Funktionen des Genes zerstören kann, wie auch das Einbringen einer Punktmutation ermöglichte, welche die Parasiten weniger empfindlich gegen Artemisinin macht.

Zur funktionellen Analyse von Proteinen in *P. falciparum* wurde SLI mit konditionellen Gen und Protein Inaktivierungstechniken, welche in anderen Organismen zur Anwendung kommen, kombiniert. Um dies zu erreichen, sowie die Zielproteine im Parasiten zu lokalisieren wurden mittels SLI die codierenden Gene mit der Sequenz welche für 2xFKBP-GFP codiert fusioniert. Die FKBP Domäne ist Teil des induzierbaren FKBP-FRB Heterodimerisierungssystems, welches mittels des Liganden Rapalog gesteuert werden kann. Das System kann für eine Methode mit dem Namen „knock sideways“ (KS) genutzt werden, welche die konditionelle Verlagerung eines Zielproteines von seinem Funktionsort in ein anderes Zielkompartiment ermöglicht. Dafür wird ein zweites Konstrukt, welches eine FRB Domäne sowie ein starkes Lokalisationssignal besitzt, verwendet (sogenannte Mislokalisierer, *engl.* „mislocalizer“). In dieser Arbeit wurden Konstrukte für die Verlagerung von Proteinen zu zwei verschiedenen Kompartimenten etabliert: den Zellkern (für nicht-nukleäre Proteine) und die Plasmamembran (für nukleäre Proteine). Die entsprechenden Mislokalisationskonstrukte wurden in den genetisch veränderten Zelllinien mit markierten Zielproteinen episomal exprimiert. Bei Zugabe des Liganden Rapalog kam es zur Dimerisierung der FKBP und FRB Domäne und das Zielprotein wurde mislokalisiert. Wenn das Zielprotein essenziell für die asexuelle Vermehrung in den Erythrozyten ist hat die Mislokalisierung einen schädlichen Effekt auf den Parasiten zur Folge. Insgesamt wurden im Rahmen dieser Arbeit 28 Proteine lokalisiert wovon 18 eine zytosolische und 9 eine nukleäre Lokalisation aufwiesen. 1 Protein wurde vom Parasiten in den Erythrozyten exportiert. Das „knock sideways“ System konnte 19 von 22 getesteten Proteinen in dieser Arbeit effizient mislokalisieren. Die Resultate wurden dabei auf genetischer Ebene von TGDs ergänzt welche auch mittels des SLI Systems durchgeführt wurden (SLI-TGD). Von allen 8 essenziellen Proteinen, welche mittels „knock sideways“ identifiziert wurden, konnten die codierenden Gene mittels SLI-TGD nicht unterbrochen werden. Im Gegensatz dazu wurde von allen 11 Proteinen, die durch die „knock sideways“ Methode als nicht essenziell identifiziert wurden, eine Zelllinie mit unterbrochenem Zielgen erhalten.

Das System wurde weiterhin genutzt um das *kelch13* Gen, welches mit einer verringerten Empfindlichkeit des Parasiten gegen den wichtigsten Anti-Malaria Arzneistoff Artemisinin assoziiert wird, zu markieren. In dieser Arbeit wurde gezeigt, dass das Protein in einem bisher unbekanntem Kompartiment lokalisiert ist und es konnte mittels KS demonstriert werden, dass es für den Übergang vom Ringstadium ins Trophozitenstadium benötigt wird. Das Herausschneiden des funktionellen Genes mittels des induzierbaren Cre rekombinase Systems (diCre) resultierte in einem vergleichbaren Phänotypen. Darüber hinaus wurde die Mutation welche Artemisinin Resistenz vermittelt ins Genome eingebracht und durch den sogenannten Ringphase-Überlebenstest (*engl.* ring stage survival assay) gezeigt dass sie zu einer verringerten Anfälligkeit der Parasiten gegenüber Artemisinin führt. Damit konnte in dieser Arbeit dieses wichtige Protein erstmal lokalisiert und inaktiviert werden.

Um potentielle Interaktionspartner von Kelch13, sowie Proteine die im selben Kompartiment anzutreffen sind ausfindig zu machen, wurde die Methode zur entfernungsbhängigen Biotin Identifikation (*engl.* proximity dependent biotin identification – BioID) mit dem FKBP-FRB Heterodimerisierungssystem kombiniert in

einem Konzept das wir DIQ-BioID nannten (dimerisierungs-induzierte quantitative BioID). Die Biotinligase BirA* wurde dabei mit der FRB Domäne fusioniert und epsiomal in der genetisch modifizierten Kelch13 Zelllinie exprimiert. Die Zugabe von Rapalog führte zur Dimerisierung mit Kelch13 und proximale Proteine wurden biotiniliert. Mittels des DIQ-BioID Untersuchung konnten 20 signifikant angereicherte Proteine identifiziert werden. 11 dieser Proteine wurden mittels SLI markiert und deren Co-Lokalisation mit Kelch13 gezeigt, welches die Spezifität des Ansatzes verdeutlicht.

Zusammengefasst werden die hier vorgestellten Methoden von SLI, KS und DIQ-BioID die Identifikation und Analyse von essenziellen Genen für die asexuelle Vermehrungsphase von *P. falciparum* erheblich beschleunigen. Darüber hinaus wird es die Identifikation von Interaktionspartnern erleichtern. Mittels SLI, welches sich als robustes System bewies, konnten in kurzer Zeit genomische Modifikationen vorgenommen werden. Es kann dabei als Plattform für das KS System verwendet werden und ermöglicht die Lokalisation von Zielproteinen, kann aber auch mit vielen anderen Systemen kombiniert werden. Letztlich werden die etablierten Methoden zur Untersuchung von Kelch13 dazu beitragen die zelluläre Funktion des Proteins aufzuklären und einen Einblick in den Artemisinin-Resistenzmechanismus zu gewinnen.

Table of contents

Summary	iv
Zusammenfassung	vi
Table of contents	ix
List of figures	xiii
List of tables	xiv
Abbreviations	xv
1 Introduction	1
1.1 Malaria	1
1.1.1 Epidemiology	1
1.1.2 Pathophysiology	3
1.1.3 Control strategies	4
1.1.3.1 Antimalarial drugs	4
1.1.4 Vaccine development	6
1.2 Biology of <i>Plasmodium falciparum</i>	8
1.2.1 Life cycle	8
1.2.1.1 Mosquito stages	9
1.2.1.2 Liver stage	9
1.2.1.3 Asexual blood stages	10
1.2.1.4 Sexual development	12
1.2.2 Cellular biology of <i>P. falciparum</i>	13
1.2.2.1 Export of proteins	14
1.3 Methods for gene and protein inactivation in <i>P. falciparum</i>	15
1.3.1 Selection markers	16
1.3.2 Methods for genome modifications	17
1.3.3 Methods for regulation of gene expression and RNA levels	19
1.3.4 Methods for post-translation control	20
1.4 The FKBP-FRB system	21
1.5 The superfamily of BTB and Kelch repeat proteins	22
1.6 Aims of the thesis	23
2 Material and Methods	24
2.1 Material	24
2.1.1 Bacterial and <i>Plasmodium</i> strains	24
2.1.2 Chemicals	24
2.1.3 DNA- and protein-ladders	26
2.1.4 Kits	26
2.1.5 Labware and disposables	27

2.1.6	Solutions, buffers and media	28
2.1.6.1	Antibodies.....	28
2.1.6.2	Enzymes, oligonucleotides & polymerases	28
2.1.6.3	Fluorescence dyes.....	28
2.1.6.4	Solutions and buffers for biochemical experiments	29
2.1.6.5	Solutions and buffers for microbiologic culture	30
2.1.6.6	Solutions and buffers for molecular biological experiments.....	31
2.1.6.7	Solutions and buffers for cell biologic experiments	32
2.1.7	Technical devices	34
2.2	Methods.....	36
2.2.1	Microbiological Methods	36
2.2.1.1	Production of competent <i>E.coli</i>	36
2.2.1.2	Transfection of chemo-competent <i>E. coli</i>	36
2.2.1.3	Overnight culture of <i>E. coli</i> for subsequent plasmid DNA preparation	36
2.2.1.4	Freezing of <i>E. coli</i>	37
2.2.2	Molecular biological methods	37
2.2.2.1	Polymerase chain reaction	37
2.2.2.2	PCR-product purification	37
2.2.2.3	DNA restriction digest.....	38
2.2.2.4	DNA ligation	38
2.2.2.5	DNA ligation by Gibson assembly	38
2.2.2.6	Plasmid preparation	39
2.2.2.7	Sequencing of plasmid DNA.....	39
2.2.2.8	Agarose gel electrophoresis.....	39
2.2.2.9	Isolation of genomic DNA	39
2.2.3	Biochemical methods	40
2.2.3.1	Discontinuous SDS-PAGE.....	40
2.2.3.2	Western blotting	40
2.2.3.3	Immunodetection of proteins.....	40
2.2.3.4	Pull down of biotinylated proteins.....	41
2.2.4	Cell biological methods.....	41
2.2.4.1	Continuous culture of <i>P. falciparum</i> (Trager and Jensen, 1976).....	41
2.2.4.2	Selection for transgenic parasites by SLI	41
2.2.4.3	<i>P. falciparum</i> cryo-stabilates.....	42
2.2.4.4	Blood smears and Giemsa staining.....	42
2.2.4.5	Synchronization of parasites.....	42
2.2.4.6	Transfection of <i>P. falciparum</i>	43
2.2.4.7	Isolation of parasites by saponin lysis	43
2.2.4.8	Biotin labeling of parasite proteins.....	44
2.2.4.9	Induction of knock sideways and diCre.....	44
2.2.4.10	Flow cytometry growth assay.....	44

2.2.5	Microscopy	45
2.2.5.1	Live cell and fluorescence microscopy.....	45
2.2.6	Software and bioinformatic tools	46
3	Results	47
3.1	Robust and efficient selection of genomic integration.....	47
3.2	Functional analysis of essential <i>P. falciparum</i> proteins with knock sideways.....	50
3.2.1	Proof of principle.....	50
3.2.2	Screen of proteins of unknown function by KS and targeted gene disruption	53
3.2.2.1	Candidate 1: PF3D7_0525000.....	54
3.2.2.2	Candidate 2: PF3D7_0526800.....	55
3.2.2.3	Candidate 3: PF3D7_0720600.....	56
3.2.2.4	Candidate 4: PF3D7_0807600.....	56
3.2.2.5	Candidate 5: PF3D7_1317400.....	57
3.2.2.6	Candidate 6: PF3D7_1445700.....	58
3.2.2.7	Candidate 7: PF3D7_1451200.....	59
3.2.2.8	Candidate 8: PF3D7_1463000.....	60
3.2.2.9	Candidate 9: PF3D7_0202400.....	61
3.2.2.10	Candidate 10 PF3D7_0205100.....	62
3.2.2.11	Candidate 11 PF3D7_0205600.....	62
3.2.2.12	Candidate 12: PF3D7_0209700.....	63
3.2.2.13	Candidate 13: PF3D7_0210200.....	64
3.2.2.14	Candidate 14: PF3D7_0211700.....	65
3.2.2.15	Candidate 15 PF3D7_0210900.....	67
3.2.2.16	Candidate 16: PF3D7_0213700.....	68
3.2.2.17	Candidate 17: PF3D7_0213900.....	68
3.2.2.18	Candidate 18: PF3D7_0218200.....	69
3.2.3	Kinetics of the knock sideways system	70
3.3	N-terminal tagging and analysis of the artemisinin resistance gene <i>kelch13</i>	73
3.4	Co-localization of Kelch13 with different cellular markers	79
3.4.1	Kelch13 does not localize to the endoplasmic reticulum	79
3.4.2	Kelch13 does not co-localize with the Golgi apparatus	80
3.4.3	Kelch13 is often found close to PI3P positive compartments	81
3.4.4	Apicoplast and K13 do not co-localize, but are often in close proximity	82
3.4.5	Kelch13 and the Kelch13-C580Y mutant display an identical localization.....	83
3.5	Identification of potential interaction partners and compartment neighbors of the Kelch13.....	84
3.6	Validation DIQ-BioID approach by tagging of potential interaction candidates.....	88
3.6.1	KBI Candidate 1 PF3D7_0606000.....	89
3.6.2	KBI Candidate 2 PF3D7_1227700.....	91
3.6.3	KBI Candidate 3 PF3D7_0914400.....	91

3.6.4	KBI Candidate 4 PF3D7_1438400.....	92
3.6.5	KBI Candidate 5 PF3D7_1246300.....	93
3.6.6	KBI Candidate 6 PF3D7_1138700.....	95
3.6.7	KBI Candidate 7 PF3D7_0609700.....	95
3.6.8	KBI Candidate 8 PF3D7_0104300.....	97
3.6.9	KBI Candidate 9 PF3D7_0813000.....	97
3.6.10	KBI Candidate 10 PF3D7_1014900.....	99
3.6.11	KBI Candidate 11 PF3D7_1442400.....	100
4	Discussion	102
4.1	SLI and KS are suitable for medium throughput screens	102
4.1.1	Integration time into the genome is dependent on the length of the targeting region .	103
4.1.2	Considerations on essentiality of gene products.....	104
4.1.3	Limitations of SLI-TGD.....	106
4.1.4	Combination of SLI and KS with existing methods for gene function analysis.....	106
4.1.5	Factors influencing the efficiency of knock sideways and potential further improvements of the system.....	107
4.1.6	Considerations for analysis of proteins refractory to mislocalization	111
4.1.7	SLI resistance markers.....	112
4.2	Analysis of Kelch13	112
4.2.1	DIQ-BioID provides high specificity for the identification of Kelch13 neighboring proteins	114
4.2.2	Role of confirmed DIQ-BioID hits and potential relation to Kelch13 function and artemisinin resistance	117
4.2.3	Absence of proteins reported to be involved in artemisinin resistance in the Kelch13 DIQ-BioID screen	119
	Bibliography	121
	Appendix A. Oligonucleotides	141
	Appendix B. Methods for directed gene and protein inactivation in <i>P. falciparum</i>	152
	Publications	155
	Danksagung	156

List of figures

Figure 1 I Worldwide distribution and prevalence in Africa.....	2
Figure 2 I Spread of artemisinin resistance indicated by day 3 positivity of patient samples.....	6
Figure 3 I Life cycle of <i>Plasmodium falciparum</i>	8
Figure 4 I Asexual blood stages.	10
Figure 5 I Development stages of gametocytes.....	12
Figure 6 I <i>P. falciparum</i> infected red blood cell.....	14
Figure 7 II Development of genetic systems.....	16
Figure 8 I Schematic of knock sideways.....	22
Figure 9 I Diagram of <i>PfKelch13</i>	23
Figure 10 I Schematic of selection linked integration strategy and knock sideways.	47
Figure 11 I Comparison of conventional drug cycling with SLI and integration check PCRs.	50
Figure 12 I Localization and KS of CDPK5.....	51
Figure 13 I Localization and KS of HP1.	52
Figure 14 I Schematic of SLI targeted gene disruption (SLI-TGD) strategy.	53
Figure 15 I Localization and KS of PF3D7_0525000 (candidate 1).	54
Figure 16 I Localization and KS of PF3D7_0526800 (candidate 2).	55
Figure 17 I Localization and KS of PF3D7_0807600 (candidate 4).	57
Figure 18 I Localization and KS of PF3D7_1317400 (candidate 5).	58
Figure 19 I Localization and KS of PF3D7_1445700 (candidate 6).	59
Figure 20 I Localization and KS of PF3D7_1451200 (candidate 7).	60
Figure 21 I Localization and KS of PF3D7_1463200 (candidate 8).	61
Figure 22 I Localization of PF3D7_0202400 (candidate 9).	62
Figure 23 I Localization and KS of PF3D7_0205600 (candidate 11).	63
Figure 24 I Localization and KS of PF3D7_0209700 (candidate 12).	64
Figure 25 I Localization and KS of PF3D7_0210200 (candidate 13).	65
Figure 26 I Localization and KS of PF3D7_0211700 (candidate 14).	66
Figure 27 I Localization and KS of PF3D7_0210900 (candidate 15).	67
Figure 28 I Localization and KS of PF3D7_0213900 (candidate 17).	69
Figure 29 I Localization and KS of PF3D7_0218200 (candidate 18).	70
Figure 30 I Kinetics of the KS system.....	71
Figure 31 I Extended growth assay with PF3D7_0205600 (candidate 11).	72
Figure 32 I N-terminal integration strategy and localization of Kelch13.....	74
Figure 33 I KS of GFP-2xFKPB-Kelch13.	75
Figure 34 I Inducible deletion of the <i>kelch13</i> gene.	76
Figure 35 I KS of 2xFKBP-GFP-2xFKBP-Kelch13.	78
Figure 36 I Simultaneous diCre-based excision and KS of Kelch13.	78
Figure 37 I Kelch13 does not co-localize with an endoplasmic reticulum marker.	80
Figure 38 I Kelch13 does not co-localize with the Sec13p.	80
Figure 39 I Kelch13 does not co-localize with the Golgi apparatus.....	81

Figure 40 I Kelch13 shows partial co-localization with the PI3P maker P40.	82
Figure 41 I Kelch13 foci are frequently in close proximity of the Apicolpast.	83
Figure 42 I Co-localization of the Kelch13-C580Y mutant with Kelch13wt.	84
Figure 43 I Schematic of DIQ-BioID approach.	85
Figure 44 I Dimersation of Kelch13 with BirA.	86
Figure 45 I Scatterplots of DIQ-BioID with Kelch13.	87
Figure 46 I Integration checks of KBI candidates.	89
Figure 47 I Localization of PF3D7_0606000 (KBI.1) and co-localization with Kelch13.	90
Figure 48 I Localization of PF3D7_1227700 (KBI.2) and co-localization with Kelch13.	91
Figure 49 I Localization of PF3D7_0914400 (KBI.3) and co-localization with Kelch13.	92
Figure 50 I Localization of PF3D7_1246300 (KBI.5) and co-localization with Kelch13.	94
Figure 51 I Localization of PF3D7_1138700 (KBI.6) and co-localization with Kelch13.	95
Figure 52 I Localization of PF3D7_0609700 (KBI.7) and co-localization with Kelch13.	96
Figure 53 I Localization of PF3D7_0104300 (KBI.8) and co-localization with Kelch13.	98
Figure 54 I Localization of PF3D7_0813000 (KBI.9) and co-localization with Kelch13.	99
Figure 55 I Localization of PF3D7_1014900 (KBI.10) and co-localization with Kelch13.	100
Figure 56 I Localization of PF3D7_1442400 and co-localization with Kelch13.	101
Figure 57 I Time to integration is influenced by length of targeting region.	103
Figure 58 I Alternative strategy for assessing the function of a 3' tagged gene by diCre.	111

List of tables

Table 1 I Top hits identified by DIQ-BioID.	88
Table 2 I Overview of analyzed genes for establishing SLI and knock sideways.	105

Abbreviations

AA	<i>amino acids</i>	KAHRP	<i>knobs-associated histidine-rich protein</i>
ACP	<i>acyl carrier protein</i>	KBI	<i>Kelch13 BioID</i>
ACT	<i>artemisinin combination therapies</i>	KS	<i>knock sideways, knock sideways</i>
AMA1	<i>apical membrane antigen 1</i>	MC	<i>Maurer's clefts</i>
AP2	<i>APETELALA2</i>	MCA2	<i>metacaspase-like protein</i>
ATc	<i>anhydrotetracycline</i>	MSP1	<i>merzoite surface protein 1</i>
BioID	<i>biotin identification</i>	MSPs	<i>merozoite surface proteins</i>
BSD	<i>blasticidin S deaminase</i>	mTOR	<i>mechanistic target of rapamycin</i>
BTB	<i>bric à brac 1, tramtrack, broad complex</i>	neo	<i>neomycin phosphotransferase II</i>
CAT	<i>chloramphenicol acetyltransferase</i>	NES	<i>nuclear export signal</i>
CD	<i>cytosine deaminase</i>	NHEJ	<i>non-homologous end joining pathway</i>
CDPK5	<i>calcium dependent protein kinase 5</i>	NLS	<i>nuclear localization signal</i>
CID	<i>chemically inducible dimerization</i>	NPC	<i>nuclear pore complex</i>
CM	<i>cerebral malaria</i>	PEXEL	<i>plasmodium export element</i>
CQ	<i>Chloroquine</i>	PfRipr	<i>RH5 interacting protein</i>
CRISPR	<i>clustered regularly interspaced short palindromic repeat</i>	PKG	<i>proteinkinase G</i>
crt	<i>chloroquine resistance transporter</i>	PNEPs	<i>PEXEL negative exported proteins</i>
CSP	<i>circumsporozoite protein</i>	POI	<i>protein of interest</i>
CyRPA	<i>cysteine-rich protective antigen</i>	PPM	<i>parasite plasma membrane</i>
DD	<i>destabilization domain</i>	PTEX	<i>plasmodium translocon of exported proteins</i>
DDD	<i>DHFR destabilizing domain</i>	PV	<i>parasitophorous vacuole</i>
DHFR	<i>dihydrofolat reductase</i>	PVM	<i>parasitophorous vacuole membrane</i>
dhfr-ts	<i>dihydrofolat reductase-thymidylate synthase</i>	RBCs	<i>red blood cells</i>
DIQ-BioID	<i>dimerization induced quantitative BioID</i>	Rhs	<i>reticulocyte-binding like homologs</i>
EBA175	<i>erythrocyte binding antigen 175</i>	RNAi	<i>RNA interference</i>
ER	<i>endoplasmic reticulum</i>	RON2	<i>roptry neck protein 2</i>
EXP2	<i>exported protein 2</i>	RONs	<i>roptry neck proteins</i>
FC	<i>flow cytometry</i>	RSA	<i>ring stage survival assay</i>
FDR	<i>false discovery rate</i>	SERA5	<i>serine repeat antigen 5</i>
FKBP	<i>FK506 binding protein</i>	SLI	<i>selection linked integration</i>
FRB	<i>FKBP rapamycin binding domain</i>	SRP	<i>signal recognition particle</i>
FV	<i>food vacuole</i>	TBV	<i>transmission blocking vaccines</i>
GAPs	<i>GTPase activating proteins</i>	tER	<i>transitional ER</i>
GEFs	<i>guanine nucleotide exchange factors</i>	TetO	<i>tetracyclin operators</i>
GFP	<i>green fluorescence protein</i>	TetR	<i>tetracycline repressor protein</i>
GlcN	<i>glucosamine</i>	TGD	<i>targeted gene disruption</i>
GOI	<i>gene of interest</i>	TK	<i>thymidine kinase</i>
hDHFR	<i>human dihydrofolat reductase</i>	TRAD	<i>transcriptional transactivator domain</i>
HP1	<i>heterochromatin protein 1</i>	TRAP	<i>thrombospondin-related anonymous protein</i>
hpi	<i>hours post infection</i>	TRX2	<i>thioredoxin 2</i>
HR	<i>homology region</i>	TVN	<i>tubovesicular network</i>
HSP101	<i>heat shock protein 101</i>	UBP1	<i>ubiquitin carboxyl terminal hydrolase 1</i>
HSPGs	<i>heparan sulfate proteoglycans</i>	UPR	<i>unfolded protein response</i>
i.a.	<i>inter alia</i>	yDHODH	<i>yeast dihydroorodotat dehydrogenase</i>
IMC	<i>inner membrane complex</i>	ZFN	<i>zinc-finger nuclease</i>
ITNs	<i>insecticide treated mosquito nets</i>		

1 Introduction

1.1 Malaria

In 1880 the parasite causing malaria was observed for the first time in red blood cells of humans suffering from that disease (Laveran, 1880) and later described in more detail (Celli, 1885). Malaria parasites are protozoans of the genus *Plasmodium*. The genus comprises more than 200 different species that are parasites of birds, mammals and reptiles. To date five of species are known to infect humans, namely *Plasmodium falciparum*, *P. vivax*, *P. ovale*, *P. malariae* and *P. knowlesi*.

The vector transmitting *Plasmodium* parasites is the female *Anopheles* mosquito. There are about 420 different species of *Anopheles* mosquitos, whereof approximately 40 are capable to transmit human malaria. The main vector of transmission is *Anopheles gambiae* (Sinka et al., 2010) (Sinka et al., 2011).

1.1.1 Epidemiology

In 2015 there were approximately 212 million malaria cases worldwide, leading to about 429,000 deaths. Children under the age of 5 are the group most at risk with about 300,000 deaths (70% of all annual deaths). It is estimated that 90% of the cases occur in Africa and 7% in South-East Asia. Since 2000 substantial progress in the eradication of malaria has been made. Worldwide, the number of malaria infections decreased by 22% and the number of fatal cases declined by 50% (WHO World Malaria Report, 2016).

About 99% of all malaria deaths are caused by *P. falciparum*. It is geographically distributed in tropical and subtropical regions, mainly Sub-Saharan Africa, South-East Asia and South America (Figure 1a). The prevalence of this malaria parasite is strongly influenced by the climate. A temperature below 18°C restricts transmission as the time required for development in the vector increases with declining temperatures (Anderson and May, 1999; Coluzzi, 1999; Sachs and Malaney, 2002; Snow et al., 2005). Evaluation of the progress made from 2000 to 2015 showed that the prevalence of infection decreased by 50% in the group of children aged 2-10 in endemic Africa (Figure 1b,c) (Bhatt et al., 2015).

Not as virulent as *P. falciparum*, but even wider distributed (due to its higher temperature tolerance) is *P. vivax*. Even though it accounts for only 4% of the malaria cases globally, it is responsible for 41% of all cases outside the African continent, such as in South-East Asia and the Eastern Mediterranean

Region (WHO World Malaria Report, 2016). Its low prevalence in Africa is attributed to the lack of expression of the Duffy antigen in the population, which is necessary for this parasite's invasion into immature red blood cells (RBCs) (Howes et al., 2011; Livingstone, 1984). However, this requirement for the Duffy antigen has been questioned lately, as *P. vivax* parasites were found in patients with Duffy-negative RBCs (Howes et al., 2016; Menard et al., 2010). In contrast to *P. falciparum*, *P. vivax* is able to survive in humans for a longer time due to its ability to form so called hypnozoites, dormant stages that remain in the liver and can cause relapses months or even years after the primary infection (Krotoski et al., 1982; Shortt et al., 1948; White, 2011).

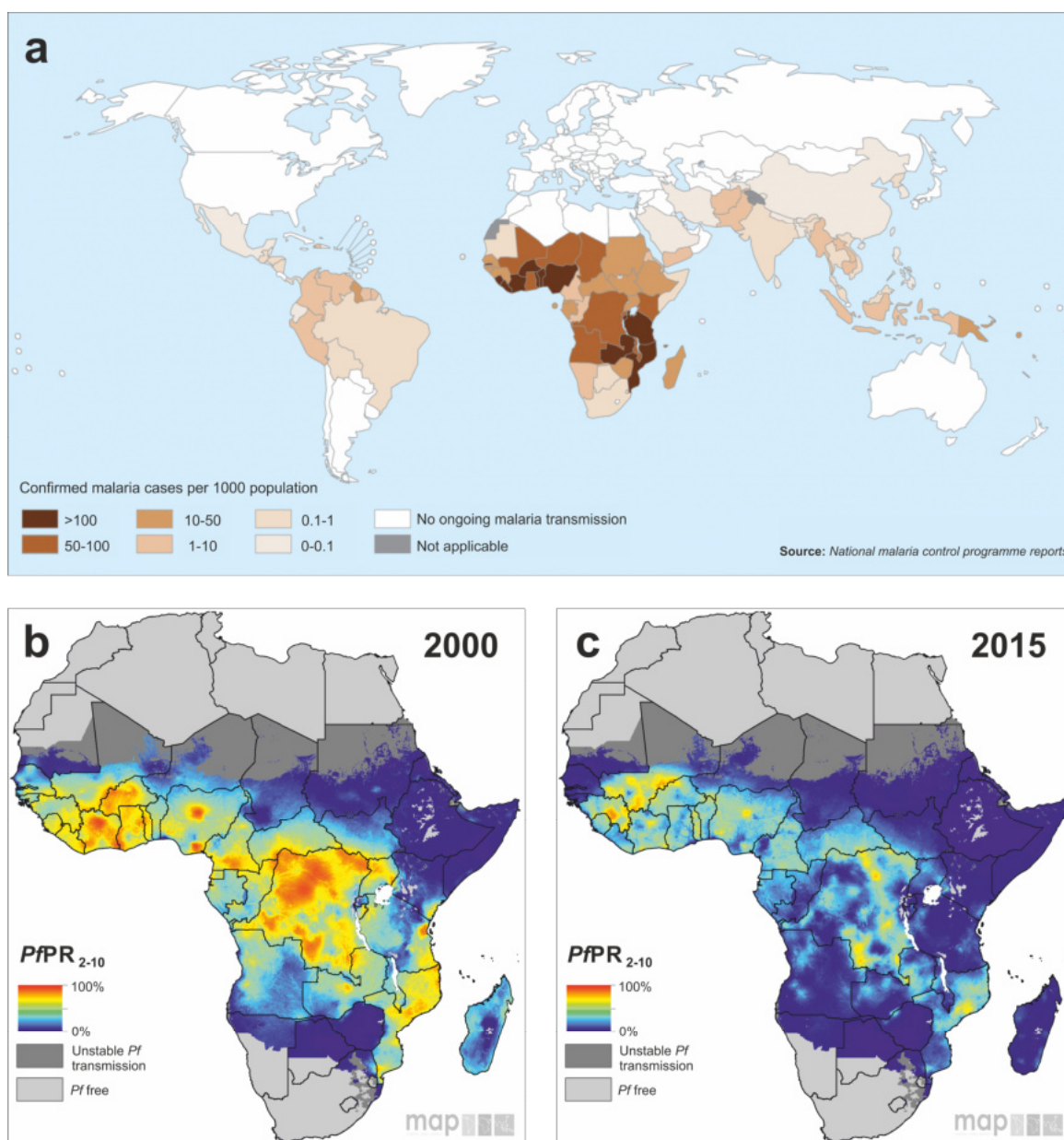


Figure 1 | Worldwide distribution and prevalence in Africa. a) Countries with ongoing transmission of malaria in 2013, cases per 1000 inhabitants are indicated in different colors (WHO World malaria report, 2013) b,c) *P. falciparum* infection prevalence in children of 2-10 years in 2000 (b) and 2015 (c) (Bhatt et al., 2015)

P. malariae and *P. ovale* rarely cause malaria deaths. *P. malariae* occurs in the same regions as *P. falciparum*. Notably this parasite does not form hypnozoites but nevertheless is capable to persist in the human host for many years. *P. ovale* is present in the western Pacific region and in Africa. The genome sequence validated evidence that it is actually two species, *P. o. wallikeri* and *P. o. curtisi* which are genetically different, although morphologically similar (Collins and Jeffery, 2005; Sutherland et al., 2010). As *P. vivax* it can generate hypnozoites, leading to relapses month or years after infection (White, 2011).

It is assumed that malaria caused by *P. knowlesi* is a zoonosis. This parasite is exclusively distributed in South-East Asia where the natural hosts, the macaques, live. Infection with *P. knowlesi* can cause severe symptoms in humans. *P. knowlesi* is morphologically similar to *P. malariae* and it is currently unclear if a host switch from monkeys to humans occurred only recently, or if previous cases had been wrongly identified as *P. malariae* (Kantele and Jokiranta, 2011; Singh and Daneshvar, 2013; Singh et al., 2004).

1.1.2 Pathophysiology

The characteristics of infection with malaria parasites differ depending on the *Plasmodium* species, but they all have in common various unspecific first symptoms such as dizziness, nausea, fever, chills, malaise and diarrhea. In *P. falciparum* the onset of symptoms starts 9-14 days after infection. *P. vivax* and *P. ovale* have a slightly later onset at days 12-18 and the *P. malariae* incubation period ranges from 18-40 days. The latency for the occurrence of symptoms is mainly influenced by the duration of the liver stage (for more information see 1.2.1.2) that precedes the continuous development phase in the blood (for more information see 1.2.1.3), which is responsible for the symptoms of the disease (Bartoloni and Zammarchi, 2012).

The typical fever is caused by the asexual replication of the parasites in red blood cells. The rupture of the host cell at the end of each development cycle (see 1.2.1.3) releases parasite antigens, hemozoin and glycosylphosphatidylinositols into the blood stream, where they act as pyrogens leading to an upregulation of TNF α followed by fever (Oakley et al., 2011; Schofield et al., 2002). This is as well responsible for the characteristic recurring fever attacks seen in patients infected by *P. vivax*, *P. ovale* and *P. malariae*. The synchronous growth of *P. vivax* and *P. ovale* with a 48h life cycle in the blood stages leads to the tertian fever characterized by fever attacks every two days, whereas *P. malariae* displays a 72h blood stage cycle, leading to fever attacks every three days (malaria quartana). As *P. falciparum* grows asynchronously, less predictable fever attacks are observed in patients infected by this parasite (Bartoloni and Zammarchi, 2012).

P. vivax, *P. ovale* and *P. malariae* rarely lead to life threatening consequences for the patient, even though there is increasing evidence of severe *P. vivax* infections (Rahimi et al., 2014). In contrast, *P.*

falciparum causes severe complications in approximately 1% of all cases. Complications can involve pulmonary or renal failure, severe anemia or cerebral malaria (CM) which usually includes coma, mostly affecting children under the age of 5 (Trampuz et al., 2003). Untreated CM is fatal in most cases, whereas the mortality in treated cases ranges between 15-20%. The underlying molecular mechanisms are not clear to date, even though there is strong evidence that the ability of *P. falciparum* infected RBCs to bind to the endothelium (cytoadherence) or to other infected RBCs (sequestration) may be involved. This causes an obstruction of blood vessels reduces the blood flow and leads to inflammation (Seydel et al., 2015; Wassmer et al., 2015).

1.1.3 Control strategies

Since the UN Millenium Declaration (UN Millenium Development Goals Report, 2015) different actions have been taken in an attempt to rapidly and effectively decrease the number of cases and the distribution of malaria. Amongst others this included plans for malaria eradication by vaccination and administration of drugs (discussed in more detail below), as well as setting up surveillance systems and controlling vector populations.

One of the most effective measurements in terms of vector control and malaria eradication was the use of insecticides. One infamous example is DDT, which was introduced in the 1940s but was banned in the 70s and 80s due to its toxicity that originates from its accumulation in fat tissue. Nevertheless, DDT helped reducing the population at risk to contract malaria from 77% (1900) to 50% (1975) (Enayati and Hemingway, 2010) and despite its negative attributes, DDT is still used for indoor residual spraying.

Since 2000 the use of insecticide treated mosquito nets (ITNs) has turned out to be one of the most successful steps in controlling malaria, significantly reducing malaria-derived child mortality. Today more than half of the African population at risk sleeps under an ITN. A current issue is the resistance of mosquitos to the pyrethroids, the only insecticides presently licensed for this purpose (Greenwood et al., 2008).

1.1.3.1 Antimalarial drugs

Numerous different antimalarial drugs are currently on the market, but over the course of time parasites developed resistances against all of them. The drugs can be classified into 4 groups:

- Quinine and derivates, such as chloroquine, mefloquine and lumefantrin
- Antifolates such as proguanil, trimethoprim and pyrimethamine
- Artemisinin and its derivates, for instance dihydroartemisinin, artesunate and artemether
- Atovaquone

The first antimalarial drug, quinine, was extracted from cinchona bark in 1820. It is active against the asexual blood stages (see 1.2.1.3). Its 4-aminoquinoline derivate Chloroquine (CQ) accumulates in the

parasite's food vacuole and inhibits polymerization of hemozoin, a step in the detoxification of hemoglobin. The resistance independently emerged in the late 1950s in South-America and South-East Asia (Payne, 1987). As the resistance to CQ is widespread, it is of only limited use today. CQ resistance is caused by a point mutation in the chloroquine resistance transporter gene (*crt*), that encodes a food vacuole transporter (Durand et al., 2001; Wellems and Plowe, 2001). The mutated protein transports chloroquine out of the food vacuole substantially faster than the wild type transporter and consequently leads to a decreased CQ sensitivity (Bray et al., 1998).

Proguanil, trimethoprim and derivatives target the parasite's folic acid metabolism. The parasite relies on *de novo* synthesis of folates. Folates, especially tetrahydrofolate, are essential cofactors in amino acid and nucleic acid metabolism. The widespread resistance is caused by a mutation in the dihydrofolate reductase (DHFR) gene that leads to an affinity loss of the drug to the tetrahydrofolate complex (Arrow and Panosian, 2004; Delves et al., 2012; Muller and Hyde, 2010). Atovaquone inhibits the electron transport chain in the parasite's mitochondria and is usually used in combination with proguanil. Resistance to this drug emerged rapidly and showed a mutation in the enzyme Cytochrome b. However, the resistance appears to prevent development in the mosquito and as a consequence cannot spread (Goodman et al., 2016). Atovaquone may therefore be an excellent partner for drug combinations and may be useable indefinitely without resistance becoming established in the parasite population.

Artemisinin was first used in traditional Chinese medicine and can be extracted from the leaves, stem and flowers of *Artemisia annua* (Klayman et al., 1984). Artemisinin was made available as a drug through the ground breaking work of Youyou Tu (Tu, 2011; Tu et al., 1981) for which she received the 2015 Nobel prize (Nobelprize.org, 2015). It is active against the asexual erythrocytic stages as well as the sexual precursor cells (gametocytes) that are passed on to the mosquito. The derivatives artesunate and artemether are prodrugs of dihydroartemisinin and due to their higher efficacy the 3 derivatives have replaced artemisinin. The therapeutic effect of artemisinin derivatives sets in rapidly, but the drugs are also rapidly eliminated from circulation with a half-life of approximately 1h. According to the WHO guidelines the first line treatment of Malaria are artemisinin combination therapies (ACTs), where a derivative of artemisinin is combined with a slower acting drug with a longer serum half life such as lumefantrine or mefloquine.

The mode of action of artemisinins is to date unclear. Some models suggest the interaction of the drug's endoperoxide bridge with heme, leading to oxidative stress and subsequent death of the parasite. Moreover it was proposed that artemisinin inhibits *Pf*ATP6, but other publications could not verify these findings (Cheeseman et al., 2012; Eckstein-Ludwig et al., 2003; Miao et al., 2013; Miotto et al., 2013). A more recent study implicated that artemisinins directly inhibits the enzyme phosphatidylinositol-3-kinase (PI3K) (Mbengue et al., 2015a).

First cases of artemisinin resistant parasites, characterized by slow parasite clearance in treated patients, were reported from South-East Asia. In the following years the resistance rapidly spread in South-East Asia (Figure 2) and now emerged independently in an African *P. falciparum* strain (Dondorp et al., 2009; Lu et al., 2017; Noedl et al., 2008; Woodrow and White, 2017). Resistance has been defined as a parasite clearance half-life ≥ 5 h following ACT (WHO, 2017). In field settings artemisinin resistance is regularly assessed by detection of parasites on day 3 after ACT (day 3 positivity) (White et al., 2015).

A mutation in the *PfKelch13* (C580Y) protein was found as a molecular marker for artemisinin resistance. It however needs to be noted that other mutations in the same region of this gene can also lead to a reduced susceptibility, even though C580Y is the most widespread mutation in South-East Asia (Ariey et al., 2014; Ashley et al., 2014). Furthermore, there have been reports of parasite isolates that showed reduced susceptibility to artemisinin derivatives that lacked mutations in *Kelch13*, suggesting that other genes may in some instances contribute or even mediate to artemisinin resistance (Mukherjee et al., 2017). So far the molecular mechanism of resistance to artemisinins is not clear. It has been proposed that the mutation in the *Kelch13* protein leads to increased PI3K levels and PI3P levels, thus antagonizing the effect of artemisinin (Mbengue et al., 2015a). Other studies indicated increased expression of unfolded protein response (UPR) pathways and an altered endoplasmic reticulum (ER) stress response (Dogovski et al., 2015; Mok et al., 2015).

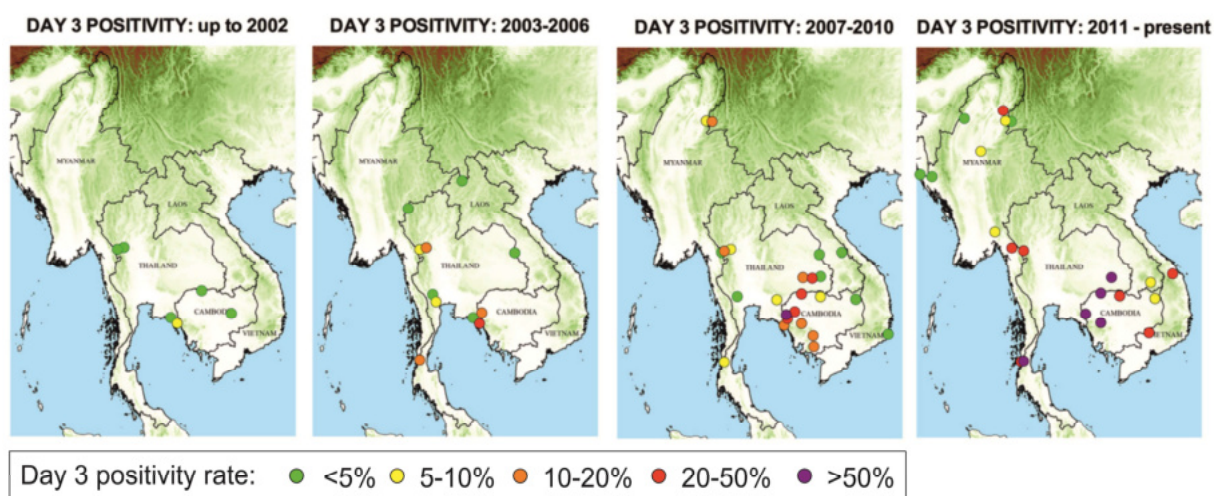


Figure 2 | Spread of artemisinin resistance indicated by day 3 positivity of patient samples. Plotted are the rates of patients with detectable parasitemia on day 3 after start of ACT analyzed by microscopy in South East Asia from 2000 to 2016. Dots mark the study sites and colors indicate the percentage of positive samples. (modified from (Woodrow and White, 2017))

1.1.4 Vaccine development

The development of a malaria vaccine has proven to be a difficult task. This is due to the parasite genetic diversity of surface proteins (antigenic variation and polymorphisms), differential expression of redundant antigens (for instance invasion ligands), the intracellular live style of the parasite and its complex life cycle. The WHO declared the goals for vaccine development in their malaria vaccine technology roadmap, that envisages a vaccine with a desired clinical efficacy of 75% that thereby could lead to a significantly decreased incidence of malaria (Malaria Vaccine Technology Roadmap, 2013). However, no vaccine with the promise of such level of efficacy is currently in the pipeline. The current candidates can be classified in three groups: transmission blocking vaccines (TBV), erythrocytic vaccines and pre-erythrocytic vaccines.

TBVs block transmission to or infection of the vector by targeting antigens important for gametes, zygotes or oocyst stages of the parasite. Lead candidate antigens are *Pfs25* and *Pfs28*, but so far no breakthrough in development was reported (Arama and Troye-Blomberg, 2014; Moreno and Joyner, 2015).

Erythrocytic vaccines usually act by preventing invasion of the so called merozoite stage into RBCs. Merozoites are the only free stages of the parasite in the blood but their short presence in the serum asks for very high levels of antibodies to prevent invasion. Lead structures are proteins expressed on the surface of merozoites i.e. erythrocyte binding antigen 175 (EBA175), apical membrane antigen 1 (AMA1), merozoite surface protein 1 (MSP1) and the parasitophorous vacuole resident protein serine repeat antigen 5 (SERA5). The main issue of erythrocytic vaccines is the high diversity of antigens based on genetic polymorphisms, highlighted by recent trials with MSP1 and AMA1 that could not demonstrate any protection (Arama and Troye-Blomberg, 2014; Ogutu et al., 2009; Sagara et al., 2009). A recently studied candidate, the reticulocyte binding homolog RH5, may circumvent these problems as it is a merozoite surface protein showing only limited diversity (Crosnier et al., 2011; Wanaguru et al., 2013). Rh5 acts in a complex with cysteine-rich protective antigen (CyRPA) and the RH5 interacting protein (*Pf*Ripr). This complex binds the protein basigin on the RBC surface, which is essential for invasion of the parasite into the RBC (Crosnier et al., 2011; Reddy et al., 2015). RH5 based vaccines have so far only been tested and shown to be effective against infection in an animal model (Douglas et al., 2015).

The only vaccine that is currently approved for use by the European Medicines Agency (EMA) is RTS,S (Mosquirix®). It consists of a recombinant antigen of the circumsporozoite protein (CSP) fused to the hepatitis B surface antigen and targets pre-erythrocytic sporozoite stages of the parasite. In a phase 3 clinical trial it showed a reduction of clinical malaria episodes compared to the control in 27% of infants and 46% in children 18 month after vaccination (Agnandji et al., 2014). A follow-up study 7 years after vaccination demonstrated that even though RTS,S initially showed some protective effect, the vaccine efficacy fades over time and a rebound effect that can lead to more clinical malaria cases compared to the control was evident (Olotu et al., 2016).

The highest efficacy to date was obtained by whole parasite based vaccination by immunization with radiation attenuated sporozoites. This approach was already tested in the 1960s, but finding the optimal levels of radiation remained a problem (Nussenzweig et al., 1967; Nussenzweig et al., 1969) and the production of sufficient numbers of sporozoites was at that time not considered feasible for a commercial vaccine. The idea was however taken up years later and the administration of attenuated, aseptic, purified, cryopreserved sporozoites led to high levels of protection (Seder et al., 2013). One solution to the radiation dose problem could be the use of genetically attenuated parasites that arrest during development in the liver (Annoura et al., 2012; Khan et al., 2012; van Dijk et al., 2005; van Schaijk et al., 2014). However, it is at present unclear if this will result in a viable vaccine. Another variation called sporozoite chemoprophylaxis vaccine was published recently. For this approach aseptic, purified, cryopreserved, non-irradiated sporozoites were administered along with chloroquine treatment. The rationale of this approach is to allow the asymptomatic liver infection which results in priming of the immune system. Drug administration then prevents the symptomatic blood stage infection but the immunity to liver infection remains. This approach led to a 100% protection rate when challenged with the same strain. Despite the very promising results, scale-up of sporozoite

extraction and long term protection will remain an issue that needs to be solved (Mordmuller et al., 2017).

1.2 Biology of *Plasmodium falciparum*

1.2.1 Life cycle

Plasmodium falciparum displays a complex life cycle (Figure 3) where it has to cope with drastic changes of environment from its definite host, the *Anopheles* mosquito to the human body. For instance there is great difference in body temperature of 20-25°C to 37°C between these hosts. Once it enters the human there are various cellular surroundings, first in the skin and blood stream to reach the liver where a first asexual development takes place in hepatocytes (the ‘liver stage’), followed by the continuous development within RBCs leading to exponential multiplication of the parasite in the blood (the ‘blood stage’) and finally the production of sexual precursor cells (gametocytes) that can be transmitted back to the mosquito.

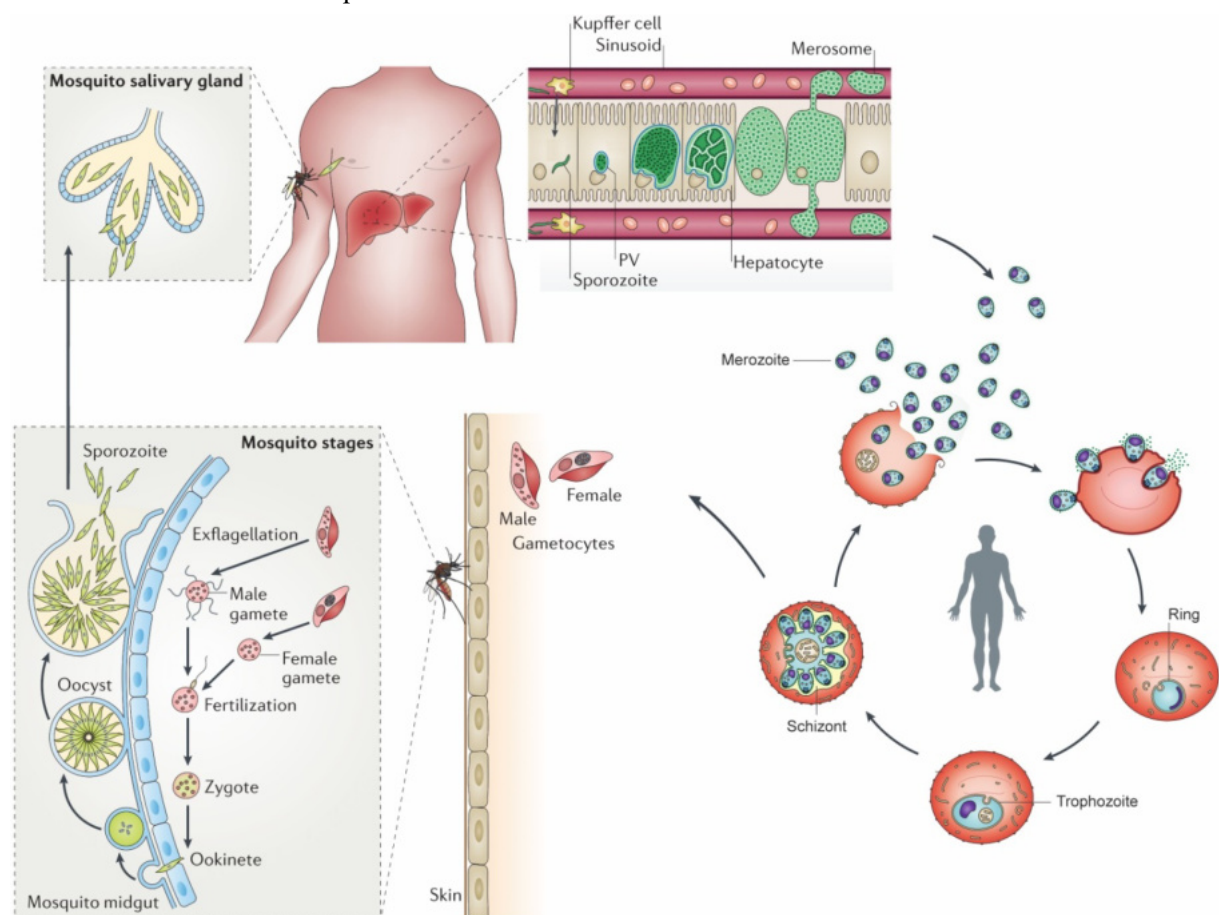


Figure 3 | Life cycle of *Plasmodium falciparum*. Sporozoites are injected into the circulation upon a bite of a female *Anopheles* mosquito and infect hepatocytes where they asexually replicate. Thousands of merozoites are subsequently released into the blood stream invading RBCs. The parasites develop from ring to trophozoite to schizont stage and ruptures. Daughter merozoites invade new RBCs and the asexual blood cycle starts again. Less than 10% of the parasites commit to sexual development and can be transmitted to an *Anopheles* mosquito. In the mosquito midgut the parasite

undergoes sexual replication, resulting in an ookinete penetrating the midgut wall. On the basal lamina ookinete arrests, develops into an oocyst and forms sporozoites that are released into the hemolymph. In the salivary gland the sporozoites can be transmitted to the human host, starting a new cycle (modified from De Niz et al., 2017 and De Koning-Ward et al., 2016)

1.2.1.1 Mosquito stages

Upon a blood meal of a female *Anopheles* mosquito on a host infected with malaria parasites, mature male and female gametocytes are taken up. Based on the change in pH, temperature and the encounter with the mosquito-derived metabolite xanthurenic-acid, the gametocytes are activated in a process termed gametogenesis (Guttery et al., 2015). Female gametocytes egress from their surrounding RBC in a protein kinase G (PKG) dependent manner and develop into fertile, haploid female gametes, the macrogametes (Billker et al., 2004; Guttery et al., 2012). The male gametocytes rapidly replicate their DNA from haploid (1N) to octoploid (8N) and produce 8 elongated male gametes that egress from the RBC in an actin dependent process termed exflagellation (Guttery et al., 2015; Sinden, 2015).

Fertilization of gametes leads to a diploid zygote that undergoes meiotic division to turn into a motile tetraploid stage termed the ookinete. This ookinete is characterized by an elongated shape and the capacity to penetrate the midgut epithelium, which occurs 12-36 h after the first ookinete epithelium interaction. Once it reaches the basal lamina of the midgut wall the ookinete arrests and develops in 10-12 days into an oocyst. In the oocysts, hundreds of elongated parasite stages termed sporozoites, develop (Aly et al., 2009; Sinden, 1974). After completion of sporozoite development in the oocyst, they egress into the hemocoel and are transported through the circulating hemolymph. Upon reaching the basal lamina of the salivary glands they attach by ligand-receptor interaction. CSP and thrombospondin-related anonymous protein (TRAP) have been shown to be essential for attachment (Kappe et al., 1999; Sultan et al., 1997). In the final step, sporozoites transit to the duct of the salivary gland and, upon a blood meal of the mosquito, are transmitted to the next human host.

1.2.1.2 Liver stage

After a bite of an infected female *Anopheles* mosquito, less than a hundred sporozoites are injected into the human host. Some of them reach a blood vessel and enter circulation, others stay in the skin or are eliminated in the lymph nodes. Once a sporozoite reaches the liver, it moves along the sinusoid and via Kupffer cells or endothelial cells and arrives at its final destination, the hepatocytes (Prudencio et al., 2006). Interestingly, sporozoites do not infect the first hepatocytes they reach, but instead travers several before invading the one they use as host cell. The attachment of sporozoites to hepatocytes was shown to be facilitated by interaction of CSP and TRAP on the sporozoite surface as well as CD81 and heparan sulfate proteoglycans (HSPGs) on the hepatocyte surface (Pinzon-Ortiz et al., 2001; Robson et al., 1995; Silvie et al., 2003; Sultan et al., 1997). Upon invasion of the parasite into the hepatocyte a parasitophorous vacuole (PV) is formed. Essential for establishing the PV is the hepatocyte receptor EphA2 and the sporozoite proteins of the 6-cys family P36 and P52 (Kaushansky et al., 2015). Within the hepatocyte the parasite develops into a trophozoite and then generates merozoites by undergoing

schizogony. In the case of *P. falciparum* several tens of thousands of merozoites can be generated per liver schizont. The completion of the parasites liver development is marked by the disintegration of the PV followed by the release of merozoites in membranous sacs termed merosomes. The merosomes reupture in the lung capillaries and release the merozoites into the circulation (Baer et al., 2007; Sturm et al., 2006). In *P. falciparum* the development in the liver takes on average 5.5 days (Bartoloni and Zammarchi, 2012).

1.2.1.3 Asexual blood stages

The asexual cycle in the blood starts with the invasion of merozoites in RBCs. In the following 48h the parasite grows inside its host cell from a so called ring stage to the trophozoite stage and finally to the schizont stage. In the final phase of the schizont stage (also termed the segmenter stage), the RBC ruptures and up to 32 new merozoites are released into circulation. These merozoites invade new RBCs, which marks the beginning of the next asexual cycle (Figure 4).

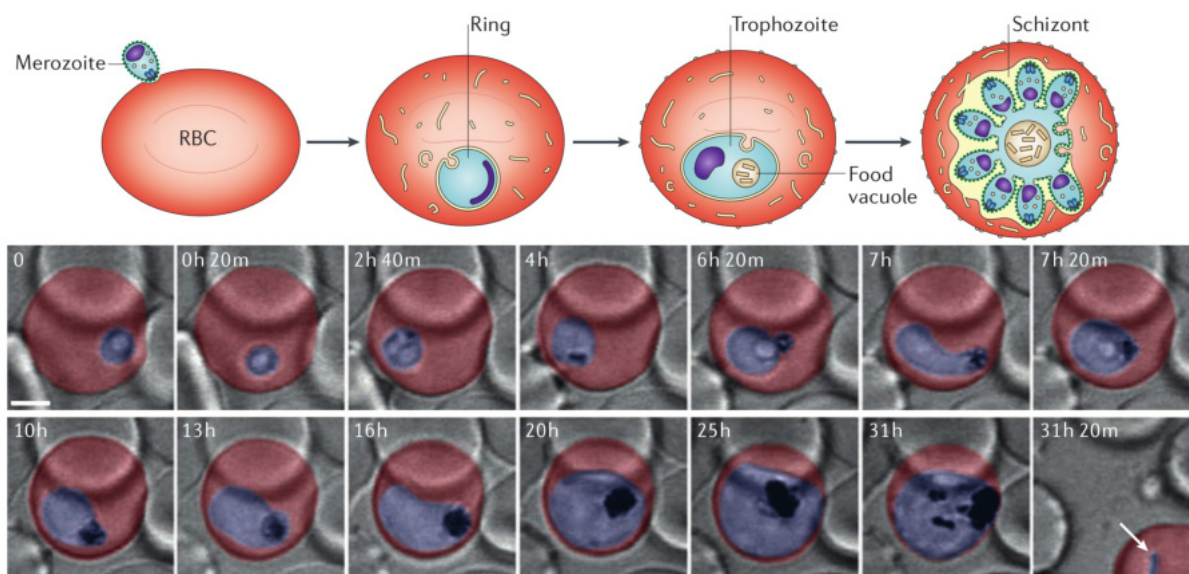


Figure 4 | Asexual blood stages. (Top panel) Scheme of the developmental stages in the asexual cycle. (Bottom panel) 4D imaging of a complete cycle of a *P. falciparum* parasite (blue) in a RBC (red) using time laps imaging. Time point in hours post infection are shown. Arrow in the last picture indicates a ring stage after reinvasion of a released merozoite (De Niz et al., 2107).

Invasion of merozoites into the RBC is a rapid, complex and highly orchestrated process. The initial contact is a low affinity interaction of merozoite surface proteins (MSPs) with the erythrocyte surface. Best characterized is the interaction of the GPI-anchored merozoite surface protein 1 (MSP1) with band 3 of the host cell, resulting in a deformation of the RBC (Goel et al., 2003). Subsequently the merozoite orientates with its apical pole towards the RBC membrane to bring the apically located organelles, required for invasion, close to the site where invasion is initiated. Irreversible attachment, as well as the reorientation is promoted by parasite ligands such as the erythrocyte binding antigens (EBAs) (stored in the micronemes) and reticulocyte-binding like homologs (Rhs) (stored in the rhoptries), which are partially redundant (O'Donnell et al., 2000). EBAs bind to glycoprotein receptors

on the RBC and this invasion pathway is sialic-acid dependent. Rh5 bind to mostly unknown receptors in a sialic-acid independent manner. It has to be noted that Rh5 plays a role downstream of the other Rh5s, which is thought to triggers the discharge of the rhoptries (Weiss et al., 2015). A tight junction is formed by interaction of AMA1 on the merozoite surface and rhoptry neck protein 2 (RON2), which is first translocated from the parasite into the host cell membrane (Srinivasan et al., 2011; Tonkin et al., 2011). The following release of lipids and proteins from the rhoptries is thought to have an important role in the formation of the PV membrane that separates the merozoite from the engulfing RBC (Cowman and Crabb, 2006). Most of the merozoite surface proteins are shed during invasion driven by the proteases (Aikawa et al., 1978; Bannister et al., 1975; Cowman and Crabb, 2006; Ladda et al., 1969). The actual invasion process into the RBC is driven by a parasite-encoded actin-myosin motor (Baum et al., 2006; Weiss et al., 2016).

Once in the RBC, the parasite enters the ring stage which lasts approximately 18h. This phase of the life cycle obtained its name from the cup shape appearance of the parasite, even though the parasite switches between ring forms and amoeboid forms (Gruring et al., 2011). At this stage extensive host cell remodeling, by export of parasite proteins into the RBC cytosol, starts to take place. 4 hours after invasion parasite modified structures in the RBC called Maurer's clefts (MC) become apparent (Gruring et al., 2011). One of the most prominent changes to the RBC is the appearance of so called knobs on the surface in the early trophozoite stage. They are important structures for mediating cytoadherence in order to avoid clearance in the spleen (see 1.2.2.1) (Leech et al., 1984; Nagao et al., 2000; Watermeyer et al., 2016). Transition to trophozoite is marked by alteration of rings to a more irregular form, a steady position in the RBC and the appearance of the food vacuole (see 1.2.2), an acidic lysosomal-like compartment. Main characteristic of the trophozoite stage is the intense growth of the parasite lasting until approximately 34 hours post infection (hpi). In order to grow the parasite needs to take up nutrients and generate space by host cell cytosol and hemoglobin uptake. The underlying mechanism conferring the nutrient uptake is not clear. It has been proposed that a PVM derived structure called tubovesicular network (TVN) is involved in this process (Lauer et al., 1997). Equally the endocytotic mechanism of hemoglobin and RBC cytosol uptake is unknown, potentially involving structures called cytostomes (Aikawa et al., 1966; Lazarus et al., 2008). The beginning of the following schizont stage the parasite is marked by asynchronous nuclear division by schizogony (Gerald et al., 2011). The parasite forms up to 32 daughter cells organized by the microtubular system. At this stage important structures for the later following reinvasion into new RBCs are assembled, the inner membrane complex (IMC) and the apical complex. The IMC contributes to structural stability of the cells and provides a scaffold for the formation of daughter cells. Furthermore it is crucial for gliding motility in the invasion process and has been shown to be essential for sexual development (Baum et al., 2006; Keeley and Soldati, 2004; Khater et al., 2004; Kono et al., 2012). After formation of the merozoites and prior to the exit from the RBC the PVM is disintegrated followed by a rupture of RBC membrane. This sequential process is triggered by proteases (Blackman and Carruthers, 2013). The releases of the daughter merozoites into circulation 48 hpi completes the asexual life cycle.

1.2.1.4 Sexual development

Of the asexually multiplying blood stages a small number, usually below 10%, commit to sexual differentiation. This process, termed gametocytogenesis, takes 10-12 days and leads the development of male and female gametocytes (Josling and Llinas, 2015). Gametocytogenesis can be divided into five subsequent stages that based on their morphology are termed stage I-V. Early stage gametocytes resemble trophozoites but with progressing in development, they become elongated and acquire a sickle shape (Figure 5) (Carter and Miller, 1979). Only stage I and V gametocytes can be found in circulation, as other stages sequester in the bone marrow (Aguilar et al., 2014; Farfour et al., 2012). After development to stage V gametocytes the parasite can be transmitted to mosquitos and start its sexual reproduction (see 1.2.1.1).

The exact time of commitment to gametocytogenesis in the asexual cycle is unknown, but as all merozoites derived from a parasite become exclusively female or male gametocytes, it must occur in the cycle preceding gametocyte development (Bruce et al., 1990; Smith et al., 2000). A protein essential for gametocytogenesis is the transcription factor AP2-G. It belongs to an apicomplexan family of proteins containing APETELALA2 (AP2) DNA-binding domains. Disruption of the AP2-G gene leads to a parasites incapable to produce gametocytes (Kafsack et al., 2014; Sinha et al., 2014). Many factors, such as spent parasite medium have been implicated in an increase in gametocyte production rates but there is no clear consensus what leads to commitment and whether not stochastic effects are at play. Recent studies implicated microvesicles derived from infected RBCs in the induction of gametocytogenesis but relations to physiological cues still need to be established (Josling and Llinas, 2015; Mantel et al., 2013; Regev-Rudzki et al., 2013).

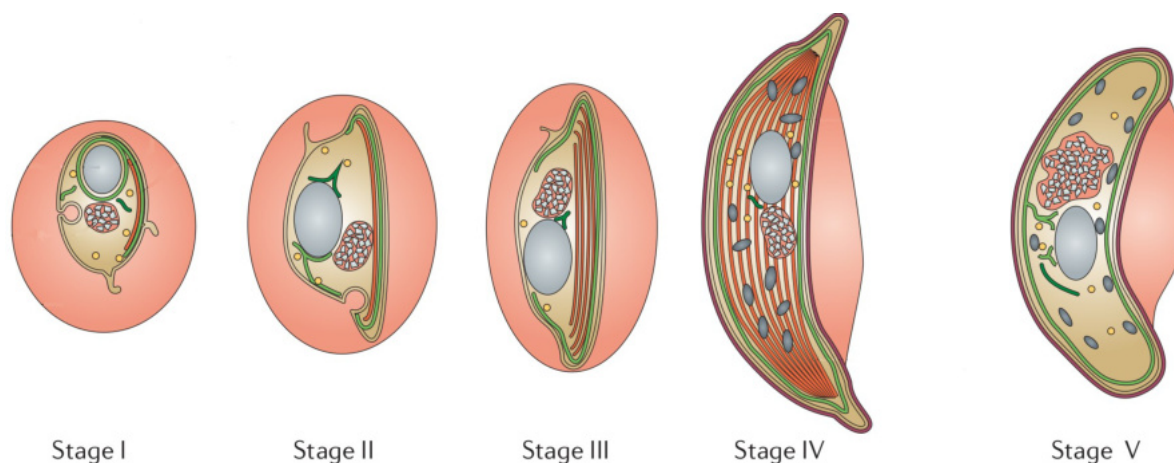


Figure 5 | Development stages of gametocytes. Only stage I and V can be found in the circulation, the other stages develop in the bone marrow. (Josling and Llinas, 2015)

1.2.2 Cellular biology of *P. falciparum*

Apart from the basic eukaryotic organelles, such as the nucleus, mitochondria, ER and Golgi-apparatus, *P. falciparum* parasites possess highly specialized organelles suited to its intracellular lifestyle (Figure 6). The most prominent of these are the apical organelles that are essential for the invasion into new RBCs. It harbors secretory organelles termed micronemes, rhoptries, exonemes and dense granules. In addition to these the parasite contains a lysosome-like organelle termed the food vacuole and a secondary endosymbiont termed the apicoplast.

The food vacuole (FV) is an acidic compartment and fundamental for the digestion of hemoglobin that is taken up in large quantities by the parasite during its development in the RBC (Francis et al., 1997; Gluzman et al., 1994; Vander Jagt et al., 1986). Unlike mitochondria or the apicoplast, the FV may be formed *de novo* with each cycle in a new host cell, as it is disposed during egress from the RBC. Its formation may be driven by the fusion of several endocytic vesicles in the late ring stage (Abu Bakar et al., 2010; Lazarus et al., 2008). The FV contains a set of proteases e.g. falcipain, plasmepsin I and plasmepsin II that drive hemoglobin digestion and detoxification (Goldberg et al., 1991; Goldberg et al., 1990). A degradation product is α -hematin, which is toxic for the parasite due to its property to induce the production of free radicals in the FV. The parasite polymerizes α -hematin into the non-toxic hemozoin, but the enzymes catalyzing this polymerization are still not entirely clear (Francis et al., 1997; Sullivan, 2002; Sullivan et al., 1996).

The apicoplast is a plastid that lost its photosynthetic function. It was acquired by secondary endosymbiosis of red algae that itself contained a prokaryotic endosymbiont (Fast et al., 2001; Kohler et al., 1997). Hence the apicoplast is a secondary endosymbiont and is surrounded by 4 membranes. It contains more than 500 proteins, but only about 50 (on the 35 kb plastid genome) are still encoded in the apicoplast itself. The remainder was transferred to the parasites nucleus and the proteins are afterwards targeted via specific signals to the apicoplast (Waller et al., 1998; Waller et al., 2000).

The apicoplast was highlighted as an Achilles heel of the parasite (Soldati, 1999). However, its role for parasite biology remained elusive for a long time but based on the proteins predicted to be trafficked to the apicoplast, roles in the biosynthesis pathways of fatty acids, Fe-S clusters, lipoic acid and isoprenoid biosynthesis were identified (Ralph et al., 2004; Seeber and Soldati-Favre, 2010; van Dooren and Striepen, 2013). A study from Yeh & deRisi showed that only the isoprenoid precursor biosynthesis is essential for the blood stages. Parasites that were cured of their apicoplast using an antibiotic could be rescued when a single isoprenoid biosynthesis precursor (isopentenyl pyrophosphate) was supplemented (Yeh and DeRisi, 2011).

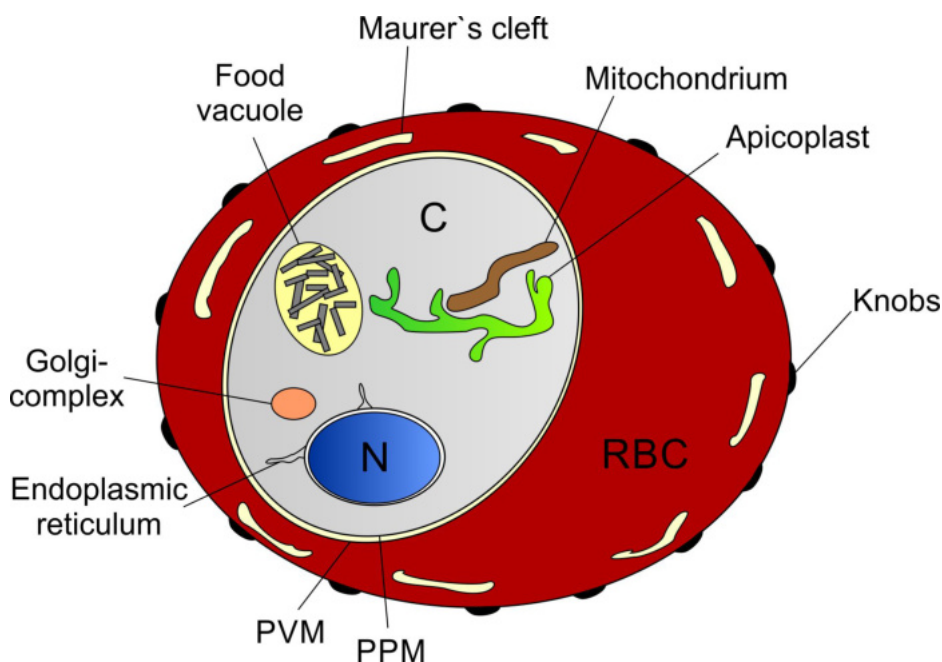


Figure 6 | *P. falciparum* infected red blood cell. Schematic of a trophozoite stage parasite within a RBC. Organelles are displayed. N, nucleus; C, cytosol of the parasite; PPM, parasite plasma membrane; PVM, parasite vacuolar membrane; RBC, red blood cell. (Image was kindly provided by Sabine Schmidt (Schmidt, 2017))

1.2.2.1 Export of proteins

Over the period of a cycle the parasite modifies its host cell extensively by transporting proteins into the cytosol and to the surface of the RBC, as well as taking up nutrients, hemoglobin and the host cells cytosol to provide space for its own growth.

Exported proteins have to enter the secretory pathway and pass two different membranes, first the parasite plasma membrane (PPM) and secondly the parasitophorous vacuole membrane (PVM). The so far best described export signal is the plasmodium export element (PEXEL), an N-terminal motif consisting of 5 amino acids (AA), RxLxE/Q/D. Upon translation the PEXEL motif of a protein is recognized by the signal recognition particle (SRP), which directs it to the endoplasmic reticulum (ER) and where it is inserted via the ER translocon Sec61 into the ER lumen. Here the PEXEL motif gets cleaved by Plasmepsin V, exposing a new n-terminus as result (Boddey et al., 2010; Hiller et al., 2004; Marti et al., 2004). However, there are a so far unknown number of exported proteins that do not contain a PEXEL motif, the PEXEL negative exported proteins (PNEPs). Often containing a transmembrane domain, all known PNEPs have a hydrophobic region in common that mediates entry into the secretory pathway (Heiber et al., 2013; Spielmann and Gilberger, 2010; Spielmann et al., 2006).

The transport from ER to the PV is mediated by vesicles, delivering the protein into the PV (Deponte et al., 2012). There is compelling evidence that trafficking across the PVM is mediated by a complex termed PTEX, plasmodium translocon of exported proteins. The identified components are EXP2 (exported protein 2), likely the pore through the membrane, HSP101 (heat shock protein 101) an

AAA+ ATPase that is responsible for unfolding of the traversing proteins and PTEX150, which has been proposed to have a structural/stabilizing function. Moreover PTEX88 and TRX2 (thioredoxin 2) are associated with PTEX, but their role is to date unclear and both are not essential for parasite survival in contrast to the first three components (Beck et al., 2014; de Koning-Ward et al., 2009; Elsworth et al., 2014; Matthews et al., 2013). Having reached the host cell most exported proteins are trafficked via or to a structure in the host cell that is termed Maurer's clefts (MC) (Deponte et al., 2012; Lanzer et al., 2006; Przyborski et al., 2003). One of the best studied MC resident proteins is REX1, having a crucial role in the morphology (McHugh et al., 2015). The MC function is not entirely clear, but they are thought to be a sorting nexus e.g. for virulence factors as EMP1 that is delivered to the RBC membrane. EMP1 is expressed on the surface and important for cytoadherence. It is thought to be the one of the main factors contributing to cerebral malaria. A recent publication has shown that binding of the EMP1 to the endothelial receptors ICAM-1 and EPCR simultaneously is associated an increased risk of developing CM (Lennartz et al., 2017). Anchored in an underlying structure called knobs it interacts with KAHRP (knobs-associated histidine-rich protein) and PfEMP3, whereat KHARP was shown to be essential for knob formation (Crabb et al., 1997; de Koning-Ward et al., 2016; Deponte et al., 2012).

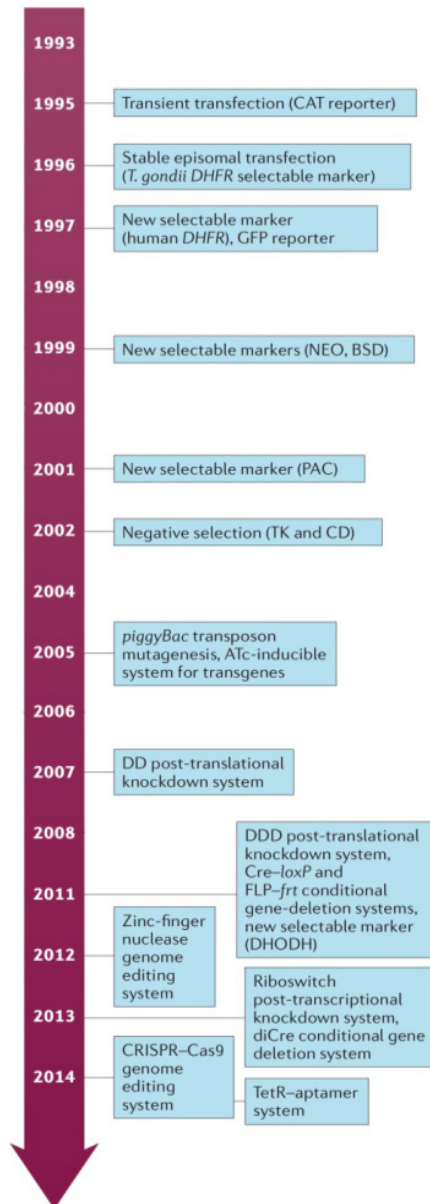
1.3 Methods for gene and protein inactivation in *P. falciparum*

The haploid genome of *Plasmodium falciparum* encompasses about 5400 genes spread on 14 chromosomes (Rutledge et al., 2017). Additionally the parasite contains the 35kb apicoplast genome and 6kb mitochondrial genome (Gardner et al., 2002). To date more than one-third of all of its predicted genes are annotated as of 'unknown function', which indicates that the protein they encode show no homology to proteins of known function found in other organisms (Plasmodb.org). This indicates that still a large part of this parasites' biology remains unknown. As many of these unknown genes are restricted to Apicomplexa or the genus Plasmodium, they are involved in parasite-specific processes that are best suited as targets for therapeutic interventions.

To find out more about the parasite specific biology, it is essential to elucidate the function of these gene products. A first step in this would be to localize these proteins in the cell, as demonstrated for instance in yeast (Huh et al., 2003). However, it has been estimated that solely localizing all *P. falciparum* proteins will take until 2050 (Webster and McFadden, 2014).

Recent years have shown great technical progress in manipulating *P. falciparum* genes and proteins that in part address the limitations hampering the study of this parasite's biology (Figure 7) (de Koning-Ward et al., 2015; Webster and McFadden, 2014). The first transient transfection of *P. falciparum* was achieved more than 20 years ago by using electroporation with a plasmid leading to the expression of chloramphenicol acetyltransferase (CAT) (Wu et al., 1995). A year later, the first stable transfection was reported (Wu et al., 1996). Since then, a few other techniques for transfection were reported, but so far the originally introduced electroporation is the only reliable method (Gopalakrishnan et al., 2013; Mamoun et al., 1999b; Webster and McFadden, 2014). While a number

of advances of the original electroporation protocol were made (Deutsch et al., 2001; Moon et al., 2013), transfection remains time intensive. An option to use 96-well plates to achieve a higher throughput was published, but has not seen much use to date (Caro et al., 2012).



After transfection plasmid DNA is usually present episomally, which is appropriate for approaches such as overexpression of a tagged protein of interest. However, for gene and protein inactivation methods changes to the parasite genome are needed. This is hampered by the fact that the integration of plasmids into the *P. falciparum* genome occurs only at very low frequency. Traditionally such genetic changes were obtained through single crossover homologous recombination based on a 500 to 1500 bp sequence on the plasmid matching a genomic region. In contrast double crossover recombination does not usually seem to occur and can only be obtained when employing negative selectable markers (Duraisingh et al., 2002; Maier et al., 2006). To obtain parasites with genomic integrations of a plasmid of interest are passively selected by cycles on and off the drug selecting for the episomal plasmid. This procedure leads to a slow enrichment of parasites with the integration and takes several weeks to many months. Unfortunately, this approach is not always successful. Especially, if the genetic change leads to a reduction in parasite fitness parasites with the integrated plasmid cannot be obtained at all (de Koning-Ward et al., 2015; Webster and McFadden, 2014).

Figure 7 | Development of genetic systems. DHFR, dihydrofolate reductase; NEO, neomycin phosphotransferase; BSD, blasticidin S deaminase; PAC, Puromycin-N-acetyltransferase; TK, thymidine kinase; CD, cytosine deaminase; ATc, anhydrotetracycline; DD, destabilization domain; DDD, DHFR destabilization domain; DHODH, dihydroorotate dehydrogenase; TetR, tetracycline repressor. (modified from de Koning-Ward et al., 2015)

1.3.1 Selection markers

Pivotal for genetic manipulations are robust positive selection markers that are encoded on the plasmid to be transfected into the parasite. For *P. falciparum* there are currently 6 selection markers available. Dihydrofolate reductase-thymidylate synthase (*dhfr-ts*) was the first selection marker used. Plasmids encoding this gene can be selected using pyrimethamine (Wu et al., 1996). Soon the set was extended by the human dihydrofolate reductase (hDHFR), which confers resistance to WR99210 (Fidock and Wellems, 1997). hDHFR is the most robust and therefore most widely used selection marker in *P.*

falciparum research. Another two years later the Goldberg lab published that the genes neomycin phosphotransferase II (*neo*) and blasticidin S deaminase (*bsd*) confer resistance to G418 and blasticidin in *P.falciparum*, respectively (Mamoun et al., 1999a). BSD turned into a frequently used marker, usually to generate double transgenic parasites that are already resistant to WR99210. In contrast, Neo turned out to be unreliable for episomal expression. Puromycin-N-acetyltransferase (PAC) conferring resistance to the drug puromycin is another infrequently used marker in *P.falciparum*. The newest positive selection marker is yeast dihydroorotat dehydrogenase (yDHODH) that is selected using atovaquone or DSM1. This marker is already well established in the field (de Koning-Ward et al., 2001; Ganesan et al., 2011; Ghorbal et al., 2014).

Two negative selection markers have also been used in *P.falciparum* research. These markers, thymidine kinase (TK) and cytosine deaminase (CD), are selected with the pro-drugs ganciclovir and 5-fluorocytosine, respectively. In parasites harboring the marker, the prodrug is turned into its active form, killing the parasite. These markers can be used for removal of episomes and selection of double-crossover recombination integrands (Duraisingh et al., 2002; Ghorbal et al., 2014).

1.3.2 Methods for genome modifications

The first gene ‘knockout’ in *P.falciparum* was done in 1997 with the simple approach termed targeted gene disruption (TGD). The gene is targeted using a 600-1200 bp long homology region (HR) in its 5’ coding region. This region is situated on an episomal plasmid that, upon single-crossover integration into the genome, truncates the gene. This leads to a truncated, preferentially unfunctional protein that however is not a true knockout (Webster and McFadden, 2014). It was shown that the truncation of KAHRP leads to RBC lacking knobs on the surface of infected RBCS and for the first time demonstrated a role of these structures in cytoadhesion and hence virulence of the parasite (Crabb et al., 1997). The TGD approach has since been used many times, but integration into the genome is done by passive selection with the above mentioned limitations (see 1.3). Moreover the truncated gene products can still be functional, especially if the gene is small in size. Furthermore, due to the inefficiency and uncertainty to obtain a TGD, it cannot be concluded that lack of integration signifies an essential function of the targeted gene.

A more recent method for genome editing is the use of Zinc-finger nucleases (ZFN). ZFNs consist of a zinc finger DNA-binding domain that recognizes a specific sequence in the genome and FokI nuclease that induces double strand breaks (DSB) in the DNA upon dimerization (Bitinaite et al., 1998). DSB can be repaired by the parasite using end joining pathways that result in disruption of the gene, as the repair mechanism is error prone and causes deletions or insertions. Alternatively the parasite can repair DSB by the homologous recombination (HR) pathway, if a donor template is provided (Webster and McFadden, 2014). Of note is that *P.falciparum* parasites do not possess the canonical non-homologous end joining pathway (NHEJ), known from higher eukaryotes, but use an alternative end joining pathway (Kirkman et al., 2014; Singer et al., 2015). ZFNs was validated for their use in *P.falciparum* parasites by inducing a DSB in an parasite line expressing green fluorescence protein (GFP) from an endogenous locus in the genome. The donor template contained flanking regions

matching the GFP locus and hDHFR as a selection marker, resulting in the elimination of the *gfp* gene upon repair of the ZFN induced DNA strand break. GFP fluorescence was completely lost within 14 days under positive selection. In a similar experiment without a selection marker a mixed population of genetically altered and non-altered parasites was obtained, making cloning of parasites a necessary step to obtain a homogenous population with the desired genetic change (Lyko et al., 2012; Straimer et al., 2012). In two other studies ZFNs were used to introduce point mutations conferring parasite drug resistance (McNamara et al., 2013; Straimer et al., 2012).

Double strand breaks and the same repair pathways as for ZNFs are used by the clustered regularly interspaced short palindromic repeat (CRISPR)-Cas9 system. Cas9 is an endonuclease causing DSBs that is guided by RNA to the targeted locus. This technique, after two proof of principle studies (Ghorbal et al., 2014; Wagner et al., 2014), is now increasingly used to modify the *P. falciparum* genome. It was used to introduce mutations in the Kelch13 gene that confers artemisinin resistance (Ghorbal et al., 2014) and to identify the amino acids that are essential for binding of the drug Mefloquin to the 80S ribosome (Wong et al., 2017). It was also used to destroy genes that are not essential for *in vitro* growth such as KAHRP and EBA175 locus (Ghorbal et al., 2014; Wagner et al., 2014) or to insert loxP sites to inducibly delete gene regions with a small molecule-controlled recombinase (see below) (Andenmatten et al., 2013; Collins et al., 2013; Jullien et al., 2007; Jullien et al., 2003; Volz et al., 2016). In comparison to ZNFs it is a simpler and cheaper approach, as ZFNs need to be engineered (de Koning-Ward et al., 2015). CRISPR/CAS9 technology has also been used in the Apicomplexan *Toxoplasma gondii* to carry out genome-wide loss of function screens (Sidik et al., 2016). however, the limited transfection efficiency and the absence of the NHEJ pathway may in the near future hamper similar approaches in *P. falciparum* parasites.

Genome editing can also be achieved by using site specific recombinases, such as Cre or FLP (Sauer, 1987; Zhu and Sadowski, 1995). These recombinases require two targeting sequences, loxP sites or *frt* sites that flank the region to be manipulated. Depending on the orientation of the targeting sequences, the region of interest is either removed or inverted. Hence, if they are placed upstream and downstream of the locus, the gene can either be removed or inverted. Comparing both recombinases, the Cre system was shown to be more efficient in *P. falciparum* (O'Neill et al., 2011). Important for the analysis of essential genes is the possibility to inducibly activate the recombinase, as premature excision would kill the parasite. This was achieved using a split Cre recombinase termed diCre. With this system the dimerization and subsequent activation of Cre is induced by addition of the ligand rapamycin (Jullien et al., 2007; Jullien et al., 2003). This system was adapted to the Apicomplexan *T. gondii* (Andenmatten et al., 2013) and then transferred to *P. falciparum* (Collins et al., 2013) and since then has been used in a number of instances, for example to study the function of the invasion protein AMA1 (Yap et al., 2014). The DiCre system therefore represents one of the most promising tools for the study of essential *P. falciparum* proteins to date.

1.3.3 Methods for regulation of gene expression and RNA levels

A commonly used system for post-transcriptional control in eukaryotes is RNA interference (RNAi) where a small RNA molecule binds to mRNA and thus inhibits its translation or leads to degradation of the mRNA (Agrawal et al., 2003; Hamilton and Baulcombe, 1999). Unfortunately *P. falciparum* lacks the corresponding machinery, making it impossible to use RNAi (Baum et al., 2009). An alternative approach is to influence promoter control. The first technique for the control of gene expression in *P. falciparum* was the Tet-off system. The promoter of a gene of interest (GOI) is first replaced by a promoter that includes several tetracyclin operators (TetO) sequences. Upon binding of a transcriptional transactivator domain (TRAD) the gene of interest gets expressed. Addition of anhydrotetracycline (ATc) to the culture inhibits binding of the TRADs to the operators and results in a knockdown of gene expression (Meissner et al., 2005). However, this system has seen little use, likely due limited levels of regulation. An improved version of this system, although so far not efficient enough for conditional gene knockdowns in *P. falciparum* (Pino et al., 2012), was successfully used in the rodent malaria parasite *P. berghei* (e.g. Elsworth et al., 2104).

A further interesting option for the control of mRNA levels are ribozymes (ribonucleic acid enzymes) that cleave the mRNA in which they are incorporated. Usually these ribozymes are situated in the 3' untranslated region (UTR). Upon activation, the 3' UTR is lost, often leading to degradation of the mRNA and a reduction in the expression of the corresponding protein. Different ribozymes have been tested in *P. falciparum* but only the glmS ribozyme is widely used (Agop-Nersesian et al., 2008; Ahmed and Sharma, 2008; Flores et al., 1997; Prommana et al., 2013). Inserted into the 3' UTR of a target gene addition of glucosamine (GlcN) induces self-cleavage of the RNA, achieving knock down levels of more than 80% (de Koning-Ward et al., 2015). The glmS ribozyme has for instance been used to regulate the expression of a component of the PETX complex or to knock down the protease processing exported proteins in the ER (Elsworth et al., 2014; Sleebs et al., 2014).

Another technique for post-transcriptional control makes use of so called aptamers. Nucleic acid aptamers are short oligonucleotide sequences that bind their target molecules with very high affinity. Constant improvements of already published aptamer systems led to the most recent aptamer method called TetR-DOZI system (Belmont and Niles, 2010; Ganesan et al., 2016; Goldfless et al., 2014; Hunsicker et al., 2009; Niles et al., 2009). A repeat of ten aptamers in the 3' UTR targets the tetracycline repressor protein (TetR) onto the mRNA. The TetR protein in turn is fused to the DOZI protein, which is the *P. falciparum* homologue of the *S. cerevisiae* mRNA decapping protein Dhh1p. The presence of this protein results in decapping of the mRNA and consequently leads to translational repression. The system is inducible, as addition of ATc leads to conformational changes in the TetR protein, which prevents aptamer interaction and consequently leads to protein expression. With the TetR-DOZI system it was shown that the suspected drug resistance protein ATPase PfATP4, is essential for parasite survival (Ganesan et al., 2016) and TRIC- θ , subunit of the TRIC chaperon complex, is necessary for asexual development but not protein export, as suggested earlier (Mbengue et al., 2015b; Spillman et al., 2017).

1.3.4 Methods for post-translation control

Two different domains have been used in *P. falciparum* to inducibly control the stability of proteins of interest. The first is based on the FK506-binding protein destabilization domain (DD) (Banaszynski et al., 2006) and the second on the DHFR destabilizing domain (DDD) (Iwamoto et al., 2010). In absence of stabilizing ligands (termed shield-1 and trimethoprim for the 2 domains, respectively), the domains promote their own degradation via the ubiquitin proteasome machinery. Fusion of these domains (either C- or N-terminally) then can lead to the degradation of the attached protein of interest together with the destabilization domain. These systems were up to date the most successful approach to functionally analyze essential *P. falciparum* proteins (Armstrong and Goldberg, 2007; de Koning-Ward et al., 2015; Muralidharan et al., 2011). One of the first examples using the DD system analyzed the function of the calcium dependent protein kinase 5 (CDPK5). Fusion of DD to endogenously expressed CDPK5 led to degradation of CDPK5 when shield was removed and resulted in an arrest in the schizont stage and demonstrated an essential role of this kinase in egress of merozoites out of the infected RBC (Dvorin et al., 2010). However, the level of regulation achieved with the DD system appears to strongly depend on the target and not all proteins can be regulated sufficiently (Webster and McFadden, 2014).

The DDD system has been shown to have a higher variability in knockdown levels than the DD system (de Koning-Ward et al., 2015). Nevertheless its use has been reported in different publications, e.g. indicating the essential role of the proteasome lid subunit 6 (Muralidharan et al., 2011). Furthermore DDD seems to be particularly suited to target chaperones. Removal of the stabilizing agent can lead to binding of the chaperone to the fusion tag, thereby inactivating, as observed when studying the PTEX component HSP101 (Beck et al 2014) and HSP110 (Muralidharan et al., 2012).

A similar method makes use of an auxin-inducible degron. It is based on the interaction of the plant hormone auxin with the auxin responsive AUX/IAA sequence that recruits an E3 ubiquitin ligase and leads to proteasomal degradation. For malaria parasites, a proof of concept has been published in 2013, but so far this system only has been applied in *P. berghei*, investigating the role of the parasite's calcineurin in the mammalian host and in the mosquito (Kreidenweiss et al., 2013; Philip and Waters, 2015).

1.4 The FKBP-FRB system

Most techniques for functional analysis of a gene or its product are based on their removal or a reduction in their abundance. In contrast, controlled changes of the localization of a target protein can be used in a variety of ways for functional studies. This can be used by virtue of a heterodimerization system of which the FRB-FKBP system has been most widely used (Putyrski and Schultz, 2012). It belongs to the class of chemically inducible dimerization (CID) systems where the interaction of the 2 components is controlled by a small molecule, here termed a heterodimerizer. The system is derived from the interaction of the immunosuppressant sirolimus (also known as rapamycin) with the cytosolic 12 kDa FK506 binding protein (FKBP, also FKBP12). The complex inhibits the mechanistic target of rapamycin, the mTOR kinase. The exact binding region of the kinase is termed FKBP rapamycin binding domain (FRB) (Belshaw et al., 1996; Chen et al., 1995; Choi et al., 1996; Liang et al., 1999). Of advantage is that no interaction of FKBP and FRB can be detected in the absence of rapamycin. Rapamycin alone binds FRB only with moderate affinity ($K_D = 26 \mu\text{M}$), whereas the rapamycin-FKBP complex ($K_D = 0.2 \text{ nM}$) binds FRB with high affinity ($K_D = 12 \text{ nM}$), rendering the dimerization nearly irreversible (Banaszynski et al., 2005). To avoid toxic effects of rapamycin a derivative called rapalog combined with a modified FRB (termed FRB*) can be used (Faivre et al., 2006).

The FRB-FKBP system has been used for a broad variety of approaches. It has found much use in the field of signal transduction, for example the manipulation of G proteins, where it can be used to inducibly localize a constitutively active GTPase to the cell membrane to identify downstream effects as well as signaling networks (Castellano et al., 2000; Fivaz et al., 2008; Inoue et al., 2005; Inoue and Meyer, 2008; Komatsu et al., 2010). Furthermore it has been used to control the localization of Rab5a to study endosome maturation (Fili et al., 2006), to dissect the role of membrane lipids as second messengers, in endocytosis and receptor trafficking (Suh et al., 2006; Varnai et al., 2006; Zoncu et al., 2007), for protein degradation via a split ubiquitin (Pratt et al., 2007) and conditional protein splicing (Mootz and Muir, 2002; Schwartz et al., 2007).

The same technique was used by different groups, in an approach called anchor-away or knock sideways, to assess the function of proteins by inducibly removing them from their native site of localization. To achieve this, the protein of interest (POI) is fused to FKBP and the FRB domain is expressed as a second protein, containing a localization signal or an anchor protein (Haruki et al., 2008; Robinson et al., 2010). Addition of rapamycin then rapidly depletes the POI from its site of action and a phenotype is displayed if the protein was essential (Figure 8). Different localization signals were used for the FRB (the anchor), including transmembrane proteins, ribosomal proteins, Tom70p (mitochondrion), and nuclear localization signals, providing versatile options for targets from different cellular compartments (Geda et al., 2008; Haruki et al., 2008; Patury et al., 2009; Robinson et al., 2010; Xu et al., 2010).

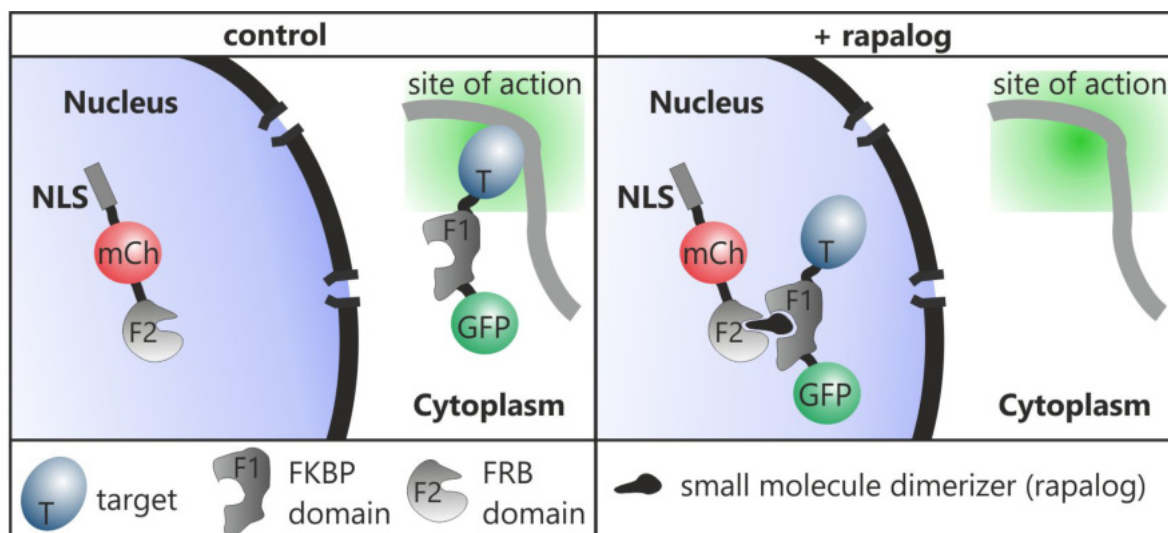


Figure 8 | Schematic of knock sideways. The protein of interest is tagged with FKBP and GFP and gets expressed under its endogenous promoter. A second protein, the so called mislocalizer, consisting of a localization signal, an FRB domain and an mCherry is expressed episomally. Addition of rapalog leads to dimerization of FKBP and FRB and subsequent the POI is relocalized to the nucleus. NLS, nuclear localization signal; mCh, mCherry; GFP, green fluorescence protein; F1, FKBP domain; F2, FRB domain; T, target protein

1.5 The superfamily of BTB and Kelch repeat proteins

The Kelch13 protein (726 AA) was shown to be a molecular marker for artemisinin resistance. Two functional domains were identified. A bric à brac 1, tramtrack, broad-complex (BTB) (also known as POZ) domain spanning AA 352 - 440 and six kelch motifs spanning AA 444 - 726 (Figure 9) (section 2.2.6). The kelch repeats form a 6 bladed kelch propeller. The N-terminal part of Kelch13 is *Plasmodium* specific, i.e., shows no homology to proteins in other organisms (reviewed in Tilley et al, 2016).

The superfamily of BTB proteins is divided into 3 subgroups: KLHL, KBTBD and KLHDC that can be distinguished in the number and type of their domains. KLHL proteins contain 5-6 Kelch repeats and one BTB/POZ domain and one BACK (BTB and C-terminal Kelch) domain. KBTBD proteins contain one BTB/POZ domain, in some cases one BACK domain and 2-4 Kelch repeats. KLHDC contain 3-7 Kelch repeats and usually no BTB/POZ or BACK domain (Dhanao et al., 2013). Thus, Kelch13 likely represents a member of KLHDC proteins.

The BTB/POZ domain was shown to be important for protein binding or homodimerization (Bardwell and Treisman, 1994; Perez-Torrado et al., 2006) and amongst others plays a role in gating of ion-channels (Kreusch et al., 1998; Minor et al., 2000), cytoskeletal regulation (Kang et al., 2004; Ziegelbauer et al., 2001) and transcriptional repression (Melnick et al., 2000). The BACK domain plays a role in the binding of ubiquitin E3 ligases. In this domain configuration, the Kelch domain would be the adapter for the substrate of the E3 ligase (Furukawa et al., 2003).

Kelch domain containing proteins have functional roles in numerous cellular processes as actin cytoskeleton regulation (Soltysik-Espanola et al., 1999), regulation of stress response (Itoh et al., 1999), control of G-proteins (Harashima and Heitman, 2002) and glucose metabolism (Murzin, 1992).

The Kelch13 protein was suggested to interact with an E3 ligase and indicated to have a similar role as the human stress response regulating protein KEAP1 as none of the other 6 Kelch repeat containing proteins in *P. falciparum* possesses a BTB/POZ domain (Ariey et al., 2014; Mbengue et al., 2015a; Tilley et al., 2016). However, as has been noted in a recent publication, *Pf*Kelch13 does not contain a BACK domain, indicating that it is potentially not interacting with an E3 ligase (Tilley et al., 2016). The identification of Kelch13 interaction partners could clarify this point and may be a next step to shed light on the cellular process the Kelch13 protein is involved in.

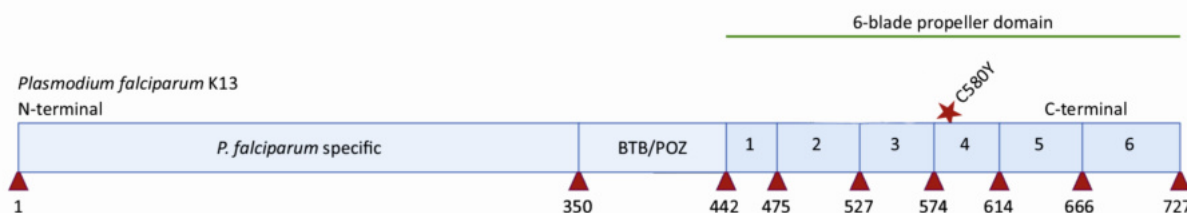


Figure 9 | Diagram of *Pf*Kelch13. Red triangles mark the indicated amino acid positions. Domains are annotated, the Kelch propeller consists of 6 Kelch repeats. Red asterisk shows the most common mutation conferring artemisinin resistance. (modified from Tilley et al., 2016)

1.6 Aims of the thesis

A lot of the *P. falciparum* specific biology remains elusive as the current tools to analyze the large number of genes of unknown function have limitations. Most of the strategies to achieve this are time consuming and complex, hampering the progress in identifying new essential genes. Hence, new methods are needed to unravel the biology of this important pathogen.

This work aims at identifying new parasite specific essential genes by developing and establishing new methods that allow the genomic manipulation of the parasite as well as the functional analysis of proteins. For this, a new method for the genomic manipulation of the parasite genome that showed promising initial results in our laboratory will be tested. In addition, this method for the genomic manipulation will be exploited to establish conditional gene and protein inactivation systems in *P. falciparum* to study essential parasite targets. Finally this will be further combined with BioID to add the interactome to the functional data. Specifically, these methods will be used to study new unknown parasite targets as well as specific targets of high interest such as the artemisinin resistance protein Kelch13.

2 Material and Methods

2.1 Material

2.1.1 Bacterial and *Plasmodium* strains

<i>Escherichia coli</i> XL-10 Gold	<i>Tet^r Δ(mcrA)183 Δ(mcrCB-hsdSMRmrr) 173 endA1 supE44 thi-1 recA1 gyrA96 relA1 lac Hte [F'proAB lacI^q Z ΔM15 Tn10 (Tet^r) Amy Cam^r]</i>
<i>Plasmodium falciparum</i> 3D7	Clone of NF54 isolate (MRA-1000) from a malaria patient near the Amsterdam airport (Walliker et al., 1987)

2.1.2 Chemicals

Acetic acid	Roth, Karlsruhe
Acrylamide/Bisacrylamide solution (40 %)	Roth, Karlsruhe
Agar LB (Lennox)	Roth, Karlsruhe
Agarose	Invitrogen
AlbumaxII	Gibco, Life Technologies, USA
Albumin bovine Fraction V (BSA)	Biomol, Hamburg
Ammonium persulfate (APS)	Applichem, Darmstadt
Ampicillin	Roche, Mannheim
Bacto™ yeast extract	BD, USA
Bacto™ Pepton	BD, USA
Biotin	Sigma, Steinheim
Blasticidin S	Invitrogen, Karlsruhe
Bromophenol blue	Merck, Darmstadt
Calcium chloride (CaCl ₂)	Sigma, Steinheim
Desoxynucleotides (dNTPs)	Thermo Scientific

4',6-diamidino-2-phenylindole (DAPI)	Roche, Mannheim
Dihydroartemisinin (DHA)	Adipogen, Switzerland
Dihydroethidium (DHE)	Cayman, Ann Arbor, USA
Dimethyl sulfoxide (DMSO)	Sigma-Aldrich, Steinheim
Dipotassium phosphate	Roth, Karlsruhe
Disodium phosphate	Roth, Karlsruhe
1,4,-dithiothreitol (DTT)	Roche, Mannheim
DSM1	BEI resources
Dulbecco's Phosphate Buffered Saline (DPBS)	Pan Biotech, Aidenbach
Ethanol	Merck, Darmstadt
Ethidium bromide	Sigma Aldrich, Steinheim
Ethylenediaminetetraacetic acid (EDTA)	Biomol, Hamburg
Ethylene glycol tetraacetic acid (EGTA)	Biomol, Hamburg
G418 disulfate salt	Sigma Aldrich, Steinheim
Gentamycin	Ratiopharm, Ulm
Giemsa's azure, eosin, methylene blue solution	Merck, Darmstadt
D-Glucose	Merck, Darmstadt
Glutardialdehyd (25 %)	Roth, Karlsruhe
Glycerol	Merck, Darmstadt
Glycine	Biomol, Hamburg
Hoechst33342	Cheomdex, Switzerland
(4-(2-Hydroxyethyl)-1-piperazineethanesulfonic acid) (HEPES)	Roche, Mannheim
Hydrochloric acid (HCl)	Merck, Darmstadt
Hypoxanthin	Biomol, Hamburg
Isopropanol	Roth, Karlsruhe
Magnesium chloride (MgCl ₂)	Merck, Darmstadt
Manganese(II) chloride (MnCl ₂)	Merck, Darmstadt
β-Mercaptoethanol	Merck, Darmstadt
Methanol	Roth, Karlsruhe
3-(N-morpholino)propansulfonic acid (MOPS)	Sigma Aldrich, Steinheim
Milk powder	Roth, Karlsruhe
Percoll	GE Healthcare, Sweden
Phenylmethylsulfonylfluorid (PMSF)	Sigma Aldrich, Steinheim
Potassium chloride	Merck, Darmstadt

Protease inhibitor cocktail ("Complete Mini")	Roche, Mannheim
Rapalog (A/C Heterodimerizer AP21967)	Clontech, Mountain View, USA
Rubidium chloride	Sigma Aldrich, Steinheim
RPMI (Roswell Park Memorial Institute)-Medium	Applichem, Darmstadt
Saponin	Sigma-Aldrich, Steinheim
Sodium acetate	Merck, Darmstadt
Sodium chloride	Gerbu, Gaiberg
Sodium bicarbonate	Sigma Aldrich, Steinheim
Sodium dodecyl sulfate (SDS)	Applichem, Darmstadt
Sodium dihydrogen phosphate	Roth, Karlsruhe
Sodium hydroxide	Merck, Darmstadt
Sorbitol	Sigma Aldrich, Steinheim
N, N, N, N-Tetramethylethylenediamin (TEMED)	Merck, Darmstadt
Tris base	Roth, Karlsruhe
Tris-EDTA (TE)	Invitrogen, Karlsruhe
Triton X-100	Biomol, Hamburg
Water for molecular biology (Ampuwa)	Fresenius Kabi, Bad Homburg
WR99210	Jacobus Pharmaceuticals, Washington, USA

2.1.3 DNA- and protein-ladders

GeneRuler™ 1 kbp ladder	Thermo Scientific, Schwerte
PageRuler™ prestained protein ladder	

2.1.4 Kits

QIAamp DNA Mini Kit	Qiagen, Hilden
QIAGEN Plasmid Midi Kit	
Western Blot ECL-Clarity Detection Kit	Bio-Rad, USA
Western Blot ECL-SuperSignal West Pico	Thermo Scientific, Schwerte
NucleoSpin. Plasmid	Macherey-Nagel, Düren
NucleoSpin. Extract II	

2.1.5 Labware and disposables

Labware and disposables	Specifications	Manufacturer
Conical falcon tubes	15 ml, 50 ml	Sarstedt, Nümbrecht
Cryotubes	1.6 ml	Sarstedt, Nümbrecht
Culture bottles	50 ml	Sarstedt, Nümbrecht
Disposable pipette tips	1-10/20-200/100-1000 μ l	Sarstedt, Nümbrecht
Eppendorf reaction tubes	1.5 / 2 ml	Sarstedt, Nümbrecht; Eppendorf, Hamburg
Filter tips	1-10/20-200/100-1000 μ l	Sarstedt, Nümbrecht
Flow cytometry tubes	55.1579	Sarstedt, Nümbrecht
Glass cover slips	24x65 mm thickness 0.13-0.16 mm	R. Langenbrinck, Emmerdingen
Glass slides		Engelbrecht, Edermünde
Gloves, latex		Kimtech Science EcoShield
Leukosilk tape		BSN medical
Multiply- μ Strip Pro 8-Strip PCR-reaction tube		Sarstedt, Nümbrecht
Nitrocellulose blotting membrane Protean	Amersham 0.45 μ m	GE Healthcare
One way canulas		Braun, Melsungen
One way syringe		Braun, Melsungen
Parafilm		Bemis, USA
Pasteur pipettes		Brand, Wertheim
Petri dishes	15x60mm / 14x90 mm	Sarstedt, Nümbrecht
Plastic pipettes	5 / 10/ 25 ml	Sarstedt, Nümbrecht
Scalpel		Braun, Melsungen
Sterile filter	0.22 μ m	Sarstedt, Nümbrecht
Transfection cuvettes	0.2 cm	Bio Rad, München

2.1.6 Solutions, buffers and media

2.1.6.1 Antibodies

Primary antibodies	anti-GFP (mouse)	1:1000 for Western blots	Roche, Mannheim
	anti-GFP (rabbit)	1:2000 for Western blots	Thermo Scientific
	anti-FKBP (rabbit)	1:2500 for Western blots	Abcam, Cambridge
Secondary antibodies	anti-mouse-HRP	1:3000 for Western blots	Dianova, Hamburg
	anti-rabbit-HRP	1:2500 for Western blots	Dianova, Hamburg
	Streptavidin-HRP	1:1000 for Western blots	Thermo Scientific
Antibody beads	coupled Streptavidin-Sepharose	For pulldown of proteins	GE Healthcare life science

2.1.6.2 Enzymes, oligonucleotides & polymerases

Enzymes	Restriction Enzymes	NEB, Ipswich, USA.
	T4 DNA-Ligase [3 U/ μ l]	NEB, Ipswich, USA.
Oligonucleotides	All oligonucleotides are listed in Appendix A	Sigma Aldrich, Steinheim
Polymerases	FirePol DNA Polymerase [5 U/ μ l]	Solis Biodyne, Taipei, Taiwan
	Phusion. High-Fidelity DNA Polymerase [2 U/ μ l]	NEB, Ipswich, USA
	Taq DNA Polymerase [5 U/ μ l]	NEB, Ipswich, USA

2.1.6.3 Fluorescence dyes

Hoechst 33342	Chemodex
Dihydroethidium	Cayman

DAPI | Roche

2.1.6.4 Solutions and buffers for biochemical experiments

SDS-PAGE and Western blot

10 x Running buffer	250 mM Tris base 1.92 M Glycine 1 % (w/v) SDS in dH ₂ O
Separating gel buffer	1.5 M Tris-HCl, pH 8.8 in dH ₂ O
Stacking gel buffer	1 M Tris-HCl, pH 6.8 in dH ₂ O
Separating gel (12 %)	2.1 ml dH ₂ O 1.25 ml running gel buffer 1.5 ml Acryl amide (40 %) 50 µl SDS (10 %) 50 µl APS (10 %) 2 µl TEMED
Stacking gel (5 %)	0.35 ml stacking gel buffer 2.17 ml dH ₂ O 375 µl Acryl amide (40 %) 30 µl SDS (10 %) 30 µl APS (10 %) 3 µl TEMED
Ammonium persulfate (APS)	10% (w/v) in dH ₂ O
6 x SDS sample buffer	375 mM tris HCl pH 6.8 12 % (w/v) SDS 60 % (v/v) Glycerol 0.6 M DTT 0.06 % (w/v) Bromophenol blue
10x Western blot transfer buffer	250 mM Tris-Base 1.92 M glycerol

	0.1 % (w/v) SDS in dH ₂ O
1x Western blot transfer buffer	10 % 10 x Western transfer buffer 20 % Methanol in dH ₂ O

2.1.6.5 Solutions and buffers for microbiologic culture

10x LB stock solution	10% NaCl 5% peptone 10% yeast extract in dH ₂ O, autoclaved
LB working solution	1% (w/v) NaCl 0.5% (w/v) peptone 1% (w/v) yeast extract in dH ₂ O
LB Agar plate solution	1.5% Agar-Agar 1x LB medium
Ampicillin stock solution	100 mg/ml in 70% ethanol
Glycerol freezing solution	50% (v/v) glycerol in 1x LB medium
TFBI buffer	30 mM acetic acid 50 nM MnCl ₂ 100 mM RbCl 10 mM CaCl ₂ 15 % (v/v) glycerol pH 5.8 (with 0.2 N Acetic acid) ad 500 ml H ₂ O
TFBII buffer	10 mM MOPS 75 mM CaCl ₂ 10 mM RbCl

15 % (v/v) glycerol
pH 7.0 (with NaOH)
ad 500 ml H₂O

2.1.6.6 Solutions and buffers for molecular biological experiments

Gibson assembly buffers

5x isothermal reaction buffer (6 ml)	3 ml 1 M Tris-HCl pH 7.5 150 µl 2 M MgCl ₂ 60 µl each of 100 mM dGTP/dATP/dTTP/dCTP 300 µl 1 M DTT 1.5 g PEG-8000 300 µl 100 nM NAD ad 6 ml dH ₂ O
Assembly master mixture (1.2 ml)	320 µl 5x isothermal reaction buffer 0.64 µl 10 U / µl T5 exonuclease 20 µl 2 U / µl Phusion DNA polymerase 160 µl 40 U / µl Taq DNA ligase ad 1.2 ml dH ₂ O

DNA gel electrophoresis

50x TAE	2 M Tris base 1 M Pure acetic acid 0.05 M EDTA pH 8,5
6x Loading buffer	40 % Glycerol (v/v) 2.5 % (w/v) Xylene cyanol 2.5 % (w/v) Bromophenol blue in dH ₂ O

DNA precipitation

Sodium acetate	3 M NaAc, pH 5.2
----------------	------------------

Tris-EDTA (TE) buffer	10 mM Tris-HCl pH 8,0 1 mM EDTA pH 8,0
-----------------------	--

2.1.6.7 Solutions and buffers for cell biologic experiments

P. falciparum in vitro culture

RPMI complete medium	1,587 % (w/v) RMPI 1640 12 mM NaHCO ₃ 6 mM D-Glucose 0.5 % (v/v) Albumax II 0.2 mM Hypoxanthine 0.4 mM Gentamycin pH 7.2 in dH ₂ O sterile filtered
Synchronization solution	5 % (w/v) D-Sorbitol in dH ₂ O sterile filtered
Parasite freezing solution (PFS)	4,2 % (w/v) D-Sorbitol 0,9 % (w/v) NaCl 28 % (v/v) Glycerol in dH ₂ O sterile filtered
Parasite thawing solution (PTS)	3,5 % (w/v) NaCl in dH ₂ O sterile filtered
Transfection buffer (Cytomix)	120 mM KCl 150 μM CaCl ₂ 2 mM EGTA 5 mM MgCl ₂ 10 mM K ₂ HPO ₄ / KH ₂ PO ₄ 25 mM Hepes pH 7.6

	<p>in dH₂O sterile filtered</p>
Amaxa transfection buffer	<p>90 mM NaPO₄ 5 mM KCl 0.15 mM CaCl₂ 50 mM HEPES pH7.3 in dH₂O sterile filtered</p>
WR99210 stock solution	<p>20 mM WR99210 in DMSO</p>
WR99210 working solution	<p>1:1000 dilution of stock solution in RPMI complete medium sterile filtered</p>
Blasticidin S (BSD) working solution	<p>5 mg/ml BSD in RPMI complete medium sterile filtered</p>
G418 working solution	<p>50 mg/ml in RPMI complete medium sterile filtered</p>
DSM1 stock solution (50x)	<p>187,5mM DSM1 in DMSO</p>
DSM1 working solution	<p>100 µl DSM1 stock solution ad 5 ml in 95% DMSO / 5% 1xPBS solution</p>
Human red blood cells	<p>Bloodgroup 0+, sterile concentrate, Blood bank Universitätsklinikum Eppendorf (UKE), Hamburg</p>
Percoll stock solution	<p>90 % (v/v) Percoll 10 % (v/v) 10x PBS</p>
60 % Percoll solution	<p>6.7 ml Percoll stock solution 3.3 ml RPMI complete medium</p>

	0.8 g Sorbitol sterile filtered
Parasite lysis buffer	4 % SDS 0.5 % Triton 0.5x PBS in dH ₂ O
DHE stock solution (10x)	5 mg DHE in 1ml DMSO
DHE working solution (1x)	0.5 mg DHE in 1ml DMSO
Ho33342 stock solution (10x)	4.5 mg Ho33342 in 1ml DMSO
Ho33342 working solution (1x)	0.45 mg Ho33342 in 1ml DMSO
FC stop solution	0.5 µl Glutaraldehyde (25%) in 40ml RPMI complete medium
Rapalog (AP21967) stock solution	500 mM in ethanol
Rapalog working solution	1:20 dilution of stock solution in RPMI complete medium

2.1.7 Technical devices

Device	Specifications	Distributor
Agarose gel chamber	Sub Cell GT basic	Bio-Rad, München
Analytical Balance	870	Kern
Blot device		
Gel holder cassettes		
Foam pads	Mini Protean Tetra	Bio-Rad, München
Electrode assembly		
Cooling unit		

	Megafuge 1.0R	Heraeus, Hannover
	J2 HS Ultracentrifuge	Beckmann Coulter, Krefeld
Centrifuge	Rotor JA-12	
	Avanti J-26S XP	Beckmann Coulter, Krefeld
	Rotor JA-14	
Table centrifuge	Eppendorf 5415 D	Eppendorf, Hamburg
Casting stand		
Casting Plates	Mini Protean	Bio-Rad, München
Casting frames		
Developer	ChemiDoc XRS+	Bio-Rad, München
Electrophoresis chamber	Mini Protean 67s	Bio-Rad, München
	Gene Pulser XCell	Bio-Rad, München
Electroporator	Nucleofector II AAD-1001N	Amaxa Biosystems, Germany
Flow cytometer	LSR II	BD Instruments, USA
Ice machine	EF 156 easy fit	Scotsmann, Venon Hills, USA
Bacterial incubator	Thermo function line	Hereaus, Hannover
<i>P. falciparum</i> cell culture incubator	Heratherm IGS400	Thermo Scientific, Langensfeld
Shaking Incubator	Max Q4000	Barnstead, Iowa, USA
Light microscope	Axio Lab A1	Zeiss, Jena
Fluorescence microscope	Axioscope 1	Zeiss, Jena
Microscope digital camera	Orca C4742-95	Hamamatsu Phototonics K.K.
Microwave	Micro 750W	Whirlpool, China
Laboratory scale	Atilon	Acculab Sartorius, Göttingen
PCR mastercycler	epgradient	Eppendorf, Hamburg
pH-meter	SevenEasy	Mettler-Toledo, Gießen
Pipettes	1-10/200/1000 µl	Gilson, Middleton, USA
Pipettor	Pipetboy acu	IBS, USA
	EV31	Consort, Belgium
Power supply	Power source 300 V	VWR, Taiwan
Roller mixer	STR6	Stuart
	Sterile Gard III Advance	Baker, Stanford, USA
Sterile laminar flow bench	Safe 2020	Thermo Scientific, Pinneberg
Thermoblock	Thermomixer compact	Eppendorf, Hamburg
Ultrapure water purification	Milli Q	Millipore

system

UV transilluminator	PHEROlum 289	Biotec Fischer, Reiskirchen
Vacuum pump	BVC Contorl	Vacuubrand, Deutschland
Vortexer	VF2	Jank & Kunkel IKA Labortechnik
Waterbath	1083	GFL, Burgwedel

2.2 Methods

2.2.1 Microbiological Methods

2.2.1.1 Production of competent *E. coli*

For increased plasmid uptake of *E. coli* the bacteria were rendered chemo-competent by using the rubidium chloride method resulting in a decreased stability of the bacterial cell wall (Hanahan, 1983). 20 ml LB medium were inoculated with a glycerol stock of the *E. coli* XL10 Gold strain and incubated overnight at 37 °C with vigorous shaking. 10 ml of this culture were transferred into a 1 L Erlenmeyer flask containing 200 ml LB medium and incubated at 37 °C with vigorous shaking until an OD₆₀₀ of 0.5-0.6 was reached. Following the harvest of the bacteria by centrifugation at 2400 x g at 4 °C for 20 min the pellet was re-suspended in 60 ml TFBI buffer. After 10 min of incubation on ice with subsequent centrifugation at 2400 x g at 4 °C the pellet was suspended in 8 ml TFBII buffer and aliquoted (100 µl) in 1.5 ml reaction tubes. The suspension was stored at -80 °C.

2.2.1.2 Transfection of chemo-competent *E. coli*

A 100 µl aliquot of the chemo-competent *E. coli* was thawed on ice. Plasmid DNA (10 µl of a ligation or 0.5 µl of a sequenced construct) was added and incubated on ice for 20min. Suspension was heat shocked at 42 °C for 30 sec and put back into ice for 1min. The complete suspension was plated on LB agar plates containing an ampicillin selection marker. The plate was incubated over night at 37 °C.

2.2.1.3 Overnight culture of *E. coli* for subsequent plasmid DNA preparation

Bacteria from an agar plate or glycerol stock were inoculated in LB medium overnight at 37 °C with vigorous shaking. For plasmid mini preparations 2 ml of LB medium in a 2 ml reaction tube were used, whereas for plasmid midi preparations 180 ml of LB medium in a 1 L Erlenmeyer flask was used.

2.2.1.4 Freezing of *E. coli*

500 μ l of *E. coli* overnight culture was mixed with 500 μ l of glycerol in a 1.5 ml reaction tube and stored at -80 °C.

2.2.2 Molecular biological methods

2.2.2.1 Polymerase chain reaction

Two different DNA polymerases were used, for amplification of a PCR product (preparative PCR) with subsequent cloning a Phusion – high fidelity polymerase (NEB), whereas for analytical PCRs (colony screens for identification of positive clones after transformation or integration checks) a FIREPol polymerase (Solis Biodyne) was used. The setting for the PCR cycler can be found below, for certain constructs settings (annealing or elongation temperature) were adjusted.

Preparative PCR		Analytical PCR	
5x Phusion buffer	10 μ l	10x FIREPol buffer	1 μ l
dNTP's	5 μ l	dNTP's	1 μ l
Primer fw	1 μ l	MgCl ₂	0.8 μ l
Primer rv	1 μ l	Primer fw	0.5 μ l
Phusion DNA polymerase	0.3 μ l	Primer rv	0.5 μ l
Template	0.3 μ l	FIREPol DNA polymerase	0.05 μ l
dH ₂ O	ad 50 μ l	Template	0.03 μ l
		dH ₂ O	ad 10 μ l

PCR program

Phase	Temperature	Time	
Denaturation	95 °C	4 min	
25-30 cycles	Denaturation	95 °C	30 sec
	Annealing	42-60 °C	30 sec
	Elongation	52-72 °C	x min

x depends on the expected size in of the PCR product and was usually 1min per 1000 bp.

2.2.2.2 PCR-product purification

For purification of PCR products and of digested DNA fragments and vectors the Nucleo Spin Gel and PCR Clean-up kit was used as instructed in the manual. Elution volume was 50 μ l of elution buffer AE.

2.2.2.3 DNA restriction digest

Preparative digests were performed for digestion of PCR products and vectors by using different DNA restriction enzymes to create sticky ends for cloning of plasmids. DpnI was used if the template of the PCR reaction was a plasmid with methylated DNA. Analytical digests were performed of mini and midi DNA preparations to exclude recombination and confirm correct insertion of PCR products into the plasmid. They were performed in 10 μ l volume including 0.3 μ l of each restriction enzyme and 1.2 μ l of plasmid DNA.

The incubation time for preparative digests was 3h, for analytical digests 1h, each at 37 °C.

Preparative PCR

10x NEB cut smart	5 μ l
Each restriction enzyme	1 μ l
DNA (PCR/plasmid)	20/10 μ l
dH ₂ O	ad 50 μ l

2.2.2.4 DNA ligation

Digested PCR products and plasmids were ligated using the T4 ligase. The ligation mix was incubated for 30-60min at room temperature.

Ligation

10x T4 ligase buffer	1 μ l
T4 ligase	1 μ l
plasmid DNA	0.5 μ l
PCR product	7.5 μ l

2.2.2.5 DNA ligation by Gibson assembly

An alternative method for ligation of insert and vector is the Gibson DNA assembly (Gibson et al., 2009). It allows the ligation of up to 6 different inserts. The ligation does not require sticky ends, thus only DpnI digest of the insert is necessary for depletion of methylated templates. For efficient ligation an overlap of 15-35 bp into the vector sequence is needed. The ligation mix was incubated at 50 °C for 60 min.

Gibson assembly

Assembly master mixture	7.5 μ l
vector DNA	1 μ l
PCR product	0.5 μ l
dH ₂ O	Ad 10 μ l

2.2.2.6 Plasmid preparation

Plasmids of 2 ml mini preparations from overnight cultures were purified with the Nucleo Spin Plasmid Kit, whereas midi preparations were purified with the QIAfilter Plasmid Midi Kit according to the manufacturer's protocols.

2.2.2.7 Sequencing of plasmid DNA

To confirm that the insert does not contain mutations it was sequenced. 3 µl of plasmid DNA from a mini preparation were mixed with 3 µl (10 mM) of a sequencing primer and dH₂O was added to 15 µl. Sequencing was performed by SeqLab (Sequence Laboratories Göttingen).

2.2.2.8 Agarose gel electrophoresis

DNA fragments can be separated according to their size in an electric field due to their negatively charged phosphate backbone by agarose gel electrophoresis. Usually gels of 1% agarose were used in this study. The agarose was mixed with 1x TAE buffer and dissolved by boiling using the microwave. Ethidium bromide was added to a final concentration of 1 µg/ml. The solution was transferred into a gel tray and combs were placed to create pockets for loading DNA samples.

After solidification of the gel it was transferred to the electrophoresis chamber that was filled with 1x TAE. The DNA samples were prepared by adding 6x DNA loading buffer and loaded into the pockets. Electrophoresis was performed at a voltage of 150 V for 15-25 min. Size of DNA fragments was analyzed under UV lights by comparison to a DNA ladder.

2.2.2.9 Isolation of genomic DNA

In order to confirm integration of a plasmid into the correct genomic locus of *P. falciparum* the genomic DNA was isolated and used for PCR analysis. 5 ml of a parasite culture at 1-10 % parasitemia was harvested and centrifuged at 1800 x g for 2 minutes. Purification of DNA from blood was performed by using the QIAamp DNA Mini Kit according to the manufacturer's protocol.

2.2.3 Biochemical methods

2.2.3.1 Discontinuous SDS-PAGE

Proteins can be separated according to their molecular weight by using the discontinuous SDS-polyacrylamide gel electrophoresis (PAGE) (Laemmli, 1970). SDS binds to the proteins, unfolds them and consequently leads to a negative net charge of the proteins irrespectively of their original charge. The SDS sample buffer contains DTT, in order to reduce the number of disulfide bonds of the protein and thus contributes to denaturation of the protein. For separation of proteins 12% polyacrylamide gels were used. The protein samples were heat denaturized (85 °C, 5-10 minutes) and loaded into pockets of the gel along with a prestained protein marker containing proteins of defined sizes. Separation of proteins was performed by applying 150 V for 60-90 minutes.

2.2.3.2 Western blotting

Proteins were identified by the transfer of the proteins, which were separated by SDS-PAGE, onto a nitrocellulose membrane using the wet transfer method. The polyacrylamide gel was layered on a nitrocellulose membrane and compressed on both sides by 3 Whatman filter papers and a sponge. After transfer into the Biorad tank blotting chamber the polyacrylamide gel faced the cathode whereas the nitrocellulose membrane faced the anode. The chamber was filled with transfer buffer and the transfer was carried out by applying a voltage of 100 V for 1 hour at 4 °C. Alternatively, the transfer can be realized overnight by applying 15 V at 4 °C.

2.2.3.3 Immunodetection of proteins

In order to detect the proteins on the nitrocellulose membrane the membrane was blocked with 5% milk powder in 1x PBS for 60 minutes at room temperature, at first. Due to proteins of the milk powder unspecific binding sites on the membrane were occupied. Afterwards the primary antibody (see 2.1.6.1) diluted in 5% milk powder in 1x PBS as added and incubated over night at 4 °C. After washing the membrane 4-6 times with 1x PBS the secondary antibody conjugated to horse radish peroxidase (HRP) (see 2.1.6.1), diluted in 5% milk powder in 1x PBS was added and incubated for 1 hour at room temperature. Again, the membrane was washed 4-6 times with 1x PBS and transferred onto a transparent film. The ECL-Western blot detection Kit was used in order to visualize the oxidation of luminol leading to chemiluminiscence by x-ray screen. The exposure times were 2-60 minutes.

2.2.3.4 Pull down of biotinylated proteins

For the pulldown of biotinylated proteins exclusively tubes and pipette tips from the company Eppendorf were used. All solutions were prepared in Ampuwa dH₂O and each step was performed on ice.

The unsynchronized parasites were harvested and lysed in saponin from 150 ml of culture as described in 2.2.4.7. The pellet in the 2ml reaction tube was washed twice with 1.5 ml DPBS (3 minutes at 16000 x g) and then dissolved by addition of 2 ml of lysis buffer (50 mM Tris-HCl pH 7.5, 500 mM NaCl, 1% Triton + freshly added 1 mM DTT, 2x protease inhibitor cocktail, 1 mM PMSF). The lysates were stored at -80 °C (until further use). For efficient extraction of proteins the lysates were thawed and frozen two times in total. After centrifugation at 16000 x g for 10 minutes the supernatant was transferred to a 15 ml reaction tube and diluted in a ratio of 1:2 with 50 mM TrisHCl pH 7.5, 2x protease inhibitor cocktail, 1 mM PMSF. 50 µl of Streptavidin-Sepharose (equilibrated in 50 mM TrisHCL pH 7.5) were added and incubated overnight at 4 °C by overhead rotation. After the incubation the 15 ml tubes were centrifuged at 1600 x g for 1 minute. Then the pellet was transferred into a 1.5 ml reaction tube. The sepharose pellet was washed 2 times in 500 µl cold lysis buffer, once in 500 µl cold dH₂O (Ampuwa), two times in 500 µl cold TrisHCl pH 7.5 and three times in 500 µl cold 100 mM TEAB. After each washing step the tube was incubated for 2 minutes on a roller mixer at room temperature and centrifuged at 1600 x g for 1 minute. After the final washing step the pellet was suspended in 50µl of 100mM TEAB. It was shipped on ice for mass spectrometry analysis. The analysis was performed by Wietike Hoijmakers (Radboud Institute, Netherlands).

2.2.4 Cell biological methods

2.2.4.1 Continuous culture of *P. falciparum* (Trager and Jensen, 1976)

The *P. falciparum* cultures were grown in 15x60 mm and 14x90 mm petri dishes at 37 °C. The atmosphere was adjusted to high carbon dioxide and low oxygen levels (5% O₂, 5% CO₂, 90% N₂). The petri dishes contained 5 ml (15x60 mm) or 10 ml (14x90 mm) RPMI complete medium and bloodgroup 0+ erythrocytes to a hematocrit of 5%. Transgenic parasites were selected with 4nM WR99210, 2 µg/ml blasticidin S or 0.9 µM DSM1. Parasites were cultured at a parasitemia of 0.1 – 5% whereas the RPMI medium was changed every other day. In parasite cultures with higher parasitemias medium was change daily.

2.2.4.2 Selection for transgenic parasites by SLI

For selection of integrants by using SLI, cultures containing an episomal plasmid selected with WR were adjusted to 2-5% parasitemia and G418 was added to a final concentration of 400 µg/ml (Birnbbaum et al., 2017). For yDHODH as SLI resistance marker a concentration of 1.5 µM DSM1 was applied. WR99210 selection pressure was discarded. The cultures were fed daily until day 7 after start

of G418 selection pressure and from then on fed every other day. On day 16 of selection parasites were taken off drug. The cultures were maintained for a maximum of 60 days, if no parasites were obtained until then the culture was discarded.

Giemsa smears were made on day 2 of selection pressure to inspect if the parasite culture. If parasitemia was above 10% 7 ml RPMI medium were added into the 15x60 mm petri dish.

Of reappearing parasite DNA was isolated with the QIAamp DNA Mini Kit and PCRs across the integration junctions and testing for leftover unmodified locus (to exclude the presence of wild type or incorrect integrants) were performed. If wild type locus was detected the parasite cultures were treated with WR99210 for 2 cycles and DNA isolation with subsequent integration check was performed again. For essentiality checks with SLI-TGD, three parallel 5-ml cultures containing the episomal plasmid were placed under G418 selection (400 µg/ml). If no correct integration occurred on two occasions (with a total of six cultures), the target was assumed to be essential (Birnbaum et al., 2017). The cultures were maintained for a maximum of 60 days, if no parasites were obtained until then the culture was discarded.

2.2.4.3 *P. falciparum* cryo-stabilates

For long term storage parasites can be stored as cryo-stabilates in liquid nitrogen. Parasites of a ring stage parasitemia of 3-10% in 15x60 mm or 14x90 mm petri dishes were transferred into a 15 ml tube and centrifuged at 1800 x g for 2 minutes. The pellet was resuspended in 1 ml parasite freezing solution, transferred into cyro tubes and frozen in liquid nitrogen.

Cryo-stabilates were thawed at 37 °C, transferred into a 15 ml tube and centrifuged at 1800 x g for 2 minutes. The supernatant was discarded and the pellet was resuspended in 1 ml parasite thawing solution. After another centrifugation step at 1800 x g for 2 minutes supernatant was discarded and the pellet was washed with RPMI medium. Supernatant was discarded again and the pellet was transferred into a 15x60 mm petri dish and resuspended in 5 ml RPMI medium. Hematocrit was adjusted to approximately 5 %. The selection drug was added after 24h.

2.2.4.4 Blood smears and Giemsa staining

The parasitemia can be assessed by Giemsa stained blood smears of parasite cultures. About 0.8 µl of the red blood cell of the culture are transferred to a glass slide. The blood droplet is smeared by using another glass slide, resulting in a monolayer of RBCs. The blood on the slide is fixated in methanol for 30 seconds and the stained with Giemsa staining solution for 10 minutes at least. After the staining period the slide is rinsed with water, thus removing the superfluous Giemsa staining solution. The smears were analyzed by an optical light microscope.

2.2.4.5 Synchronization of parasites

For synchronization of parasites the culture was transferred to a 15 ml tube and centrifuged at 1800 x g for 3 minutes. The supernatant was discarded, whereas the pellet was resuspended in 5% D-sorbitol in

dH₂O and incubated at 37 °C for at least 10 minutes. After the incubation period the tube was centrifuged at 1800 x g for 3 minutes and washed with RPMI medium. After another centrifugation step at 1800 x g for 3 minutes the pellet was transferred into a petri dish containing RPMI medium. A culture was obtained containing only parasites at 0-18 hours post infection.

2.2.4.6 Transfection of *P. falciparum*

Transfection of *P. falciparum* parasites is performed by electroporation. For the BioRad system 100 µg of DNA from a DNA midi preparation were precipitated in a 1.5 ml reaction tube by addition of 1/10 volume of 3 M sodium acetate and 3 volumes of ethanol abs. The tube was centrifuged at 16000 x g for 10 minutes. The supernatant was discarded and the pellet was washed with ethanol 70%. After another centrifugation step at 16000 x g for 5 minutes the pellet was air dried. The pellet was solved in 15 µl TE buffer and 385 µl cytomix.

250 µl of RBCs containing synchronized ring stage parasites at a parasitemia of 5-10% were pelleted. The dissolved DNA was mixed with the infected RBCs and transferred to an electroporation cuvette (2 mm, BioRad). For the electroporation the Gene Pulser Xcell (350V, 50 µF, ∞ Ω) was utilized. Subsequent, the parasites were transferred to a 15x60 mm petri dish containing RPMI. After 24h the selection drug was added. For the first 5 days RPMI medium was changed daily, afterwards every other day.

For transfection with the Amaxa system only 50 µg of DNA are needed and electroporation is performed with late schizonts. Precipitation was performed as described above. The dried pellet is dissolved in 10 µl TE buffer and 90 µl of Amaxa transfection solution is added. Schizonts were isolated by adding 4 ml 60% percoll solution into a 15 ml tube and layering 5-10 ml infected RBCs above. After centrifugation at 2000 x g for 6 minutes the schizonts can be seen in a layer clearly distinguishable from the RBC pellet at to bottom of the tube. The schizonts were extracted by using a pipette, washed one in RPMI and centrifuged at 1800 x g for 4 minutes. The supernatant was discarded. 10-15 µl of the schizont pellet were mixed with the DNA solution and tranferred into an electroporation cuvette (2 mm, BioRad). For electroporation the Nucleofector II AAD-1001N, program U-033 was utilized. After electroporation the parasites were transferred into a 2 ml reaction tube containing 300 µl uninfected RBC and 100 µl RPMI medium prewarmed to 37 °C. The 2 ml reaction tube was incubated for 15-60 minutes at 37 °C under rigorous shaking. Then the parasites were transferred into a 15x60 mm petri dish containing RPMI medium. The section drug was added 24 h later. For the first 5 days RPMI medium was changed daily, afterwards every other day.

2.2.4.7 Isolation of parasites by saponin lysis

Parasite can be isolated from RBC by lysing in low concentration of saponin. Saponin lyses the RBC and the parasitophorous vacuole membrane but the parasite plasma membrane remains intact. 5-10 ml of parasite culture at a parasitemia of 5-10% were harvested (1800 x g, 3 minutes) and supernatant was discarded. The pellet was dissolved in 10 pellet volumes of ice-cold 0.03% (w/v) saponin in PBS and

incubated on ice for 5-20 minutes. The mixture was transferred into a 2 ml reaction tube and centrifuged for 5 min at 16000 x g. Washing of the pellet and subsequent centrifugation was repeated until no hemoglobin was visible in the supernatant any more. 1 μ l of 25x protease inhibitor cocktail was added to the pellet and then the pellet was resuspended in 25-150 μ l SDS-lysis buffer. Until further use the pellet was stored at -20 °C.

After thawing the pellet was centrifuged for 5 min at 16000 x g. Then the supernatant was transferred to a 1.5 ml reaction tube and 6x SDS sample buffer was added. The solution was incubated for 5 min at 85 °C. 8 μ l per sample were usually used for SDS-PAGE.

2.2.4.8 Biotin labeling of parasite proteins

For mass spectrometry analysis of biotin labeled proteins larger amounts of parasites need to be harvested. The GFP-2xFKBP-Kelch13 cell line was transfected with BirA*-FRB-FRB-mCherry. The parasite cell line was cultured in 3x 50 ml culture flasks (Sarstedt) totaling 150 ml of culture. 24 h before harvesting of the parasites each 50 ml flask was splitted into two and the hematocrit was adjusted to 5%. Biotin was added to the RPMI medium. 3 of the flasks were the control whereas to the 3 corresponding flasks rapalog (AP21967) was added to a final concentration of 250 nM, inducing the dimerization. Harvesting of the cells was performed at a parasitemia of 5-10 %. The parasites were saponin lysed and used for mass spectrometry analysis (2.2.3.4). For assessment of biotinylation by SDS-PAGE and Western blot 10 ml of a parasite culture at 5-10% parasitemia was used.

2.2.4.9 Induction of knock sideways and diCre

For the knock sideways and diCre based excision integrants were transfected with a plasmid leading to the episomal expression of a mislocalizer or the diCre construct. The plasmids were selected with 2 μ g/ml blasticidin S or 0.9 μ M DSM1. In case of blasticidin S the concentration was increased to 9-18 μ M to increase expression (Epp et al., 2008). For the KS or diCre-based gene excision, the culture was split into two dishes. To one of these dishes, rapalog (AP21967, Clontech) was added to a final concentration of 250 nM and the other dish served as a control. Mislocalization, as compared with the control culture, was verified microscopically after 16 h if not indicated otherwise (Birnbaum et al., 2017).

Rapalog was stored at -20 °C as a 500 mM stock in ethanol, and working stocks were kept as 1:20 dilutions in RPMI at 4 °C for a maximum of 3 weeks.

2.2.4.10 Flow cytometry growth assay

For growth assays the parasitemia of the culture was adjusted to 0.1 % and split into a control 2 ml dish and a rapalog treated (250 nM) 2 ml dish. The parasitemia was measured every 24h for 5 consecutive days. Medium was changed daily. The flow cytometry assay is based on a previous publication (Malleret et al., 2011), but the used of PBS in the publication is substituted by RPMI.

For assessment of the parasitemia the parasites need be stained. For staining 80 μ l of RPMI medium were added to a 1.5 ml Eppendorf tube. This was followed by addition of 1 μ l of HO33342 working solution and 1 μ l of DHE working solution to the 1.5 ml tube.

The parasite culture to be analyzed was thoroughly resuspend by pipetting up and down and transfer 20 μ l into a flow cytometry tube. 80 μ l of RPMI dye mix were added to the flow cytometry tube with the parasite suspension and mix by shaking the tube. The mix was incubated for 20 min in the dark and afterwards 400 μ l of FC stop solution as added. Then the parasitemia was measured to second decimal place using the LSRII, with the gating as described (Malleret et al., 2011).

2.2.5 Microscopy

2.2.5.1 Live cell and fluorescence microscopy

Live cell and fluorescence microscopy images were taken with a Zeiss AxioImager M1 equipped with a Hamamatsu Orca C4742-95 camera and the Zeiss Axiovision software (v 4.7). A 100 \times /1.4–numerical aperture lens or a 63 \times /1.4–numerical aperture lens was used. The images were processed in Corel Photo paint (Birnbaum et al., 2017).

500 μ l of a parasite culture were transferred into a 1.5 ml reaction tube and incubated with DAPI (final concentration of 1 μ g/ml) for 10 minutes at room temperature. The tube was centrifuged at 6000 x g for 1 minute and the supernatant was discarded up to a 1:1 ration of pellet and supernatant. The suspension RBCs were resuspended and 4 μ l were transferred to a glass slide and covered with a coverslip.

2.2.6 Software and bioinformatic tools

ApE plasmid editor	http://biologylabs.utah.edu/jorgensen/wayned/ape/
Corel DRAW X6 v16.4.1.1281	Corel Corporation
Corel PhotoPaint X6 v16.4.1.1281	Corel Corporation
Image Lab v 5.2.1	BioRad Laboratories
GraphPad Prism 5	GraphPad Software
FACS Diva v 6.1.3	BD Bioscience
BLAST	https://blast.ncbi.nlm.nih.gov/Blast.cgi
HHpred	https://toolkit.tuebingen.mpg.de/#/tools/hhpred
PlasmoDB	Plasmodb.org
Compute pI/Mw	http://web.expasy.org/compute_pi/
MotifScan	http://myhits.isb-sib.ch/cgi-bin/motif_scan
AxioVision v 4.7	Carl Zeiss Microscopy
Microsoft Office v 14.0.7182.5000	Microsoft Corporation

BLAST, HHpred and MotifScan were used as bioinformatical tools to identify homologies to proteins of known function or domain of known function for all targets in this study. If possible the species *Plasmodium* was excluded from the search. For BLAST search the expected threshold in the category algorithm parameters was changed from 10 to 1000.

3 Results

3.1 Robust and efficient selection of genomic integration

Integration of plasmids into the genome is crucial for functional studies and to localize endogenous proteins by tagging. However, integration into the genome of *P. falciparum* is difficult to obtain. This is due to the low frequency of homologous crossover recombination of episomal plasmids and the fact that selection of cells with an integrated plasmid (henceforth ‘integrants’) is a passive process (see 1.3) (de Koning-Ward et al., 2015; Webster and McFadden, 2014). To overcome this issue and to enable the analysis of new parasite specific proteins, a method termed ‘selection linked integration’ (SLI) was developed. In a promoter-less construct a targeting region of 500-1000bp length for the gene of interest was linked to a sequence coding for a skip peptide (Straimer et al., 2012; Szymczak et al., 2004), followed by an additional positive selection marker (Figure 10). The plasmid is transfected and episomally maintained by a DHFR selection cassette (Fidock and Wellem, 1997). Plasmids usually integrate by single crossover integration. Upon integration of the SLI plasmid, the complete GOI as well as the additional positive selection marker (SLI resistance marker) become expressed under the promoter of the GOI. However, due to the skip peptide, (which leads to skipping of the protein translation) the GOI and the additional resistance are not attached but are expressed as separate polypeptides. Consequently, parasites carrying the integration can be selected by addition of the selection drug corresponding to the SLI resistance marker.

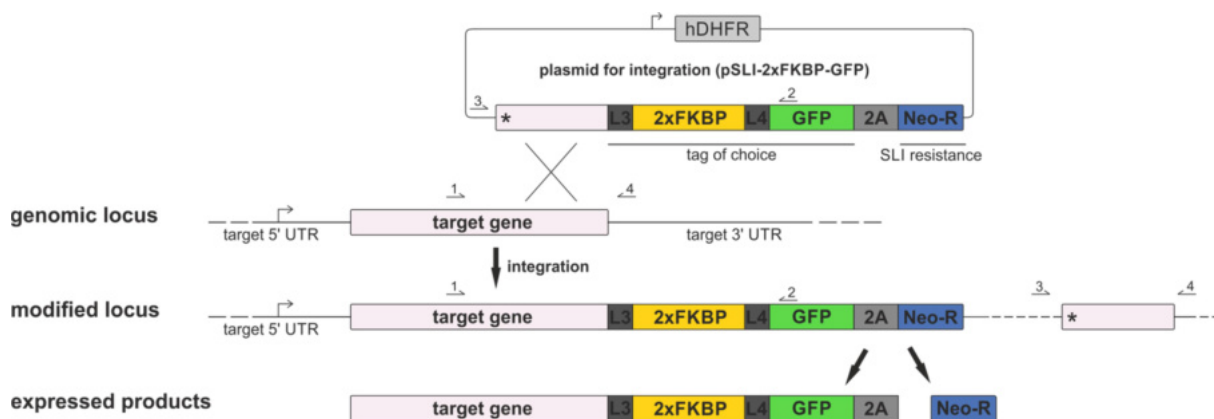


Figure 10 | Schematic of selection linked integration strategy and knock sideways. Usually the last 500-1000 bp (without the stop codon) are inserted into the pSLI-2xFKBP-GFP plasmid as homology region for integration into the target's genomic locus. Upon integration the SLI resistance marker is expressed under the target's endogenous promoter. Due to the 2A skip peptide, the SLI resistance is independent of tagged target protein. L3 and L4 are linkers (Varnai et al., 2006); 2A, T2A skip peptide; Asterisk, stop codon; Neo-R, neomycin phosphotransferase II gene.

To test this approach, the neomycin phosphotransferase II was used as SLI resistance marker (Mamoun et al., 1999a; Wang et al., 2002). Endogenous genes were tagged with the green fluorescence protein (GFP) coding sequence, enabling localization of the native protein.

Four random genes were chosen in a first trial. After transfection, parasites carrying the episomal plasmid were obtained. The SLI approach for integration was then compared to conventional drug cycling. All integration cell lines using the SLI approach could be obtained in 5 to 18 days. An integration check by PCR showed that all integrations occurred in the correct genomic locus and wild type locus was non-detectable. In contrast, using the conventional cycling approach only two cell lines could be obtained after 59 days. The two remaining cell lines were not obtained after 90 days of cycling (Figure 11a,c). The quantitative skipping of the Neo selection marker from the protein of interest for the SLI integrants was verified by western blot (Figure 11b).

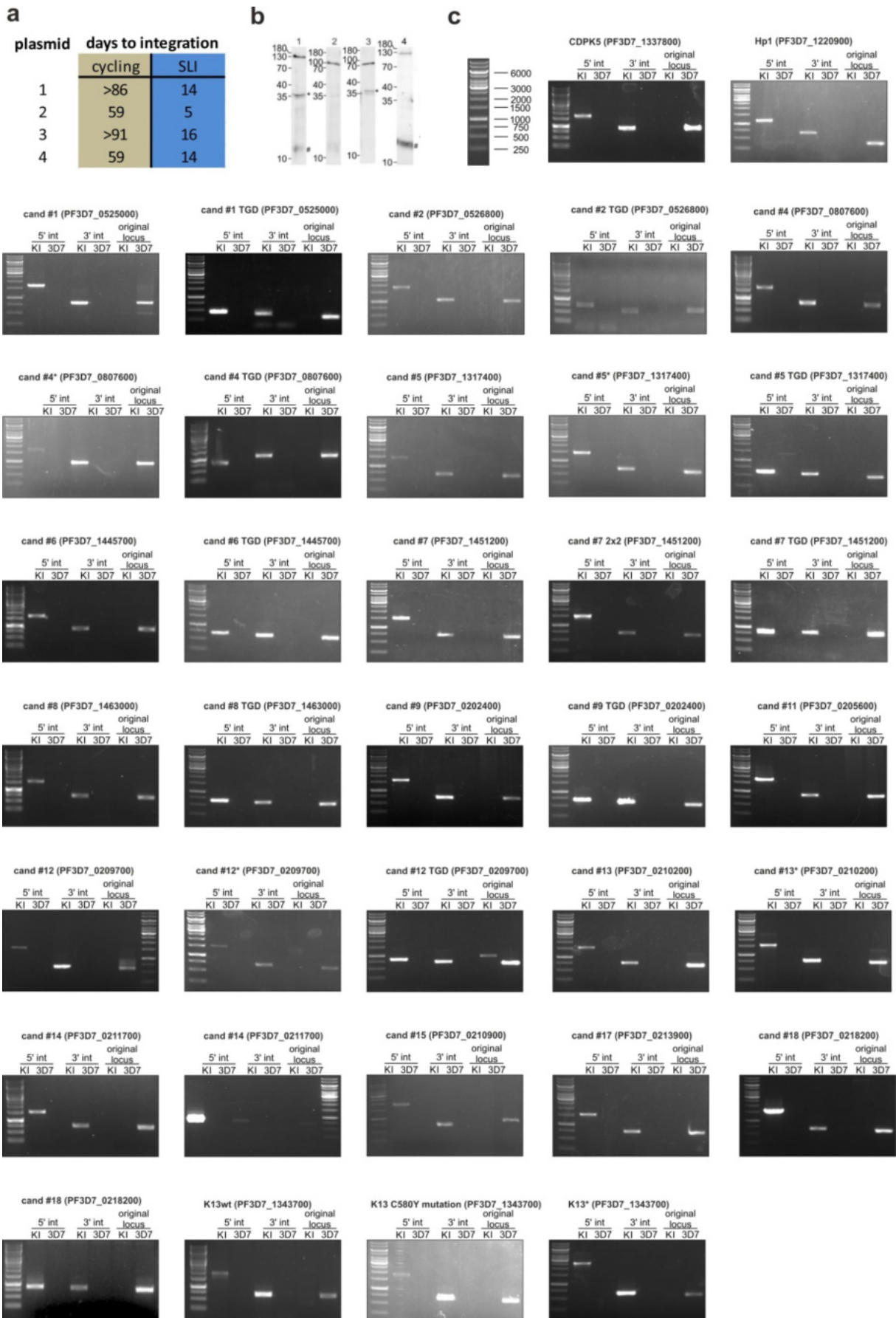


Figure 11 | Comparison of conventional drug cycling with SLI and integration check PCRs. **a)** The graph displays the time required for plasmid integration with cycling and SLI method. Plasmids 1,2,3 and 4 are candidates #1, #2, #8 and CDPK5 from Figure 11c, respectively. **b)** Immunoblots of cell lines corresponding to a) show quantitative skipping. The expected sizes for skipped proteins are 137, 100, 93 and 123 kDa, respectively. Non-skipping of proteins would add 29 kDa for the neomycin phosphotransferase II. Detection was done using anti-GFP. Asterisk, frequently observed GFP degradation product; hash, antibody independent ECL signal of hemoglobin. **c)** Integration checks for all integration cell lines generated by SLI. Agarose gels with PCR products from genomic DNA of each parasite line indicated above the gels. The primers used are indicated in figure 7. Primers spanning the 5' prime junction were 1+2, spanning the 3' junction were 3+4 and correspond to 5' int and 3' int, respectively. Absence of original locus, showing that no parasite with wild type locus remained, was confirmed by combination of primers 1+4. Sizes of the marker bands are shown in the first panel from the top. KI, knock-in cell line; 3D7, wild type parasite line; TDG, targeted gene disruption using SLI; Asterisks indicate fusion of gene using pSLI-sandwich vector (including a 2xFKBP-GFP-2xFKBP tag), all other cell lines carry 2xFKBP-GFP tag.

3.2 Functional analysis of essential *P. falciparum* proteins with knock sideways

Current tools for functional analysis of *P. falciparum* genes or their gene products are currently limited. For this reason a method called knock sideways (KS) (see 1.4) (Geda et al., 2008; Haruki et al., 2008; Patury et al., 2009; Robinson et al., 2010; Xu et al., 2010) was chosen as a new mean to functionally analyze proteins in *P. falciparum*. This method acts rapidly and circumvents problems that arise from genetic manipulation of the target.

3.2.1 Proof of principle

In a proof of principal experiment the knock sideways method was tested with two known essential proteins, CKDP5 (Figure 12) (Dvorin et al., 2010) and heterochromatin protein 1 (HP1) (Brancucci et al., 2014). SLI was used for endogenous tagging of the GOI with two *fkbp* domains (*2xfkbp*) and *gfp*, and correct integration was confirmed by PCR (Figure 11c). CDPK5-2xFKPB-GFP localized throughout the cytoplasm with multiple small foci. HP1-2xFKPB-GFP localized, as published, at the nucleus and accumulates in foci (Figure 13) (Brancucci et al., 2014).

The general approach of the KS system was to mislocalize POIs to a distinct cellular compartment when FKBP and FRB* are dimerized by the small molecule rapalog. For nuclear proteins, such as HP1, mislocalization to the parasite's plasma membrane was chosen. For proteins residing in the cytosol, such as CDPK5, relocation into the nucleus was chosen. The mislocalizers consisted of the corresponding localization signal fused to an FRB* domain and mCherry. Localization signals were a nuclear localization signal (NLS) (Kalderon et al., 1984) or a signal, consisting of the 13 N-terminal AA of the human Lyn kinase, targeting the construct to the parasite plasma membrane (PPM) (Toth et al., 2012; Varnai et al., 2007).

Addition of rapalog led to efficient relocation of CDPK5 from the cytosol into the nucleus, whereas 95.8% (s.d. 3.7%, n=11 cells) of HP1 translocated to the plasma membrane (Figure 12a, 13a). In a flow cytometry (FC) based growth assay, starting from an identical culture that was grown with or without rapalog (KS and control, respectively), the effect on the parasite proliferation were assessed

over the course of 5 days. Confirming the published data, a growth defect was observed for the KS with each of the two proteins (Figure 12b, 13b).

A more detailed analysis with synchronized parasites showed that KS of CDPK5 led to an arrest in the schizont stage, verifying the published egress phenotype (Figure 12c) (Dvorin et al., 2010). Mislocalization of HP1 led to a dramatic increase in the production of gametocytes 8 days after addition of rapalog, which is in line with a previous publication (Figure 13c) (Brancucci et al., 2014). Altogether this shows that the method is applicable to study essential proteins in *P. falciparum*.

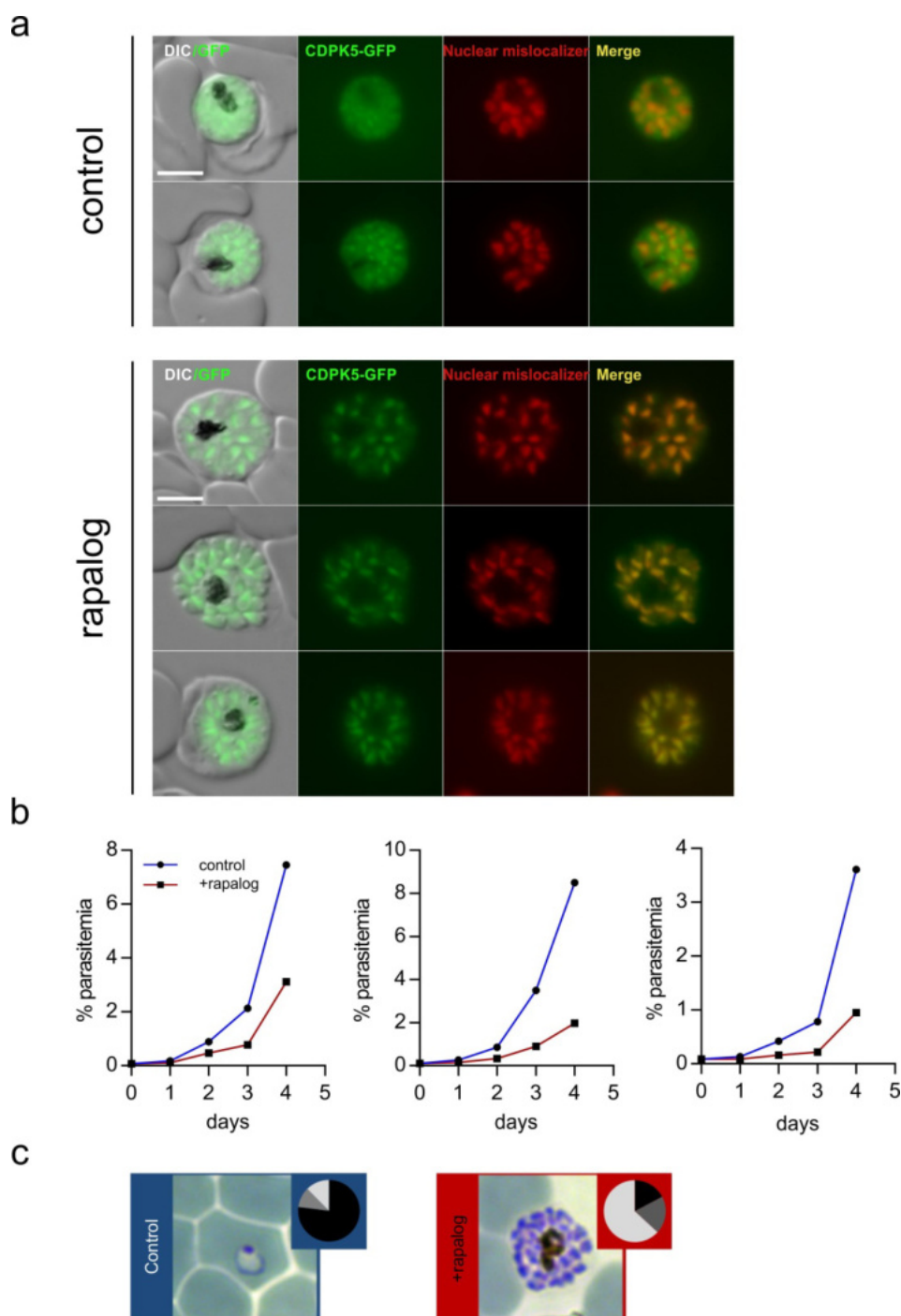


Figure 12 | Localization and KS of CDPK5. **a)** Knock-in cell line of CDPK5-2xFKBP-GFP transfected with a plasmid promoting episomal expression of the 1xNLS-FRB-mCherry mislocalizer. Live cell fluorescence images of control and rapalog-treated

cells were taken after 16h. **b)** Flow cytometry (FC) growth curves from 3 independent experiments, each going over 5 days. Parasitemia of the cultures show development of the control and the cell grown in the presence of 250nM rapalog **c)** Giemsa smears of control and rapalog treated, tightly synchronized parasites 48 hours post infection (hpi). Pie charts display quantification of different stages (number of stages compared to all parasites) observed at this time point (rings, black; trophozoites, dark grey; schizonts, light gray; n = 226 and 255 cells for control and +rapalog, respectively). One representative of 3 independent experiments is shown. DIC, differential interference contrast; merge, merged GFP and mCherry signal. Scale bars, 5 μ m.

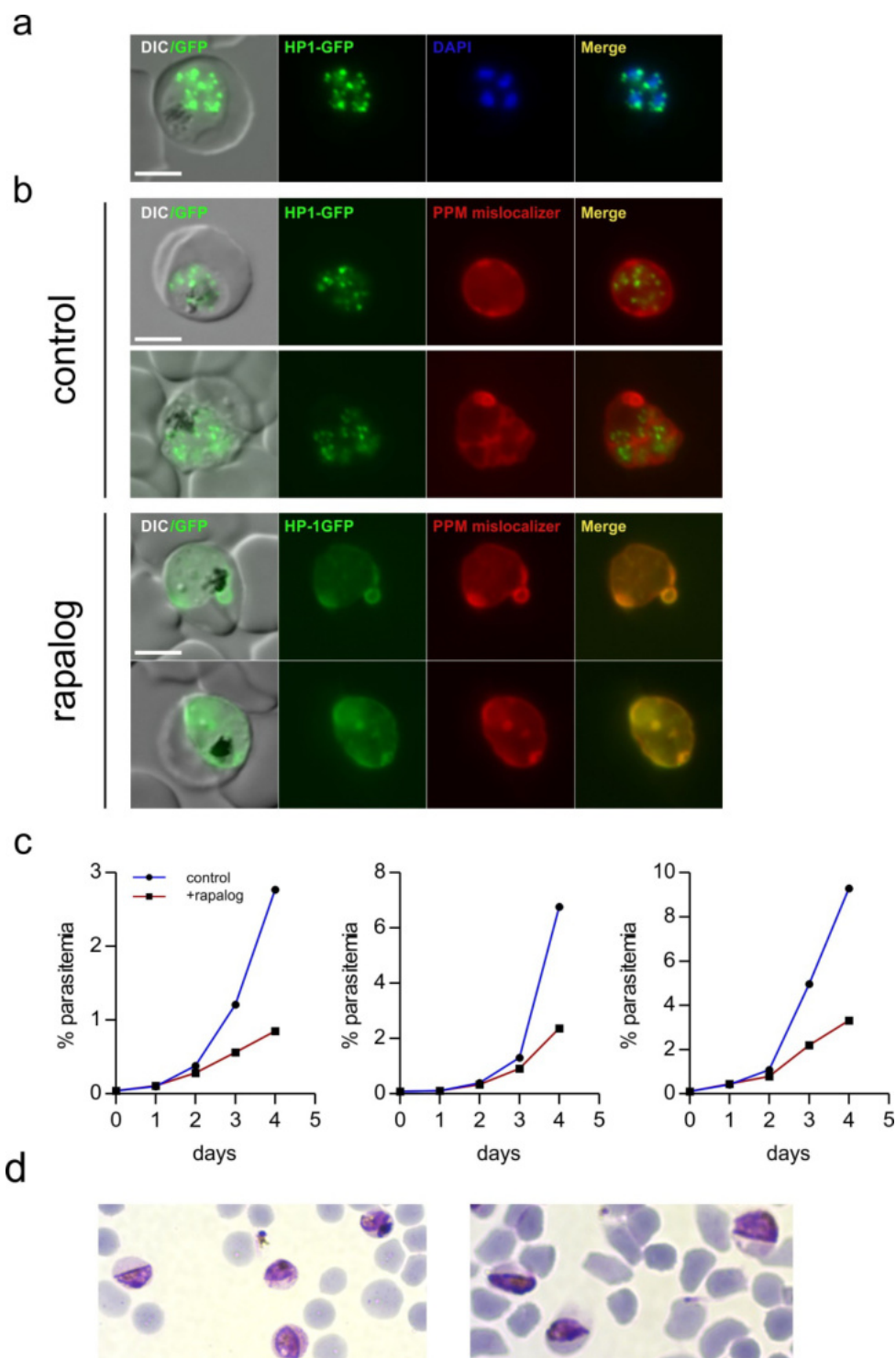


Figure 13 | Localization and KS of HP1. a,b) Live cell images of knock-in cell line of HP1. **a)** Cell line stained with DAPI nuclear stain. **b)** Knock-in cell line of HP1-2xFKPB-GFP transfected with an episomal plasmid leading to the expression of the

PPM mislocalizer, images of control and rapalog-treated cells were taken after 16h. **c)** FC growth curves from 3 independent experiments, each going over 5 days showing development of control and cell line treated with 250nM rapalog **d)** Giemsa smears show gametocytes on day 8 after start of KS experiment (one representative of two independent experiments is shown). DIC, differential interference contrast; merge, merged GFP and mCherry signal. Scale bars, 5µm.

3.2.2 Screen of proteins of unknown function by KS and targeted gene disruption

To demonstrate versatility, efficiency and robustness of our system we chose 8 arbitrary genes from different chromosomes and, in a more systematic approach, 10 genes from chromosome 2. All selected targets fulfilled the following two selection requirements: first, lack of any homology outside the Apicomplexans and second, lack of a signal peptide or transmembrane domain(s), as proteins entering the secretory pathway are not expected to be accessible for functional analysis by KS. Knock in cell lines were created tagging the POI C-terminally with 2xFKBP-GFP to localize them and functionally analyze them using KS. As for some proteins the level of mislocalization was not compelling, the number of FKBP domains on the target was increased (see below). To this end, the plasmid pSLI sandwich, resulting in fusion of the target with 2xFKBP-GFP-2xFKBP was used for integration into the genome. The localization and KS results with the here selected 18 targets are shown in the following sections (3.2.2.1-3.2.2.18).

To complement the data of the knock sideways, which acts on protein level, SLI was used to attempt disruption of each of the 18 target genes (Figure 14). This method is based on the traditionally used passively enriched targeted gene disruption (TGD) (see 1.3.2) but with SLI these parasites can be selected (termed SLI-TGD), dramatically increasing the speed to obtain integrants and potentially also enabling the selection of mildly disadvantageous disruptions. If parasites with the disrupted gene can be selected with SLI, the gene must be dispensable for parasite survival. Conversely, if no correct integrants could be selected with SLI on at least 6 occasions, the gene was considered as important for parasite survival (henceforth termed ‘essential’, see also 4.1.2). The SLI-TGD for the 18 selected candidates is presented together with the localization and KS studies (section 3.2.2.1-3.2.2.18).

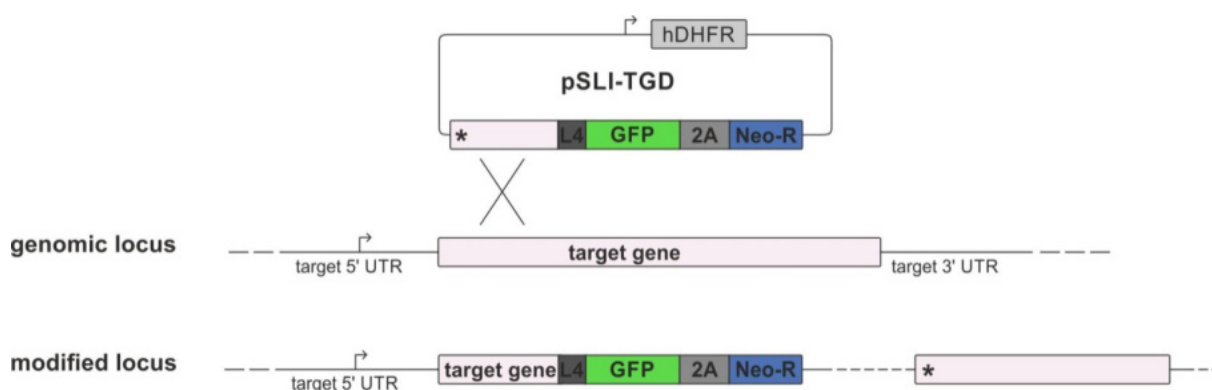


Figure 14 | Schematic of SLI targeted gene disruption (SLI-TGD) strategy. The gene is targeted in the front and can be selected via SLI. Asterisk, stop codon; arrows, promoters; 2A, T2A skip peptide

3.2.2.1 Candidate 1: PF3D7_0525000

The protein PF3D7_0525000 encompasses 704 AA and has a predicted zinc-finger domain spanning AA 24-121 (see section 2.2.6) for prediction tools used for all candidates). Correct integration of the plasmid into the genome, leading to endogenous fusion of candidate 1 with the sequence coding for 2xFKBP-GFP, was confirmed by PCR (Figure 11c). The protein was expressed from early trophozoite stage to schizont stage (Figure 15a,b) and localizes in the parasites cytosol.

A nuclear mislocalizer was chosen for knock sideways. Upon addition of rapalogs, to induce the knock sideways, the candidate was efficiently mislocalized to the nucleus (Figure 15b). A growth assay over 5 days was carried out but showed no difference in parasites where candidate 1 had been knocked aside compared to the control (Figure 15c). In agreement with a dispensable role of this protein for blood stage parasite development, the corresponding gene was successfully disrupted using SLI-TGD (Figure 11c). Hence the protein is considered not to be essential in the asexual blood stages.

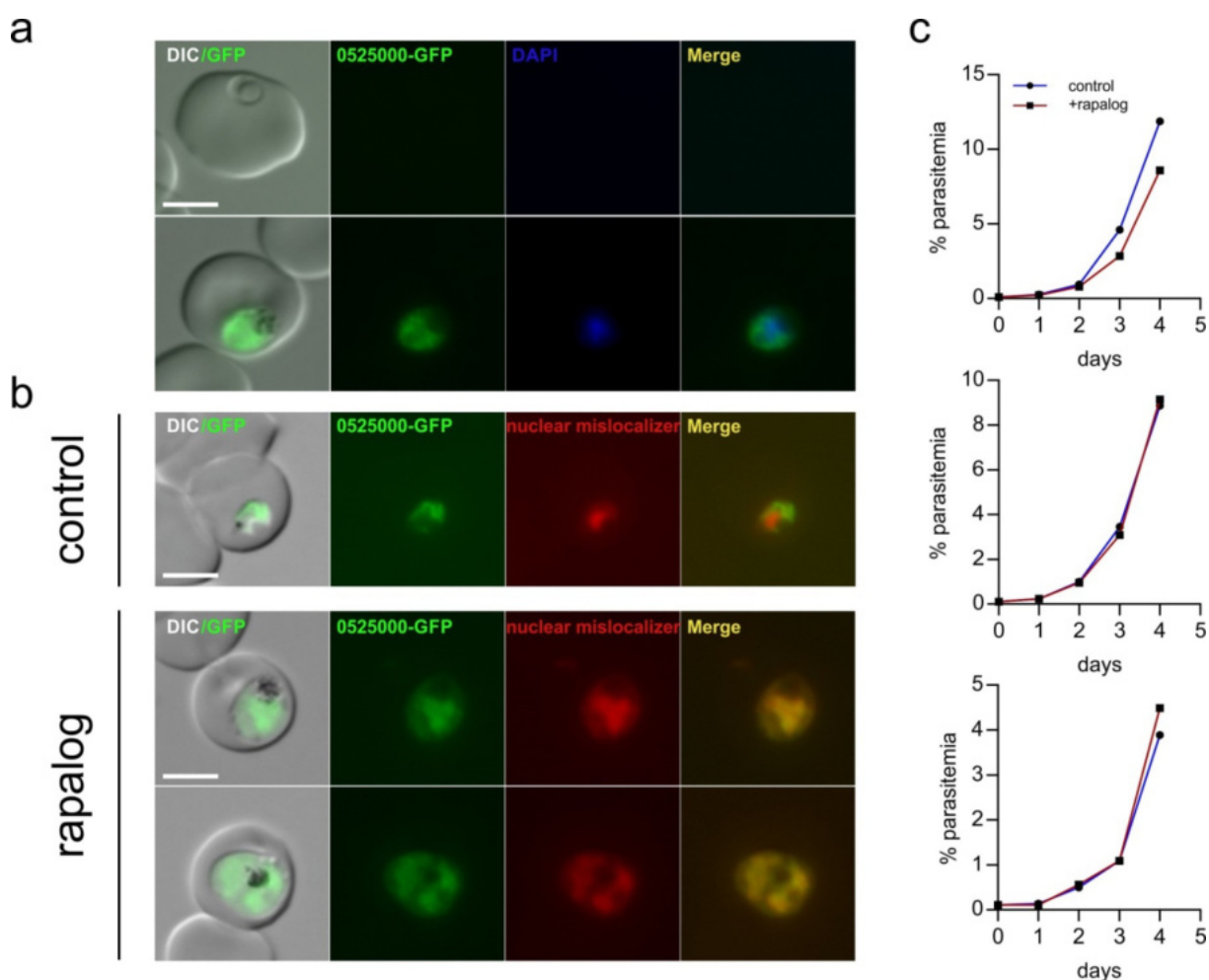


Figure 15 | Localization and KS of PF3D7_0525000 (candidate 1). **a,b)** Live cell images of knock-in cell line of candidate 1 fused to 2xFKBP-GFP. **a)** Cell line stained with DAPI nuclear stain. **b)** Knock-in cell line transfected with an episomally expressed 1xNLS-FRB-mCherry mislocalizer. Live cell fluorescence images of control and rapalogs-treated cells were taken after 16h. **c)** FC growth curves over the course of 5 days from 3 independent experiments showing development of control and culture grown in the presence with 250 nM rapalogs. Scale bars, 5 μ m.

3.2.2.2 Candidate 2: PF3D7_0526800

Candidate 2 (PF3D7_0526800) is a protein of 368 AA. No similarities to known domains could be identified (see section 2.2.6). Correct integration of the plasmid into the genome, leading to endogenous fusion of candidate 2 with the sequence coding for 2xFKBP-GFP, was confirmed by PCR (Figure 11c). The protein was expressed from ring stage to schizont stage and localized to the nucleus, as evident from the co-localization of the GFP signal with the DAPI nuclear stain (Figure 16a,b). For candidate 2 the PPM mislocalizer was chosen. After addition of rapalogs to induce the knock sideways a majority of the candidate 2 protein population was relocalized to the PPM (Figure 16b). In trophozoites a small amount of the target protein remained in the nucleus (Figure 16b). As evident in a representative fluorescence picture (Figure 16b, lower panel), mislocalization in the schizont stage was less efficient. A growth assay over 5 days was carried out but showed no difference in parasites where candidate 2 had been knocked aside compared to the control. As the gene encoding candidate 2 could be disrupted with SLI-TGD (Figure 11c), this protein was considered not to be essential for the parasite in asexual blood stages.

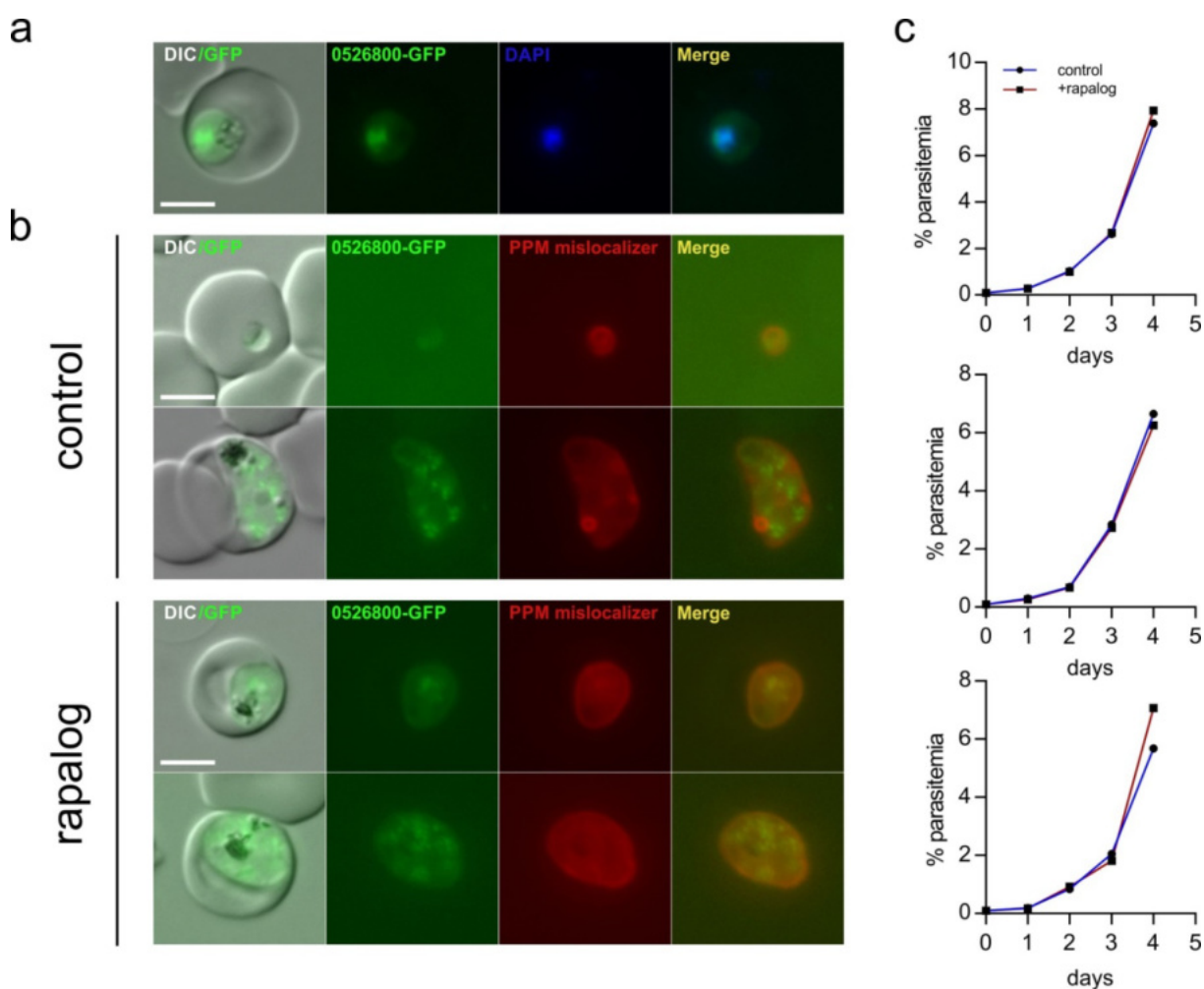


Figure 16 | Localization and KS of PF3D7_0526800 (candidate 2). **a,b)** Live cell images of knock-in cell line of candidate 2 fused to 2xFKBP-GFP. **a)** Cell line stained with DAPI nuclear stain. **b)** Knock-in cell line transfected with an episomally expressed Lyn-FRB-mCherry mislocalizer. Live cell fluorescence images of control and rapalogs-treated cells were taken after

16h. c) FC growth curves over the course of 5 days from 3 independent experiments showing development of control and culture treated with 250 nM rapalog. Scale bars, 5 μ m.

3.2.2.3 Candidate 3: PF3D7_0720600

Candidate 3 (PF3D7_0720600) is a protein of 236 AA. No similarities to other proteins or domains could be found by *in silico* analysis and no other homologies to known domains or other proteins outside the Apicomplexa were identified (see section 2.2.6). As Rab proteins have clear signatory domains and are generally highly conserved (reviewed in (Stenmark, 2009)), and no such homology was found with this candidate, the relevance of its resemblance to the leishmania Rab6-like protein is unclear. All attempts to C-terminally tag candidate 3 in the genome failed. In line with this, no disruption of this gene by SLI-TGD could be obtained (Table 2). PF3D7_0720600 is therefore potentially essential to the *P. falciparum* parasite, but could not be localized nor functionally analyzed.

3.2.2.4 Candidate 4: PF3D7_0807600

PF3D7_0807600 is a protein of 1334 AA. No similarities to other proteins or domains could be found by *in silico* analysis (see section 2.2.6). Correct integration of the plasmid into the genome, leading to endogenous fusion of candidate 4 with the sequence coding for 2xFKBP-GFP, was confirmed by PCR (Figure 11c). The protein was expressed throughout all asexual stages (Figure 17a,b). It localizes to the nucleus and the nuclear periphery. First attempts to mislocalize the protein to the PPM using KS were not successful. Hence, the gene was fused to a *2xfkbp-gfp-2xfkbp* tag via SLI and the correct integration was confirmed (Figure 11c). KS analysis of this cell line resulted in complete mislocalization to the parasite plasma membrane (Figure 17b). No difference in growth was observed in growth assays when the protein was knocked aside and compared to control cells (Figure 17c). A SLI-TGD was obtained for this cell line (Figure 11c). Taken together, these results indicate that this candidate is not essential for the growth of parasite blood stages.

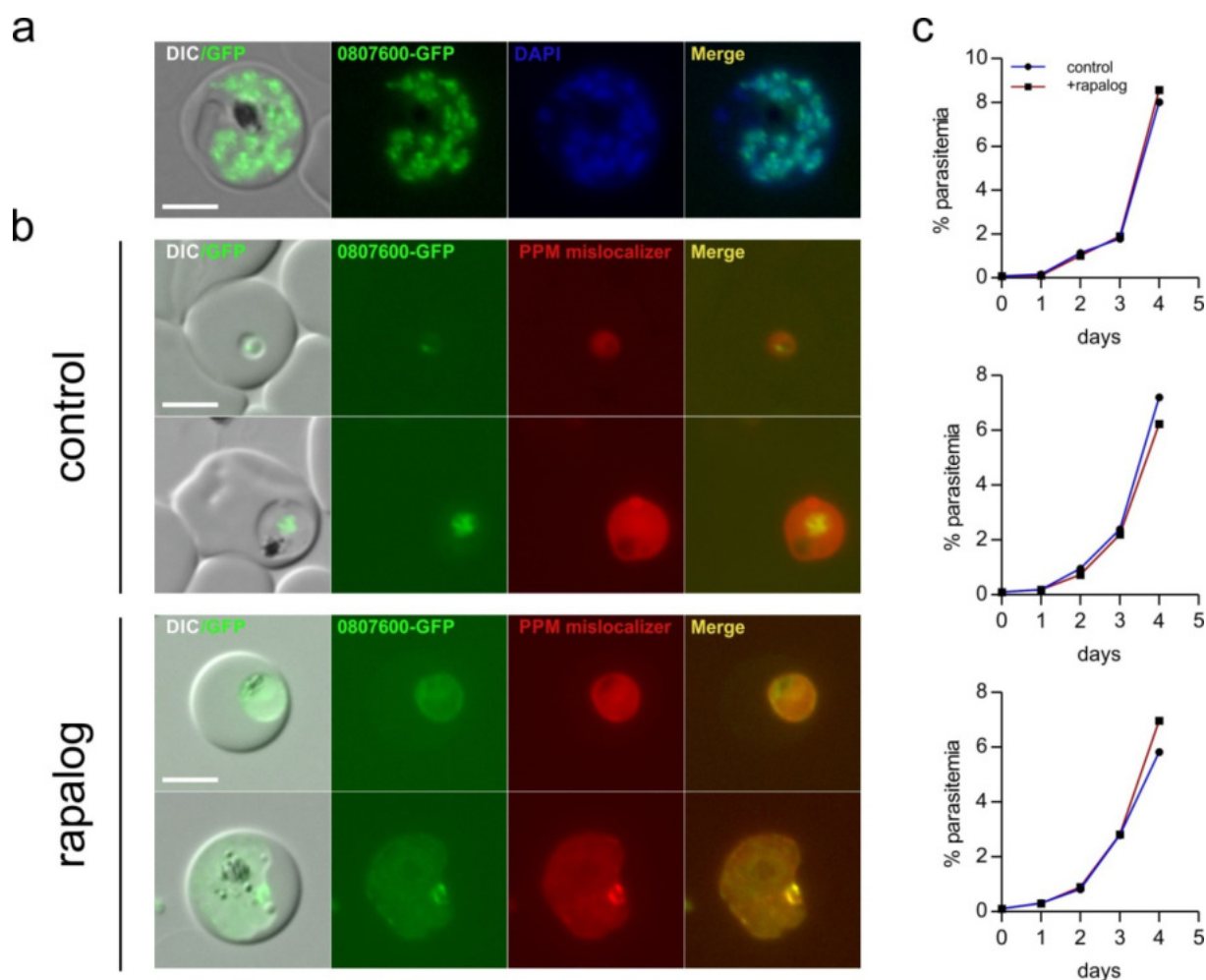


Figure 17 | Localization and KS of PF3D7_0807600 (candidate 4). **a,b)** Live cell images of knock-in cell line of candidate 4 fused to 2xFKBP-GFP-2xFKBP. **a)** Cell line stained with DAPI nuclear stain. **b)** Knock-in cell line transfected with an episomally expressed Lyn-FRB-mCherry mislocalizer. Live cell fluorescence images of control and rapalog-treated cells were taken after 16h. **c)** FC growth curves over the course of 5 days from 3 independent experiments showing development of control and culture treated with 250 nM rapalog. Scale bars, 5 μ m.

3.2.2.5 Candidate 5: PF3D7_1317400

For PF3D7_1317400 a zinc finger domain was found spanning AA 1-30 (see section 2.2.6). The protein consists of 205AA. Integration of the SLI plasmid for FKBP-GFP tagging was confirmed by PCR (Figure 11c). Candidate 5 was expressed from trophozoite stage to schizont stage (Figure 18a,b). As evident from the GFP signal that co-localized with DAPI stain, the protein was found in the nucleus. A PPM mislocalizer was chosen for the KS analysis. Similar to Candidate 4, the improved version of the KS vector was used, as fusion of the Protein to 2xFKBP-GFP showed insufficient effect upon addition of rapalog (Figure 18b). The KS of the protein fused to 2xFKBP-GFP -2xFKBP was efficient, even though traces of the protein remained in the nucleus after mislocalization. The growth assay of the cells grown with rapalog showed no difference to the control (Figure 18c). In agreement, a disruption of the gene encoding candidate 5 was obtained using SLI-TGD (Figure 11c). This indicates that candidate 5 is not essential for the asexual blood stage of the parasite.

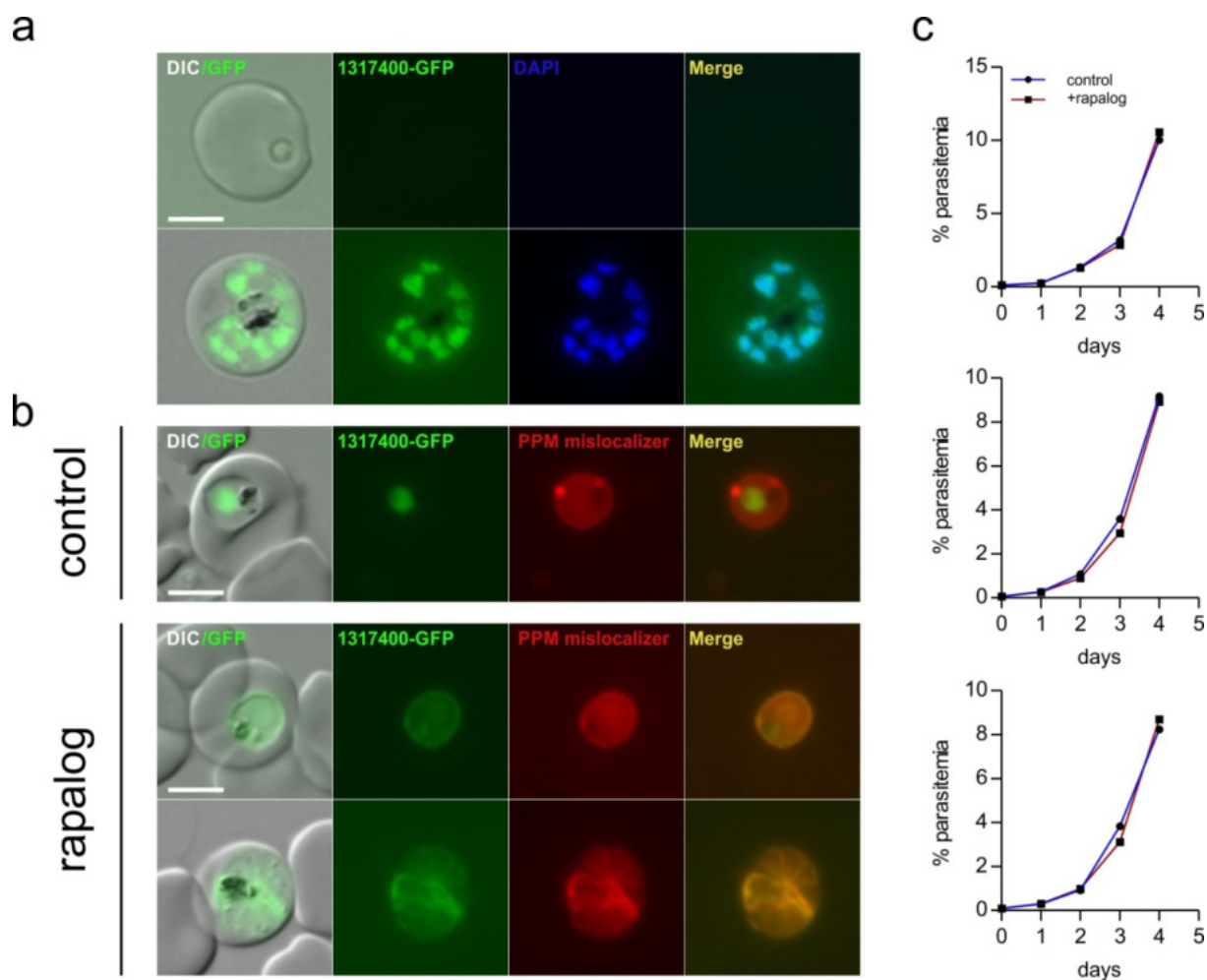


Figure 18 | Localization and KS of PF3D7_1317400 (candidate 5). **a,b**) Live cell images of knock-in cell line of candidate 5 fused to 2xFKBP-GFP-2xFKBP. **a**) Cell line stained with DAPI nuclear stain. **b**) Knock-in cell line transfected with an episomally expressed Lyn-FRB-mCherry mislocalizer. Live cell fluorescence images of control and rapalog-treated cells were taken after 16h. **c**) FC growth curves from 3 independent experiments showing development of control and culture treated with 250 nM rapalog. Scale bars, 5 μ m.

3.2.2.6 Candidate 6: PF3D7_1445700

PF3D7_1445700 encompasses 351 AA and no homology to known domains could be detected (see section 2.2.6). Correct integration into the targeted genomic loci was assessed by PCR (Figure 11c). The protein was exclusively expressed in schizont stage and showed a plasma membrane or IMC-like localization (Figure 19). A nuclear mislocalizer was used but no mislocalization was observed after addition of rapalog (Figure 19, lower panel). Hence no growth assay was carried out. In a first successful approach, SLI-TGD truncated the gene by 49.4% (Figure 11c). A second, more recent approach with a different targeting region, similar in size to the first one, but resulting in the truncation of 86% of the gene was not successful. This may indicate that this gene is nevertheless essential but that the second half is dispensable for its function.

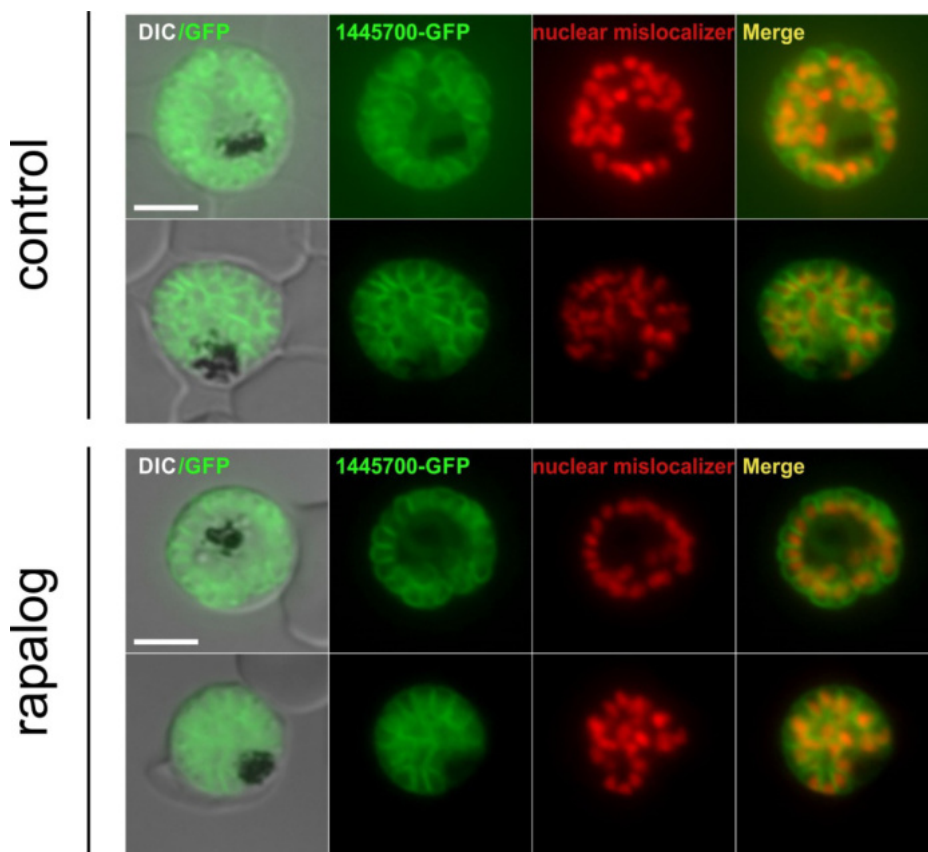


Figure 19 | Localization and KS of PF3D7_1445700 (candidate 6). Live cell images of knock-in cell line of candidate 6 fused to 2xFKBP-GFP. The knock-in cell line was transfected with an episomally expressed 3xNLS-FRB-mCherry mislocalizer. Live cell fluorescence images of control and rapalog-treated cells were taken after 16h. Scale bars, 5 μ m.

3.2.2.7 Candidate 7: PF3D7_1451200

PF3D7_1451200 is a protein of 1504 AA. No known domains were found for candidate 7 (see section 2.2.6). Correct integration of the SLI plasmid fusing the gene with *fkbp* and *gfp* was confirmed by PCR (Figure 11c). The GFP tagged candidate 7 showed fluorescence in the parasite's nucleus as evident in the co-localization with DAPI stain and was expressed in all asexual stages (Figure 20a,b). The nuclear fluorescence generally overlapped with DAPI but also included foci in trophozoite and schizont stage (Figure 20a, lower panel). Based on the nuclear localization, a PPM mislocalizer was chosen for KS analysis of this candidate. In this case the 2xFKBP-GFP tag was insufficient to mediate efficient mislocalization, and thus the 2xFKBP-GFP-2xFKBP tag was used in a second cell line (Figure 11c). Despite the improved KS vector the addition of rapalog to the culture led only to a very inefficient mislocalization of the protein, and a large part of the protein remained in the nucleus (Figure 20b). Nevertheless, a growth assay was performed showing no effect on parasite growth of the cells grown with rapalog compared to control (Figure 20c). A SLI-TGD was obtained for this candidate (Figure 11c), which indicates that the gene is not required for development of parasite blood stages.

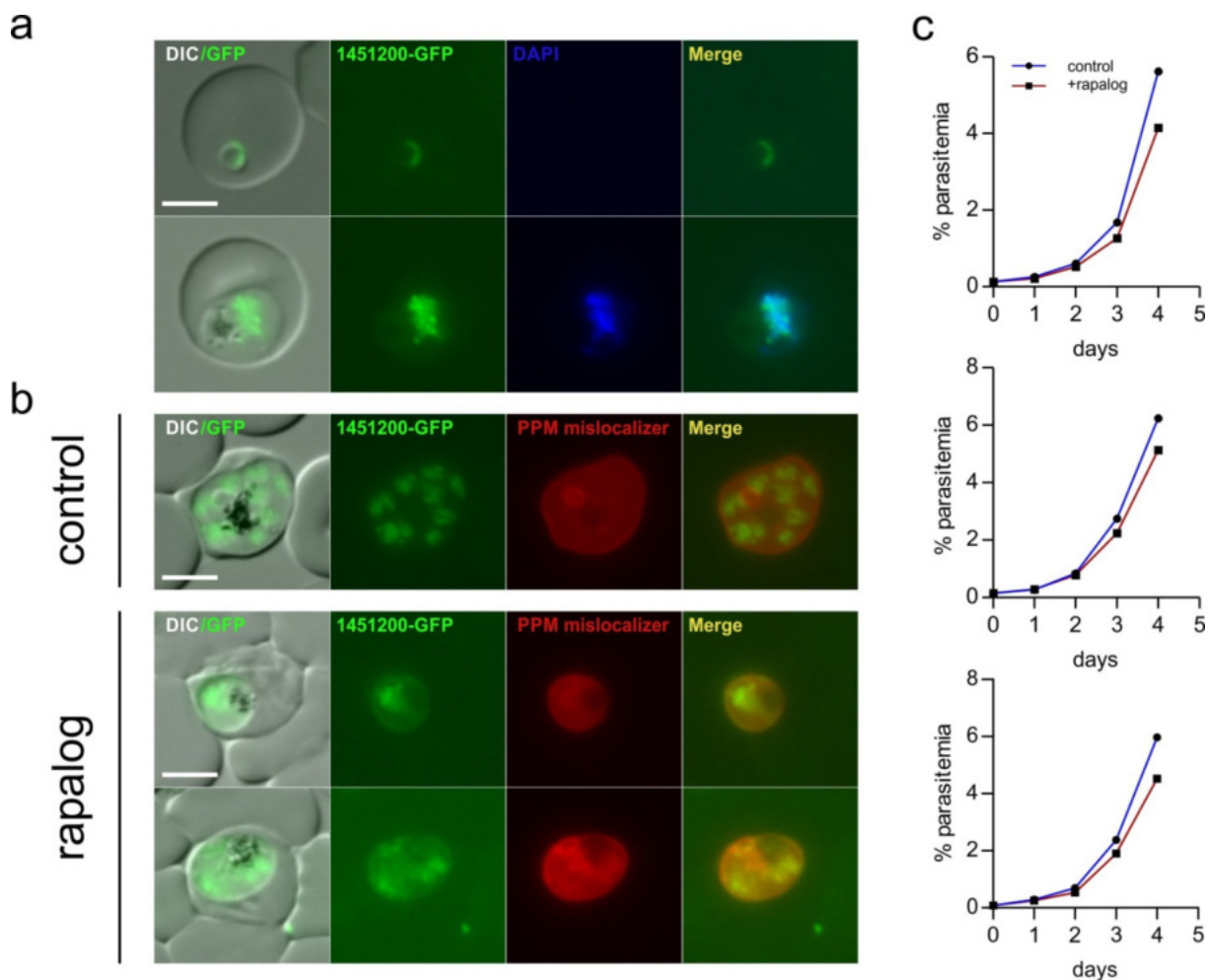


Figure 20 | Localization and KS of PF3D7_1451200 (candidate 7). **a,b)** Live cell images of knock-in cell line of candidate 7 fused to 2xFKBP-GFP-2xFKBP. **a)** Cell line stained with DAPI nuclear stain. **b)** Knock-in cell line transfected with an episomally expressed Lyn-FRB-mCherry mislocalizer. Live cell fluorescence images of control and rapalog-treated cells were taken after 16h. **c)** FC growth curves from 3 independent experiments showing development of control and culture treated with 250 nM rapalog. Scale bars, 5 μ m.

3.2.2.8 Candidate 8: PF3D7_1463000

PF3D7_1463000 encompasses 308 AA. No known domains were found by *in silico* analysis (see section 2.2.6). Integration in the targeted genomic locus was confirmed by PCR (Figure 11c). The protein localized to the nucleus and included one to multiple foci in trophozoite and schizont stage with a faint cytosolic pool as can be seen in the co-localization with DAPI (Figure 21a, lower panel). It was expressed from ring stage to schizont stage (Figure 21a,b). The KS, using a PPM mislocalizer, efficiently relocated the protein to the PPM (Figure 21b). A growth assay over 5 days was carried out but showed no difference in parasites where candidate 8 had been knocked aside compared to control (Figure 21c). Moreover a SLI-TGD was obtained (Figure 11c), confirming the dispensability of candidate 8 in asexual blood stage parasites.

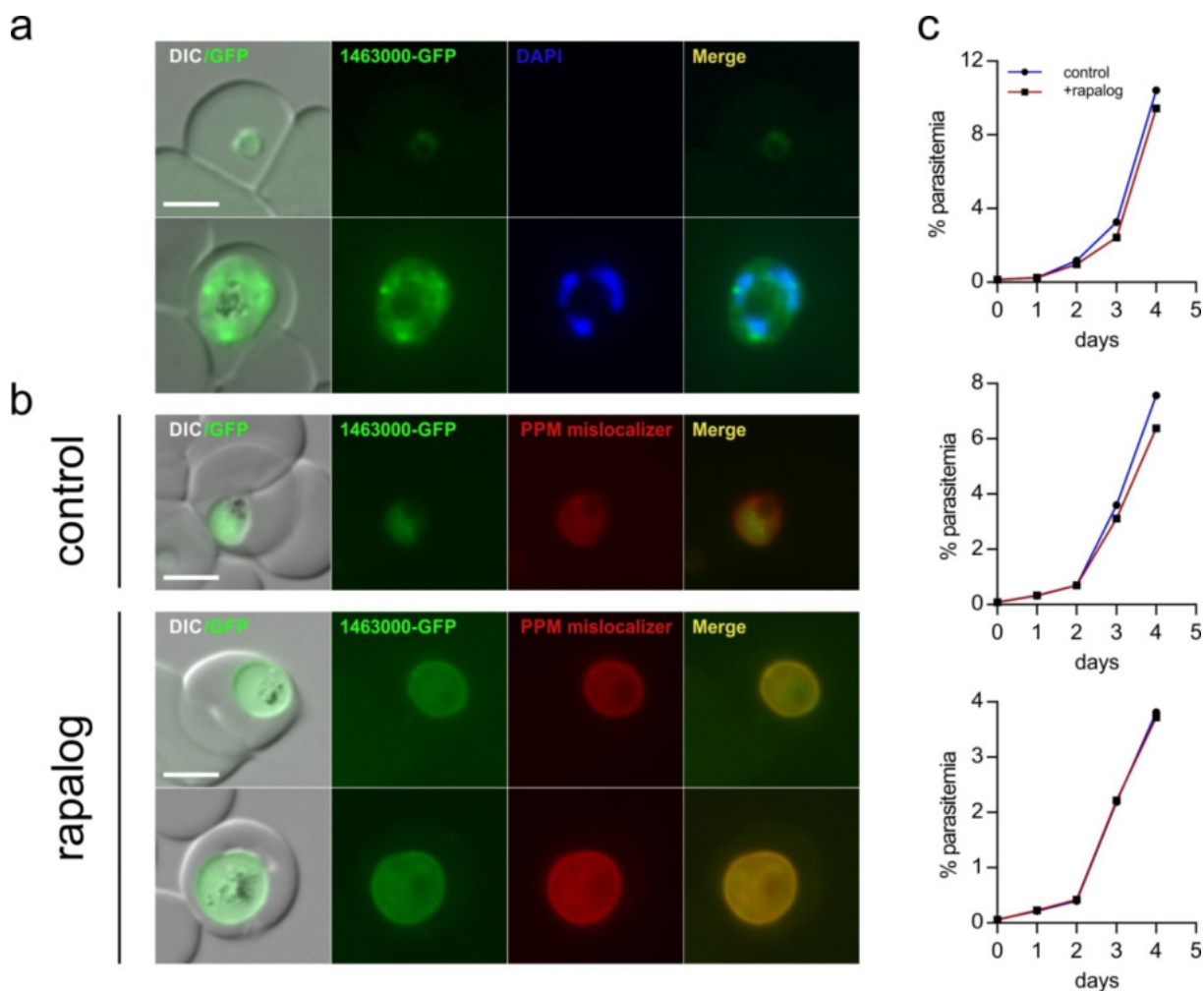


Figure 21 | Localization and KS of PF3D7_146300 (candidate 8). **a,b)** Live cell images of knock-in cell line of candidate 8 fused to 2xFKBP-GFP. **a)** Cell line stained with DAPI nuclear stain. **b)** Knock-in cell line transfected with an episomally expressed Lyn-FRB-mCherry mislocalizer. Live cell fluorescence images of control and rapalog-treated cells were taken after 16h. **c)** FC growth curves from 3 independent experiments showing development of control and culture treated with 250 nM rapalog. Scale bars, 5 μ m.

3.2.2.9 Candidate 9: PF3D7_0202400

Candidate 9 is a protein of 1192 AA. No homology to known domains could be assigned (see section 2.2.6). The correct integration into the targeted genomic locus was confirmed by PCR (Figure 11, kindly performed by Nick Reichard). Unexpectedly, the candidate was found to be exported (Figure 22 (Reichard, 2015)). No classical PEXEL motif was detectable in the protein. This indicates that the protein represents a new PEXEL negative exported protein (Spielmann and Gilberger, 2010). Exported proteins cannot be targeted by KS with the mislocalizers currently available. Nevertheless, the protein could be disrupted with SLI-TGD (Figure 11c) and hence is not essential for the growth of asexual blood stage parasites.

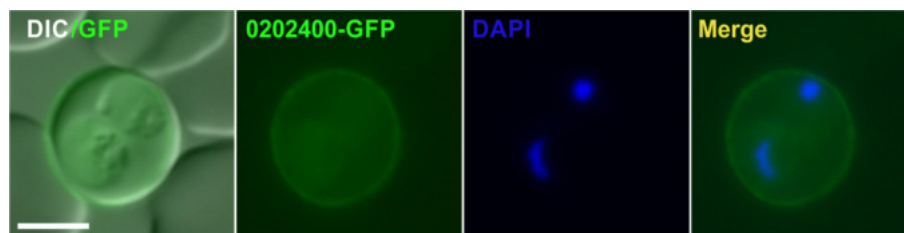


Figure 22 | Localization of PF3D7_0202400 (candidate 9). Live cell images of knock-in cell line of candidate 9 fused to 2xFKBP-GFP. Cell line stained with DAPI nuclear stain. Images were taken by Nick Reichard. Scale bar, 5 μ m.

3.2.2.10 Candidate 10 PF3D7_0205100

PF3D7_0205100 is a protein of 705 AA. *In silico* analysis could not identify homologies to known domains (see section 2.2.6). All attempts to C-terminally tag candidate 10 in the genome failed. In line with this, no disruption of this gene by SLI-TGD could be obtained (Table 2). PF3D7_0205100 therefore likely is essential to *P. falciparum* blood stage parasites, but could neither be localized nor functionally analyzed.

3.2.2.11 Candidate 11 PF3D7_0205600

PF3D7_0205600 is a protein of 635 AA. No homologies to domains outside the Apicomplexa were identified (see section 2.2.6). A 2xFKBP-GFP knock-in cell line was created and the integration into the correct genomic locus was confirmed by PCR (Figure 11c) (Reichard, 2015). The protein was found to be expressed from trophozoite to schizont stage and localized to the nucleus with a faint cytosolic pool, as shown by co-localization of the GFP signal with a DAPI signal (Figure 23a,b) (Reichard, 2015). Focal GFP staining was observed in the nucleus or at the nuclear periphery (Figure 23a, lower panel). A PPM mislocalizer was chosen to carry out KS analysis. Upon addition of rapalog the target was efficiently targeted to the plasma membrane (Figure 23b). A growth assay over the course of 5 days showed a clearly reduced growth in the rapalog treated culture compared to the control (Figure 23c) (Reichard, 2015). This result was supported by failure to truncate the gene by SLI-TGD (Table 2). Hence, candidate 11 can be considered to be essential for the development of asexual blood stage parasites.

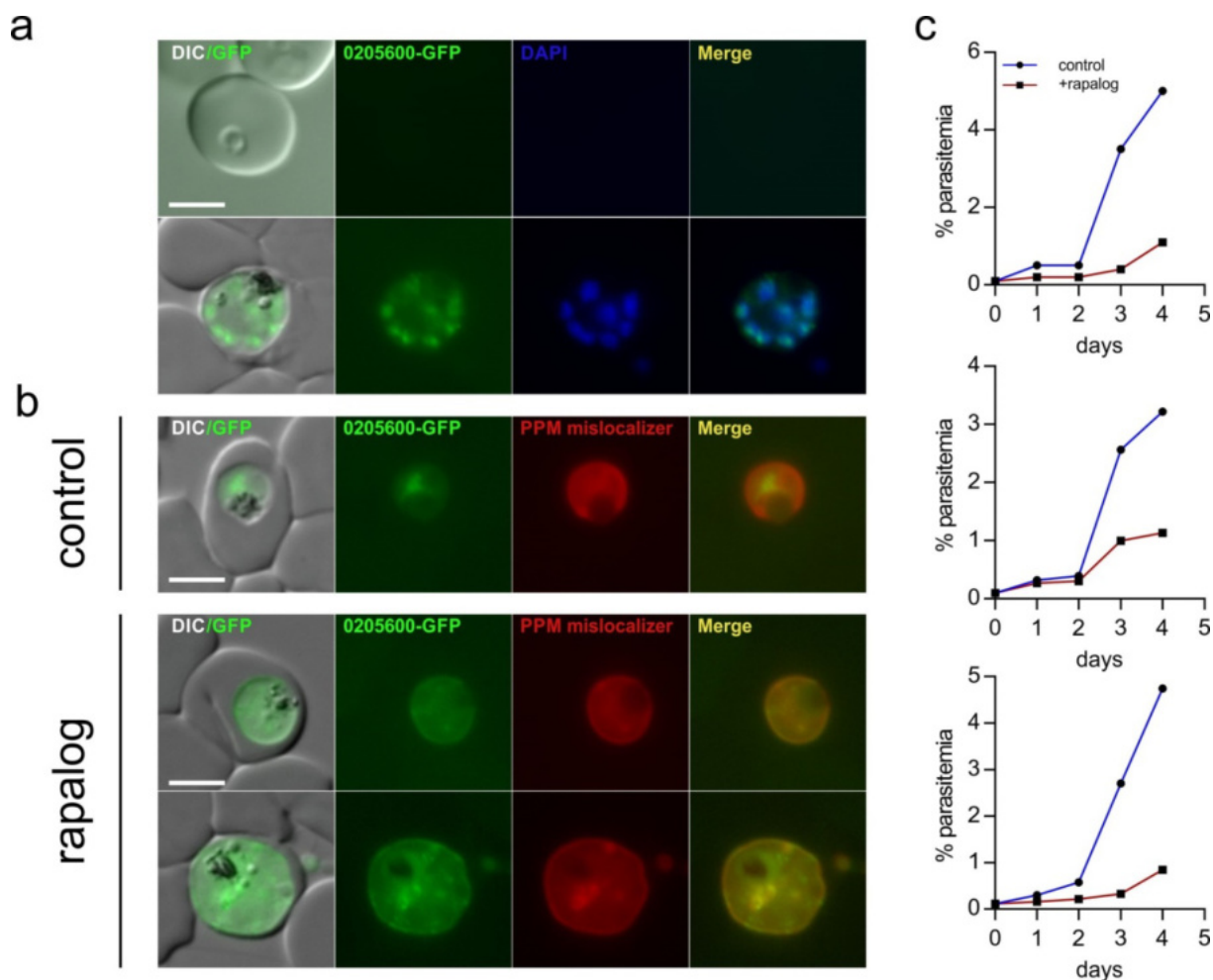


Figure 23 | Localization and KS of PF3D7_0205600 (candidate 11). **a,b)** Live cell images of knock-in cell line of candidate 11 fused to 2xFKBP-GFP. **a)** Cell line stained with DAPI nuclear stain (Reichard, 2015) **b)** Knock-in cell line transfected with an episomally expressed Lyn-FRB-mCherry mislocalizer. Live cell fluorescence images of control and rapalog-treated cells were taken after 16h. **c)** FC growth curves from 3 independent experiments showing development of control and culture treated with 250 nM rapalog. Scale bars, 5 μ m.

3.2.2.12 Candidate 12: PF3D7_0209700

PF3D7_0209700 is annotated as a putative RING zinc finger protein in Plasmodb (Plasmodb.org). It contains a potential SPX (name is derived from Syg1, Pho81, XPR1 proteins) domain spanning from 1-173 and a zinc finger domain from AA 214 to 254 (see section 2.2.6). SPX domains are involved in signal transduction of G-proteins (Spain et al., 1995). The complete protein encompasses 1707 AA. The protein was fused to 2xFKBP-GFP-2xFKBP and the integration into the correct genomic locus was confirmed by PCR (Figure 11c) (Reichard, 2015). The GFP signal showed a cytosolic localization and was expressed in all asexual stages (Figure 24a,b). For KS a nuclear mislocalizer was chosen. Addition of rapalog led to complete mislocalization from the cytosol to the nucleus (Figure 24b). The growth assay showed no effect on parasite development in the parasites grown in the presence of rapalog when compared to control (Figure 23c). Moreover parasites with a truncated gene were

obtained by SLI-TGD (Figure 11c). Consequently, the gene is not essential for the growth of asexual blood stage parasites.

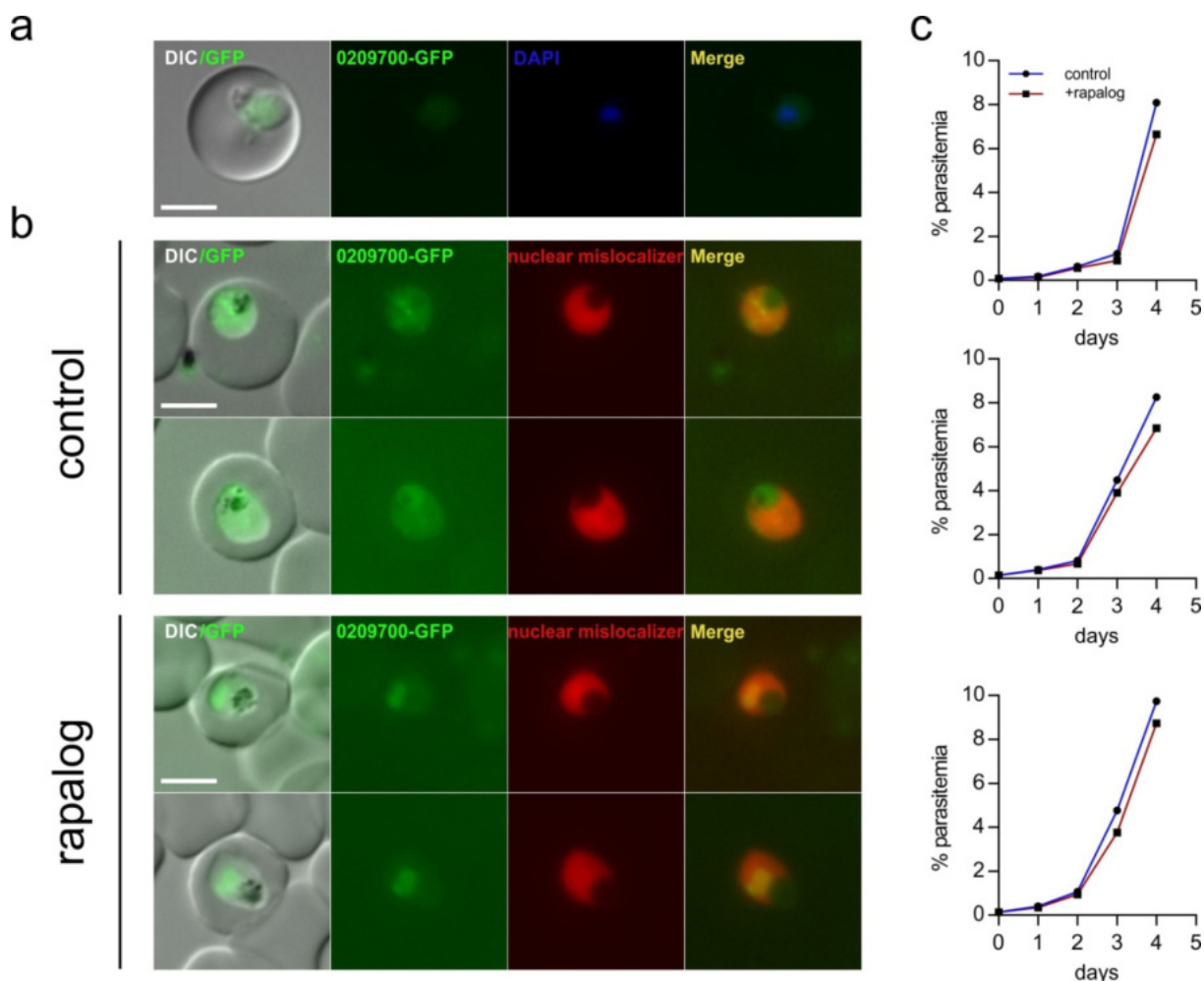


Figure 24 | Localization and KS of PF3D7_0209700 (candidate 12). **a,b)** Live cell images of knock-in cell line of candidate 12 fused to 2xFKBP-GFP-2xFKBP. **a)** Cell line stained with DAPI nuclear stain. Images by Nick Reichard **b)** Knock-in cell line transfected with an episomally expressed 1xNLS-FRB-mCherry mislocalizer. Live cell fluorescence images of control and rapalog-treated cells were taken after 16h. **c)** FC growth curves from 3 independent experiments showing development of control and culture treated with 250 nM rapalog. Scale bars, 5 μ m.

3.2.2.13 Candidate 13: PF3D7_0210200

PF3D7_0210200 is a protein of 2588 AA. No homologies to known domains could be identified in this candidate except for a potential nuclear localization signal spanning AA 890 to 904 (see section 2.2.6). The protein was endogenously tagged with 2xFKBP-GFP-2xFKBP using SLI. Integration into the correct genomic locus was confirmed by PCR (Figure 11c). The protein showed a nuclear localization, evident by co-localization of the GFP signal with the DAPI nuclear stain (Figure 25a). Its expression was detected from trophozoite stage to schizont stage but not in ring stages (Figure 25a,b). For the knock sideways a PPM mislocalizer was chosen. In the cells treated with rapalog, the protein was efficiently depleted from the nucleus and translocated to the plasma membrane (Figure 25b). A

growth assay over the course of 5 days showed a growth defect of the parasites grown in the presence of rapalog compared to untreated parasites (Figure 25c). In line with this result, all attempts to disrupt the gene by SLI-TGD were unsuccessful (Table 2). Hence, the protein is essential for the development of asexual blood stages.

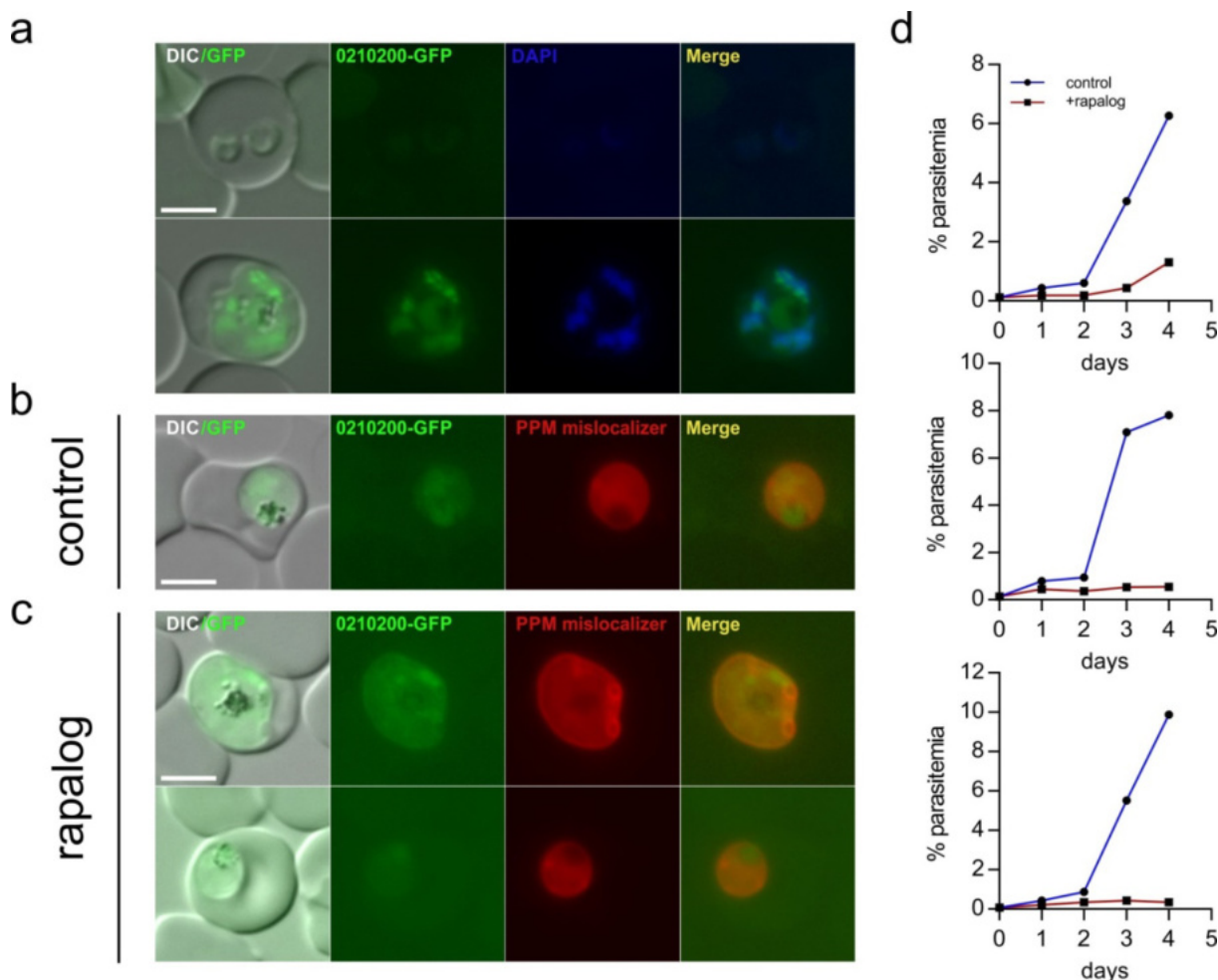


Figure 25 | Localization and KS of PF3D7_0210200 (candidate 13). **a,b)** Live cell images of knock-in cell line of candidate 13 fused to 2xFKBP-GFP-2xFKBP. **a)** Cell line stained with DAPI nuclear stain. **b)** Knock-in cell line transfected with an episomally expressed Lyn-FRB-mCherry mislocalizer. Live cell fluorescence images of control and rapalog-treated cells were taken after 16h. **c)** FC growth curves from 3 independent experiments showing development of control and culture treated with 250 nM rapalog. Scale bars, 5 μ m.

3.2.2.14 Candidate 14: PF3D7_0211700

PF3D7_0211700 is annotated as a putative tyrosin-kinase like protein (Plasmodb.org). It comprises 1233 amino acids. The kinase domain was identified to span AA 952-1204 (see section 2.2.6). The gene was fused to *2xfkbp-gfp* using SLI and the correct integration was confirmed by PCR (Figure 11c) (kindly performed by Nick Reichard). The protein was expressed at extremely low levels which made it impossible to assess to localization by fluorescence microscopy (Figure 26a), in accordance with the low transcription levels of this gene (Le Roch et al., 2003). Consequently the growth assay

was carried out for a cell line containing a nuclear mislocalizer and a cell line containing the PPM mislocalizer, despite the fact that the effectiveness of the knock sideways could not be visually assessed (Figure 26b,c). For both assays no difference in rapalog treated cells compared to control was evident. Moreover the gene was successfully truncated by SLI-TGD (Figure 11c). Hence, candidate 14 was classified as not essential for the growth of asexual blood stage parasites.

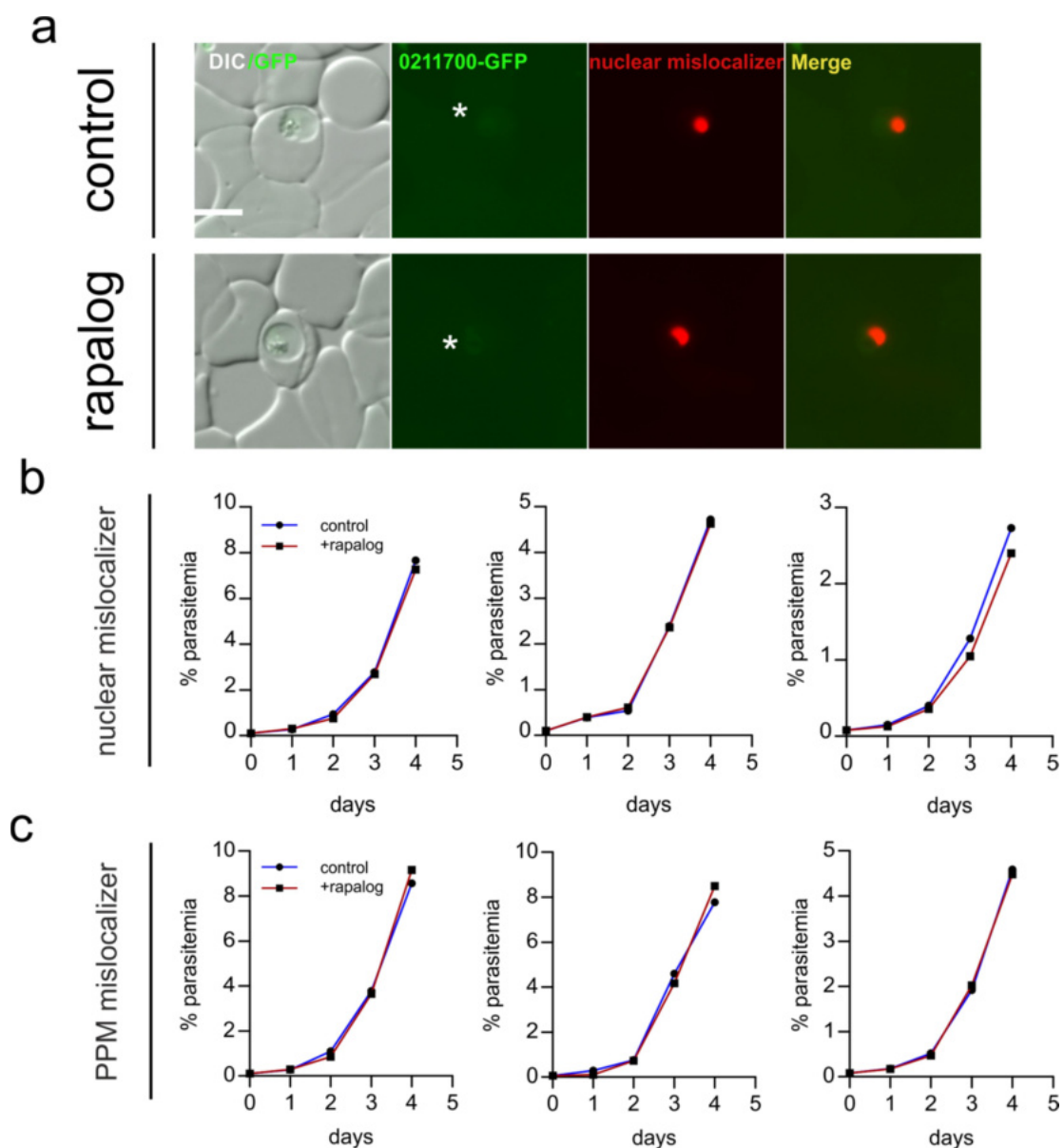


Figure 26 | Localization and KS of PF3D7_0211700 (candidate 14). **a)** Live cell images of knock-in cell line of candidate 14 fused to 2xFKBP-GFP. Knock-in cell line transfected with an episomally expressed 3xNLS-FRB-mCherry mislocalizer. Live cell fluorescence images of control and rapalog-treated cells were taken after 16h. **b)** FC growth curves over 5 days from 3 independent experiments showing development of control and culture treated with 250 nM rapalog for nuclear and PPM mislocalizer, respectively. Asterisk, autofluorescence of the food vacuole. Scale bar, 5 μ m.

3.2.2.15 Candidate 15 PF3D7_0210900

Candidate 15 comprises 284 amino acids. No homologies to known domains were identified by *in silico* analysis (see section 2.2.6). The protein was endogenously tagged with 2xFKBP-GFP using SLI and integration into the correct genomic locus was confirmed by PCR (Figure 11c) (kindly performed by Nick Reichard). The protein localized to the nucleus and the nuclear periphery as assessed by colocalization of the GFP signal with the DAPI nuclear stain (Figure 27a). Notably, the staining pattern with this protein did not fully overlap with the nuclear stain in trophozoite stage parasites but showed some signal extending over the confines of the DAPI signal (Figure 27a, bottom panel). Candidate 15 was expressed from ring stage to the schizont stage (Figure 27a,b). For knock sideways analysis a PPM mislocalizer was chosen. The addition of rapalog led to a relocalization of the protein with a very weak GFP signal left in the nucleus (Figure 27b). Subsequently a growth assay was performed. Comparison of the control and the rapalog treated culture showed a severe growth defect after mislocalizing the protein (Figure 27c). This indicated the essentiality of candidate 15 for the development of blood stage parasites. In agreement, all attempts to obtain a truncated gene using SLI-TGD failed (Table 2).

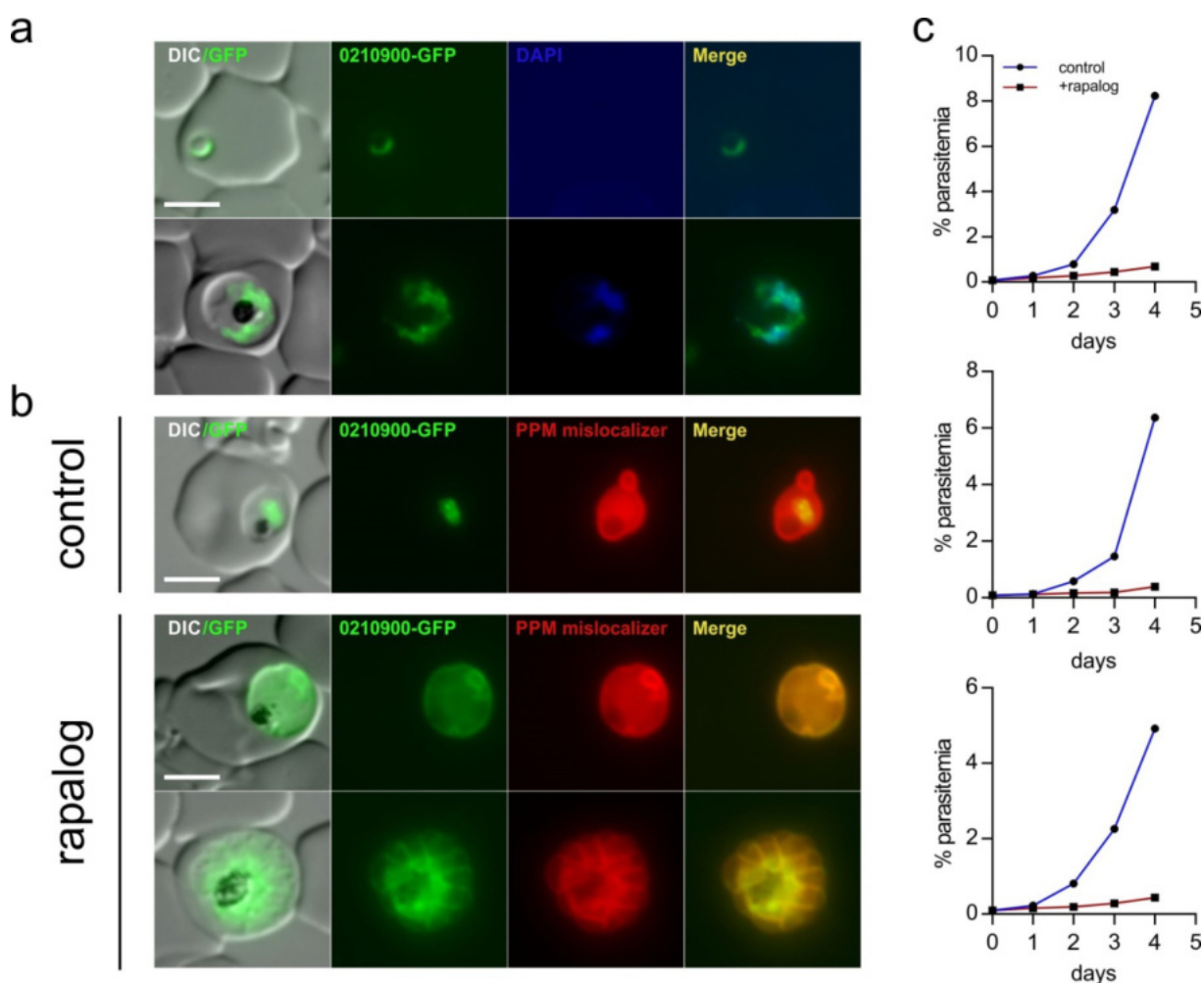


Figure 27 | Localization and KS of PF3D7_0210900 (candidate 15). **a,b**) Live cell images of knock-in cell line of candidate 15 fused to 2xFKBP-GFP. **a**) Cell line stained with DAPI nuclear stain. **b**) Knock-in cell line transfected with an episomally

expressed Lyn-FRB-mCherry mislocalizer. Live cell fluorescence images of control and rapalog-treated cells were taken after 16h. c) FC growth curves from 3 independent experiments showing development of control and culture treated with 250 nM rapalog. Scale bars, 5 μ m.

3.2.2.16 Candidate 16: PF3D7_0213700

PF3D7_0213700 is a protein of 154 AA. Homology search revealed a domain of unknown function 842 (DUF) (Marchler-Bauer et al., 2017) (see section 2.2.6). The domain of unknown function spans almost the entire protein from amino acids 21 to 143. All attempts to C-terminally tag candidate 10 in the genome failed. In line with this, no disruption of this gene by SLI-TGD could be obtained (Table 2). PF3D7_0205100 is therefore potentially essential to the *P. falciparum* parasite, but could neither be localized nor functionally analyzed.

3.2.2.17 Candidate 17: PF3D7_0213900

The protein consists of 1166 amino acids. *In silico* analysis identified no homologies to known domains (see section 2.2.6). The gene was fused to *2xfkbp-gfp* by using SLI. Integration into the correct genomic locus was confirmed by PCR (Figure 11c). Co-localization of the GFP tagged protein with DAPI nuclear stain showed an exclusively cytosolic localization with the protein being absent from the nucleus (Figure 28a). Thus, a nuclear mislocalizer was chosen (Figure 28b). Addition of rapalog led to no change in the cellular distribution of the protein (Figure 28b). Consequently no growth assay was carried out. The gene could not be truncated by SLI-TGD (Table 2), and hence it is considered essential for asexual blood stage development of the parasite.

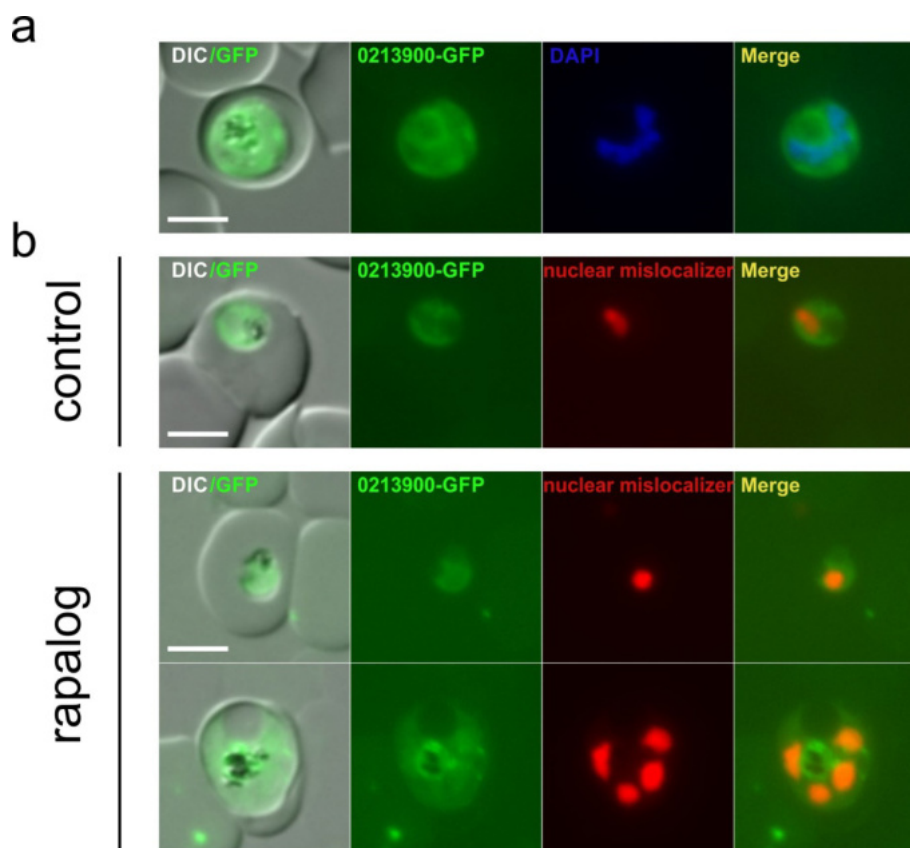


Figure 28 | Localization and KS of PF3D7_0213900 (candidate 17). **a,b)** Live cell images of knock-in cell line of candidate 17 fused to 2xFKBP-GFP. **a)** Cell line stained with DAPI nuclear stain. **b)** Knock-in cell line transfected with an episomally expressed 1xNLS-FRB-mCherry mislocalizer. Live cell fluorescence images of control and rapalog-treated cells were taken after 16h. Scale bars, 5 μm .

3.2.2.18 Candidate 18: PF3D7_0218200

PF3D7_0218200 is a protein of 807 amino acids. An EF-hand domain was identified, encompassing amino acids 89 to 101 (see section 2.2.6), but no other homologies were found. EF-hand domains bind Ca^{2+} , playing a role in various cellular functions (Lewit-Bentley and Rety, 2000). The protein was C-terminally tagged with 2xFKBP-GFP. The integration was confirmed by PCR (Figure 11c) (kindly performed by Nick Reichard). The protein was detected by fluorescence microscopy starting from the trophozoite stage to the merozoite stage but not in ring stages (Figure 29a,b). It localized throughout the cytosol of the parasite but appeared to be absent from the nucleus (Figure 29a). For this candidate a nuclear mislocalizer was chosen. The KS, initiated through the addition of rapalog, led to an efficient relocalization of candidate 18 to the nucleus (Figure 29b). The subsequent growth assay over the course of 5 days showed no difference of the control to the cell line treated with rapalog (Figure 29c). In line, parasites with a truncated gene were obtained by using SLI-TGD (Figure 11c). Hence, the gene is not essential for the development of asexual blood stage parasites.

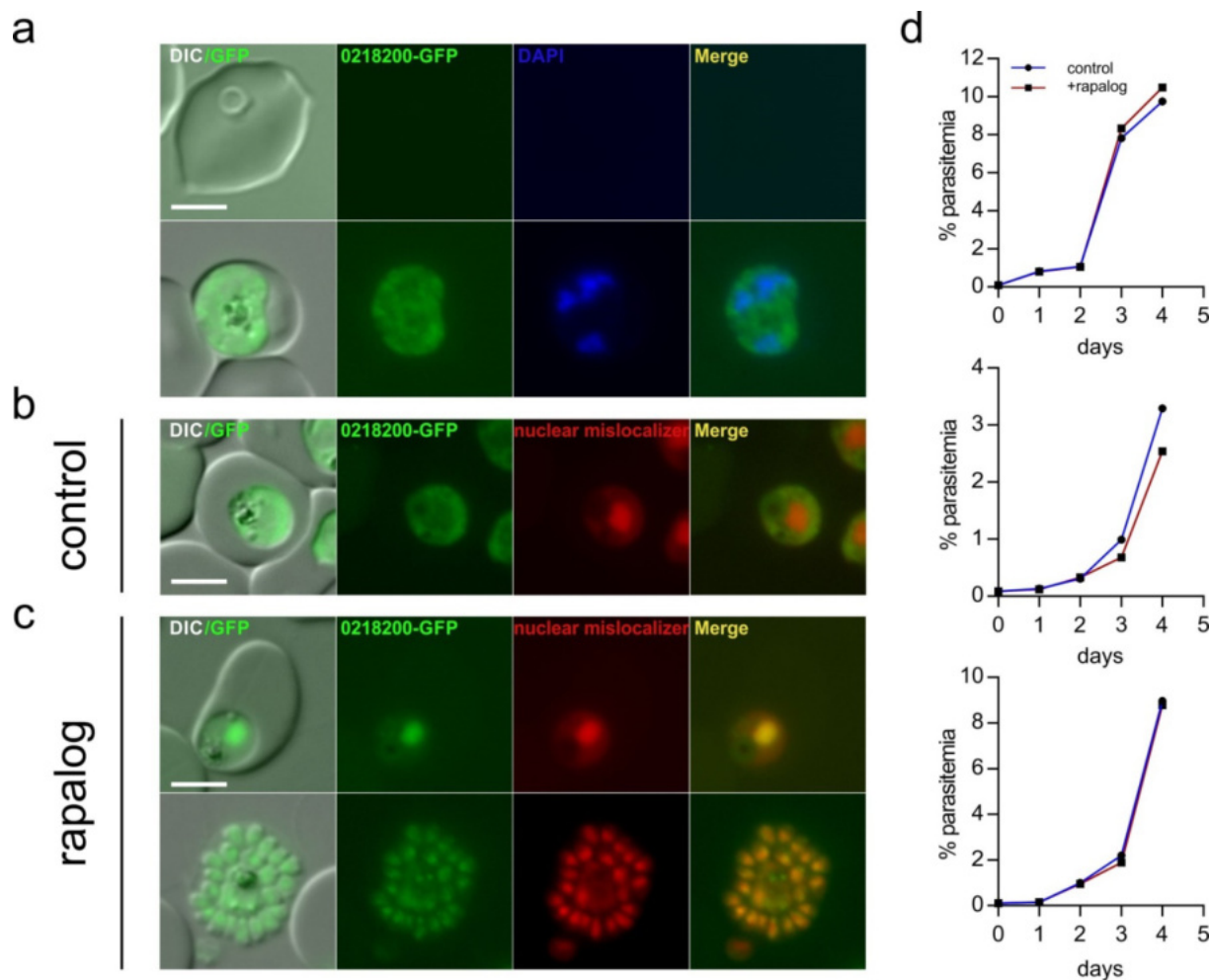


Figure 29 | Localization and KS of PF3D7_0218200 (candidate 18). **a,b** Live cell images of knock-in cell line of candidate 18 fused to 2xFKBP-GFP (Reichard, 2015). **a**) Cell line stained with DAPI nuclear stain. **b**) Knock-in cell line transfected with an episomally expressed 1xNLS-FRB-mCherry mislocalizer. Live cell fluorescence images of control and rapalog-treated cells were taken after 16h. **c**) FC growth curves from 3 independent experiments over 5 days showing development of control and culture treated with 250 nM rapalog. Scale bars, 5 μ m

3.2.3 Kinetics of the knock sideways system

The kinetics of mislocalization was analyzed for 2 nuclear and 1 cytoplasmic proteins to gain a better understanding of the knock sideways system in *P. falciparum* parasites. Five different time points at 0h, 1h, 4h and 8h after addition of rapalog were assessed for candidates 11, 13 and 18 (Figure 30). An additional time point at 16h was taken for candidate 11 as mislocalization was not completed before that (Figure 30b). Candidate 18, a cytosolic protein, was rapidly mislocalized to the nucleus. At the 1h mark almost all cells showed complete relocation from cytosol to nucleus (Figure 30a). For both nuclear proteins (candidates 11 and 13) mislocalization took longer compared to candidate 18. After 8h most cells displayed efficient translocation to the plasma membrane for candidate 13 (Figure 30c). In contrast, at the same time point, only one-third of the cells showed complete mislocalization for candidate 11 (Figure 30b). Efficient mislocalization was achieved for most cells after 16h. This may indicate superiority of the nuclear mislocalizer over the PPM mislocalizer for KS.

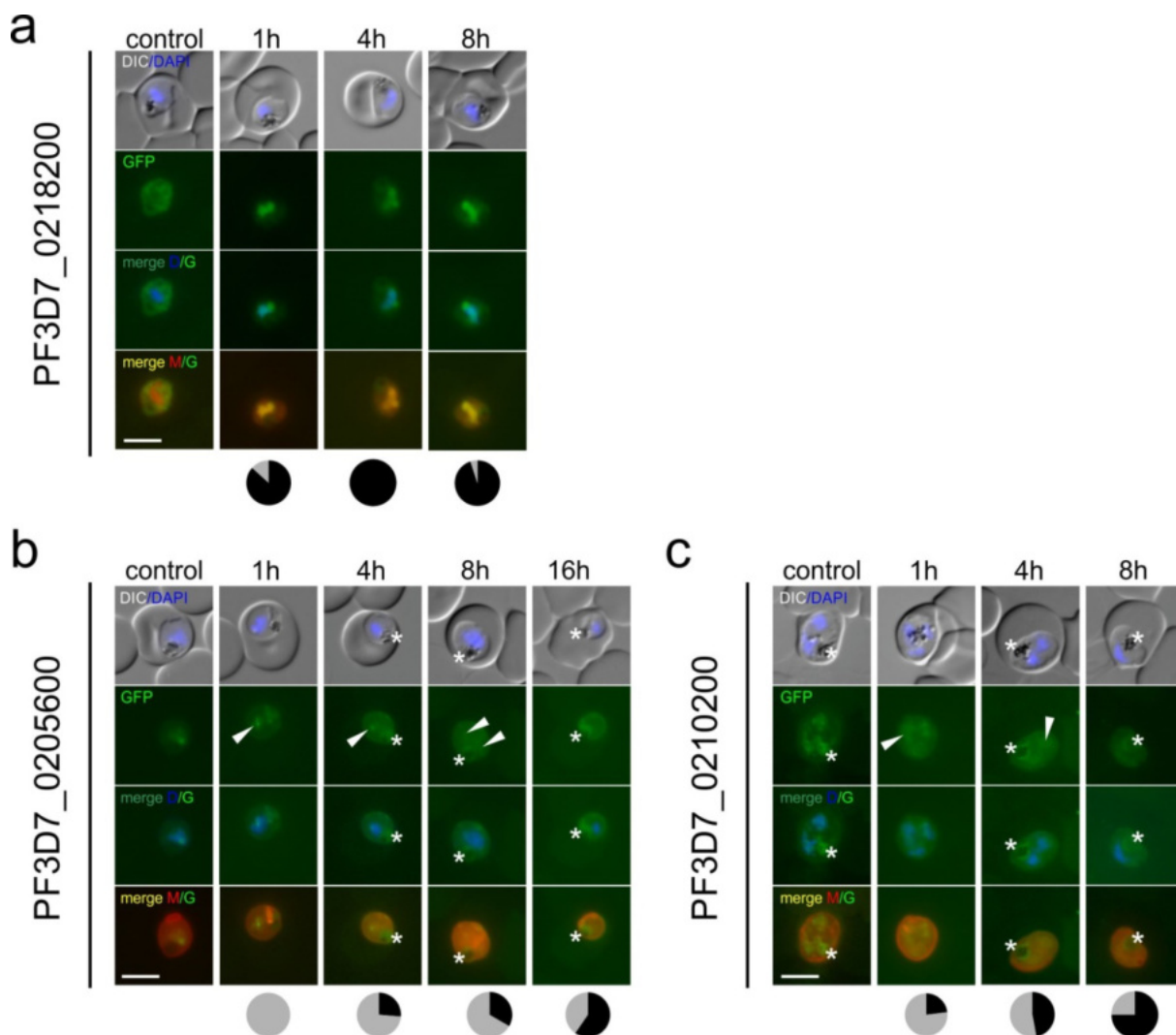


Figure 30 | Kinetics of the KS system. Time course for the onset and completion of mislocalization for different proteins after addition of rapalog. **a)** Disperse cytosolic protein PF3D7_0218200 (candidate 18) with a nuclear mislocalizer. Pie charts for PF3D7_0218200-GFP show proportion of cells where the GFP signal fully co-localized with the mislocalizer, suggesting full mislocalization (black) or cells where GFP signal did not fully co-localize, suggesting incomplete mislocalization (grey); **b,c)** Two nuclear proteins PF3D7_0205600 and PF3D7_0210200 (candidate 11 and 13, respectively) relocated to the PPM. $n = 30, 22,$ and 20 cells for PF3D7_0218200-GFP, for 1 h, 4 h, and 8 h. For the nuclear proteins PF3D7_0205600-GFP and PF3D7_0210200-GFP) incomplete mislocalization was defined as focal or dispersed GFP signal in the area occupied by the DAPI nuclear stain. Pie charts show proportion of cells with incomplete mislocalization (grey) versus cells with complete mislocalization (black). For PF3D7_0205600-GFP $n = 24, 19, 39,$ and 52 cells for 1 h, 4 h, 8 h, and 16 h, respectively; for PF3D7_0210200-GFP $n = 26, 20,$ and 16 cells, for 1 h, 4 h, 8 h, and 16 h, respectively. Shown is one of two independent experiments. Asterisks, food vacuole autofluorescence; Arrows, non-mislocalized protein. Time points are indicated above the panels. DIC: differential interference contrast; DAPI: parasite nuclei; merge D/G: merge DAPI and GFP; merge M/G: merge mislocalizer and GFP; Size bars, $5 \mu\text{m}$.

An extended growth assay was performed with PF3D7_0205600-2xFKBP-GFP (candidate 11) (Figure 31a) in order to evaluate the slowly growing population of parasites that appeared in the rapalog treated cell line at day 4 of the initial assay (Figure 23c). Over the course of 9 days, a slowly expanding population of parasites expressing low levels of the mislocalizer was identified (Figure 31b,c). This indicates the existence of a small founder population with low levels of

mislocalizer where the knock sideways is inefficient enough to permit parasite growth. Selection of these parasites, despite continued drug pressure to maintain the mislocalizer plasmid, highlights the selection the KS exerts on the cells and hence the importance of the target for parasite growth.

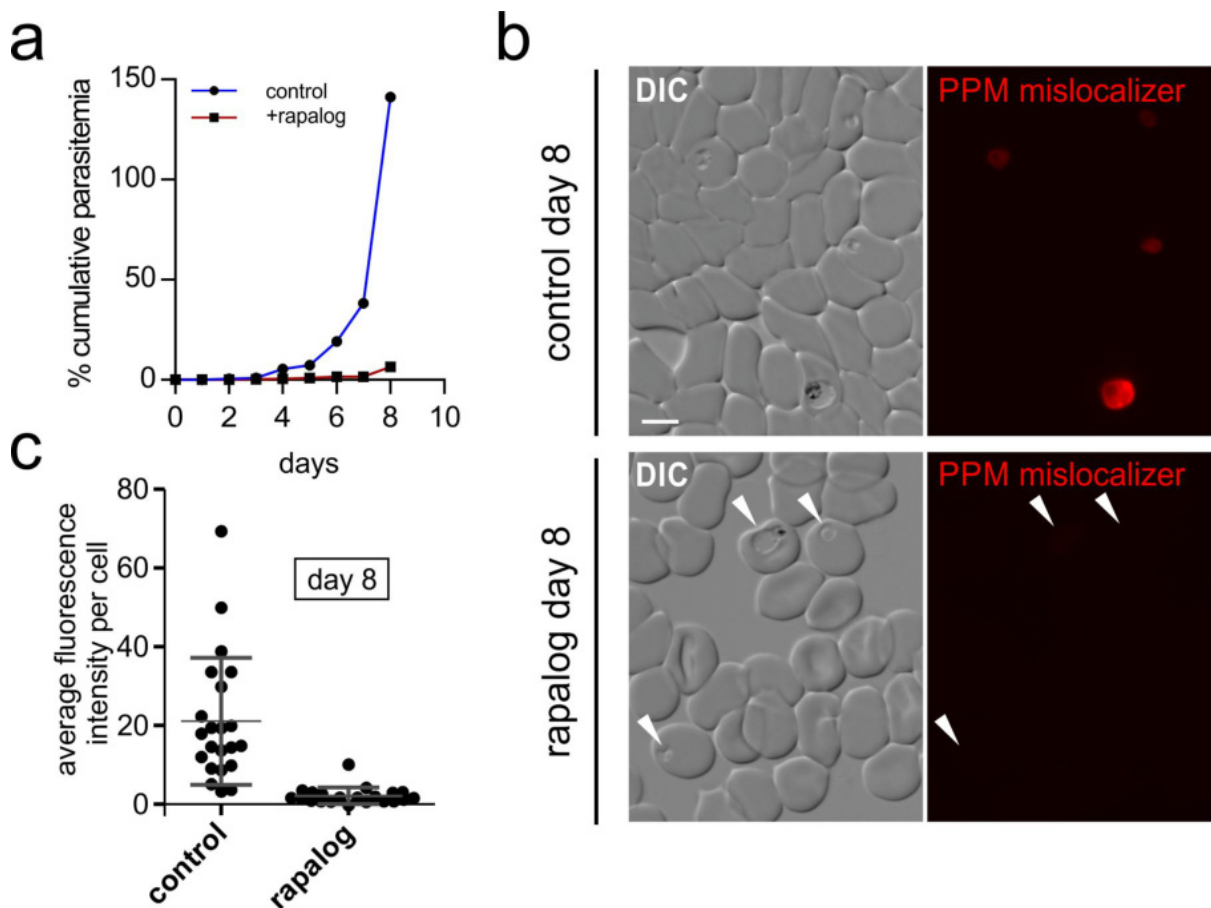


Figure 31 | Extended growth assay with PF3D7_0205600 (candidate 11). **a**) FC growth curve extended to day 8 after addition of 250 nM rapalog. **b**) Top panel showing the intensity of expression of the Lyn-FRB-mCherry mislocalizer in an untreated culture on day 8 of the experiment; Bottom panel showing the expression intensity of the same mislocalizer in the rapalog-treated culture. Pictures are taken with same exposure time. Arrows indicate parasites in DIC and fluorescence picture. **c**) Quantification of average fluorescence intensity per cell of control and rapalog-treated cells ($n = 22$ and $n = 21$, respectively) on day 8. Size bars, 5 μm .

3.3 N-terminal tagging and analysis of the artemisinin resistance gene

kelch13

The Kelch13 protein was identified as a molecular marker for artemisinin resistance (see 1.1.3.1) (Ariey et al., 2014). Despite of the high level of attention it has received, it has not been localized nor functionally analyzed so far (Tilley et al., 2016). It was therefore chosen as a further target to test the system to localize and functionally analyze *P. falciparum* proteins.

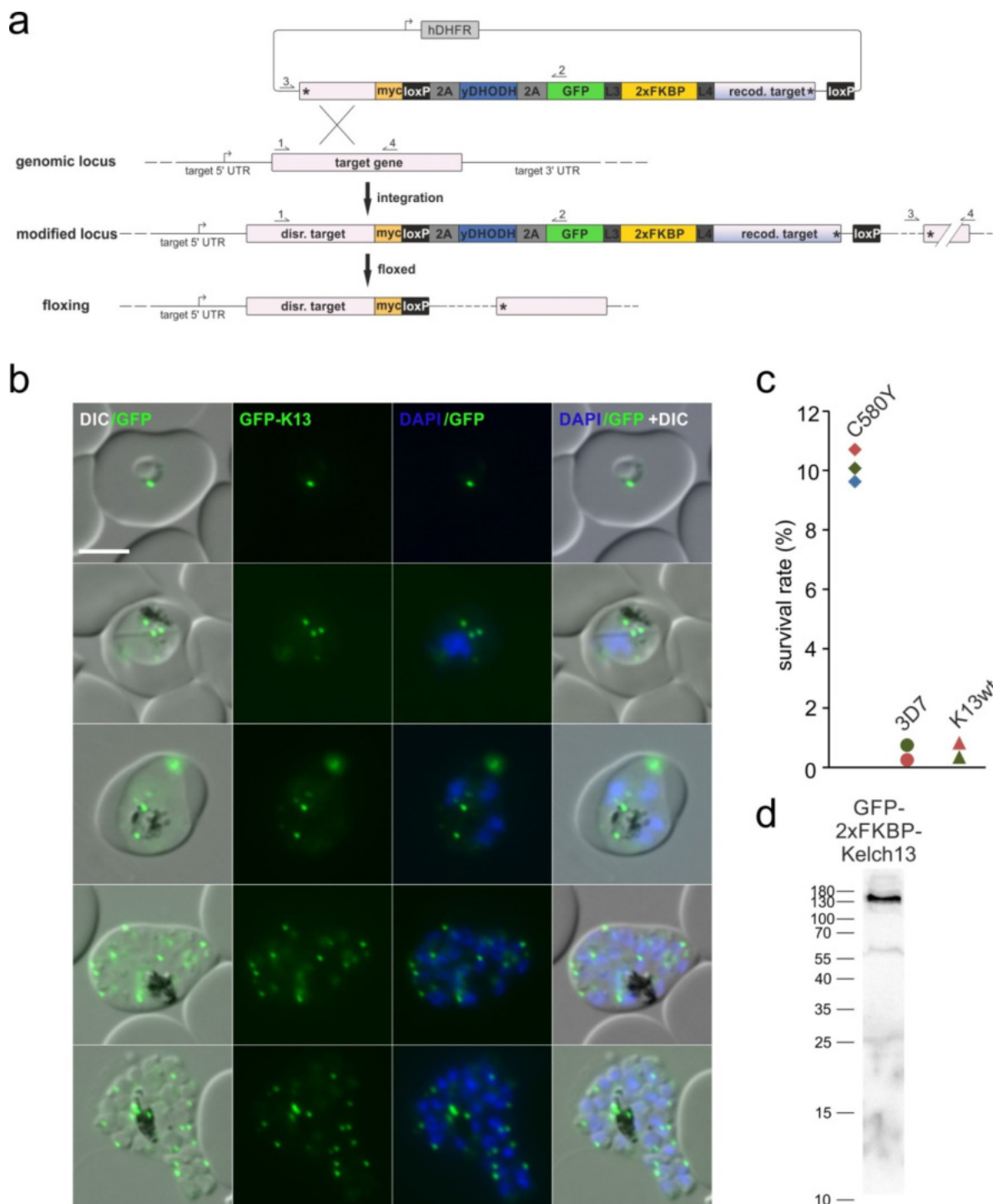
Initially it was attempted to fuse the endogenous gene in its genomic locus with *2xfkbp-gfp* at its 3' end. However, all four attempts using SLI failed and no parasites with the correct integration could be recovered. In line with this, no parasite cell line with a truncated *kelch13* gene could be obtained in 6 attempts by SLI-TGD. Hence, the protein was considered to be essential for the asexual blood stages and tagging of the C-terminus likely interferes with its physiological function.

Consequently we tested an N-terminal tagging approach (Figure 32a) for which we adopted a previously used strategy to obtain N-terminally tagged Rab7 (Flemming, 2015). With this approach the endogenous copy of the *kelch13* gene is truncated while at the same time a codon changed functional copy, separated by a skip peptide (Straimer et al., 2012; Szymczak et al., 2004), is provided. The functional copy was fused to *gfp-2xfkbp* at the 5' end. Moreover we placed loxP sites 5' and 3' of the codon adjusted version, allowing the excision of the gene via the diCre system (see 1.3.2) (Andenmatten et al., 2013; Collins et al., 2013; Jullien et al., 2007; Jullien et al., 2003). Additionally, in contrast to the previously used system (Flemming, 2015), DHODH as a second selectable marker (Ganesan et al., 2011) was linked to a skip peptide and added to the expression cassette, making the N-terminal integration approach amenable to SLI. The integration into the correct genomic locus was assessed by PCR and a band of the expected size of 138 kDa was observed on western blot (Figure 32d).

The *kelch13* protein was located in one to several foci in the cytosol of all asexual blood stages of the parasite. At least one focus was always found in close proximity to the food vacuole (Figure 32b). In the ring stage the focus of Kelch13 was constantly moving. In the trophozoite stage most foci were at a fixed position in the parasite, whereas single foci still showed movement. Movement of foci was not observed in later stages.

The C580Y mutation of the *kelch13* protein has been demonstrated to confer resistance to artemisinin and its derivatives (Ariey et al., 2014). A second knock-in cell line was generated carrying this modification in the newly inserted and functional copy of Kelch13 (GFP-2xFKBP-Kelch13^{C580Y}). Integration into the correct genomic locus was confirmed by PCR (Figure 11c). A ring stage survival assay (RSA) was performed (Witkowski et al., 2013). Expectedly, an increase survival rate of parasites harboring the mutation, compared to 3D7 and parasites containing the wild type GFP-2x-FKBP-K13 was found (Figure 32c). The level of resistance matched previously published results

(Straimer et al., 2015; Witkowski et al., 2013). This demonstrated that SLI can be used to test resistance alleles and that the copy of *kelch13* replacing the endogenous, truncated gene, is active.



C580Y knockin cell line (GFP-2xFKBP-Kelch13^{C580Y}). **d**) Immunoblot with protein extracts of GFP-2xFKBP-Kelch13 knock-in cell line (138 kDa) probed with rabbit anti-GFP.

To functionally assess the Kelch13 protein, a knock sideways was carried out with a cell line containing a nuclear mislocalizer. Upon addition of rapalog the protein was efficiently transferred into the nucleus with only faint foci remaining in the cytosol (Figure 33a). Surprisingly, in a growth assay no difference to the control was observed (Figure 33b). Quantification of the mislocalized protein showed that approximately 90% of Kelch13 was relocated to the nucleus (Figure 33c), indicating that small amounts of the protein are sufficient for parasite survival.

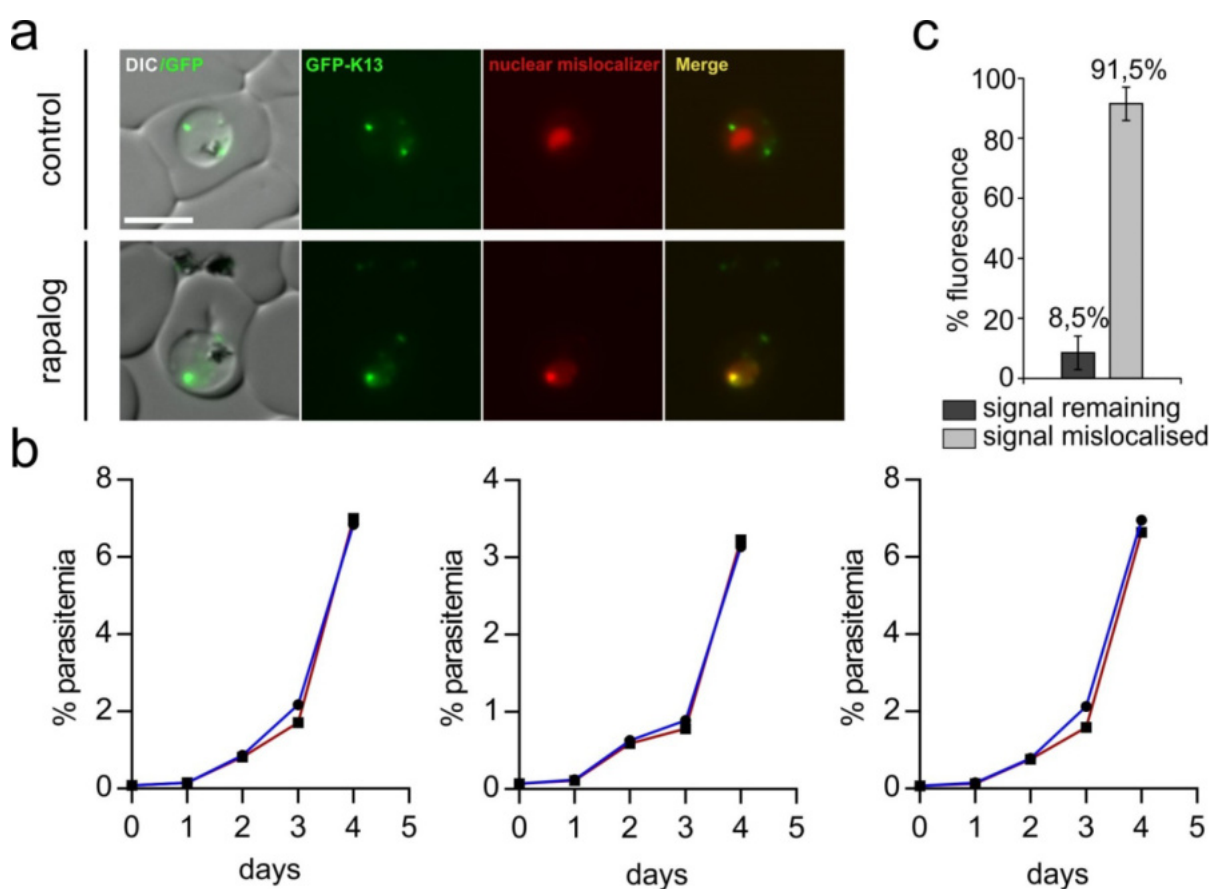


Figure 33 | KS of GFP-2xFKBP-Kelch13. **a**) Live cell fluorescence images of the control and rapalog treated parasites after 16 h. Parasites were transfected with an episomal plasmid expressing a 1xNLS-FRB-mCherry mislocalizer. Size bar, 5 μ m. **b**) FC growth curves from 3 independent experiments over 5 days showing development of control and the culture grown in the presence of 250 nM rapalog. **c**) Quantification of mislocalized FKBP-K13 (n = 10, error bars show SD).

For genomic excision of the functional copy of the *kelch13* gene, diCre was inducibly activated by addition of rapalog. Quantification of the fluorescence intensity showed that the Kelch13 protein was still detectable up to 3 days after initiation of diCre based excision of the active *kelch13* gene (Figure 34a). In agreement with this, a reduced growth compared to the control was observed on day 3 of the growth assay (Figure 34b). Thereafter growth stopped and only ring stage parasites were visibly in the rapalog treated culture. In contrast, the control grew normally and showed all stages (Figure 34a).

western blot (Figure 11c and Figure 35d). In the KS experiment with this version of the Kelch13 protein (2xFKBP-GFP-2xFKBP-K13), mislocalization into the nucleus was complete (Figure 35a) and resulted in a rapid growth defect in the growth assay (Figure 35b). To more closely analyze the stage of the growth defect, knock sideways was initiated in synchronized ring stage parasites. In these parasites an instant arrest in the ring stage was observed, whereas control parasites grew normally and turned into trophozoites followed by transition to schizonts (Figure 35c). Similarly to the result observed in the diCre *kelch13* gene-elimination experiment, the parasites turned into condensed forms over a time frame of several days. Thus, the phenotype was reproduced, but KS showed a dramatically faster response time than the diCre based gene excision.

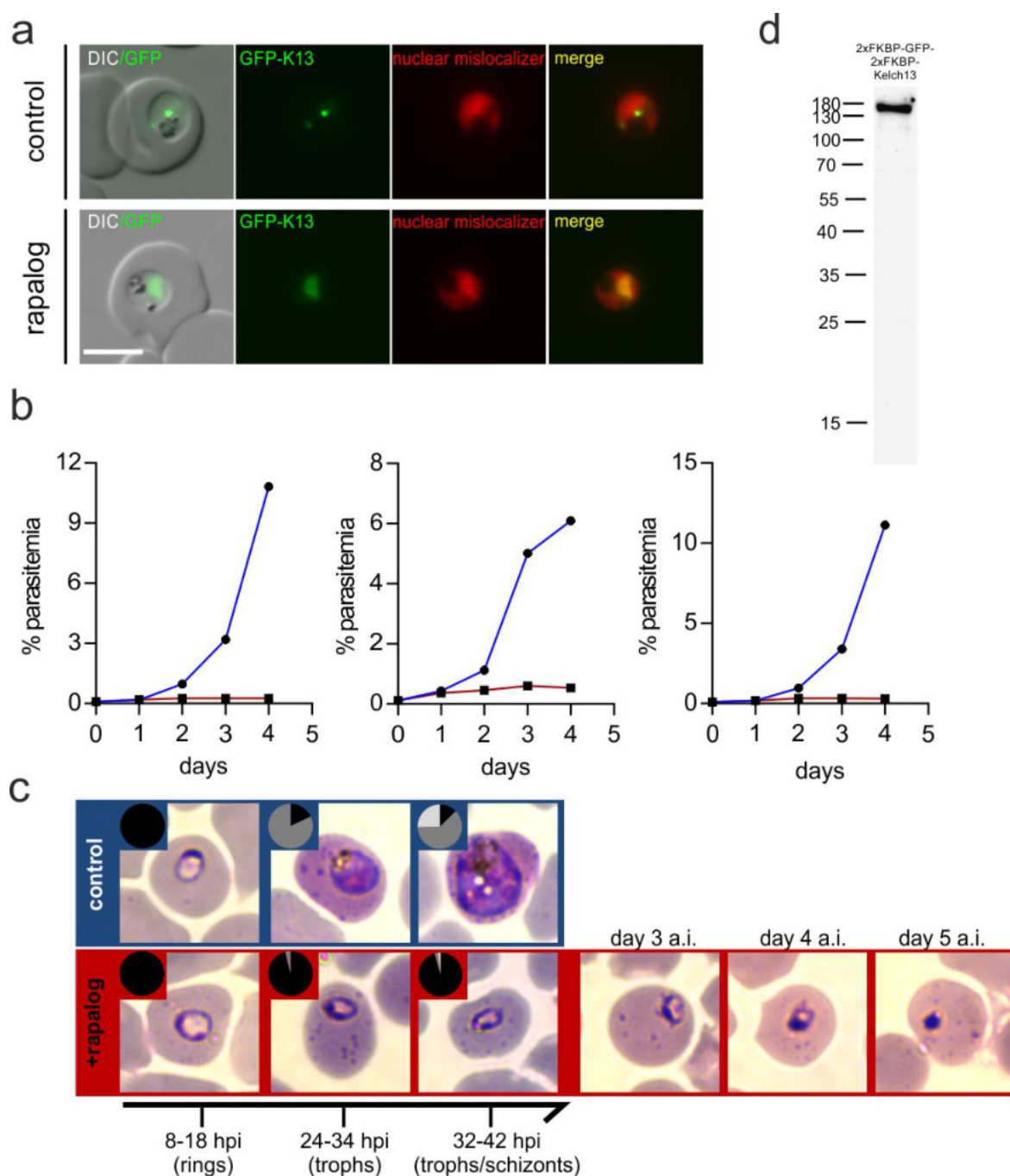


Figure 35 | KS of 2xFKBP-GFP-2xFKBP-Kelch13. **a)** Live cell images of control and rapalog treated parasites 16 h after addition of rapalog. The knock-in cell line was transfected with an episomal plasmid expressing 1xNLS-FRB-mCherry. **b)** FC growth curves from 3 independent experiments over 5 days showing development of control and culture treated with 250 nM rapalog. **c)** Giemsa smears of synchronized parasites grown in the presence (rapalog) or absence (control) of rapalog. Timeline and expected stages are indicated below. Pie charts show quantification of the proportion of stages observed (black, rings; dark gray, trophozoites; light gray, schizonts; n = 119, 105 and 117 control cells and 120, 184 and 118 rapalog-treated cells for the 8–18, 24–34 and 32–42 hours post invasion (hpi) time points, respectively; one representative of 3 independent experiments is shown. Condensation of arrested rings is shown for days 3, 4 and 5 after induction of the KS (a.i.). **d)** Immunoblot with protein extracts of 2x-FKBP-GFP-2xFKBP-Kelch13 knock-in cell line (165 kDa) probed with rabbit anti-FKBP. DIC, differential interference contrast; DAPI, parasite nuclei; merge, merged red and green signal. Scale bars, 5 μ m.

Moreover, a cell line was created where simultaneous nuclear mislocalization and diCre-based excision was possible, leading to the phenotype observed with the KS or the diCre mediated gene excision (Figure 36). In contrast to the diCre induced gene deletion, an immediate effect on the rapalog treated cell line was observed, visible in fluorescence images (Figure 36b) and in the FC growth assay (Figure 36a). Hence, the combination of KS (here with the nuclear mislocalizer) and diCre provides a further option, if the diCre strategy or KS alone are insufficient to achieve a sufficient and fast enough response with difficult targets.

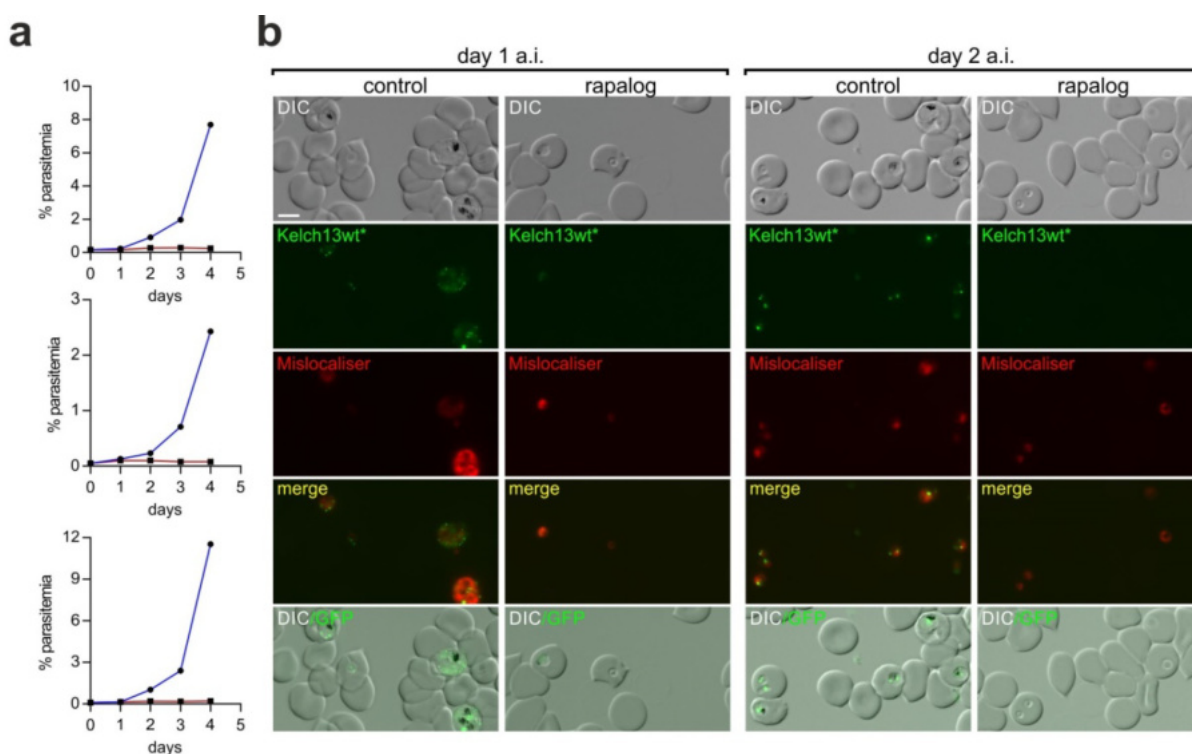


Figure 36 | Simultaneous diCre-based excision and KS of Kelch13. **a)** FC growth curves from 3 independent experiments over 5 days showing development of control and culture treated with 250 nM rapalog. The 2xFKBP-GFP-2xFKBP-Kelch13 cell line was transfected with a plasmid leading to the simultaneous expression of 1xNLS-FRB-mCherry and diCre and subsequent simultaneous KS and excision of the target. **b)** Live cell images of untreated (control) and rapalog treated parasites one or two days after induction of diCre-based excision and KS (images shown are from one of four independent experiments). All GFP fluorescence images were taken with the same exposure time. DIC, differential interference contrast; merge, merged red and green signal.

3.4 Co-localization of Kelch13 with different cellular markers

To characterize the localization of the Kelch13 protein in more detail, co-localization experiments were carried out with markers for food vacuole proximal compartments and with markers relevant for the supposed altered PI3P levels and increased expression of unfolded protein response pathways in artemisinin resistant parasites (see 1.1.3.1) (Mbengue et al., 2015a; Mok et al., 2015) The markers (including markers for the endoplasmic reticulum (ER), Golgi apparatus, PI3P, and Apicoplast) were transfected as mCherry fusions into the cell line expressing GFP-2xFKBP-Kelch13 from the endogenous locus (section 1.3).

3.4.1 Kelch13 does not localize to the endoplasmic reticulum

Two different markers were used for co-localization with the ER. In order to visualize the ER lumen, the K13 cell line was transfected with a construct marking the ER (Kulzer et al., 2009). This construct consists of a signal sequence, mScarlet and a C-terminal ER retention signal (SDEL) (Munro and Pelham, 1987). For detection by fluorescence microscopy, the recently published red fluorescent protein mScarlet (Bindels et al., 2017) was used instead of mCherry. Fluorescence microscopy of this parasite line revealed that the Kelch13 protein was often found in close proximity to the ER, but in the majority of cells did not co-localize (Figure 37).

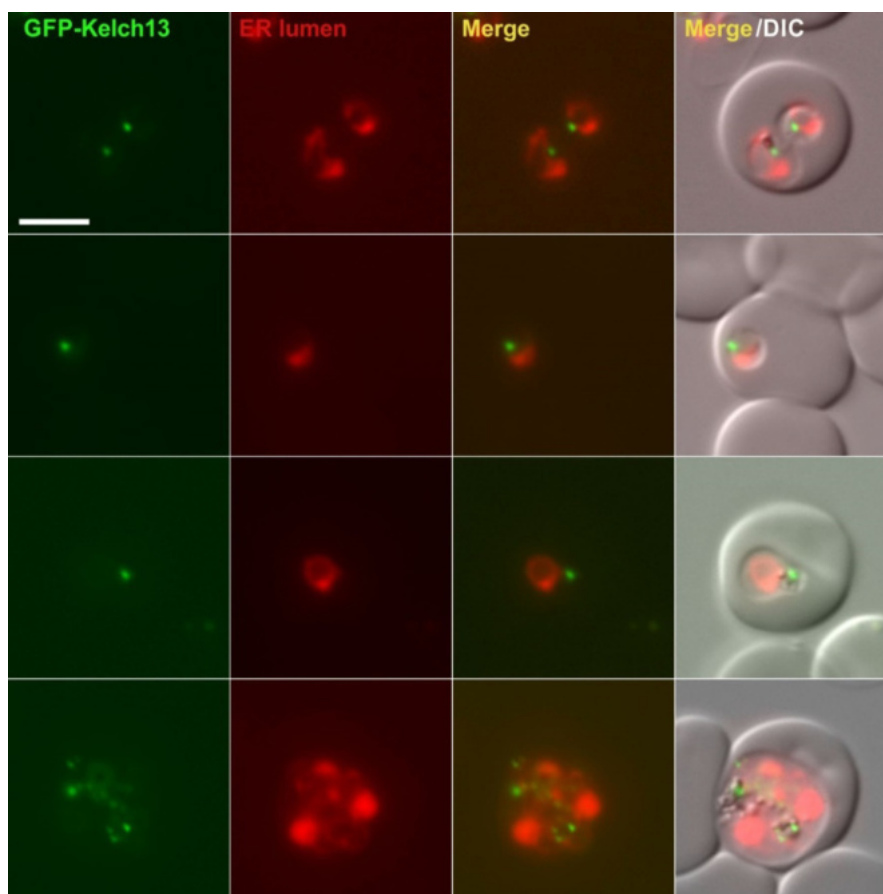


Figure 37 | Kelch13 does not co-localize with an endoplasmic reticulum marker. Live cell images of the GFP-2xFKBP-Kelch13 knock-in cell line transfected with an episomal plasmid expressing Stevor1-30-mScarlet-SDEL that marks the ER lumen. Merge, GFP + mCherry signal; DIC, differential interference contrast; Size bar, 5 μ m.

To evaluate if Kelch13 overlaps with transitional ER sites the marker Sec13p was used. The transitional ER (tER) sites, important for vesicle transport from ER to Golgi are part of the COPII complex (Deponte et al., 2012; Salama et al., 1993; Struck et al., 2008). Evaluation of the K13 GFP signal with the mCherry signal of Sec13p showed no co-localization with the tER (Figure 38).

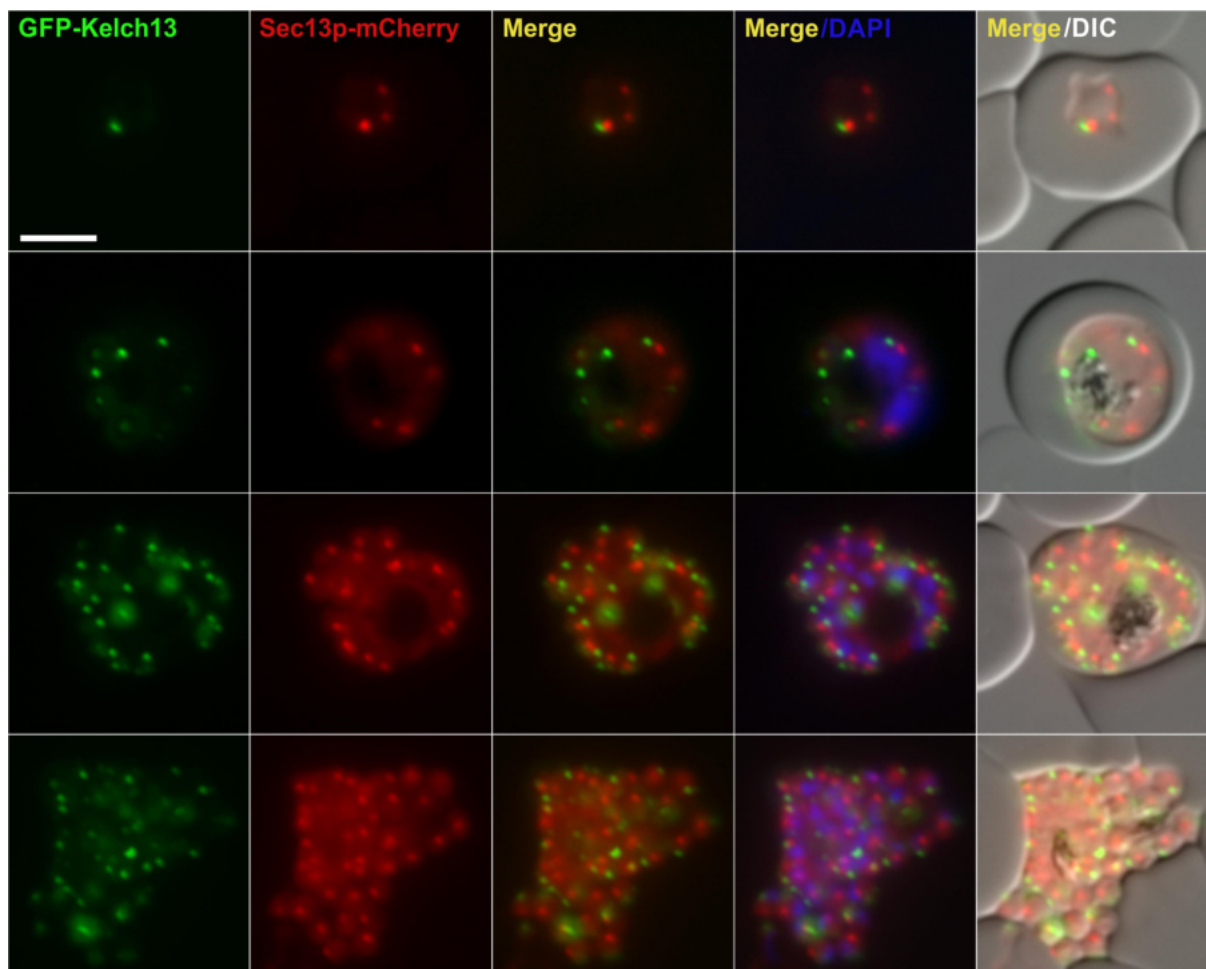


Figure 38 | Kelch13 does not co-localize with the Sec13p. Live cell images of the GFP-2xFKBP-Kelch13 knock-in cell line episomally expressing Sec13p-mCherry. Merge, GFP + mCherry signal; DIC, differential interference contrast; Size bar, 5 μ m.

3.4.2 Kelch13 does not co-localize with the Golgi apparatus

To evaluate the spatial organization of the Kelch13 protein in relation to the Golgi apparatus, the GFP-2xFKBP-Kelch13 knock-in cell line was transfected with the episomally expressed Golgi marking construct GRASP1-mCherry. The Golgi did not co-localize with the Kelch13 protein and was only unregularly found in close proximity in ring and trophozoite stages (Figure 39).

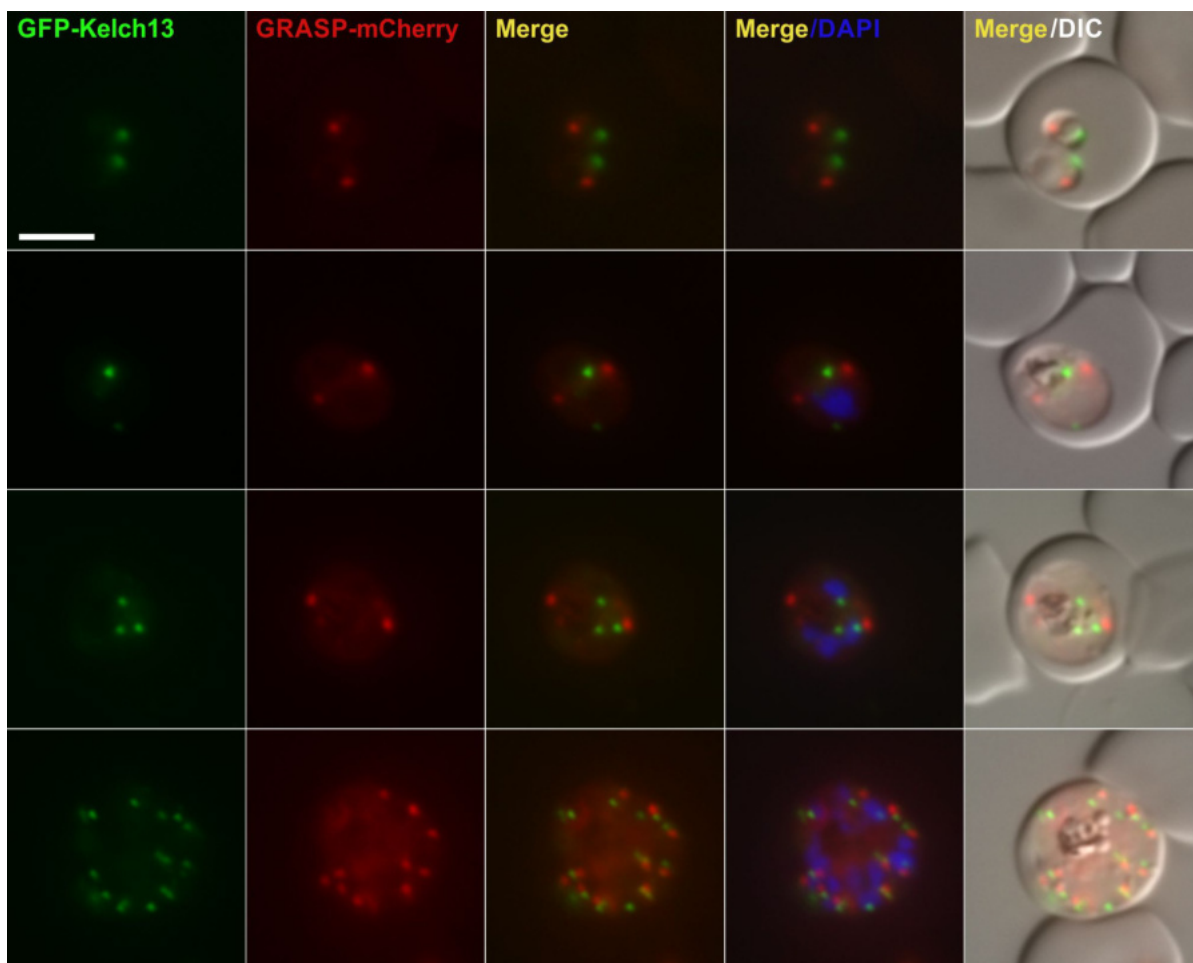


Figure 39 | Kelch13 does not co-localize with the Golgi apparatus. Live cell images of the GFP-2xFKBP-Kelch13 knock-in cell line transfected with episomally expressed GRASP1-mCherry. Merge, GFP + mCherry signal; DIC, differential interference contrast; Size bar, 5 μ m.

3.4.3 Kelch13 is often found close to PI3P positive compartments

PI3P was reported to be involved in the Artemisinin resistance mechanism (Mbengue et al., 2015a). Moreover it was shown to associate with the Apicoplast and the parasite's food vacuole (Flemming, 2015; Tawk et al., 2010). In order to evaluate if PI3P and the Kelch13 protein share the same compartment, the GFP-2xFKBP-Kelch13 knock-in cell line was transfected with the episomal PI3P reporter P40-mCherry (Boddey et al., 2016; Ponting, 1996). The Kelch13 protein was found close to or overlapping with the periphery of a PI3P positive compartment that corresponded to the food vacuole (as judged by the hemozoin evident in the DIC at this site) (Figure 40, arrows). Not all Kelch13 foci showed a co-localization with the PI3P marker and there were PI3P positive structures outside the food vacuole that did not overlap with Kelch13 foci (Figure 40).

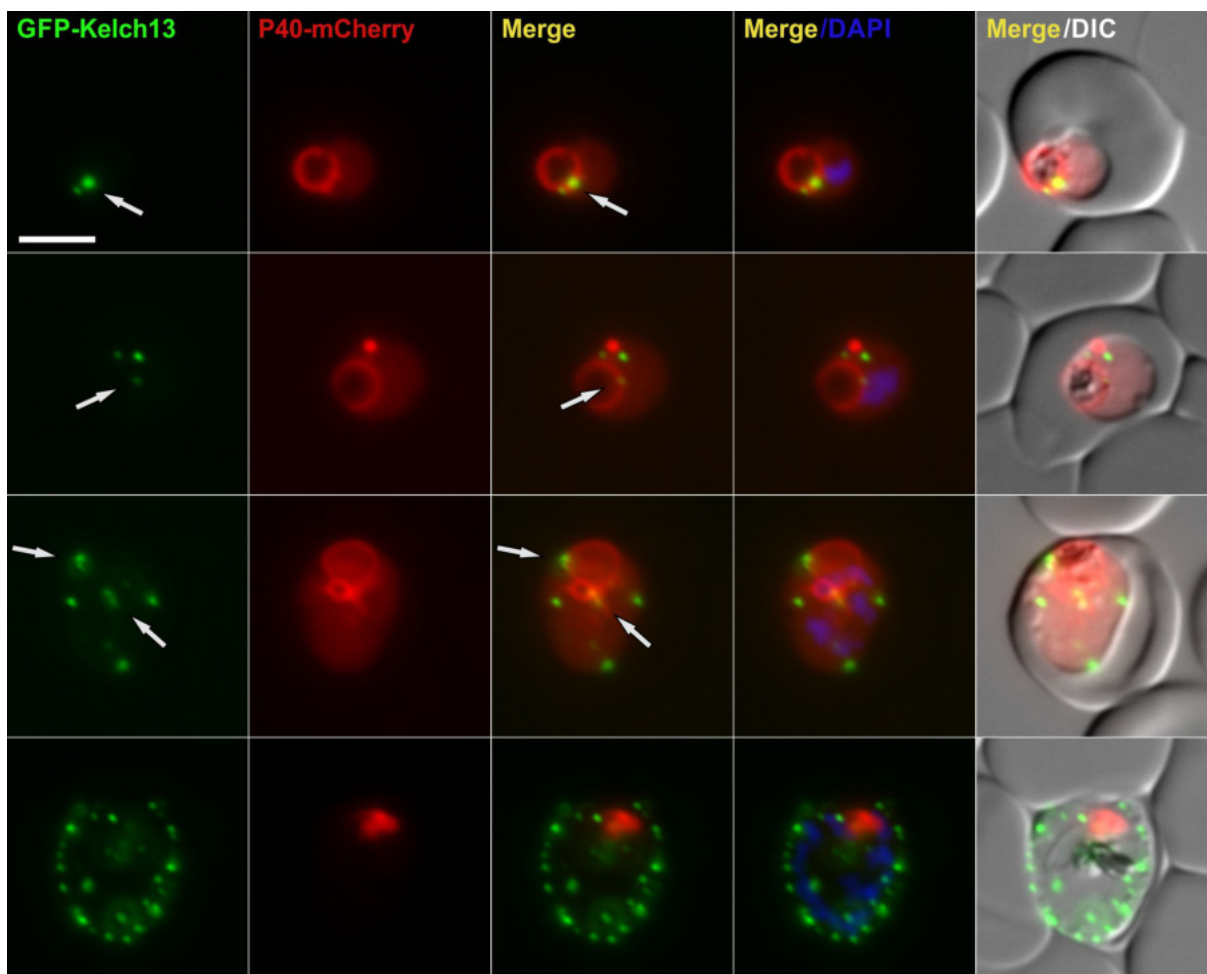


Figure 40 | Kelch13 shows partial co-localization with the PI3P maker P40. Live cell images of the GFP-2xFKBP-Kelch13 knock-in cell line transfected with an episomal plasmid expressing P40-mCherry that marks PI3P positive compartments. Arrows indicate sites of co-localization; Merge, GFP + mCherry signal; DAPI, parasite nuclei; DIC, differential interference contrast; Size bar, 5 μ m.

3.4.4 Apicoplast and K13 do not co-localize, but are often in close proximity

For co-localization with the Apicoplast the Kelch13 knock-in cell line was transfected with a plasmid to episomally express mCherry tagged acyl carrier protein (ACP) (Tonkin et al., 2004; Waller et al., 2000). In fluorescence images it was found that the Kelch13 protein did not co-localize with ACP-mCherry throughout all stages (Figure 41). However, at least one foci of the Kelch13 protein was frequently found in close proximity to the Apicoplast and in some cells seemed to overlap with the ACP signal (Figure 41). It cannot be determined from these experiments whether there is any true spatial link between Apicoplast and Kelch13 foci or whether this is coincidental due to the proximity of both of these structures with the food vacuole. Of note, and as described before, the structure of the Apicoplast was different from the structure seen with the PI3P marker, indicating that the Apicoplast is not always or in its entirety marked by the PI3P probe P40 (Flemming, 2015).

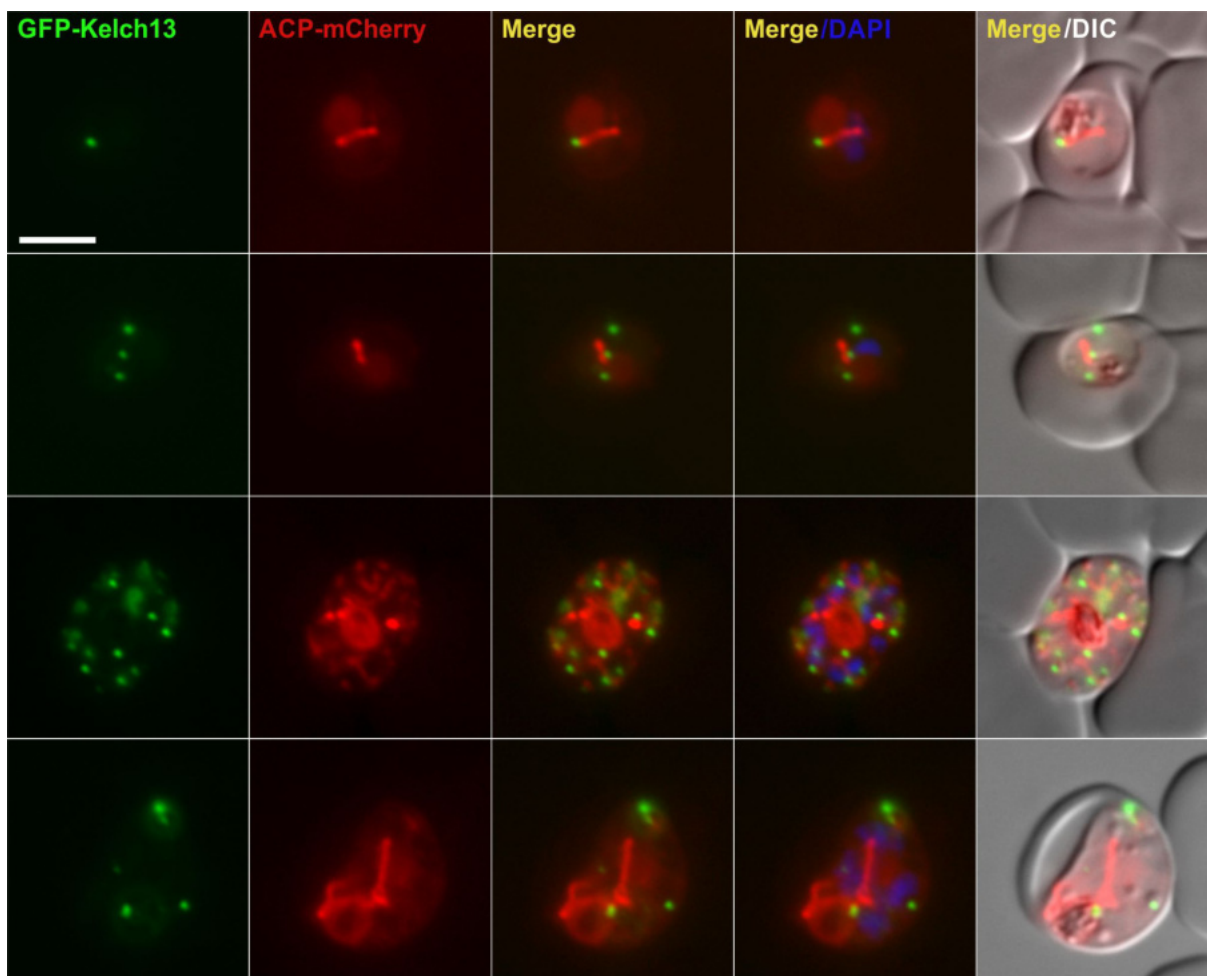


Figure 41 | Kelch13 foci are frequently in close proximity of the Apicoplast. Live cell images of the GFP-2xFKBP-Kelch13 knock-in cell line transfected with a plasmid expressing ACP-mCherry that marks the Apicoplast. Merge, GFP + mCherry signal; DAPI, parasite nuclei; DIC, differential interference contrast; Size bar, 5 μ m.

3.4.5 Kelch13 and the Kelch13-C580Y mutant display an identical localization

To examine if the resistance conferring C580Y mutation altered the localization of the Kelch13 protein, the GFP-2xFKBP-Kelch13^{C580Y} knock-in was co-transfected with a plasmid expressing mCherry-Kelch13^{wt}. As evident from a fluorescence microscopy analysis, the mutation did not lead to a change in subcellular localization (Figure 42). In some cells additional Kelch13^{wt} foci were found, but this could not be observed regularly (Figure 42, arrows).

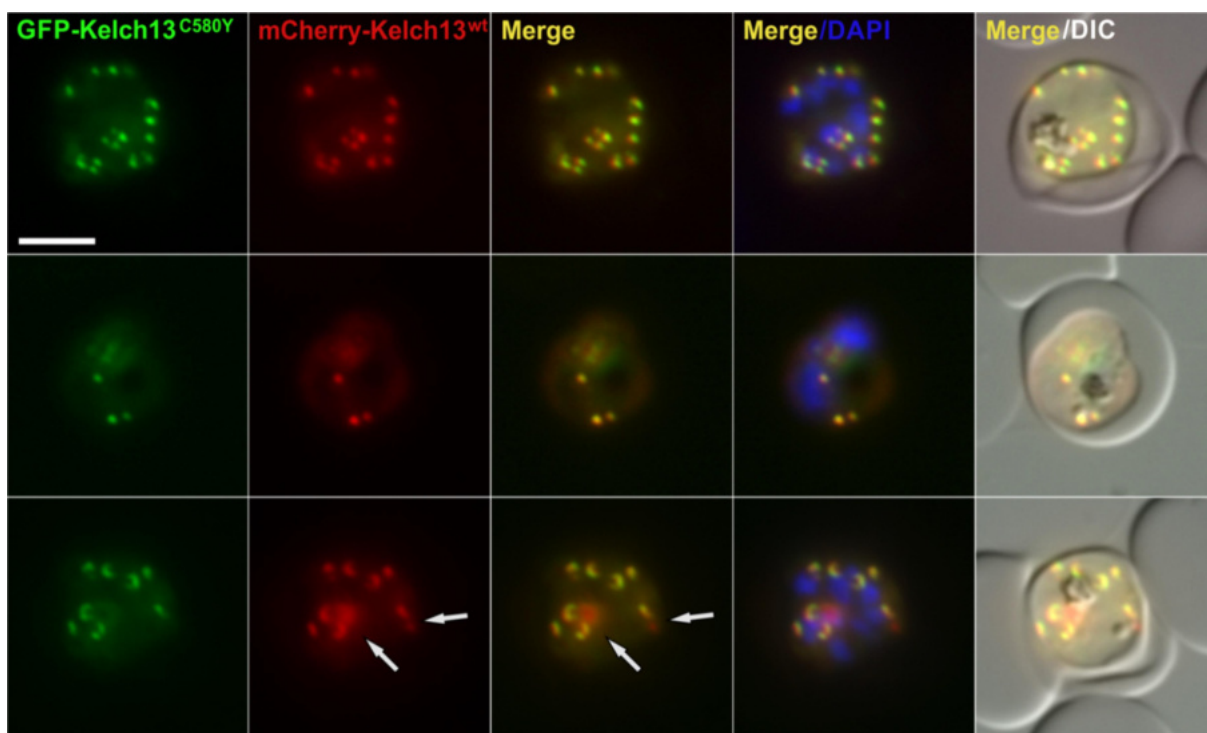


Figure 42 | Co-localization of the Kelch13-C580Y mutant with Kelch13wt. Live cell images of the GFP-2xFKBP-Kelch13^{C580Y} knock-in cell line transfected with an episomal mCherry-Kelch13^{wt} plasmid. Arrows indicate foci that could be attributed to overexpression of mCh-Kelch13wt. Merge, GFP + mCherry signal; DAPI, parasite nuclei; DIC, differential interference contrast; Size bar, 5 μ m.

3.5 Identification of potential interaction partners and compartment neighbors of the Kelch13

The identification of interaction partners and proteins localized to the same compartment can provide important clues to identify the function of proteins or protein complexes. As there are no known direct effectors of the Kelch13 protein, a method called BioID (biotin identification) (Blancke-Soares, 2016; Roux et al., 2012) was adapted to the FKBP-FRB heterodimerization approach in order to obtain the interactome of the Kelch13 protein.

The BioID method is based on proximity dependent labeling of proteins by the promiscuous biotin ligase BirA*. The *E. coli*-derived ligase bears the R118G mutation, leading to unspecific biotinylation of the amino acid lysine in a radius of approximately 10 nm, if biotin is present (Choi-Rhee et al., 2004; Cronan, 2005; Kim et al., 2016; Roux et al., 2012). Subsequently all biotinylated proteins can be purified by streptavidin beads and analyzed by mass spectrometry (Blancke-Soares, 2016; Roux et al., 2012).

To make BioID feasible for the quantitative approach comparing the same cell culture with or without BirA* dimerized onto the target, it was N-terminally fused to FRB-FRB-mCherry. The construct was kindly provided by Ernst Jonscher. It was assumed that for a quantitative and specific readout it is of advantage to have a low expression of the BirA construct, as excess unbound BirA could contribute to

background due to an increased biotinylation of unspecific proteins in the parasite. Hence, the 1000 bp 5' upstream region of the *sf3a2* gene (PF3D7_0619900) was chosen as promoter as it was previously shown to display very low expression levels (Le Roch et al., 2003). We termed the overall approach 'dimerization induced quantitative BioID' (DIQ-BioID) (Figure 43).

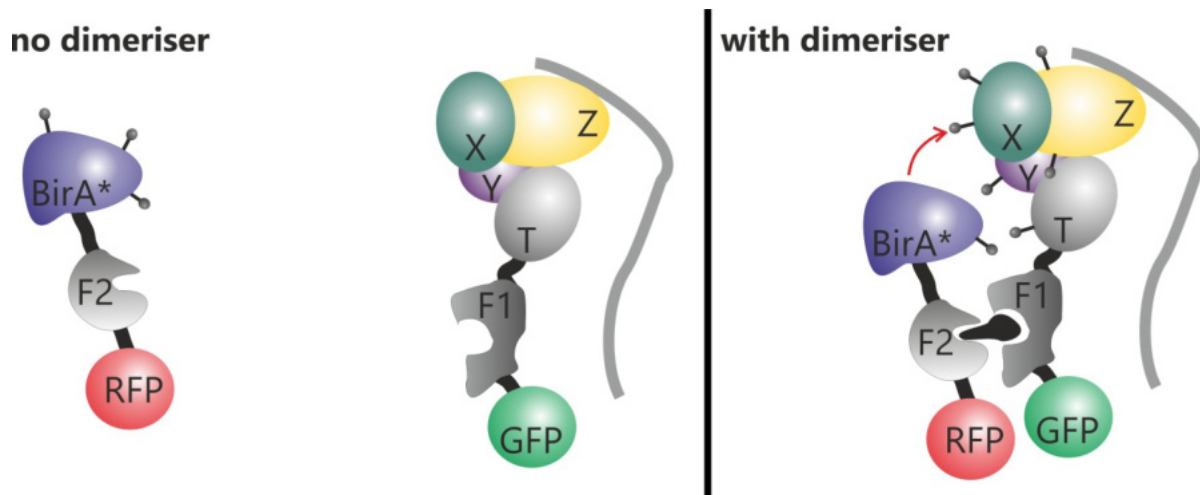


Figure 43 | Schematic of DIQ-BioID approach. Left side showing BirA construct and target protein without rapalog. Right side showing dimerization of BirA-FRB-mCherry with target protein. Pins indicate biotinylation of proximal proteins.. GFP, green fluorescence protein; RFP, red fluorescence protein; F1, FKBP domain; F2, FRB domain; T, target protein; X/Y/Z, different direct and indirect interaction partners of target protein, BirA*, promiscuous biotin ligase.

The BirA*-FRB-FRB-mCherry (BirA-nT) (Figure 44a) construct was found in the parasite cytosol with a mild enrichment in the nucleus in some cells (Figure 44b). This may be attributed to the DNA binding domain of the biotin ligase (Choi-Rhee et al., 2004; Kim et al., 2016). Addition of rapalog to the parasite cell line led to dimerization of FRB with the Kelch13 FKBP domains as evident from a relocation of the complete pool of BirA* to the GFP-2xFKBP-Kelch13 foci (Figure 44b).

A culture was split in 250 nM rapalog-treated and control. Both were incubated for 24 h after addition of biotin. Whole cell lysates were prepared and western blot showed biotinylation of proteins by probing with streptavidin-HRP (Figure 44c). A band at approximately 140 kDa that was exclusively found in the rapalog treated cell line. This matches the size of the Kelch13 protein, with an expected molecular weight of 138 kDa. Except for the Kelch13 band control and rapalog-treated samples displayed an unspecific biotinylation pattern.

The BioID experiments were carried out as described in the material and methods section (see 2.2.3.4). The mass spectrometry samples were run and analyzed by Wieteke Hoeijmaker (Bartfai Lab, Radbound University, Netherlands).

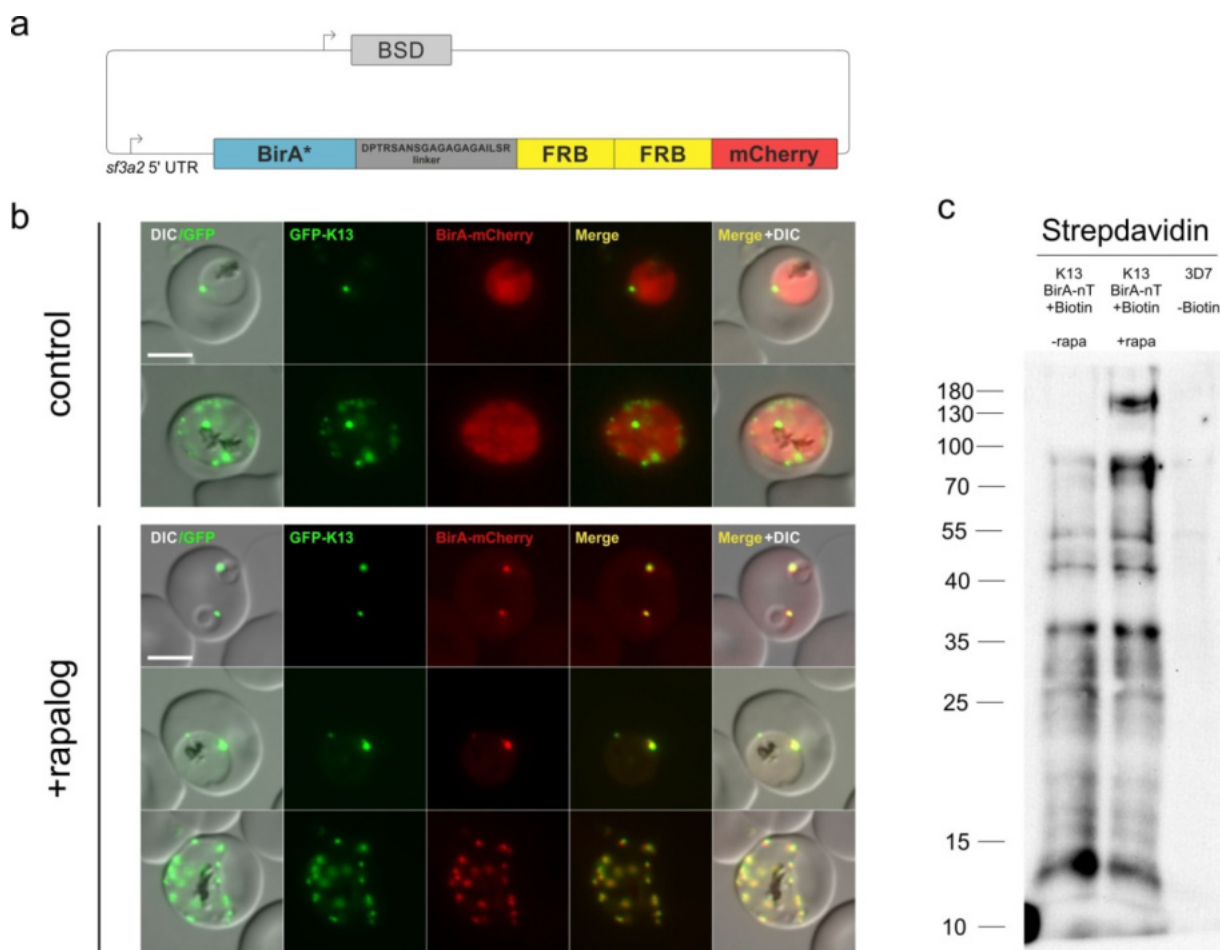


Figure 44 | Dimersation of Kelch13 with BirA. **a)** Schematic of the construct BirA-nT used for DIQ-BioID. **b)** Live cell imaging of GFP-2xFKBP-Kelch13 transfected with episomally expressed BirA-nT. Images show control and rapalog treated parasites after 16 h. **c)** Western blot analysis of control (referred to as -rapa) and rapalog treated culture after 24 h incubation with biotin. Rapalog and biotin were added at the same time. Samples were probed with streptavidin-HRP. 3D7 is the negative control. K13, GFP-2xFKBP-Kelch13; rapa, rapalog; Size bar, 5 μ m.

The experiment was performed in two biological replicas. The results are displayed in plots with enrichment of rapalog treated culture over the control. The replicas are plotted as log₂-normalized ratio on x and y axis (Figure 45, Table 1). The significance of the single hits is indicated by different colors in the plot. In this plot the significance is equivalent to the false discovery rate (FDR) that describes the expected proportion of false hits amongst all hits. 8 proteins were identified with an FDR < 10⁻¹⁰ and 20 proteins down to an FDR of < 10⁻² (Figure 45). The hit identified with highest enrichment in the rapalog treated culture over the control in both replicas is the Kelch13 protein (Figure 45, Table 1). This verifies that the BirA construct was dimerized to Kelch13 and the biotinylation was successful.

14 out of the top 20 hits were proteins annotated as of 'unknown function', indicating that the process is unique to *Plasmodium spp.* or *Apicomplexa*. Proteins found with homologies to known gene products included the metacaspase-like protein (MCA2), a protein annotated in PlasmodB as formin 2 and ubiquitin carboxyl-terminal hydrolase 1 (UBP1). UBP1 has previously been linked to artemisinin

resistance (Borrmann et al., 2013; Cerqueira et al., 2017; Hunt et al., 2007; Hunt et al., 2010) and hits 8 (PF3D7_1138700) and 9 (PF3D7_0609700) were identified as Kelch13 interaction partners in a genome wide 2-hybrid screen (LaCount et al., 2005). Overall this suggests that the hit lists consist of viable candidates interacting with Kelch13 or contributing to the function of the same biological process.

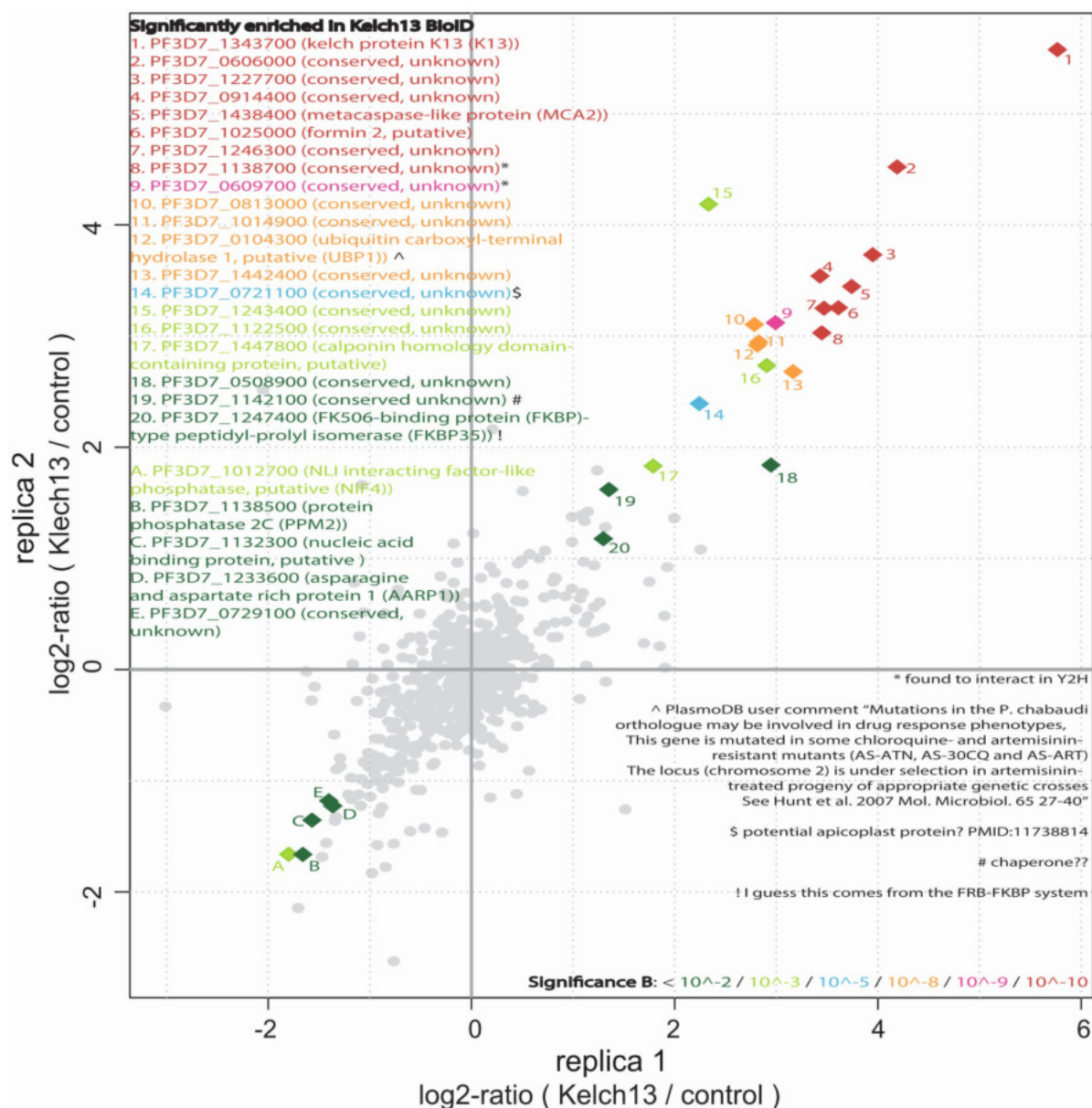


Figure 45 | Scatterplots of DIQ-BioID with Kelch13. Plotted are the log₂-ratios of rapalog-treated culture over the control (referred to as Kelch13/control) obtained from duplicates. Significance (=FDR) of the hits is indicated by a color code in the bottom part of the plot with red equaling a significance of 10⁻¹⁰. Numbers marking the diamonds in the plot correspond to the numbers and ID of proteins displayed on the left side.

Table 1 | Top hits identified by DIQ-BioID. Table shows the protein IDs identified with the highest significance in a log₂-ratio. Number of peptides gives the absolute number of peptides identified for each hit in both replicas. Column assigned as indicates the given Kelch13 BioID number to the corresponding protein ID.

Protein ID	Product description	log ₂ ratio Kelch13 / control		Number of peptides	Assigned as
		replica 1	replica 2		
PF3D7_1343700	Kelch protein K13	5,766	5,576	49	-
PF3D7_0606000	conserved, unknown	4,189034	4,520819	64	KBI.1
PF3D7_1227700	conserved, unknown	3,948881	3,731225	46	KBI.2
PF3D7_0914400	conserved, unknown	3,430553	3,539939	9	KBI.3
PF3D7_1438400	metacaspase-like protein, MCA2	3,741467	3,445802	31	KBI.4
PF3D7_1025000	formin 2, putative	3,610464	3,254565	30	-
PF3D7_1246300	conserved, unknown	3,469625	3,250303	17	KBI.5
PF3D7_1138700	conserved, unknown	3,447315	3,028793	30	KBI.6
PF3D7_0609700	conserved, unknown	2,991626	3,120043	24	KBI.7
PF3D7_0813000	conserved, unknown	2,783687	3,103829	14	KBI.9
PF3D7_1014900	conserved, unknown	2,828022	2,946305	103	KBI.10
PF3D7_0104300	Ubiquitin carboxyl-terminal hydrolase 1	2,814161	2,91866	50	KBI.8
PF3D7_1442400	conserved, unknown	3,165365	2,679642	36	KBI.11

3.6 Validation DIQ-BioID approach by tagging of potential interaction candidates

To confirm the results from the Kelch13 BioID (KBI) experiments the top 13 significantly enriched candidates, with the exception of the Formin2 (already analyzed by Flemming, 2015), were selected to be fused to 2xFKBP-GFP-2xFKBP in their endogenous genomic locus by using SLI (Table 1). Apart from MCA2 which likely cannot be C-terminally tagged, all integrations were obtained. For KBI.8, only an integration with the 2xFKBP-GFP tag but not 2xFKBP-GFP-2xFKBP tag was successful (Table 1).

To evaluate the co-localization with the Kelch13 protein, the cells lines of the GFP tagged candidate knock ins were co-transfected with the episomally expressed mCherry-Kelch13 construct and analyzed by fluorescence microscopy. To identify the essential genes among the KBI candidates SLI-TGD was attempted. The candidates suggested to be essential by SLI-TGD, in addition to 3 non-essential controls, were then further analyzed by KS.

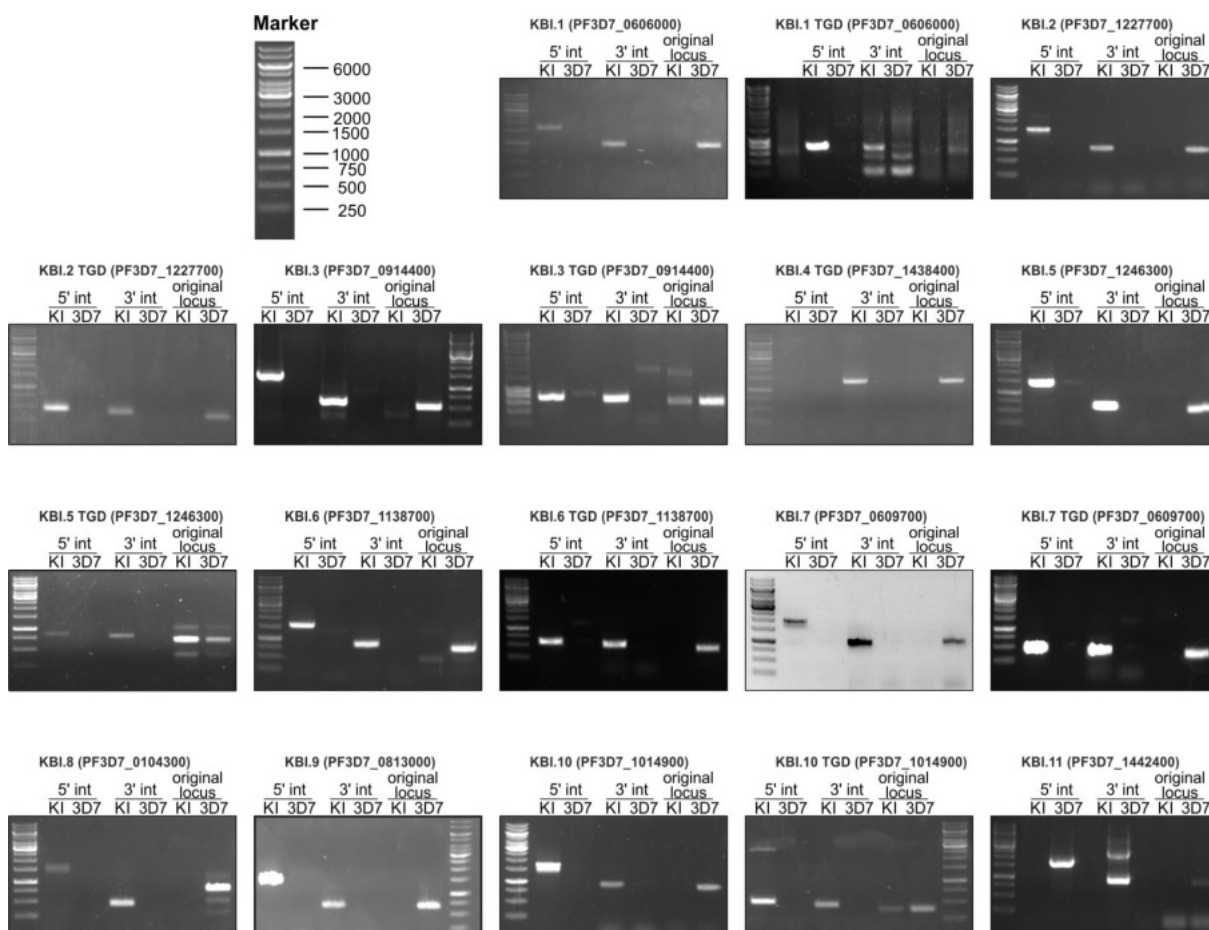


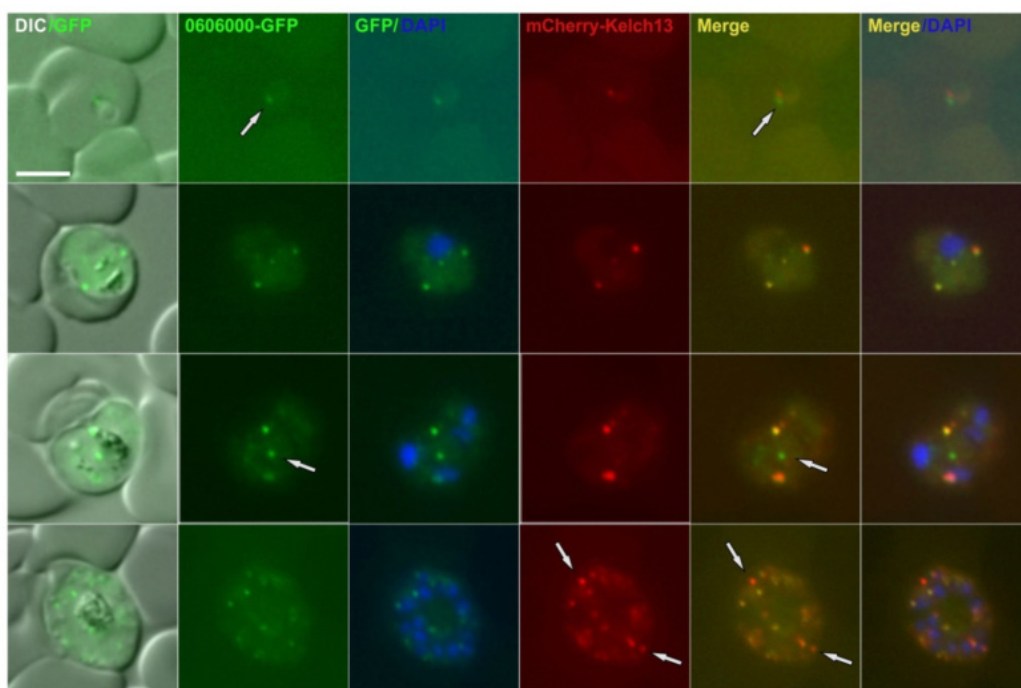
Figure 46 | Integration checks of KBI candidates. Integration checks for integration cell lines generated by SLI. For all cell lines with C-terminal tagging the pSLI-sandwich vector was used except of KBI.8 (PF3D7_0104300) that was tagged with 2xFKBP-GFP. Agarose gels with PCR products from genomic DNA of each parasite line indicated above the gels. The primers used are indicated in figure 7. Primers spanning the 5' prime junction were 1+2, spanning the 3' junction were 3+4 and correspond to 5' int and 3' int, respectively. Absence of original locus, showing that no parasite with wild type locus remained, was confirmed by combination of primers 1+4. Sizes of the marker bands are shown in the first panel from the top. KI, knock-in cell line; 3D7, wild type parasite line; TDG, targeted gene disruption using SLI.

3.6.1 KBI Candidate 1 PF3D7_0606000

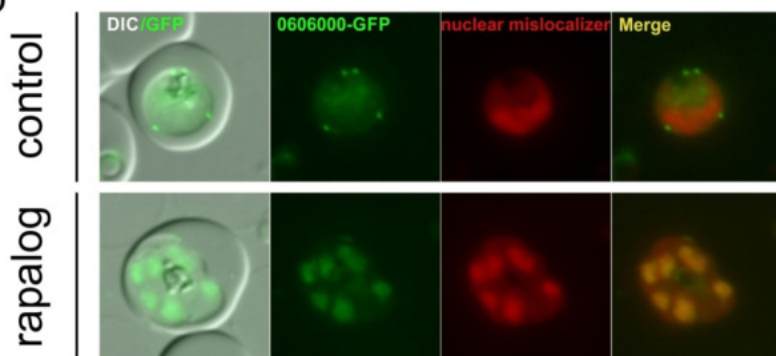
PF3D7_0606000 is a protein of 1063 AA. No functional domains or homologies to known proteins could be assigned using bioinformatic searches (Section 2.2.6). The gene was fused to *2xfkbp-gfp-2xfkbp* using SLI and the correct integration was confirmed by PCR (Figure 46). KBI.1 is expressed in all asexual blood stages and showed a similar staining pattern like the Kelch13 protein with one or more foci found in proximity of the food vacuole (Figure 47a). The majority, but not all of

the KBI.1 foci co-localized with the Kelch13 foci (Figure 47a, arrows). In the ring stages foci not co-localizing with mCherry-Kelch13 were attributed to the already mentioned movement of the foci (see 3.3). Manual inspection of ring stage parasites under the fluorescence microscope showed an identical localization. In the trophozoite and schizont stage foci that were not overlapping could be seen in some of the cells (Figure 47a, arrows). KBI.1 tagged with 2xFKBP-GFP-2xFKBP was efficiently mislocalized using a nuclear mislocalizer (Figure 47b) and no growth defect was observed (Figure 47c). In line with that the gene encoding KBI.1 was successfully truncated by SLI-TGD (Figure 46). Hence, the protein is not crucial for the development of asexual blood stage parasites.

a



b



c

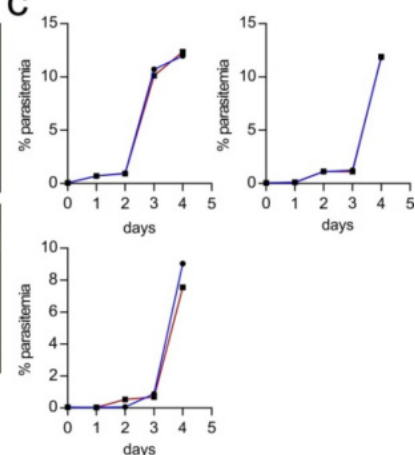


Figure 47 | Localization of PF3D7_0606000 (KBI.1) and co-localization with Kelch13. a) Panel shows representative live cell images of PF3D7_0606000-2xFKBP-GFP-2xFKBP knock-in cell line transfected with mCherry-Kelch13 for co-localization. Arrows indicate foci of KBI.1 or Kelch13 that are not co-localizing. **b)** Knock-in cell line transfected with an episomally expressed 1xNLS-FRB-mCherry mislocalizer. Live cell fluorescence images of control and rapalog-treated cells were taken after 16h. **c)** FC growth curves from 3 independent experiments showing development of control and culture treated with 250 nM rapalog. DIC, differential interference contrast; DAPI, parasite nuclei, Size bar, 5 μ m.

3.6.2 KBI Candidate 2 PF3D7_1227700

KBI.2 (PF3D7_1227700) is a protein of 771 AA. Blast search identified a homology to the *T. gondii* proteophosphoglycan PPG1, covering AA 321-615 (49 % similarity, 23% identities) (Section 2.2.6). Correct integration into the genome, leading to endogenous fusion of KBI.2 with the sequence coding for 2xFKBP-GFP-2xFKBP, was confirmed by PCR (Figure 46). The protein is expressed from ring stage to schizont stage (Figure 48). Most KBI2 foci co-localized with the K13 foci, but the relative intensity of the foci differed between KBI.2 and the Kelch protein (Figure 48). As the gene encoding KBI.2 could be disrupted with SLI-TGD (Figure 46), this protein is considered not to be essential for the parasite.

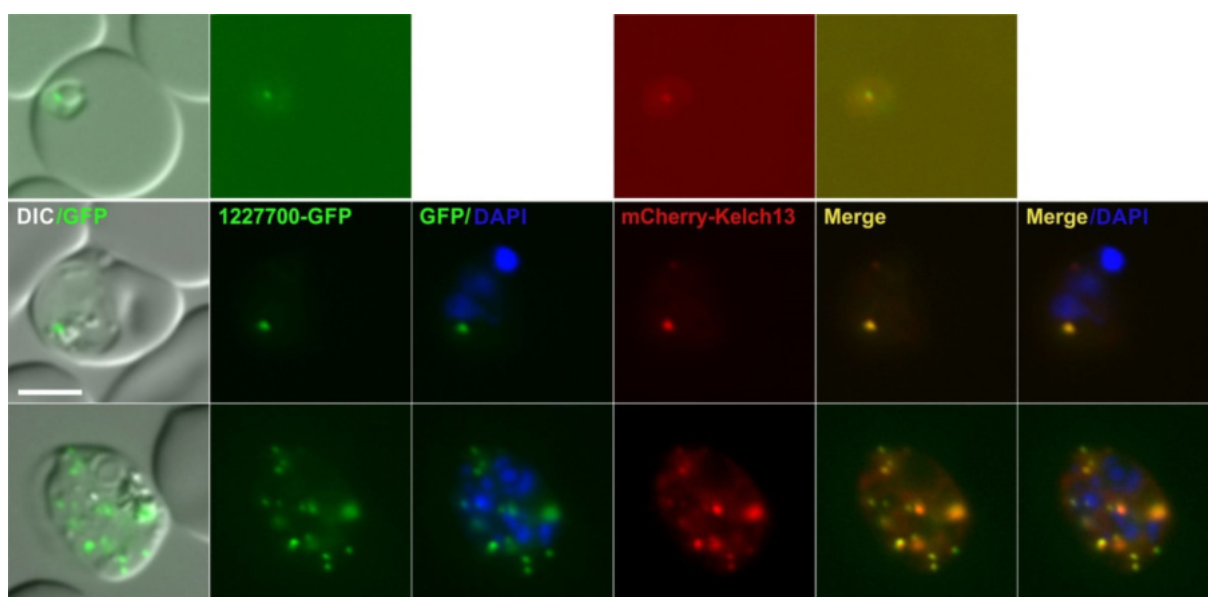


Figure 48 | Localization of PF3D7_1227700 (KBI.2) and co-localization with Kelch13. Panel shows representative live cell images of PF3D7_1227700-2xFKBP-GFP-2xFKBP knock-in cell line transfected with mCherry-Kelch13 for co-localization. Ring stages showed no DAPI signal, hence DAPI images were not included. DIC, differential interference contrast; DAPI, parasite nuclei, Size bar, 5µm.

3.6.3 KBI Candidate 3 PF3D7_0914400

PF3D7_0914400 encompasses 249 AA. No homology to known proteins or domains from other organisms could be identified (section 2.2.6). Integration into the correct genomic locus was assessed by PCR (Figure 46). The protein is expressed from ring to schizont stage and localized in foci (Figure 49). Candidate 3 co-localized with at least one Kelch13 focus in every cell but foci positive for either Kelch13 or KBI.3 alone were frequently observed (Figure 49). In late stages more foci were positive for both proteins, but the number of GFP foci exceeded the number of mCherry-K13 foci (Figure 49 bottom panel). The gene encoding for KBI.3 was disrupted by SLI-TGD (Figure 46). A band for original locus was detected by PCR in the integration cell line, but selection is still ongoing. Hence, the gene is not essential for development of asexual blood stages.

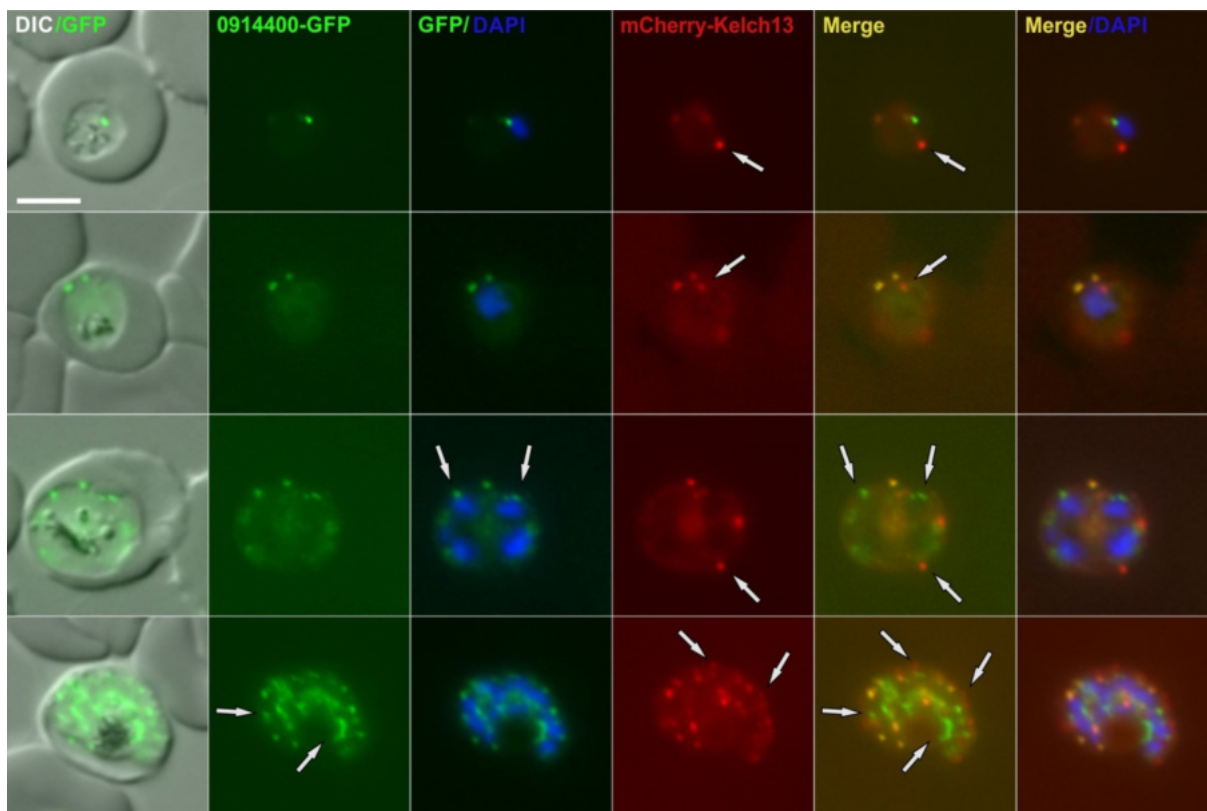


Figure 49 | Localization of PF3D7_0914400 (KBI.3) and co-localization with Kelch13. Panel shows representative live cell images of PF3D7_0914400-2xFKBP-GFP-2xFKBP knock-in cell line transfected with mCherry-Kelch13 for co-localization. Arrows indicate foci of KBI.3 or Kelch13 that are not co-localizing. DIC, differential interference contrast; DAPI, parasite nuclei, Size bar, 5 μ m.

3.6.4 KBI Candidate 4 PF3D7_1438400

KBI.4 is annotated as metacaspase-like protein (MCA2). Its gene product comprises 2020 AA. All attempts to fuse the gene under its endogenous locus with a sequence coding for 2xFKBP-GFP-2xFKBP or with the smaller 2xFKBP-GFP sequence failed, indicating that a C-terminal fusion had a detrimental effect on the parasites. Unexpectedly, truncation of the gene encoding KBI.4 was possible using SLI-TGD (Figure 46). This suggests that either the C-terminal fusion with the tag was not obtained for independent reasons (inaccessibility of this part of the gene to recombination) or that its C-terminal fusion has a dominant negative effect. It should be noted that other metacaspase-like proteins exist in the parasite and that these could take over some of the functions. Nevertheless, based on these data, the gene encoding KBI4 has to be considered as not essential for the growth of asexual blood stage parasites.

3.6.5 KBI Candidate 5 PF3D7_1246300

PF3D7_1246300 is a protein of 888 AA. In its C-terminal region, spanning from AA 643-883, a homology to adaptin c-terminal domain containing protein in *T. gondii* was detected by NCBI Blast (44% positives) (Section 2.2.6). The gene was fused to *2xfkbp-gfp-2xfkbp* using SLI and the correct integration was confirmed by PCR (Figure 46). Fluorescence imaging with the 2xFKBP-GFP-2xFKBP knock in cell line showed that KBI.5 localized in foci in a pattern similar to Kelch13 (Figure 50a,b). Co-localization experiments with K13 showed that both proteins were present in the same foci (Figure 50b). In the schizont stage the GFP signal showed a diffuse staining pattern and only few KBI.5 foci were co-localizing with Kelch13 (Figure 50b, bottom panel). The Kelch13 foci outnumbered the KBI.5 foci (Figure 50b, bottom panel). KS led to an efficient relocalization of the protein to the nucleus (Figure 50c), but no growth defect was observed (Figure 50d). The gene encoding for KBI.5 was truncated by SLI-TGD (Figure 46). A band for original locus was detected by PCR in the integration cell line, but selection is still ongoing. Hence, the gene is no essential for the parasite's asexual blood stages.

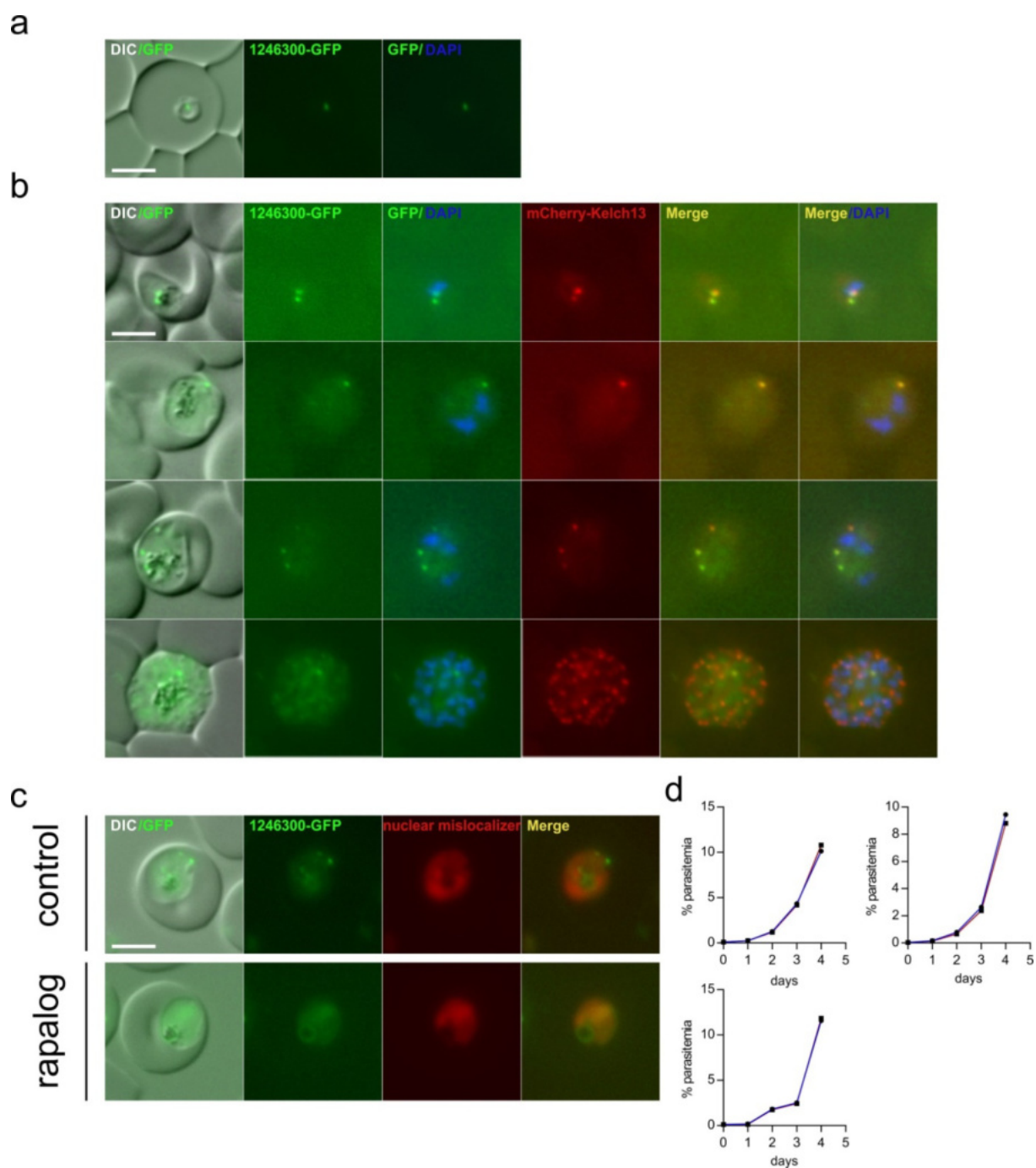


Figure 50 | Localization of PF3D7_1246300 (KBI.5) and co-localization with Kelch13. a-c) Panels show representative live cell images of PF3D7_1246300-2xFKBP-GFP-2xFKBP knock-in cell line **a)** Cell line stained with DAPI nuclear stain **b)** Knock-in cell line transfected with plasmid episomally expressing mCherry-Kelch13 for co-localization. **c)** Knock-in cell line transfected with an episomally expressed 1xNLS-FRB-mCherry mislocalizer. Live cell fluorescence images of control and rapalog-treated cells were taken after 16h. **d)** FC growth curves from 3 independent experiments showing development of control and culture treated with 250 nM rapalog. DIC, differential interference contrast; DAPI, parasite nuclei, Size bar, 5 μ m.

3.6.6 KBI Candidate 6 PF3D7_1138700

KBI.6 comprises 1870 amino acids. No domains or homologies to proteins of known function were found (Section 2.2.6). Integration into the correct genomic locus, leading to endogenous fusion of KBI.6 with the sequence coding for 2xFKBP-GFP-2xFKBP, was confirmed by PCR (Figure 46). PF3D7_1138700 was expressed throughout all asexual blood stages (Figure 51). It was localized in one to multiple foci, whereof one focus was always in close proximity to the food vacuole (Figure 51b). Most foci co-localized with the K13 protein (Figure 51b). Notably, and in contrast to other candidates such as KBI.9, a strong fluorescence intensity of Kelch13 foci positively correlated with a strong GFP signal of KBI.6. The gene was disrupted by using SLI-TGD (Figure 46) and thus is considered not to be essential for the asexual blood stages.

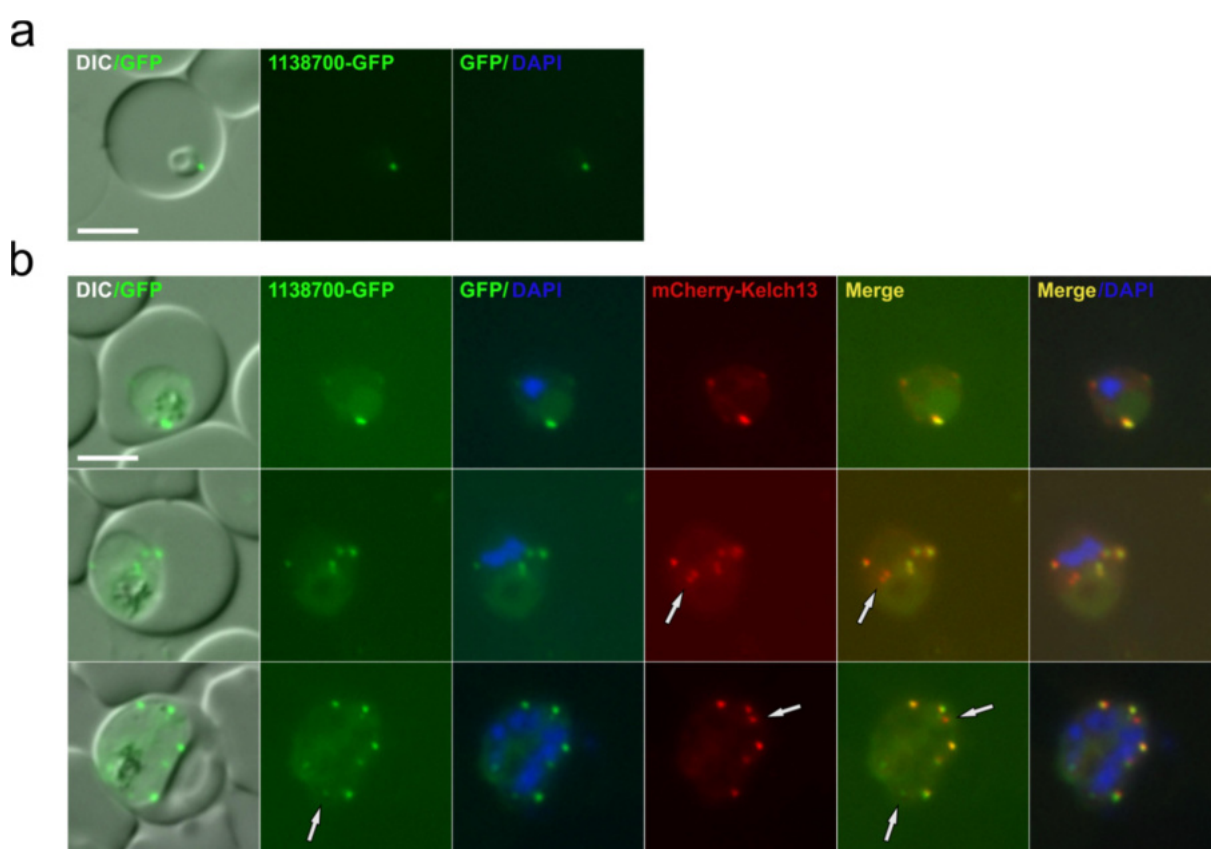


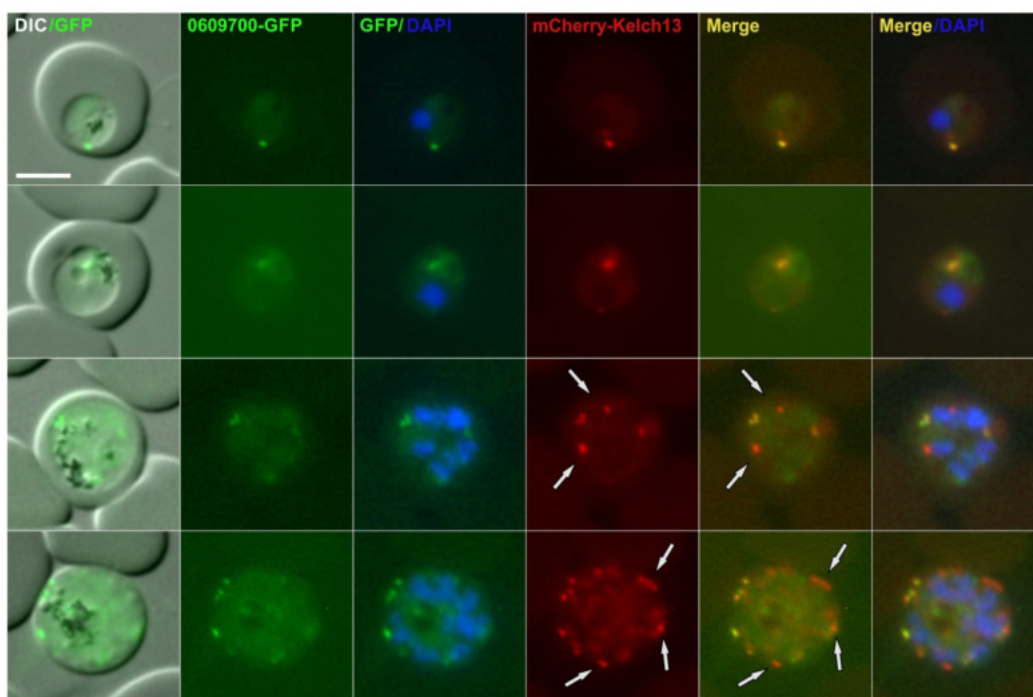
Figure 51 | Localization of PF3D7_1138700 (KBI.6) and co-localization with Kelch13. a,b) Panels show representative live cell images of PF3D7_1138700-2xFKBP-GFP-2xFKBP knock-in cell line **a)** Cell line stained with DAPI nuclear stain **b)** Cell line transfected with a plasmid episomally expressing mCherry-Kelch13 for co-localization. Arrows indicate foci of KBI.6 or Kelch13 that are not co-localizing. DIC, differential interference contrast; DAPI, parasite nuclei, Size bar, 5µm.

3.6.7 KBI Candidate 7 PF3D7_0609700

PF3D7_0609700 is a protein of 1901 AA. No functional domains or homologies to known proteins from other organisms could be detected by *in silico* analysis (Section 2.2.6). Correct integration into the genome of the plasmid leading to the fusion of KBI.7 the sequence coding for 2xFKBP-GFP-2xFKBP, was confirmed by PCR (Figure 46). Endogenously GFP-tagged KBI.7 was found in

multiple foci in the parasites cytosol of which at least one was close to the food vacuole, reminiscent to the pattern observed with Kelch13 (Figure 52a). Most of the KBI.7 foci co-localized with Kelch13 (Figure 52a). In the schizont stage the Kelch13 foci outnumber the foci of KBI.7 (Figure 52a, arrows). Knock sideways of KBI.7-2xFKBP-GFP-2xFKBP transfected with an episomally expressed nuclear mislocalizer resulted in a partial relocation into the nucleus with KBI.7 still remaining in foci in the cytosol (Figure 52b). No effect on the development in a growth assay could be observed (Figure 52c). The gene encoding KBI.7 was successfully disrupted by using SLI-TGD (Figure 46). Hence, the gene is not of importance for the asexual blood stage development.

a



b

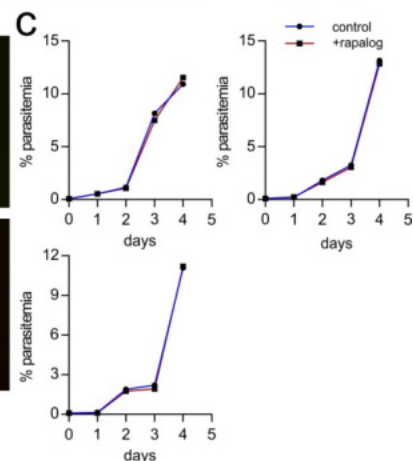
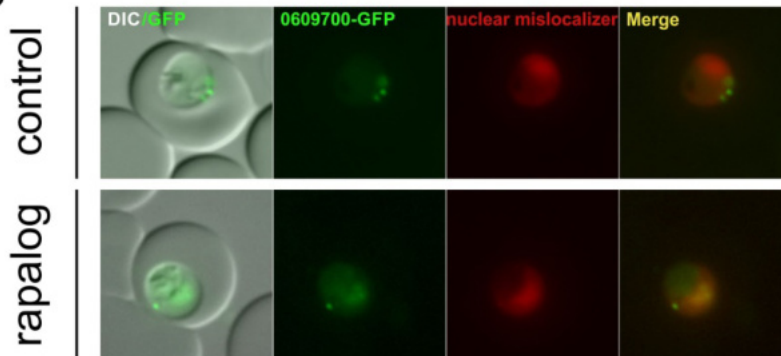


Figure 52 | Localization of PF3D7_0609700 (KBI.7) and co-localization with Kelch13. a-c) Panels show representative live cell images of PF3D7_0609700-2xFKBP-GFP-2xFKBP knock-in cell line a) Cell line stained with DAPI nuclear stain b) Knock-in cell line transfected with plasmid episomally expressing mCherry-Kelch13 for co-localization. Arrows indicate foci of KBI.7 or Kelch13 that are not co-localizing. c) Knock-in cell line transfected with an episomally expressed 1xNLS-FRB-mCherry mislocalizer. Live cell fluorescence images of control and rapalog-treated cells were taken after 16h. d) FC growth curves from 3 independent experiments showing development of control and culture treated with 250 nM rapalog. DIC, differential interference contrast; DAPI, parasite nuclei, Size bar, 5 μ m.

3.6.8 KBI Candidate 8 PF3D7_0104300

PF3D7_0104300 is the gene coding for the ubiquitin carboxyl-terminal hydrolase (UBP1) and encompasses 3499 amino acids. The ubiquitin hydrolase domain is situated in AA 3168-3487. UBP1 is a deubiquitinating enzyme that recognizes the carboxyl terminal amino acid Glycine of ubiquitin. It hydrolyses the peptide bond of ubiquitin to its target protein.

Correct integration of the plasmid used to fuse the gene encoding for KBI.8 to *2xfkbp-gfp* was confirmed by PCR (Figure 46). The protein is expressed throughout all asexual blood stages (Figure 53a). It was found in usually one to up to 5 foci (mostly late stages) in the parasite's cytosol. The single focus was generally found at the food vacuole (Figure 53a). The UBP1 focus co-localized with one of the food vacuole proximal Kelch13 foci, even though co-localization was not observed for all foci (Figure 53a, arrows). The gene encoding UBP1 could not be disrupted by SLI-TGD (Table 2) and consequently is essential for the asexual blood stages.

The cell line of UBP1 fused to 2xFKBP-GFP was transfected with a nuclear mislocalizer to assess the function in more detail (Figure 53b). Even though the translocation into the nucleus was incomplete (Figure 53b) it was sufficient to observe a growth defect (Figure 53c).

3.6.9 KBI Candidate 9 PF3D7_0813000

Candidate 9 (PF3D7_0813000) is a protein of 599 amino acids. A homology to a GTPase-activating proteins (GAP) domain was identified by HHpred (probability 86.13%) stretching from AA 1-80 (Section 2.2.6). Integration into the correct locus leading to the fusion of KBI.7 the sequence coding for 2xFKBP-GFP-2xFKBP was confirmed by PCR (Figure 46). PF3D7_0813000 was expressed in all asexual stages (Figure 54a,b). KBI9 localized in foci in the parasite cytosol. Notably, most foci were found in close proximity to the food vacuole, similar to the pattern observed with UBP1. The Kelch13 protein co-localized with KBI.9, but the number of K13 foci exceeded that of the target protein in late stages (Figure 54a, arrows). The intensity of the foci of KBI.9 and Kelch13 was inversely proportional. All attempts to disrupt *kbi.9* using SLI-TGD were not successful (Table 2). Hence, KBI9 likely is essential for the asexual blood stages. The parasites expressing KBI9-2fkbp-gfp-2xfkbp were therefore transfected with a nuclear mislocalizer and KS was carried out. The target protein was efficiently relocated to the nucleus (Figure 54b). The culture grown with rapalog displayed a marked growth defect compared to the control (Figure 54c). Altogether it can be concluded that KBI.9 is a protein co-localizing with the food vacuole proximal foci of Kelch13 that is essential for the growth of blood stage parasites.

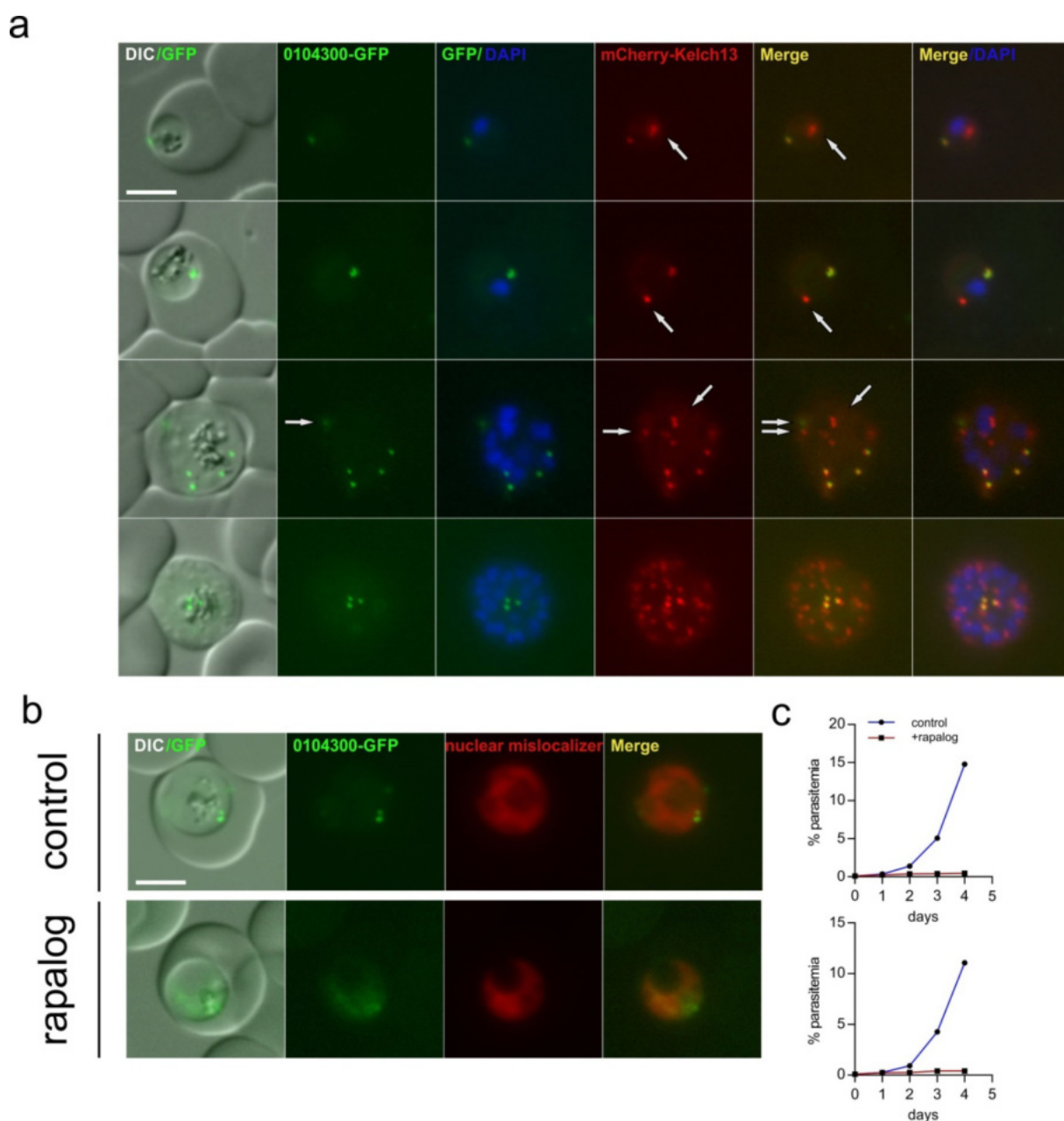


Figure 53 | Localization of PF3D7_0104300 (KBI.8) and co-localization with Kelch13. a-c) Panels show representative live cell images of PF3D7_0104300-2xFKBP-GFP knock-in cell line **a)** Cell line stained with DAPI nuclear stain **b)** Knock-in cell line transfected with plasmid episomally expressing mCherry-Kelch13 for co-localization. Arrows indicate foci of KBI.8 or Kelch13 that are not co-localizing. **c)** Knock-in cell line transfected with an episomally expressed 1xNLS-FRB-mCherry mislocalizer. Live cell fluorescence images of control and rapalog-treated cells were taken after 16h. **d)** FC growth curves from 2 independent experiments showing development of control and culture treated with 250 nM rapalog. DIC, differential interference contrast; DAPI, parasite nuclei, Size bar, 5 μ m.

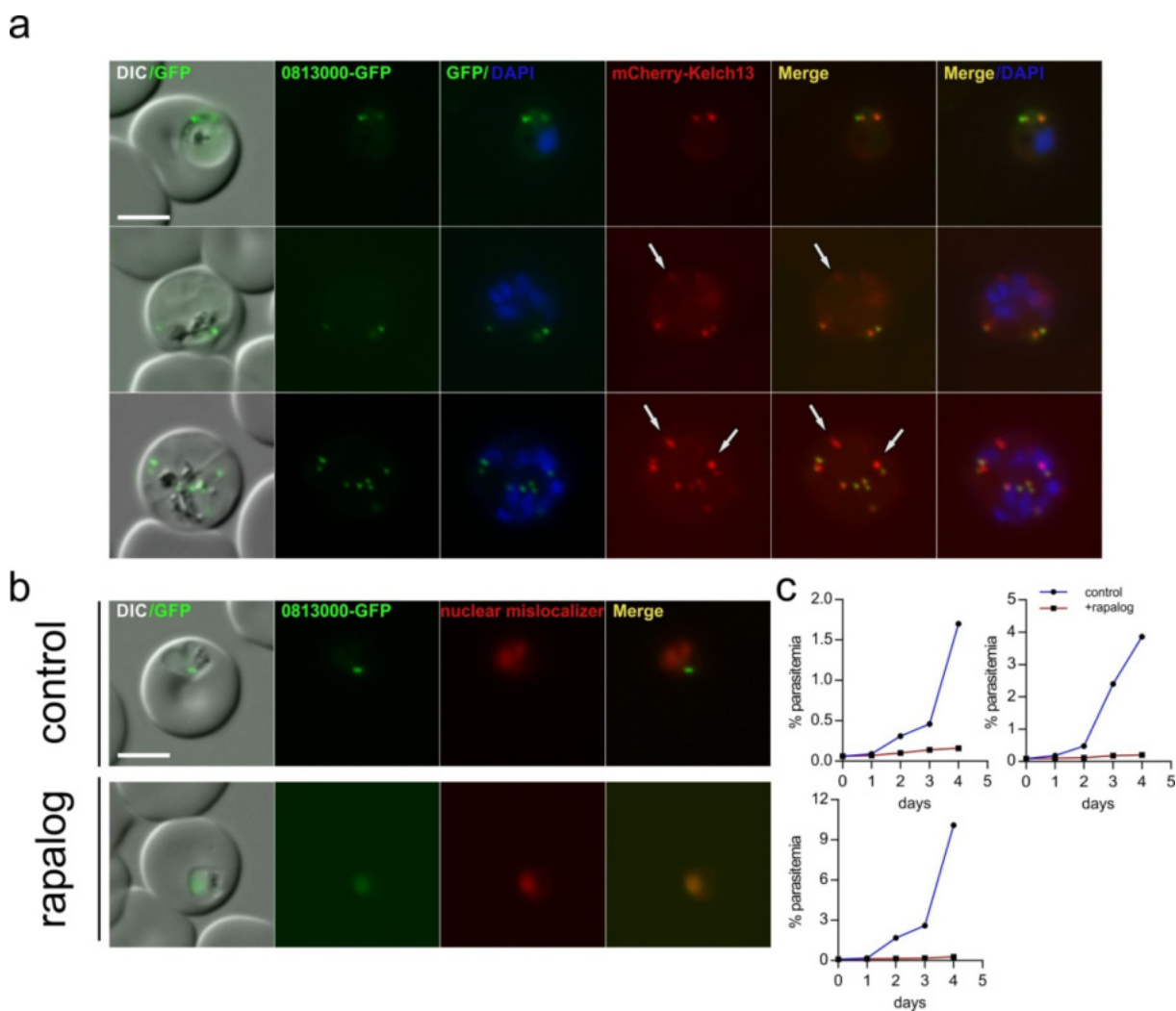


Figure 54 | Localization of PF3D7_0813000 (KBI.9) and co-localization with Kelch13. a,b) Panels show representative live cell images of PF3D7_0813000-2xFKBP-GFP-2xFKBP knock-in cell line **a)** Knock-in cell line transfected with plasmid episomally expressing mCherry-Kelch13 for co-localization. Arrows indicate foci of KBI.9 or Kelch13 that are not co-localizing. **b)** Knock-in cell line transfected with an episomally expressed 1xNLS-FRB-mCherry mislocalizer. Live cell fluorescence images of control and rapalog-treated cells were taken after 16h. **c)** FC growth curves from 3 independent experiments showing development of control and culture treated with 250 nM rapalog. DIC, differential interference contrast; DAPI, parasite nuclei, Size bar, 5 μ m.

3.6.10 KBI Candidate 10 PF3D7_1014900

PF3D7_1014900 encompasses 2279 AA. No functional domains or homologies to proteins of other organisms were identified (Section 2.2.6). The protein was fused to 2xFKBP-GFP-2xFKBP using SLI and integration of the corresponding plasmid was confirmed by PCR (Figure 46). A GFP signal was exclusively detectable in schizont stage parasites whereas all other stages showed no expression (Figure 55). The protein localized to multiple foci in the parasites cytosol (Figure 55). Analysis of the cell line expressing mCherry-Kelch13 revealed that all KBI.10 foci co-localized with a Kelch13 focus but that there existed also Kelch13 foci where no KBI.10 was detectable (Figure 55, arrows). It is at this stage unclear if these foci simply correspond to the additional foci observed due to the Kelch13

overexpression (see 3.4.5) or if this reflects true differences in the distribution of these proteins. However, the comparably high frequency of extra Kelch13 foci (extra foci in the overexpression cell line were rare), argues for a differing distribution. The *kbi.10* gene was successfully disrupted by SLI-TGD (Figure 46). A band for original locus was detected by PCR in the integration cell line, but selection is still ongoing. Hence the gene is not essential for the development of the asexual blood stages.

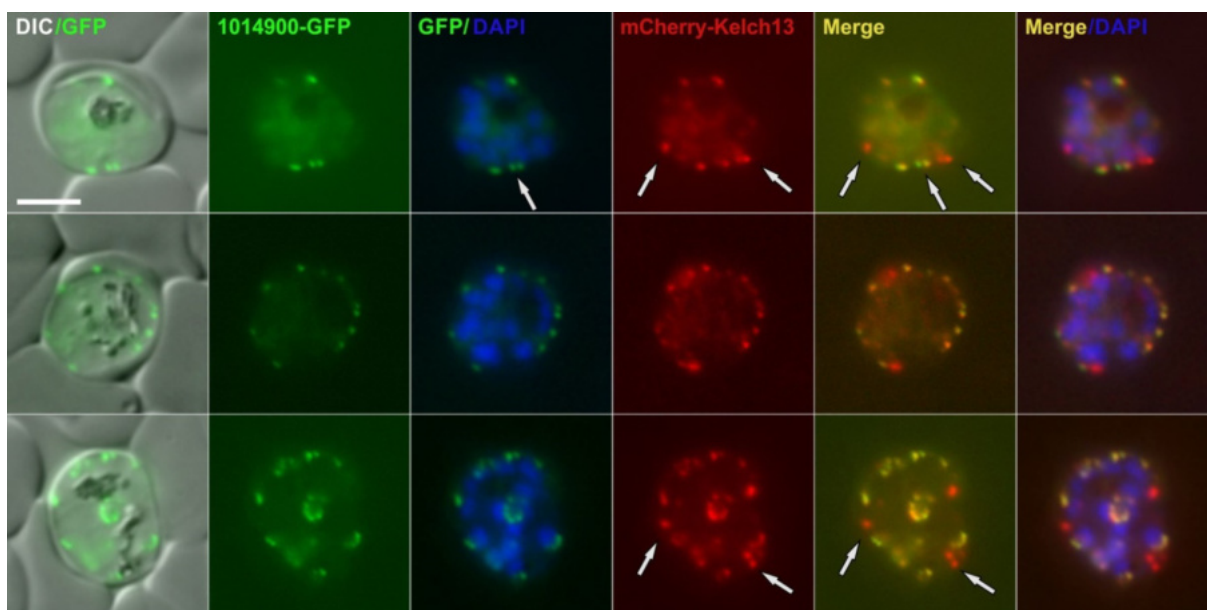


Figure 55 | Localization of PF3D7_1014900 (KBI.10) and co-localization with Kelch13. Panel shows representative live cell images of PF3D7_1014900-2xFKBP-GFP-2xFKBP knock-in cell line transfected with plasmid episomally expressing mCherry-Kelch13 for co-localization. Arrows indicate foci of KBI.10 or Kelch13 that are not co-localizing. DIC, differential interference contrast; DAPI, parasite nuclei, Size bar, 5 μ m.

3.6.11 KBI Candidate 11 PF3D7_1442400

PF3D7_1014900 is a protein of 2113 AA. No homology or functional domains were detected by *in silico* analysis (Section 2.2.6). Integration of the plasmid, leading to the fusion of *kbi.11* to *2xfkbp-gfp-2xfkbp*, into the correct genomic locus was confirmed by PCR (Figure 46). KBI.11 was expressed in all stages except for the rings stage (Figure 56, top panel). It localized in foci within the parasite, similar to the other KBIs (Figure 56). One focus was regularly found in close proximity to the food vacuole. Co-localization of the protein with Kelch13 was confirmed by episomal expression of mCherry-Kelch13 in the KBI.11 integration cell line (Figure 56). Generally there were more Kelch13 foci than KBI.11 foci (Figure 56, arrows), especially in schizonts where KBI.11 showed a more diffuse and dispersed staining pattern (Figure 56, bottom panel). So far no disruption of the gene using SLI-TGD was obtained, but selection of parasites carrying the truncated gene is still ongoing (Table 2).

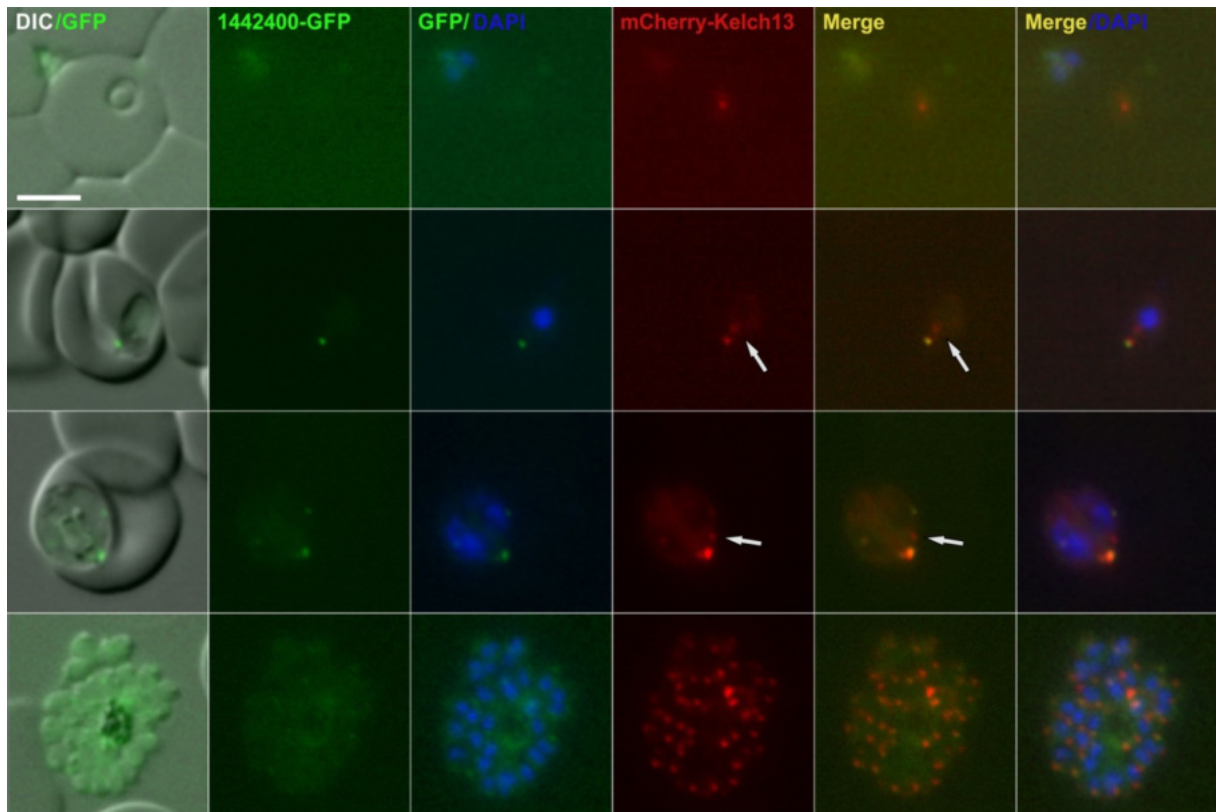


Figure 56 | Localization of PF3D7_1442400 and co-localization with Kelch13. Panel shows representative live cell images of PF3D7_1442400-2xFKBP-GFP-2xFKBP knock-in cell line transfected with plasmid episomally expressing mCherry-Kelch13 for co-localization. Arrows indicate foci of Kelch13 that are not co-localizing with KBI.11. DIC, differential interference contrast; DAPI, parasite nuclei, Size bar, 5 μ m.

4 Discussion

4.1 SLI and KS are suitable for medium throughput screens

Genomic modifications and tagging of endogenous genes in *P. falciparum* has been noted as important tools to study the biology of this parasite (de Koning-Ward et al., 2015; Webster and McFadden, 2014). However, the techniques to achieve this have so far been challenging (de Koning-Ward et al., 2015; Webster and McFadden, 2014). Moreover none of the to date described systems for the functional analysis of essential targets of this parasite are generally applicable (Armstrong and Goldberg, 2007; Crabb et al., 1997; Ghorbal et al., 2014; Meissner et al., 2005; Muralidharan et al., 2011; Prommana et al., 2013; Straimer et al., 2012; Wagner et al., 2014). The here presented method permitted rapid genomic changes and proved to be very reliable. In this thesis, the SLI system was used to create 57 integration cell lines. The localization of 28 native proteins was described in this work. The knock sideways was tested on 22 different proteins (excluded was the exported protein and 5 candidates from the Kelch13 compartment screen by DIQ-BioID as the SLI-TGDs of the corresponding genes were already obtained) and was successful for 19 of the tagged proteins. Out of those 8 proteins were found to be essential (as per definition in this thesis, see section 4.1.2 for a discussion of this point) for parasite development (Table 2). Two of the essential proteins have been described before, namely HP1 and CDPK5, but a localization was only published for HP1 (Brancucci et al., 2014; Dvorin et al., 2010). Candidates 11, 13 and 15 were proteins of unknown function and all showed a nuclear localization. The Kelch13 protein was localized in foci in the cytosol and KS revealed its essential function for parasite growth. Of the potential Kelch13 interaction partners, which were identified by DIQ-BioID, UBPI and KBI.9 were found to be essential by KS.

4 more genes were shown to be important for the asexual stages by SLI-TGD. Of these, candidate 17 was C-terminally tagged but not accessible by knock sideways, whereas the gene products of candidates 3, 10 and 16 were refractory to C-terminal tagging.

Protein localization data and whole genome screens to identify essential genes have proven to be very useful in the past to classify proteins by localization and to select genes for a further analysis, respectively (Gomes et al., 2015; Huh et al., 2003; Modrzynska et al., 2017; Sidik et al., 2016). The genome wide CRISPR screen in the Apicomplexa model organism *T. gondii* (Sidik et al., 2016) can indicate potential essential genes that have a homologue in the *P. falciparum* genome. For non-conserved genes and/or genes involved in cellular processes specific for *P. falciparum* the data should be evaluated carefully.

In the mouse malaria model *P. berghei* a different approach was chosen to identify essential genes (Gomes et al., 2015). Knock out mutants were created and identified by a barcode system (Smith et al., 2009). The close relation of *P. berghei* and *P. falciparum* should make the data of essential genes more reliable for the use in *P. falciparum*. Nevertheless, the *P. falciparum* orthologs of essential genes in *P. berghei* are not necessarily important for the development of the asexual blood stages as was observed e.g. for candidate 1 (PF3D7_0525000) of the here presented study. Its *P. berghei* ortholog

PBANKA_1239800 is annotated as essential (<http://plasmogem.sanger.ac.uk>), but in *P. falciparum* parasites carrying the truncated gene were obtained and KS showed no effect in a growth assay (section 3.2.2.1).

For *P. falciparum* combination of SLI with a high throughput transfection method (Caro et al., 2012) should make a medium to high throughput for localization and targeted gene disruption achievable and subsequently enable an efficient screen of gene products unique to *P. falciparum* or *Apicomplexan sp.* that help to uncover more about the parasite specific biology. Thereby, the SLI-TGD method is expected to replace the traditional TGD where selection of integrants is done by time intense on- and off-drug cycling. Consequently, SLI-TGD should be the first step of a work flow to rapidly assess the essentiality of a gene before starting a more detailed, time consuming analysis e.g. by diCre and KS.

4.1.1 Integration time into the genome is dependent on the length of the targeting region

The mean integration time of the plasmid into the targeted genomic locus, of all cell lines in which neomycin was used as resistance marker for C-terminal tagging, was 15.2 (± 4.8) days. The time for integration of each candidate was plotted versus the length of the targeting region (Figure 57a) or the transcription levels of the target (Figure 57b). As apparent from the regression line in the plot the length of the targeting-region is reciprocally proportional to the integration time (Figure 57a). In contrast, the average expression levels had no influence on the integration time of the plasmid into the genome (Figure 57b). Notably, the regression line indicates that integration into the genome with a homology region length of 0 bp would be possible, but this does not reflect true ratios of integration time to homology region length. For very short (and very long) homology region lengths it is rather likely to be an exponential function. Consequently, this would result in a very long selection time of genetically modified parasites, if targeting of a gene with very short homology region e.g. 50 bp is possible at all. This should be especially considered regarding SLI-TGD. Hence, it is advisable to use homology regions of at least 200 bp for integration of the plasmid into the genome.

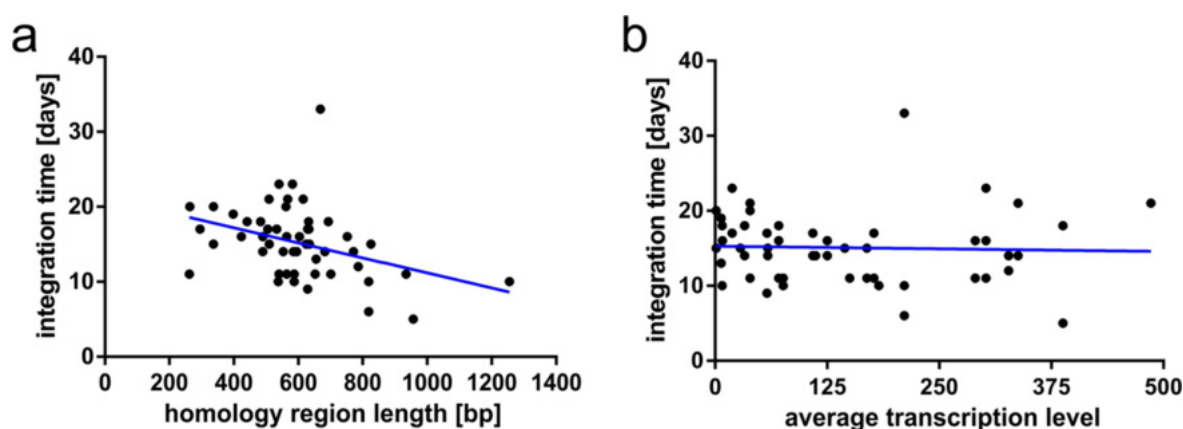


Figure 57 | Time to integration is influenced by length of targeting region. Plotted are all integration cell lines in this study in which neomycin was used as resistance marker for C-terminal integration. **a)** Integration time of plasmids into the

genome plotted versus the length of the homology region. **b)** Integration time of plasmids into the genome plotted versus the average expression levels of the target according to Le Roch et al., 2003.

4.1.2 Considerations on essentiality of gene products

It needs to be noted that the description of an essential gene or an essential gene product in this study that is identified by SLI-TDG or KS has limitations. First, the word ‘essential’ implies an absolute phenotype. However, it cannot be excluded that some of the genes here described as essential may simply reduce but not totally ablate growth. Strictly speaking, they then could not be considered to be ‘essential’. In addition the KS phenotype may be partially leaky (see also below), making it difficult to assess whether small levels of residual growth occur due to technical limitations or because the gene is not fully essential. This may not be the case for SLI-TGD. However, given the mentioned mean integration time into the genome of 15.2 (± 4.8) days and a maximum selection time of 60 days (section 2.2.4.2) parasites with a reduced growth rate of 75% or more, caused by the truncation of a gene by SLI-TGD, could not be obtained. Hence, the gene would be erroneously considered as essential.

Second, the tested targets were assessed for their function in asexual blood stages only. Hence, genes presumed dispensable may still have essential functions in other parasite stages. Third, all analyses were carried out in parasites grown in *in vitro* culture which may not in all cases reflect the situation in the actual host. For instance proteins important for cytoadherence as KAHRP can be disrupted *in vitro* but *in vivo* this would lead to inefficient cytoadherence and subsequent elimination of infected RBC in the spleen (Crabb et al., 1997; Ghorbal et al., 2014; Rug et al., 2014).

All proteins identified as essential by knock sideways displayed a slowly expanding population of parasites in the rapalog treated cell line in the FC growth assay (section 3.2.2). This could indicate that the protein is not essential as the parasites proliferate, but only leads to a severe growth phenotype. Alternatively the KS system could be leaky leading to limited amounts, under the limit of detection, of the target protein remaining at the site of action, able to maintain the molecular function. To assess the leakiness of the KS system an extended growth assay was performed. A population of parasites was found that expressed only low levels of the mislocalizer (section 3.2.3). This implies the mislocalizer must have at least an equimolar number of molecules to the target and indicates that the level of mislocalization was as well influenced by the properties of the target. However, potentially the target protein cannot be entirely depleted from its compartment. Even low amounts of the POI remaining at its site of action can sustain the molecular function for some proteins as has been observed here for the Kelch13 protein (section 3.3). Other examples include Plasmeprin V that was knocked down by the ribozyme system (Sleebbs et al., 2014).

Interestingly, intermediate types of mislocalization displaying growth defects of about 30-70% were not observed for any of the targets studied in the work presented here. However, this may be due to the small number of samples.

Table 2 | Overview of analyzed genes for establishing SLI and knock sideways. SLI column indicates time to integration in days; check marks in the correct integration column indicate integration into the correct genomic locus without remaining original locus; check marks in the knock sideways column indicate efficient KS; red check marks indicate essentiality of target by knock sideways analysis; check mark in parenthesis indicate inefficient KS; x marks unsuccessful KS; n.d., not done; exclamation marks indicate proteins important for parasite proliferation; question mark indicates unclear localization and KS efficiency due to low expression levels; Asterisks show genes fused to 2xFKBP-GFP-2xFKBP; in SLI-TGD column check marks indicate successful disruption of gene, x marks unsuccessful integration, which indicates essentiality.

Candidate	Gene ID	SLI (days)	Localization	Knock sideways	SLI-TGD
HP1	PF3D7_1220900	17	nuclear	✓!	x
CDPK5	PF3D7_1337800	14	cytosolic	✓!	x
1	PF3D7_0525000	14	cytosolic/foci	✓	✓
2	PF3D7_0526800	5	nuclear	✓	✓
3	PF3D7_0720600	x	-	-	x
4	PF3D7_0807600	10	nuclear	✓*	✓
5	PF3D7_1317400	23	nuclear	✓*	✓
6	PF3D7_1445700	11	PPM/IMC/cytosolic	x	✓
7	PF3D7_1451200	11	nuclear	(✓)*	✓
8	PF3D7_1463000	16	nuclear	✓	✓
9	PF3D7_0202400	14	exported	n.d.	✓
10	PF3D7_0205100	x	-	-	x
11	PF3D7_0205600	11	nuclear	✓!	x
12	PF3D7_0209700	11	cytosolic/foci	✓*	✓
13	PF3D7_0210200	9	nuclear	✓*!	x
14	PF3D7_0211700	23	?	?	✓
15	PF3D7_0210900	21	nucleus proximal	✓!	x
16	PF3D7_0213700	x	-	-	x
17	PF3D7_0213900	11	cytosolic	x	x
18	PF3D7_0218200	10	cytosolic	✓	✓
Kelch13	PF3D7_1343700	18	foci in cytosol	✓*!	x
KBI.1	PF3D7_0606000	12	foci in cytosol	✓*	✓
KBI.2	PF3D7_1227700	15	foci in cytosol	n.d.	✓
KBI.3	PF3D7_0914400	31	foci in cytosol	n.d.	✓
KBI.4	PF3D7_1438400	-	-	-	✓
KBI.5	PF3D7_1246300	15	foci in cytosol	✓*	✓
KBI.6	PF3D7_1138700	14	foci in cytosol	n.d.	✓
KBI.7	PF3D7_0609700	11	foci in cytosol	✓*	✓
KBI.8	PF3D7_0104300	14	foci in cytosol	✓!	x
KBI.9	PF3D7_0813000	15	foci in cytosol	✓*!	x
KBI.10	PF3D7_1014900	15	foci in cytosol	n.d.	✓
KBI.11	PF3D7_1442400	16	foci in cytosol	n.d.	?

4.1.3 Limitations of SLI-TGD

It needs to be noted that SLI-TGD leads to a disruption of a gene and not its knock-out. This needs to be considered especially for small genes as the homology region to target the gene should have a size of 200 bp or larger (section 4.1.1). Hence, the remaining part of the gene may in some cases retain partial or full functionality. Generally it can be assumed that the smaller the remaining part of the truncated gene is the higher is the likelihood of avoiding this case.

This could be circumvented by using the CRISPR/Cas9 system (section 1.3.2). It has the advantage that targeting of the gene of interest is mediated by a short guide RNA that can be designed to target the gene directly after the start codon. Thus, insertions or deletion can be placed in the genome resulting in a frameshift and consequently a non-functional gene. In contrast to SLI, in which the complete plasmid is integrated into the genome, editing of the genome by CRISPR/Cas9 leaves no such fingerprint in the DNA. However, off-target effects are a frequently observed problem of the CRISPR/Cas9 system (Tsai et al., 2015; Veres et al., 2014). Another issue is the already mentioned absence of NHEJ pathways in *P. falciparum* (section 1.3.2).

Additionally, to a truncated gene that can remain partially functional by using SLI-TGD, the truncated protein can show a dominant negative function and lead to a detrimental effect on the parasite. This would lead to the assumption of the gene being essential, but in fact a complete knock-out would show a different result. Here again, it can be assumed that the smaller the remaining part of the truncated gene is the higher is the likelihood of avoiding a dominant negative mutation, as a smaller part of the protein gets expressed. Moreover, in the current study no evidence for such a case was found as the SLI-TGD data correlated with knock sideways experiments.

4.1.4 Combination of SLI and KS with existing methods for gene function analysis

SLI and KS can also be used to improve existing methods for genome editing or for functional analysis of proteins. Especially SLI is combinable with many molecular systems as it decreases the time for integration into the genome dramatically.

The DD (destabilization domain) system (see section 1.3.4) for functional analysis of proteins in *P. falciparum* requires fusing the target gene with the sequence coding for the DD domain in the endogenous genomic locus. During the selection process for integration into the genome it needs to be stabilized by the ligand Shield-1, as otherwise the DD tagged protein gets degraded. Thus, degradation of an essential protein would prevent obtaining the modified parasites. Combination of SLI with the DD system would decrease the high costs of the stabilizing ligand Shield-1 that needs to be added throughout the selection process as it decreases the integration time (Armstrong and Goldberg, 2007). The benefit of reducing the time of integration into the genome would also be seen for other systems as the ribozyme based mRNA degradation system by glmS (Prommana et al., 2013) and it would also reduce the time required for placing loxP site containing artificial introns (Jones et al., 2016). A

summary of ways to improve other methods can be found in Appendix B, which moreover provides an overview of advantages and disadvantages of the particular systems.

The SLI system was also used in this work to knock-in a mutated allele of the *kelch13* that reduces susceptibility to artemisinins. Another technique that has previously been used to modify the same and other genes is the CRISPR/Cas9 system and zinc finger nucleases (Ghorbal et al., 2014; Mbengue et al., 2015a; Straimer et al., 2015; Straimer et al., 2012; Wagner et al., 2014; Wong et al., 2017). Gene editing by CRISPR/Cas9 or zinc finger nucleases leave no fingerprint other than the desired change in the genome. However, time and labor intense cloning of the parasites is required. In contrast, the use of SLI permits changes in the genome without cloning of parasites making it possible to assess different mutations rapidly, but leads to a comparably large change due to the integration of the whole plasmid into the genome. Also, the same types of limitations that apply to SLI-TGD due to a remaining truncated functional gene (4.1.3) apply to C-terminal tagging by SLI or knock-in of resistance alleles. Additionally, CRISPR/Cas9 needs transfection of two plasmids compared to one plasmid for the SLI system and SLI circumvents the high costs to generate zinc fingers that need to be designed to act on a particular DNA sequence of choice. Off-target effects are a common problem of CRISPR/Cas9 mediated modifications in the genome (4.1.3) and targeting subtelomeric genes for homology directed repair (HDR) is hampered by the repair of the induced double strand breaks (DSB) with a telomeric repeat rather than the desired sequence of the helper plasmid. However, in contrast to SLI, genomic modifications by CRISPR/Cas9 do not require the generation of an episomal cell line.

A major disadvantage of the CRISPR/Cas9 system to date is that changes in the genome with detrimental effects to the parasite cannot be obtained as the system is not inducible and hence it is not clear if the transfection was not successful or if the genomic modification is fatal to the parasite. The FRB-FKBP system could be used obtain an inducible version of the CRISPR/Cas9 system by regulating the localization of the Cas9 protein. Fusion to a PPM localization signal would leave the nucleus depleted of Cas9 and upon addition of rapalog the Cas9 can be localized to the nucleus by using the nuclear mislocalizer. In a recent publication the FRB-FKBP system has already been used for inducible activation of Cas9 in an approach termed split Cas9 (Zetsche et al., 2015). The split Cas9 system is designed analogous to the diCre system (Andenmatten et al., 2013; Collins et al., 2013; Jullien et al., 2007; Jullien et al., 2003), as upon addition of rapalog both fragments are assembled and become active. So far no study used the split Cas9 system in *P. falciparum*.

4.1.5 Factors influencing the efficiency of knock sideways and potential further improvements of the system

The knock sideways system has been used for a broad variety of approaches in other organisms (see 1.4) (Castellano et al., 2000; Haruki et al., 2008; Robinson et al., 2010; Suh et al., 2006; Xu et al., 2010). For the proteins analyzed in this study efficient mislocalization was observed for 19 out of 22 proteins. Notably, for 6 proteins a tag consisting of 2xFKBP-GFP-2xFKBP was used as the initial

2xFKBP-GFP tag did not sufficiently mislocalize these proteins. Hence, the 2xFKBP-GFP-2xFKBP tag was used for all potential Kelch13 interaction candidates and is now used as tag of choice for functional analysis by knock sideways in general. The improved success of the 2xFKBP-GFP-2xFKBP tag can potentially be attributed to two different, non-mutually exclusive, possibilities.

First, proteins that were refractory to mislocalization with the smaller tag were accessible by knock sideways by using the improved tag. This indicates that the 2xFKBP-GFP tag was buried in a complex or sterically interfered with the surrounding proteins leaving no contact surface for the mislocalizer. The two additional FKBP domains increased the length of the tag and the surface area and thereby potentially protrude from the complex providing a platform for interaction with the mislocalizer, even though structural studies would be needed to clarify the hypothesis. Only for UBP1 the increased size of the 2xFKBP-GFP-2xFKBP tag may have led to a detrimental effect on the parasite as the corresponding cell line was not obtained, but tagging with the smaller 2xFKBP-GFP tag was successful.

Second, in some cases an inefficient mislocalization or a reversed localization, which describes the event of mislocalizer relocated to the target protein, was observed. Hence, this suggests that the localization signal of the mislocalizer was not strong enough. Using the 2xFKBP-GFP-2xFKBP tag 4 mislocalizers are potentially able to bind the target, leading to a duplication of localization signals by the mislocalizer compared to the 2xFKBP-GFP tag and an improved transfer into the mislocalizers' cellular compartment.

In contrast, an increased number of FRB domains in the mislocalizer construct are not expected to lead to an increased efficiency of the KS. It would decrease the number of signals on the target protein, as it may bind two FKBP domains on the target. Alternatively it may bind more than one target per mislocalizer. In both cases this would decrease the mislocalization force, and hence also the efficiency of the KS.

Furthermore, weak localization signals such as 1xNLS displayed a bigger cytosolic pool than strong localization signals like 3xNLS. For the knock sideways of cytosolic proteins, a larger cytosolic pool of the mislocalizer potentially leads to an increased number of encounters with the target and thus increased the efficiency of the knock sideways.

This may also explain the fast response of cytosolic proteins over nuclear proteins, as the availability of the PPM mislocalizer in the nucleus is smaller. Consequently, a weakened Lyn localization signal could be beneficial for the knock sideways of nuclear proteins. However, this was not experimentally tested in this work. Another option to improve the mislocalization for nuclear resident proteins may be the use of other mislocalizers than the Lyn signal peptide. Haruki *et al.* used the ribosomal protein RPL13A, that transits into the nucleus, with great success to target nuclear proteins (Haruki *et al.*, 2008). All of the more than 40 tested nuclear proteins were successfully mislocalized. BLAST search identified the gene PF3D7_0814000 as the homologue of RPL13A, indicating the applicability of the ribosomal mislocalizer in *P. falciparum*.

A slightly different approach to improve the mislocalization could be the generation of a hybrid mislocalizer that contains 2 different localization signals, each fused to an FRB domain and separated by a T2A skip peptide. For instance a plasmid expressing the construct of Lyn-FRB-T2A-RPL13A-FRB-mCherry could possibly improve the mislocalization result as the ribosomal mislocalizer would transit into the nucleus and back to the cytosol and thereby increase the likelihood of an encounter of

the target protein with the Lyn mislocalizer, which would anchor the target at the parasite plasma membrane.

A further option could be the use of a nuclear export signal (NES) (Klemm et al., 1997), however all attempts to stably express a mislocalizer containing a NES in *P. falciparum* were not successful (data not shown).

For some applications it might be desirable to target more than one protein. With the system presented here only one protein can be targeted. An interesting option for the knock sideways of more than one protein would be to combine the FKBP-FRB system with an orthogonal CID system e.g. based on abscisic acid (ABA) (Liang et al., 2011; Nishimura et al., 2009), the gibberellin induced dimerization system that uses the gibberellin analog GA₃-AM as trigger (Miyamoto et al., 2012) or the rush system that utilizes the interaction of biotin and streptavidin (Boncompain et al., 2012). Moreover, assays for hemoglobin uptake and vesicular trafficking could benefit from the use of reversible CID systems as the mentioned rush system, the rCD1 based system or the SLF²-TMP system (Boncompain et al., 2012; Feng et al., 2014; Liu et al., 2014).

Due to the lack of suitable mislocalizers, knock sideways can at present not target proteins entering the secretory pathway. In addition proteins with TMs pose further problems. One solution could be the use of a mislocalizer situated within the secretory pathway. Such constructs have already been used in other systems but were called ‘hooks’ and used to control the simultaneous release of an entire population of labelled target proteins from the ER to follow the trafficking pathway of these proteins (Boncompain et al., 2012). A simple way to obtain an ER-mislocalizer would be to fuse a FRB domain to the mScarlet-SDEL ER marker used in this work (section 3.4.1). Thus, upon addition of rapalog the POI could be retained in the ER. However, it remains to be tested whether this would be successful, as the accumulation of the POI in the ER could have detrimental effects or potentially the folding of the mislocaliser may be too slow to actually capture the POI.

There are further factors that can influence the efficiency of knock sideways such as the individual properties of the POI and the complex the target protein is interacting with. It has been reported from knock sideways experiments in *S. cerevisiae* that proteins that interact with five or less proteins on average are accessible by knock sideways, whereas proteins that interact in complexes of twenty or more proteins in average are refractory to mislocalization (Patury et al., 2009; Xu et al., 2010). Due to the small sample size of about 20 tested proteins the numbers should be considered with caution, but could indicate a trend. Unsuccessful mislocalization could be due to either structural reasons (coverage of the FKBP binding site on the target by interacting proteins) as described above or due to the sum of the complex’s localization signal that might overpower the localization signal of the mislocalizers. In any of these cases the complex dissociation constant K_d of the POI for the complex is deciding, as the proportion of POI not in the complex at a given time can be mislocalized, driving the equilibrium away from the correct interaction. Finally, other components of the complex could also be anchored to a structure that can’t be mislocalized e.g. the membrane. In this case, if the mislocalizer re-directs the entire complex away (see also below), the KS would show no effect. This would be indicated in live cell imaging by a reverse localization of the mislocalizer.

Given the mentioned above number of a complex size of at most 5 proteins for successful mislocalization and considering the used of only one dimerization domain on each target protein in the study (Xu et al., 2010), it is likely that the here presented knock sideways system can mislocalize proteins that are constituents of complexes with a protein count that is higher than 5. In support of this, it was here shown that the Kelch13 protein (tagged with 2x-FKBP-GFP-2xFKBP, see section 3.3) can be efficiently mislocalized. Based on the data from the DIQ-BioID experiments it can be assumed that likely the Kelch13 protein has many interaction partners (see section 3.5). If only half of the proteins highly enriched in the DIQ-BioID experiments interact in a complex with Kelch13 at a given live cycle stage, complexes with a size of >5 members are accessible for knock sideways. While this likely will vary with the properties and composition of each complex, it nevertheless suggests that the system with multiple FKBP domains is less affected by the previously noted complex size restriction. An interactome study in human cells showed that more than two thirds of the analyzed complexes have 10 or fewer members (Huttlin et al., 2015). Assuming that *P. falciparum* is an organism of similar or lower complexity, the knock sideways system described here should be applicable for most of its proteins that are not in the secretory pathway.

It should be considered that not only single proteins can be relocalized to different compartments by knock sideways, but also a complex of proteins. In fact, the technique has been used to demonstrate interaction between proteins based on their co-mislocalization (Gallego et al., 2013). There is also the possibility that the mislocalized protein leads to unrelated negative effects on the site it was mislocalized to. There are however several indications that this did not affect the results of the experiments shown here. First, and even though only a small number of proteins have been analyzed so far, for all 19 mislocalized proteins no deviation from the SLI-TGD result was observed (Table 2). Moreover the published phenotype of CDPK5 and HP1 was reproduced. This data is important for assessing potential side effects of the mislocalization of the target protein into another compartment as well. The protein is still functional and hence could lead to detrimental effects on the parasite upon relocalization, but as before no evidence was identified for such side effects, as all 11 non-essential successfully mislocalized proteins had no effect on parasite growth and a SLI-TGD was obtained. Vice versa, if the observed growth defect for 8 proteins in the FC growth assay was based on unrelated detrimental effects, it should have been possible to disrupt those genes by SLI-TGD. Second, mislocalization of Rab5a and complementation with an active copy that is not-mislocalizable lead to a similar growth of control and rapalog treated cell line (Birnbaum et al., 2017). This showed that the observed phenotype upon depletion of Rab5a from its site of action was not caused by a side effect of the relocalization into the nucleus. Third, excision of the active *kelch13* gene copy by diCre and the knock sideways both showed an arrest of the parasite in the ring stage (this work). Excision of the active *rab5a* gene copy and knock sideways of Rab5a both showed a schizont development phenotype (Birnbaum et al., 2017).

However, the possibility of indirect effects cannot completely be excluded for all of the targets analyzed in this work and also for future work it is advisable to take this possibility into account. In order to reduce the risk of a false result of a knock sideways with new targets, it is recommended to

first use SLI-TGD to assess the essentiality of the target gene and if possible to carry out complementation and/or deletion of the gene using diCre.

4.1.6 Considerations for analysis of proteins refractory to mislocalization

Proteins that cannot be mislocalized can still be functionally analyzed e.g. by excision of the gene using the diCre system (Andenmatten et al., 2013; Collins et al., 2013; Jullien et al., 2007; Jullien et al., 2003) as shown for *kelch13* (see 3.3). Here this was done by disrupting the endogenous copy and adding a new functional copy flanked by loxP sites. With the aid of skip peptides the entire construct was expressed under the endogenous gene promoter. This was possible by shifting the frame of the loxP site 5' to the active copy so that it did not contain a stop codon. In this study the *kelch13* gene was the only one tagged at the 3' end. However, the same strategy to use loxP sites and diCre can be adapted to 3' tagging and has been done for an integral transmembrane protein that is not accessible by knock sideways (Mesén-Ramírez et al., unpublished) (Figure 58). In the case of Kelch13, the SLI-resistance was placed 3' of the active copy, separated by a skip peptide. Irrespective of the position of the tagging of the active copy, the SLI resistance could in principle be placed on either side. However, if C-terminal tagging is not possible, there is a chance that placing the SLI resistance to the C-terminal end might equally affect the target's function, as the skip peptide leaves a 28 AA overhang.

Many more approaches using diCre could be envisaged. For instance proteins going through the secretory pathway could be targeted by bringing an S/KDEL retention signal to the C-terminus of the target.

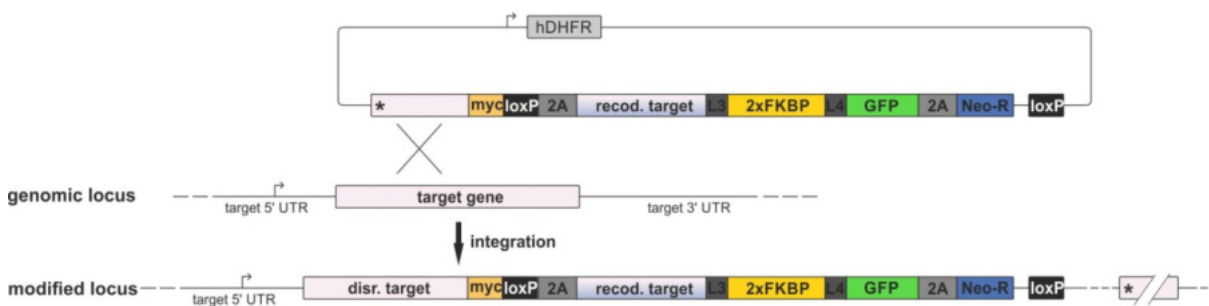


Figure 58 | Alternative strategy for assessing the function of a 3' tagged gene by diCre. The endogenous copy is disrupted and a codon optimized c-terminally tagged copy is provided (without the stop codon). SLI resistance gets expressed with the tag upon integration under the target's endogenous promoter. Due to the 2A skip peptide, the SLI resistance is independent of the tagged target protein. The active codon optimized copy can be excised from the genome by using inducible Cre recombinase. L3 and L4 are linkers (Varnai et al., 2006); 2A, T2A skip peptide; Asterisk, stop codon; Neo-R, neomycin phosphotransferase II gene.

4.1.7 SLI resistance markers

In this study the neomycin phosphotransferase II (NPT II) was the resistance of choice for selection of C-terminal tagged proteins by SLI as it was found to be very robust. A vast advantage of the resistance marker was that even proteins with a very low transcription levels (Le Roch et al., 2003) can be selected, such as candidate 14 (PF3D7_0211700), which could not be localized. Hence, SLI potentially enables targeting of most *P. falciparum* proteins.

It has also been demonstrated that BSD can be used as SLI resistance marker, by selecting for the C-terminal fusion of two exported proteins to GFP-T2A-BSD (Birnbaum et al., 2017). Nevertheless, it was not evaluated if genes with low transcription levels can be targeted as well.

However, the use of the NPT II for N-terminal tagging was not successful. All attempts to select for parasite expressing the *kelch13* gene fused to *gfp-2xfkbp* at its 5' end failed. The approach was identical to the integration strategy shown in this study (Figure 32a), whereas the yDHODH resistance marker was replaced by the NPT II. Due to the skip peptides the NPT II is fused to an additional prolin at its N-terminus and a 28 AA overhang at the C-terminus. It has been described that fusions to the carboxy-terminal end can influence the activity of NPT II depending on the added AA sequence (Reiss et al., 1984).

Hence, yDHODH as a resistance marker was successfully chosen for selection of N-terminal tagged of proteins. The number of tagged proteins by this approach is limited so far, but the strong selection pressure exerted by the corresponding selection drug DSM1, observed with cell lines carrying episomally selected plasmids, indicates that a high expression levels of the target is necessary for successful selection.

The use of BSD has recently been tested for the N-terminal tagging strategy, but so far no parasites showing integration of the plasmid into the correct genomic locus were obtained.

4.2 Analysis of Kelch13

The functional analysis of the Kelch13 protein has shown that it is necessary for transition from the ring stage to trophozoite stage in the asexual blood cycle. This result was obtained by using two different methods, knock sideways and excision of the active gene copy by diCre (section 3.3). Other effects on the development of the parasites were not observed and are unlikely, as the FC growth assays (for both, knock sideways and diCre excision of the gene) were carried out with unsynchronized parasites and both led to the accumulation of ring stages (Figure 34,35). Furthermore no increased number of dead cells or other evidence for reduced growth or changed morphology in other stages was observed in these parasites. It needs to be noted that the excision via diCre can distort the functional analysis as maybe only the earliest phenotype in the cell cycle will be detected. The excision is not as rapid as the knock sideways and significant levels of mRNA and protein can remain in the cell that can also be easily carried over in the following multiplication cycle. In this regard it is particularly noteworthy that as little as 10% of the Kelch13 protein remaining at its site of action did not result in any effect on parasite growth (Figure 33). Thus, a small amount of protein remaining after

diCre-based elimination of the *kelch13* gene may be sufficient to support parasite growth. This is clearly reflected in the timing for the onset of the phenotype after induction of diCre and the Kelch13 protein levels in these cultures. In contrast to this, an additional function of AMA1 in the resealing of the RBC after invasion was revealed by analysis with the diCre system that has not been identified with other methods (Yap et al., 2014). Hence, the diCre system will be a valuable asset for functional analysis, but as other methods has its limitations.

For N-terminal tagging of Kelch13, the *kelch13* gene was disrupted identically to the SLI-TGD approach. The chosen homology region resulted in a truncated version that had lost the region coding for the BTB and the Kelch-domain, but the complete *P. falciparum* specific parts remained (comprising approximately 50% of the gene). The disrupted endogenous copy is still expressed and cannot be mislocalized. Thus, it could still perform a function. The truncated gene encodes a C-terminal myc-tag and an immune fluorescence assay using anti-myc antibodies could show whether the truncated product shows a differing localization to the wt protein and hence would likely be non-functional. However, given the lethal phenotype of the diCre and KS with this cell line, it seems unlikely that further essential functions remain with the truncated product.

Co-localization experiments with markers for ER, Golgi apparatus, PI3P positive compartments and the Apicoplast did not result in any clear indication where the Kelch13 positive compartment fits into the scheme of cellular compartments (see 3.4). The ER and Golgi markers showed a different localization than Kelch13 throughout the asexual blood cycle. Some foci were found in close proximity in some cells, but were not consistently found and therefore likely were coincidental due to the small size of the parasite cell. It is also noteworthy that the Kelch13 foci often moved rapidly, especially in rings and trophozoites, which was not the case for the other components and hence they could not consistently be co-localising. This however could obscure a directed movement to and from one of the compartments, as each image would show a different stage in such a process. However, none of the imaging experiments indicated such a directed movement, even though this was not systematically tested in timelapse imaging.

Interestingly, in the schizont stage foci of Kelch13 were found adjacent to foci marking the ER or the Golgi. This may be attributed to the limited space inside the forming merozoites.

A PI3P positive compartment was reported to localize to the FV in previous publications (Flemming, 2015; Tawk et al., 2010). The focus of the Kelch13 protein that localized proximal to the FV was often found close to the PI3P positive compartment in this study. The Apicoplast and the Kelch13 protein were often found in close proximity, as well.

It needs to be noted that from those experiments it is difficult to assess if there is a spatial link between two structures as both are close to the FV and hence overlaps can be observed by chance. This analysis is limited by the resolution of conventional fluorescence microscopes in xy and particularly in z (which is around 0.5 μ m). Additionally the movement of foci of the Kelch13 protein complicated the analysis. To get a more detailed analysis confocal imaging and 3D reconstruction would give a higher spatial resolution.

4.2.1 DIQ-BioID provides high specificity for identification of Kelch13 neighboring proteins

Since its publication in 2012, the proximity dependent biotin identification (BioID) method has been used in numerous studies to identify interaction partners and proteins residing in a compartment of interest in a cellular context (Blancke-Soares, 2016; Chen et al., 2015; Guo et al., 2014; Kim et al., 2014; Kim et al., 2016; Lambert et al., 2015; Roux et al., 2012). The BioID method can be carried out in the living cells to capture physiological interactions. It thereby circumvents problems of biochemical approaches that often are hampered by insolubility of target complexes under suitable lysis conditions or by weak interactions as proteins are biotinylated before the solubilization that are not preserved during cell lysis (Roux et al., 2012).

In the published approaches the POI was tagged with the promiscuous biotin ligase BirA* and often separated from the POI by a linker. Taking the well characterized nuclear pore complex (NPC) as an example, the use of a long flexible linker before the BirA fused to the NPC POI was demonstrated to improve the detection rate of proximal proteins (Kim et al., 2016). It was shown that the radius of detection in this case was about 10 nm. However, BirA* did not biotinylate all proteins in the detection radius, indicating sterical restrictions or the inability to biotinylate some proteins (in further detail discussed below) (Kim et al., 2014).

In the here presented study the BirA* was not directly fused to the POI. Instead the FRB-FKBP heterodimerization system was utilized in an approach termed DIQ-BioID (section 3.5) by transfecting the GFP-2xFKBP-Kelch13 cell line with a plasmid coding for FRB-FRB-mCherry fused to an N-terminal BirA* (BirA-nT). Control of the dimerization of the GFP tagged Kelch13 protein and the mCherry tagged BirA construct in the rapalog treated culture in the fluorescence microscope was confirmed and hence showed the proximity of BirA to the target. Evaluation of the quantitative mass spectrometry data indicated that the BirA* supposed to be dimerized onto Kelch13 was indeed in close proximity to the Kelch13 protein, as this protein was the hit with the highest significance and a protein of the expected size stood out in biotin Western blots of cultures grown in the presence of rapalog compared to controls. All DIQ-BioID hits that were so far tagged for validation in this work showed a similar staining pattern to the Kelch13 protein and were found to overlap with at least one, but usually most to all Kelch13 foci (section 3.6). This is clear evidence for the high specificity of this approach. Using the same heterodimerization system as used for the knock sideways has the obvious benefit that no new integration cell line with the POI linked to BirA* needs to be created. Instead the already obtained integration cell line with the POI fused to 2xFKBP and GFP can be used, which significantly decreases the time needed for analysis of the POI as transfection of the mislocalizer for the knock sideways and transfection of the BirA construct can be done in parallel. A vast advantage of DIQ-BioID over conventional BioID is the provision of a matched control for the quantitative mass spectrometry by splitting the identical starting culture into a rapalog treated and untreated part before addition of biotin. This cannot be underestimated as there is a profound stage-specificity of gene expression levels over the 48h asexual development cycle (Bozdech et al., 2003; Le Roch et al., 2003) which results in large differences if two separately grown cultures – that will have a different

distribution of stages - are compared. It needs to be noted that for identification of the potential Kelch13 interaction partners an unsynchronized culture was used in order to assess interactions in all asexual life cycle stage in the blood as the Kelch13 protein is expressed in all stages.

The BioID method was described to be able to identify transient protein-protein interactions (Roux et al., 2012). However, it is not clear if the kinetics of biotinylation reaction is fast enough to capture short-lived interactions. It is possible that proteins escape the identification by this approach. A requirement for biotinylation by BirA* is the accessibility of the primary amine of predominantly lysine residues. If the primary amine is not accessible to BirA*, it is not biotinylated and the interacting protein cannot be purified and detected. This may for instance occur, if there is an unfavorable spatial arrangement between the dimerized BirA* and the interaction partner. This is strongly influenced by the structure of the target and its complex as well as the FRB-FKBP interaction. Having used the BirA nT construct containing two FRB domains the BirA could be sterically restricted and thus avoid the biotinylation of proximal proteins. Nevertheless, the experiment with the BirA nT construct identified 8 proteins with a FDR of 10^{-10} and 20 proteins with a minimal FDR of 10^{-2} .

In order to assess sterical restrictions, identify new proteins in the Kelch13 compartment and verify the potential interaction partners of the previous mass spectrometry experiment DIQ-BioID was tested with a new BirA construct, consisting of mCherry-FRB-BirA* (BirA cT). In contrast to the BirA nT construct the BirA cT construct contained only one FRB domain and a longer linker between BirA* and FRB domain that led to improved detection of proximal proteins by BioID in a previous publication (Kim et al., 2016). Consequently the GFP-2xFKBP-Kelch13 protein can bind two BirA cT proteins. Combined with the long flexible linker this provides a higher degree of freedom for BirA* to reach interactors of the POI and can improve the biotinylation result of proximal proteins. Moreover, the two FRB domains result in an increased variation of the targets reached.

Except for the BirA construct the DIQ-BioID experiment was carried out with an identical protocol as before.

Comparison of the top 20 identified proteins from preliminary data with the BirA cT construct and the DIQ-BioID experiment using the BirA nT construct (section 3.5) revealed that 16 proteins were shared in both datasets, indicating that the influence of linker length and FRB domains is not as important as initially assumed, at least in case of the Kelch13 protein complex (section 3.5). The experiment with the BirA nT construct identified 8 proteins with a FDR of 10^{-10} whereas the experiment with BirA cT identified 14 proteins with this level of significance. If a FDR of 10^{-2} is taken as the cut off, 20 to 27 proteins, respectively, suggesting an improved biotinylation and/or range of the biotinylation. However, it should also be noted that the coverage and quality of individual MS experiments can vary considerably, and hence these differences may also be coincidental. This may in part be less of a limitation in the here shown data as two independent biological replicas were used. Moreover, most of the top hits were reproducibly found with different BirA constructs, which indicates the robustness of the DIQ-BioID system.

The DIQ-BioID experiments were done with GFP-2xFKBP-Kelch13 cell line. Transfection of the BirA plasmids into the 2xFKBP-GFP-2xFKBP-Kelch13 cell line, which was used as basis for the

successful knock sideways and subsequent quantitative mass spectrometry analysis, would probably increase the number of identified proteins. However, at the same time this might increase the number of non-interacting proximal proteins detected, as the two additional FKBP domains are separated by GFP from the Kelch13 proximal FKBP domains and thus could result in tagging of proteins in an increased distance to the POI.

The DIQ-BioID for the Kelch13 proteins revealed 10 proteins confirmed to be in the same compartment and many more unconfirmed hits with a FDR sufficiently high that it may contain further true positives. The identified candidates could be direct or indirect interaction partners of the Kelch13 protein or only reside in the same location. Even if the proteins only share the same location with the Kelch13 protein it is likely that they contribute to common processes or are otherwise functionally linked to the Kelch13 protein. So far for all of the C-terminally tagged proteins except of PF3D7_0104300 (UBP1), PF3D7_0813000 and PF3D7_1442400 a TGD was obtained by using SLI (section 3.5). This high proportion of dispensable proteins may indicate a high redundancy in this process, and in turn could indicate a high importance for the parasite.

Moreover, the ubiquitin carboxyl-terminal hydrolase 1 (UBP1) (PF3D7_0104300) was associated with reduced artemisinin susceptibility in genome wide association studies (GWAS) (Borrmann et al., 2013; Cerqueira et al., 2017; Henriques et al., 2015) and another study identified a mutation in the *ubp1* gene leading to decreased artemisinin susceptibility in the mouse malaria model *P. chabaudi* (Hunt et al., 2007). A discussion of the potential role of UBP1 in the Kelch13 complex can be found below (section 4.2.2). The data from the reports on UBP1 give a further validation to the dataset obtained by DIQ-BioID of the Kelch13 protein.

One prospect of the identification of potential interaction partners was finding proteins of known or suspected functions that may provide clues on the function of the Kelch13 protein or the compartment it resides in. Surprisingly, most of the confirmed Kelch13 DIQ-BioID hits showed no homology to known proteins from other organisms. Hits with homologies to proteins of known function were a metacaspase-like protein (MCA2) (PF3D7_1438400), formin 2 (PF3D7_1025000) and the ubiquitin carboxyl-terminal hydrolase 1 (UBP1) (PF3D7_0104300). Additional proteins with known homologies identified in the second DIQ-BioID experiment using the BirA cT construct were the 6-phosphofruktokinase (PFK9) (PF3D7_0915400), a calponin-homology domain containing protein (PF3D7_1447800), a lysine decarboxylase (PF3D7_0405700), myosin C (PF3D7_1329100) and a GTPase-activating protein (PF3D7_0907200).

Of the eleven proteins that were co-localized with mCherry-Kelch13 only UBP1 (PF3D7_0104300) (section 3.6.8) and PF3D7_0813000 (section 3.6.9) were found to be essential for the asexual blood stages by knock sideways and SLI-TGD. A more detailed analysis using knock sideways with synchronized parasites needs to be done to determine a potential phenotype.

4.2.2 Role of confirmed DIQ-BioID hits and potential relation to Kelch13 function and artemisinin resistance

Most BioID hits showed no relation to proteins of known function, besides the above mentioned proteins as UBP1, MCA2 and formin 2 and a homology to an adaptin-like domain in PF3D7_1246300 (section 3.6.5). The protein with the strongest homology was the metacaspase.

In this work it was shown that MCA2 can be disrupted by using SLI-TGD and hence is considered not to be essential for the asexual stages (section 3.6.4). Unexpectedly, it was refractory to C-terminal tagging of the full length protein.

The genome of *P. falciparum* encodes for 3 different metacaspases (Plasmodb.org). The metacaspase 1 (MCA1) (PF3D7_1354800), the Kelch13 proximal metacaspase-like protein (MCA2) (PF3D7_1438400) and another metacaspase-like protein (MCA3) (PF3D7_1416200). Metacaspases are cysteine-dependent proteases and amongst others have been shown to play a role in cell cycle regulation in *Trypanosoma brucei* (Helms et al., 2006) and *Leishmania major* (Ambit et al., 2008) (the role of metacaspases have been reviewed by (Tsiatsiani et al., 2011) and (Shrestha and Megeney, 2012)).

In *T. brucei* it was shown that the metacaspases *TbMCA2/3/5* are redundant and co-localize with *TbRab11*. *TbMCA5* was identified as *PfMCA2* by blast search (Plasmodb.org). However, no Rab protein was found to be enriched in the DIQ-BioID screen of the Kelch13 compartment. It needs to be noted that the *PfMCA2* protein is about four times larger than its *T. brucei* homologue and the homology region spans AA 1541-1704 (52% similarities). Interestingly, overexpression of a metacaspase lacking the C-terminal region showed an increased number of hypodiploid cells (Laverriere et al., 2012), which suggests a function of the metacaspases and could indicate why all attempts to tag the full length protein of *PfMCA2* C-terminally were unsuccessful. Moreover, in *S. cerevisiae* the metacaspase YCA1 was shown to be involved in cell stress and protein homeostasis, which is mediated by controlling the stability of protein aggregates and thus could have a cytoprotective role (Lee et al., 2010). In *Aspergillus fumigatus* metacaspases were shown to play a role in stress response in the ER potentially regulating the unfolded protein response (UPR) pathways (Richie et al., 2007). Upregulation of expression of the UPR pathways in *P. falciparum* parasites has been proposed to be an important mechanism in artemisinin resistance (Mok et al., 2015) and this idea was also supported by data in *P. berghei* where the action of artemisinins were linked to cellular stress responses as well (Dogovski et al., 2015). Mok et al. used transcriptomics data of patients with acute malaria, but none of the identified genes in the study were found in the here presented screen of interaction partners of Kelch13. Thus, MCA2 could be an interesting link to the cellular stress response, but the dispensability of the MCA2 complicates the analysis. It should also be noted that the limited homologies of the metacaspases in *P. falciparum* to that of other organisms could suggest more or other functions of these proteins in the parasite. N-terminal tagging and co-localization with Kelch13 would be the first step to validate if MCA2 is a true positive hit. Functional analysis by using knock sideways would likely not display a phenotype as MCA2 is not essential for the asexual blood stages and possibly redundant to MCA1 and/or MCA3. However, the identification of interaction

partners by DIQ-BioID could provide important information if MCA2 plays a role in stress response in *P. falciparum*.

The DIQ-BioID hit annotated as Formin2 (PF3D7_1025000) was previously analyzed and there classified as Eps15-like (Flemming, 2015). However, the homology to other eukaryotes is restricted to the N-terminal 150 AAs of the 980 AA protein, indicating a plasmodium specific function.

Eps15 type proteins were shown in other organisms to be involved in different cellular processes in other organisms where it acts as an adaptor protein (reviewed in (van Bergen En Henegouwen, 2009)), for instance in the formation of clathrin coated vesicles (Benmerah et al., 1995; Schmid et al., 2006; Teckchandani et al., 2012), in binding to inositol lipids (Naslavsky et al., 2007) and in the regulation of cellular stress responses with subsequent regulation of cell proliferation (Yamada et al., 2013). Moreover it was reported to be important for internalization of receptors for instance EGFR and the transferrin receptor (Carbone et al., 1997; Huang et al., 2004). Interestingly, Eps15 is monoubiquitinated and the ubiquitination is sufficient for recruitment of Eps15 to the endosomes (Gucwa and Brown, 2014; van Delft et al., 1997). The ubiquitination was found to be mediated by two ubiquitin E3-ligases, Nedd4 and Parkin which lead to regulation of EGFR internalization (Fallon et al., 2006; Woelk et al., 2006). In turn Eps15 was reported to be deubiquitinated by the ubiquitin carboxyl-terminal hydrolase UBPY (Mizuno et al., 2006). Interestingly, in the DIQ-BioID screen the ubiquitin carboxyl-terminal hydrolase 1 (UBP1) (PF3D7_0104300) was identified, indicating a potential interaction of both proteins. However, homology of hUBPY to *Pf*UBP1 is limited to AA 3170-3486 of *Pf*UBP1 with 39% positives. Moreover, hUBPY is one-third of the size of *Pf*UBP1. The role of UBP1 in the Kelch13 complex and in artemisinin resistance is discussed in more detail below.

Kelch motif containing proteins have been demonstrated to control Eps15 activity and thereby to regulate the formation of filamentous actin (Gould et al., 2014). In *P. falciparum* Eps15 was shown to localize to the FV and the parasite plasma membrane (Flemming, 2015). In the same study, analysis by correlative light and electron microscopy (CLEM) indicated a localization of Eps15 to what appeared to be host cell cytosol filled vesicles, which indicated a function of this protein in the uptake of host cell cytosol.

Another protein that was found in the DIQ-BioID experiments is PF3D7_1246300 (KBI.5). In vitro analysis by NCBI Blast indicated a C-terminal homology to an adaptin-like domain spanning from AA 642-888 (see 3.6.5). This could be a further hint for a function in endocytosis, but it is not clear if the protein directly or indirectly interacts with the Kelch13 protein or rather with Eps15.

One of the most interesting hits of the screen is the ubiquitin carboxyl-terminal hydrolase 1 (UBP1) (PF3D7_0104300) as a mutation in the gene has been linked to artemisinin resistance in the rodent malaria model *P. chabaudi* (Hunt et al., 2007). The mutations found in *P. chabaudi* parasites were thought to reduce the deubiquitination activity of UBP1, however this was not experimentally confirmed (Hunt et al., 2007; Hunt et al., 2010). So far six mutations in the gene have been associated with increased parasite clearance time, two described in the original study with *P. chabaudi* and four identified by the analysis of samples from patients infected with *P. falciparum* (Borrmann et al., 2013; Cerqueira et al., 2017; Henriques et al., 2015). UBP1 was shown to have a similar localization as the Kelch13 protein and SLI-TGD indicates that the *ubp1* gene is essential. However, it is not clear if the

Kelch13 protein, Eps15 (see above) or other proteins are substrates for UBP1. Moreover, the extent of artemisinin resistance these mutations confer is unclear and it will be important to determine this in cultured parasites. It also needs to be demonstrated if any of these mutations have an influence on the parasite's fitness as this is important for occurrence of a stable population of mutated parasites in malaria endemic regions. The effect of the different mutations could be rapidly assessed by using the SLI system. Given the published data of the role of UBP1 in artemisinin resistance and the co-localization with Kelch13, it is highly likely that Kelch13 and UBP1 take part in the same cellular process.

In yeast it was demonstrated that Kelch proteins can act as G-protein subunit adaptors and control growth via the G protein coupled receptor Gpr1 that is activated by glucose and by the inhibition of the small G-protein (or small GTPase) Ras (Harashima et al., 2006; Harashima and Heitman, 2002). Small GTPases are activated by guanine nucleotide exchange factors (GEFs) and thereby antagonize the function of GTPase activating proteins (GAPs). Small GTPases are, amongst others, important regulators of cell proliferation and vesicle trafficking.

In the DIQ-BioID screen 4 proteins were found that could act in a similar way in *P. falciparum*. PF3D7_1447800 is a calponin homology domain-containing protein. Calponin homology-domain containing proteins have been shown to act as GEFs in other organisms (Groysman et al., 2000; Han et al., 1998). Two GTPase activating proteins, that are physiological antagonists of GEFs, were also identified in the screen, namely PF3D7_0907200 and PF3D7_0813000, whereof the latter was shown to be essential for parasite development in the asexual blood stages in this study. As essential component of the glucose metabolism the 6-phosphofructokinase (PF3D7_0915400) was found (Mony et al., 2009).

This could indicate potential function of the Kelch13 protein in cell cycle proliferation, which would be in line with the observed phenotype of parasite arresting in transition from the ring to trophozoite stage.

4.2.3 Absence of proteins reported to be involved in artemisinin resistance in the Kelch13 DIQ-BioID screen

A reported mode of action for artemisinin resistance was an effect of the Kelch13 mutation on the PI3P levels via phosphatidylinositol-3-kinase (PI3K) (Mbengue et al., 2015a). However, Kelch13 was found in close proximity to PI3P in this study, but the reported direct interaction of the Kelch13 protein with PI3K was not detected in the DIQ-BioID screen. This might either indicate that PI3K is only very transiently at the Kelch13 compartment, or it may not have been tagged with biotin due to sterical or other technical problems (section 4.2.1) or it may in fact not be present on this compartment.

A notable absentee from the DIQ-BioID screen besides the PI3K is a protein involved into the ubiquitin-proteasome machinery. It has been shown that proteins in artemisinin resistant parasites are

less ubiquitinated (Dogovski et al., 2015). Another publication claimed that an artemisinin resistance conferring mutation in the Kelch13 protein decreases the ubiquitination of the potential substrate PI3K of the Kelch13-E3 ligase complex and thus showed increased PI3P levels in mutated parasites (Mbengue et al., 2015a). The Kelch13 protein itself was suspected to act as an E3 ligase adaptor already before this (Ariey et al., 2014) as it has been shown for proteins of the KHLH family (Dhanoa et al., 2013). No protein of the ubiquitin machinery could be identified to be significantly enriched in the DIQ-BioID experiment and thus are potentially not present in the Kelch13 compartment or not have not been detected due to above mentioned problems (section 4.2.1). This suggests that the Kelch13 protein does not act as an E3 ligase adaptor. This has already been indicated in another publication that highlighted the missing BACK domain in the Kelch13 protein, which is necessary for the protein to bind the E3 ligase complex (Tilley et al., 2016). Thus, Kelch13 likely does not represent a protein of the KHLH family, but is rather a member of the KLHDC (section 1.5) family. The observed difference in ubiquitination levels of artemisinin sensitive to artemisinin resistant parasites could be attributed to different stress response mechanisms or be realized up- or downstream of the cellular process Kelch13 contributes to. The identification of the ubiquitin carboxyl-terminal hydrolase (UBP1) implicates that an ubiquitinated protein is part of the Kelch13 complex or compartment. Eps15 was shown to be regulated by this modification (see above) (Fallon et al., 2006; Woelk et al., 2006), but other candidates or the Kelch13 itself could also be the ubiquitinated target. However, proteins that have a role in the resistance to artemisinins are not necessarily essential for the physiological function of the Kelch13 complex or need to be part of it.

The most intriguing question, the function of Kelch13 in the parasite and likely related, its role in DHA resistance, cannot be answered by the data presented here. DiQ-BioID has revealed many proteins residing in the same compartment or potentially directly interacting with the Kelch13 protein. It is interesting to note that the compartment Kelch13 resides in, based on the co-localizing PfEps15-like, is filled with host cell cytosol (Flemming, 2015) but that there was no indication in this work for a role of Kelch13 in hemoglobin uptake. However, the DIQ-BioID screen and the essential proteins that have been identified, with a detailed analysis needs to be carried out in the near future, will be an important resource for probing into the function of this compartment and of Kelch13.

Bibliography

- Abu Bakar, N., Klonis, N., Hanssen, E., Chan, C., and Tilley, L. (2010). Digestive-vacuole genesis and endocytic processes in the early intraerythrocytic stages of *Plasmodium falciparum*. *J Cell Sci* *123*, 441-450.
- Agnandji, S., Lell, B., Schellenberg, D., and Rts, S.C.T.P. (2014). Efficacy and safety of the RTS,S/AS01 malaria vaccine during 18 months after vaccination: a phase 3 randomized, controlled trial in children and young infants at 11 African sites. *PLoS Med* *11*, e1001685.
- Agop-Nersesian, C., Pfahler, J., Lanzer, M., and Meissner, M. (2008). Functional expression of ribozymes in Apicomplexa: towards exogenous control of gene expression by inducible RNA-cleavage. *Int J Parasitol* *38*, 673-681.
- Agrawal, N., Dasaradhi, P.V., Mohmmmed, A., Malhotra, P., Bhatnagar, R.K., and Mukherjee, S.K. (2003). RNA interference: biology, mechanism, and applications. *Microbiol Mol Biol Rev* *67*, 657-685.
- Aguilar, R., Magallon-Tejada, A., Achtman, A.H., Moraleda, C., Joice, R., Cistero, P., Li Wai Suen, C.S., Nhabomba, A., Macete, E., Mueller, I., *et al.* (2014). Molecular evidence for the localization of *Plasmodium falciparum* immature gametocytes in bone marrow. *Blood* *123*, 959-966.
- Ahmed, A., and Sharma, Y.D. (2008). Ribozyme cleavage of *Plasmodium falciparum* gyrase A gene transcript affects the parasite growth. *Parasitol Res* *103*, 751-763.
- Aikawa, M., Huff, C.G., and Spinz, H. (1966). Comparative feeding mechanisms of avian and primate malarial parasites. *Mil Med* *131*, Suppl:969-983.
- Aikawa, M., Miller, L.H., Johnson, J., and Rabbege, J. (1978). Erythrocyte entry by malarial parasites. A moving junction between erythrocyte and parasite. *J Cell Biol* *77*, 72-82.
- Aly, A.S., Vaughan, A.M., and Kappe, S.H. (2009). Malaria parasite development in the mosquito and infection of the mammalian host. *Annu Rev Microbiol* *63*, 195-221.
- Ambit, A., Fasel, N., Coombs, G.H., and Mottram, J.C. (2008). An essential role for the *Leishmania major* metacaspase in cell cycle progression. *Cell Death Differ* *15*, 113-122.
- Andenmatten, N., Egarter, S., Jackson, A.J., Jullien, N., Herman, J.P., and Meissner, M. (2013). Conditional genome engineering in *Toxoplasma gondii* uncovers alternative invasion mechanisms. *Nat Methods* *10*, 125-127.
- Anderson, R.M., and May, R.M. (1999). *Infectious Diseases of Humans: Dynamics and Control*
- Annoura, T., Ploemen, I.H., van Schaijk, B.C., Sajid, M., Vos, M.W., van Gemert, G.J., Chevalley-Maurel, S., Franke-Fayard, B.M., Hermsen, C.C., Gego, A., *et al.* (2012). Assessing the adequacy of attenuation of genetically modified malaria parasite vaccine candidates. *Vaccine* *30*, 2662-2670.
- Arama, C., and Troye-Blomberg, M. (2014). The path of malaria vaccine development: challenges and perspectives. *J Intern Med* *275*, 456-466.
- Ariey, F., Witkowski, B., Amaratunga, C., Beghain, J., Langlois, A.C., Khim, N., Kim, S., Duru, V., Bouchier, C., Ma, L., *et al.* (2014). A molecular marker of artemisinin-resistant *Plasmodium falciparum* malaria. *Nature* *505*, 50-55.
- Armstrong, C.M., and Goldberg, D.E. (2007). An FKBP destabilization domain modulates protein levels in *Plasmodium falciparum*. *Nat Methods* *4*, 1007-1009.
- Arrow, K.J., and Panosian, C. (2004). Saving Lives, Buying Time: Economics of Malaria Drugs in an Age of Resistance. In *Saving Lives, Buying Time: Economics of Malaria Drugs in an Age of Resistance*, K.J. Arrow, C. Panosian, and H. Gelband, eds. (Washington (DC)).

- Ashley, E.A., Dhorda, M., Fairhurst, R.M., Amaratunga, C., Lim, P., Suon, S., Sreng, S., Anderson, J.M., Mao, S., Sam, B., *et al.* (2014). Spread of artemisinin resistance in *Plasmodium falciparum* malaria. *N Engl J Med* *371*, 411-423.
- Baer, K., Klotz, C., Kappe, S.H., Schnieder, T., and Frevert, U. (2007). Release of hepatic *Plasmodium yoelii* merozoites into the pulmonary microvasculature. *PLoS Pathog* *3*, e171.
- Banaszynski, L.A., Chen, L.C., Maynard-Smith, L.A., Ooi, A.G., and Wandless, T.J. (2006). A rapid, reversible, and tunable method to regulate protein function in living cells using synthetic small molecules. *Cell* *126*, 995-1004.
- Banaszynski, L.A., Liu, C.W., and Wandless, T.J. (2005). Characterization of the FKBP.rapamycin.FRB ternary complex. *J Am Chem Soc* *127*, 4715-4721.
- Bannister, L.H., Butcher, G.A., Dennis, E.D., and Mitchell, G.H. (1975). Structure and invasive behaviour of *Plasmodium knowlesi* merozoites in vitro. *Parasitology* *71*, 483-491.
- Bardwell, V.J., and Treisman, R. (1994). The POZ domain: a conserved protein-protein interaction motif. *Genes Dev* *8*, 1664-1677.
- Bartoloni, A., and Zammarchi, L. (2012). Clinical aspects of uncomplicated and severe malaria. *Mediterr J Hematol Infect Dis* *4*, e2012026.
- Baum, J., Papenfuss, A.T., Mair, G.R., Janse, C.J., Vlachou, D., Waters, A.P., Cowman, A.F., Crabb, B.S., and de Koning-Ward, T.F. (2009). Molecular genetics and comparative genomics reveal RNAi is not functional in malaria parasites. *Nucleic Acids Res* *37*, 3788-3798.
- Baum, J., Richard, D., Healer, J., Rug, M., Krnajski, Z., Gilberger, T.W., Green, J.L., Holder, A.A., and Cowman, A.F. (2006). A conserved molecular motor drives cell invasion and gliding motility across malaria life cycle stages and other apicomplexan parasites. *J Biol Chem* *281*, 5197-5208.
- Beck, J.R., Muralidharan, V., Oksman, A., and Goldberg, D.E. (2014). PTEX component HSP101 mediates export of diverse malaria effectors into host erythrocytes. *Nature* *511*, 592-595.
- Belmont, B.J., and Niles, J.C. (2010). Engineering a direct and inducible protein-RNA interaction to regulate RNA biology. *ACS Chem Biol* *5*, 851-861.
- Belshaw, P.J., Ho, S.N., Crabtree, G.R., and Schreiber, S.L. (1996). Controlling protein association and subcellular localization with a synthetic ligand that induces heterodimerization of proteins. *Proc Natl Acad Sci U S A* *93*, 4604-4607.
- Benmerah, A., Gagnon, J., Begue, B., Megarbane, B., Dautry-Varsat, A., and Cerf-Bensussan, N. (1995). The tyrosine kinase substrate eps15 is constitutively associated with the plasma membrane adaptor AP-2. *J Cell Biol* *131*, 1831-1838.
- Bhatt, S., Weiss, D.J., Cameron, E., Bisanzio, D., Mappin, B., Dalrymple, U., Battle, K.E., Moyes, C.L., Henry, A., Eckhoff, P.A., *et al.* (2015). The effect of malaria control on *Plasmodium falciparum* in Africa between 2000 and 2015. *Nature* *526*, 207-211.
- Billker, O., Dechamps, S., Tewari, R., Wenig, G., Franke-Fayard, B., and Brinkmann, V. (2004). Calcium and a calcium-dependent protein kinase regulate gamete formation and mosquito transmission in a malaria parasite. *Cell* *117*, 503-514.
- Bindels, D.S., Haarbosch, L., van Weeren, L., Postma, M., Wiese, K.E., Mastop, M., Aumonier, S., Gotthard, G., Royant, A., Hink, M.A., *et al.* (2017). mScarlet: a bright monomeric red fluorescent protein for cellular imaging. *Nat Methods* *14*, 53-56.
- Birnbaum, J., Flemming, S., Reichard, N., Soares, A.B., Mesen-Ramirez, P., Jonscher, E., Bergmann, B., and Spielmann, T. (2017). A genetic system to study *Plasmodium falciparum* protein function. *Nat Methods* *14*, 450-456.

- Bitinaite, J., Wah, D.A., Aggarwal, A.K., and Schildkraut, I. (1998). FokI dimerization is required for DNA cleavage. *Proc Natl Acad Sci U S A* *95*, 10570-10575.
- Blackman, M.J., and Carruthers, V.B. (2013). Recent insights into apicomplexan parasite egress provide new views to a kill. *Curr Opin Microbiol* *16*, 459-464.
- Blancke-Soares (2016). Identification of trafficking determinants in novel PNEPs of the human malaria parasite *Plasmodium falciparum*.
- Boddey, J.A., Hodder, A.N., Gunther, S., Gilson, P.R., Patsiouras, H., Kapp, E.A., Pearce, J.A., de Koning-Ward, T.F., Simpson, R.J., Crabb, B.S., *et al.* (2010). An aspartyl protease directs malaria effector proteins to the host cell. *Nature* *463*, 627-631.
- Boddey, J.A., O'Neill, M.T., Lopaticki, S., Carvalho, T.G., Hodder, A.N., Nebl, T., Wawra, S., van West, P., Ebrahimzadeh, Z., Richard, D., *et al.* (2016). Export of malaria proteins requires co-translational processing of the PEXEL motif independent of phosphatidylinositol-3-phosphate binding. *Nat Commun* *7*, 10470.
- Boncompain, G., Divoux, S., Gareil, N., de Forges, H., Lescure, A., Latreche, L., Mercanti, V., Jollivet, F., Raposo, G., and Perez, F. (2012). Synchronization of secretory protein traffic in populations of cells. *Nat Methods* *9*, 493-498.
- Borrmann, S., Straimer, J., Mwai, L., Abdi, A., Rippert, A., Okombo, J., Muriithi, S., Sasi, P., Kortok, M.M., Lowe, B., *et al.* (2013). Genome-wide screen identifies new candidate genes associated with artemisinin susceptibility in *Plasmodium falciparum* in Kenya. *Sci Rep* *3*, 3318.
- Bozdech, Z., Llinas, M., Pulliam, B.L., Wong, E.D., Zhu, J., and DeRisi, J.L. (2003). The transcriptome of the intraerythrocytic developmental cycle of *Plasmodium falciparum*. *PLoS Biol* *1*, E5.
- Brancucci, N.M., Bertschi, N.L., Zhu, L., Niederwieser, I., Chin, W.H., Wampfler, R., Freymond, C., Rottmann, M., Felger, I., Bozdech, Z., *et al.* (2014). Heterochromatin protein 1 secures survival and transmission of malaria parasites. *Cell Host Microbe* *16*, 165-176.
- Bray, P.G., Mungthin, M., Ridley, R.G., and Ward, S.A. (1998). Access to hemozoin: the basis of chloroquine resistance. *Mol Pharmacol* *54*, 170-179.
- Bruce, M.C., Alano, P., Duthie, S., and Carter, R. (1990). Commitment of the malaria parasite *Plasmodium falciparum* to sexual and asexual development. *Parasitology* *100 Pt 2*, 191-200.
- Carbone, R., Fre, S., Iannolo, G., Belleudi, F., Mancini, P., Pelicci, P.G., Torrissi, M.R., and Di Fiore, P.P. (1997). eps15 and eps15R are essential components of the endocytic pathway. *Cancer Res* *57*, 5498-5504.
- Caro, F., Miller, M.G., and DeRisi, J.L. (2012). Plate-based transfection and culturing technique for genetic manipulation of *Plasmodium falciparum*. *Malar J* *11*, 22.
- Carter, R., and Miller, L.H. (1979). Evidence for environmental modulation of gametocytogenesis in *Plasmodium falciparum* in continuous culture. *Bull World Health Organ* *57 Suppl 1*, 37-52.
- Castellano, F., Montcourrier, P., and Chavrier, P. (2000). Membrane recruitment of Rac1 triggers phagocytosis. *J Cell Sci* *113 (Pt 17)*, 2955-2961.
- Celli, M.a. (1885).
- Cerqueira, G.C., Cheeseman, I.H., Schaffner, S.F., Nair, S., McDew-White, M., Phyto, A.P., Ashley, E.A., Melnikov, A., Rogov, P., Birren, B.W., *et al.* (2017). Longitudinal genomic surveillance of *Plasmodium falciparum* malaria parasites reveals complex genomic architecture of emerging artemisinin resistance. *Genome Biol* *18*, 78.
- Cheeseman, I.H., Miller, B.A., Nair, S., Nkhoma, S., Tan, A., Tan, J.C., Al Saai, S., Phyto, A.P., Moo, C.L., Lwin, K.M., *et al.* (2012). A major genome region underlying artemisinin resistance in malaria. *Science* *336*, 79-82.

- Chen, A.L., Kim, E.W., Toh, J.Y., Vashisht, A.A., Rashoff, A.Q., Van, C., Huang, A.S., Moon, A.S., Bell, H.N., Bentolila, L.A., *et al.* (2015). Novel components of the *Toxoplasma* inner membrane complex revealed by BioID. *MBio* *6*, e02357-02314.
- Chen, J., Zheng, X.F., Brown, E.J., and Schreiber, S.L. (1995). Identification of an 11-kDa FKBP12-rapamycin-binding domain within the 289-kDa FKBP12-rapamycin-associated protein and characterization of a critical serine residue. *Proc Natl Acad Sci U S A* *92*, 4947-4951.
- Choi-Rhee, E., Schulman, H., and Cronan, J.E. (2004). Promiscuous protein biotinylation by *Escherichia coli* biotin protein ligase. *Protein Sci* *13*, 3043-3050.
- Choi, J., Chen, J., Schreiber, S.L., and Clardy, J. (1996). Structure of the FKBP12-rapamycin complex interacting with the binding domain of human FRAP. *Science* *273*, 239-242.
- Collins, C.R., Das, S., Wong, E.H., Andenmatten, N., Stallmach, R., Hackett, F., Herman, J.P., Muller, S., Meissner, M., and Blackman, M.J. (2013). Robust inducible Cre recombinase activity in the human malaria parasite *Plasmodium falciparum* enables efficient gene deletion within a single asexual erythrocytic growth cycle. *Mol Microbiol* *88*, 687-701.
- Collins, W.E., and Jeffery, G.M. (2005). *Plasmodium ovale*: parasite and disease. *Clin Microbiol Rev* *18*, 570-581.
- Coluzzi, M. (1999). The clay feet of the malaria giant and its African roots: hypotheses and inferences about origin, spread and control of *Plasmodium falciparum*. *Parassitologia* *41*, 277-283.
- Cowman, A.F., and Crabb, B.S. (2006). Invasion of red blood cells by malaria parasites. *Cell* *124*, 755-766.
- Crabb, B.S., Cooke, B.M., Reeder, J.C., Waller, R.F., Caruana, S.R., Davern, K.M., Wickham, M.E., Brown, G.V., Coppel, R.L., and Cowman, A.F. (1997). Targeted gene disruption shows that knobs enable malaria-infected red cells to cytoadhere under physiological shear stress. *Cell* *89*, 287-296.
- Cronan, J.E. (2005). Targeted and proximity-dependent promiscuous protein biotinylation by a mutant *Escherichia coli* biotin protein ligase. *J Nutr Biochem* *16*, 416-418.
- Crosnier, C., Bustamante, L.Y., Bartholdson, S.J., Bei, A.K., Theron, M., Uchikawa, M., Mboup, S., Ndir, O., Kwiatkowski, D.P., Duraisingh, M.T., *et al.* (2011). Basigin is a receptor essential for erythrocyte invasion by *Plasmodium falciparum*. *Nature* *480*, 534-537.
- de Koning-Ward, T.F., Dixon, M.W., Tilley, L., and Gilson, P.R. (2016). *Plasmodium* species: master renovators of their host cells. *Nat Rev Microbiol* *14*, 494-507.
- de Koning-Ward, T.F., Gilson, P.R., Boddey, J.A., Rug, M., Smith, B.J., Papenfuss, A.T., Sanders, P.R., Lundie, R.J., Maier, A.G., Cowman, A.F., *et al.* (2009). A newly discovered protein export machine in malaria parasites. *Nature* *459*, 945-949.
- de Koning-Ward, T.F., Gilson, P.R., and Crabb, B.S. (2015). Advances in molecular genetic systems in malaria. *Nat Rev Microbiol* *13*, 373-387.
- de Koning-Ward, T.F., Waters, A.P., and Crabb, B.S. (2001). Puromycin-N-acetyltransferase as a selectable marker for use in *Plasmodium falciparum*. *Mol Biochem Parasitol* *117*, 155-160.
- Deitsch, K., Driskill, C., and Wellems, T. (2001). Transformation of malaria parasites by the spontaneous uptake and expression of DNA from human erythrocytes. *Nucleic Acids Res* *29*, 850-853.
- Delves, M., Plouffe, D., Scheurer, C., Meister, S., Wittlin, S., Winzeler, E.A., Sinden, R.E., and Leroy, D. (2012). The activities of current antimalarial drugs on the life cycle stages of *Plasmodium*: a comparative study with human and rodent parasites. *PLoS Med* *9*, e1001169.
- Deponte, M., Hoppe, H.C., Lee, M.C., Maier, A.G., Richard, D., Rug, M., Spielmann, T., and Przyborski, J.M. (2012). Wherever I may roam: protein and membrane trafficking in *P. falciparum*-infected red blood cells. *Mol Biochem Parasitol* *186*, 95-116.

- Dhanao, B.S., Cogliati, T., Satish, A.G., Bruford, E.A., and Friedman, J.S. (2013). Update on the Kelch-like (KLHL) gene family. *Hum Genomics* 7, 13.
- Dogovski, C., Xie, S.C., Burgio, G., Bridgford, J., Mok, S., McCaw, J.M., Chotivanich, K., Kenny, S., Gnädig, N., Straimer, J., *et al.* (2015). Targeting the cell stress response of *Plasmodium falciparum* to overcome artemisinin resistance. *PLoS Biol* 13, e1002132.
- Dondorp, A.M., Nosten, F., Yi, P., Das, D., Phyto, A.P., Tarning, J., Lwin, K.M., Ariey, F., Hanpithakpong, W., Lee, S.J., *et al.* (2009). Artemisinin resistance in *Plasmodium falciparum* malaria. *N Engl J Med* 361, 455-467.
- Douglas, A.D., Baldeviano, G.C., Lucas, C.M., Lugo-Roman, L.A., Crosnier, C., Bartholdson, S.J., Diouf, A., Miura, K., Lambert, L.E., Ventocilla, J.A., *et al.* (2015). A PfRH5-based vaccine is efficacious against heterologous strain blood-stage *Plasmodium falciparum* infection in aotus monkeys. *Cell Host Microbe* 17, 130-139.
- Duraisingh, M.T., Triglia, T., and Cowman, A.F. (2002). Negative selection of *Plasmodium falciparum* reveals targeted gene deletion by double crossover recombination. *Int J Parasitol* 32, 81-89.
- Durand, R., Jafari, S., Vauzelle, J., Delabre, J.F., Jesic, Z., and Le Bras, J. (2001). Analysis of pfert point mutations and chloroquine susceptibility in isolates of *Plasmodium falciparum*. *Mol Biochem Parasitol* 114, 95-102.
- Dvorin, J.D., Martyn, D.C., Patel, S.D., Grimley, J.S., Collins, C.R., Hopp, C.S., Bright, A.T., Westenberger, S., Winzeler, E., Blackman, M.J., *et al.* (2010). A plant-like kinase in *Plasmodium falciparum* regulates parasite egress from erythrocytes. *Science* 328, 910-912.
- Eckstein-Ludwig, U., Webb, R.J., Van Goethem, I.D., East, J.M., Lee, A.G., Kimura, M., O'Neill, P.M., Bray, P.G., Ward, S.A., and Krishna, S. (2003). Artemisinins target the SERCA of *Plasmodium falciparum*. *Nature* 424, 957-961.
- Elsworth, B., Matthews, K., Nie, C.Q., Kalanon, M., Charnaud, S.C., Sanders, P.R., Chisholm, S.A., Counihan, N.A., Shaw, P.J., Pino, P., *et al.* (2014). PTEX is an essential nexus for protein export in malaria parasites. *Nature* 511, 587-591.
- Enayati, A., and Hemingway, J. (2010). Malaria management: past, present, and future. *Annu Rev Entomol* 55, 569-591.
- Epp, C., Raskolnikov, D., and Deitsch, K.W. (2008). A regulatable transgene expression system for cultured *Plasmodium falciparum* parasites. *Malar J* 7, 86.
- Faivre, S., Kroemer, G., and Raymond, E. (2006). Current development of mTOR inhibitors as anticancer agents. *Nat Rev Drug Discov* 5, 671-688.
- Fallon, L., Belanger, C.M., Corera, A.T., Kontogianna, M., Regan-Klapisz, E., Moreau, F., Voortman, J., Haber, M., Rouleau, G., Thorarinsdottir, T., *et al.* (2006). A regulated interaction with the UIM protein Eps15 implicates parkin in EGF receptor trafficking and PI(3)K-Akt signalling. *Nat Cell Biol* 8, 834-842.
- Farfour, E., Charlotte, F., Settegrana, C., Miyara, M., and Buffet, P. (2012). The extravascular compartment of the bone marrow: a niche for *Plasmodium falciparum* gametocyte maturation? *Malar J* 11, 285.
- Fast, N.M., Kissinger, J.C., Roos, D.S., and Keeling, P.J. (2001). Nuclear-encoded, plastid-targeted genes suggest a single common origin for apicomplexan and dinoflagellate plastids. *Mol Biol Evol* 18, 418-426.
- Feng, S., Laketa, V., Stein, F., Rutkowska, A., MacNamara, A., Depner, S., Klingmuller, U., Saez-Rodriguez, J., and Schultz, C. (2014). A rapidly reversible chemical dimerizer system to study lipid signaling in living cells. *Angew Chem Int Ed Engl* 53, 6720-6723.
- Fidock, D.A., and Wellems, T.E. (1997). Transformation with human dihydrofolate reductase renders malaria parasites insensitive to WR9210 but does not affect the intrinsic activity of proguanil. *Proc Natl Acad Sci U S A* 94, 10931-10936.

- Fili, N., Calleja, V., Woscholski, R., Parker, P.J., and Larijani, B. (2006). Compartmental signal modulation: Endosomal phosphatidylinositol 3-phosphate controls endosome morphology and selective cargo sorting. *Proc Natl Acad Sci U S A* *103*, 15473-15478.
- Fivaz, M., Bandara, S., Inoue, T., and Meyer, T. (2008). Robust neuronal symmetry breaking by Ras-triggered local positive feedback. *Curr Biol* *18*, 44-50.
- Flemming, S. (2015). Visualization and characterization of endocytic processes in the human Malaria parasite *P. falciparum* (Welch, 1897).
- Flores, M.V., Atkins, D., Wade, D., O'Sullivan, W.J., and Stewart, T.S. (1997). Inhibition of *Plasmodium falciparum* proliferation in vitro by ribozymes. *J Biol Chem* *272*, 16940-16945.
- Francis, S.E., Sullivan, D.J., Jr., and Goldberg, D.E. (1997). Hemoglobin metabolism in the malaria parasite *Plasmodium falciparum*. *Annu Rev Microbiol* *51*, 97-123.
- Furukawa, M., He, Y.J., Borchers, C., and Xiong, Y. (2003). Targeting of protein ubiquitination by BTB-Cullin 3-Roc1 ubiquitin ligases. *Nat Cell Biol* *5*, 1001-1007.
- Gallego, O., Specht, T., Brach, T., Kumar, A., Gavin, A.C., and Kaksonen, M. (2013). Detection and characterization of protein interactions in vivo by a simple live-cell imaging method. *PLoS One* *8*, e62195.
- Ganesan, S.M., Falla, A., Goldfless, S.J., Nasamu, A.S., and Niles, J.C. (2016). Synthetic RNA-protein modules integrated with native translation mechanisms to control gene expression in malaria parasites. *Nat Commun* *7*, 10727.
- Ganesan, S.M., Morrisey, J.M., Ke, H., Painter, H.J., Laroia, K., Phillips, M.A., Rathod, P.K., Mather, M.W., and Vaidya, A.B. (2011). Yeast dihydroorotate dehydrogenase as a new selectable marker for *Plasmodium falciparum* transfection. *Mol Biochem Parasitol* *177*, 29-34.
- Gardner, M.J., Hall, N., Fung, E., White, O., Berriman, M., Hyman, R.W., Carlton, J.M., Pain, A., Nelson, K.E., Bowman, S., *et al.* (2002). Genome sequence of the human malaria parasite *Plasmodium falciparum*. *Nature* *419*, 498-511.
- Geda, P., Patury, S., Ma, J., Bharucha, N., Dobry, C.J., Lawson, S.K., Gestwicki, J.E., and Kumar, A. (2008). A small molecule-directed approach to control protein localization and function. *Yeast* *25*, 577-594.
- Gerald, N., Mahajan, B., and Kumar, S. (2011). Mitosis in the human malaria parasite *Plasmodium falciparum*. *Eukaryot Cell* *10*, 474-482.
- Ghorbal, M., Gorman, M., Macpherson, C.R., Martins, R.M., Scherf, A., and Lopez-Rubio, J.J. (2014). Genome editing in the human malaria parasite *Plasmodium falciparum* using the CRISPR-Cas9 system. *Nat Biotechnol* *32*, 819-821.
- Gibson, D.G., Young, L., Chuang, R.Y., Venter, J.C., Hutchison, C.A., 3rd, and Smith, H.O. (2009). Enzymatic assembly of DNA molecules up to several hundred kilobases. *Nat Methods* *6*, 343-345.
- Gluzman, I.Y., Francis, S.E., Oksman, A., Smith, C.E., Duffin, K.L., and Goldberg, D.E. (1994). Order and specificity of the *Plasmodium falciparum* hemoglobin degradation pathway. *J Clin Invest* *93*, 1602-1608.
- Goel, V.K., Li, X., Chen, H., Liu, S.C., Chishti, A.H., and Oh, S.S. (2003). Band 3 is a host receptor binding merozoite surface protein 1 during the *Plasmodium falciparum* invasion of erythrocytes. *Proc Natl Acad Sci U S A* *100*, 5164-5169.
- Goldberg, D.E., Slater, A.F., Beavis, R., Chait, B., Cerami, A., and Henderson, G.B. (1991). Hemoglobin degradation in the human malaria pathogen *Plasmodium falciparum*: a catabolic pathway initiated by a specific aspartic protease. *J Exp Med* *173*, 961-969.
- Goldberg, D.E., Slater, A.F., Cerami, A., and Henderson, G.B. (1990). Hemoglobin degradation in the malaria parasite *Plasmodium falciparum*: an ordered process in a unique organelle. *Proc Natl Acad Sci U S A* *87*, 2931-2935.

- Goldfless, S.J., Wagner, J.C., and Niles, J.C. (2014). Versatile control of *Plasmodium falciparum* gene expression with an inducible protein-RNA interaction. *Nat Commun* 5, 5329.
- Gomes, A.R., Bushell, E., Schwach, F., Girling, G., Anar, B., Quail, M.A., Herd, C., Pfander, C., Modrzynska, K., Rayner, J.C., *et al.* (2015). A genome-scale vector resource enables high-throughput reverse genetic screening in a malaria parasite. *Cell Host Microbe* 17, 404-413.
- Goodman, C.D., Siregar, J.E., Mollard, V., Vega-Rodriguez, J., Syafruddin, D., Matsuoka, H., Matsuzaki, M., Toyama, T., Sturm, A., Cozijnsen, A., *et al.* (2016). Parasites resistant to the antimalarial atovaquone fail to transmit by mosquitoes. *Science* 352, 349-353.
- Gopalakrishnan, A.M., Kundu, A.K., Mandal, T.K., and Kumar, N. (2013). Novel nanosomes for gene delivery to *Plasmodium falciparum*-infected red blood cells. *Sci Rep* 3, 1534.
- Gould, C.J., Chesarone-Cataldo, M., Alioto, S.L., Salin, B., Sagot, I., and Goode, B.L. (2014). *Saccharomyces cerevisiae* Kelch proteins and Bud14 protein form a stable 520-kDa formin regulatory complex that controls actin cable assembly and cell morphogenesis. *J Biol Chem* 289, 18290-18301.
- Greenwood, B.M., Fidock, D.A., Kyle, D.E., Kappe, S.H., Alonso, P.L., Collins, F.H., and Duffy, P.E. (2008). Malaria: progress, perils, and prospects for eradication. *J Clin Invest* 118, 1266-1276.
- Groysman, M., Russek, C.S., and Katzav, S. (2000). Vav, a GDP/GTP nucleotide exchange factor, interacts with GDIs, proteins that inhibit GDP/GTP dissociation. *FEBS Lett* 467, 75-80.
- Gruring, C., Heiber, A., Kruse, F., Ungefehr, J., Gilberger, T.W., and Spielmann, T. (2011). Development and host cell modifications of *Plasmodium falciparum* blood stages in four dimensions. *Nat Commun* 2, 165.
- Gucwa, A.L., and Brown, D.A. (2014). UIM domain-dependent recruitment of the endocytic adaptor protein Eps15 to ubiquitin-enriched endosomes. *BMC Cell Biol* 15, 34.
- Guo, Z., Neilson, L.J., Zhong, H., Murray, P.S., Zanivan, S., and Zaidel-Bar, R. (2014). E-cadherin interactome complexity and robustness resolved by quantitative proteomics. *Sci Signal* 7, rs7.
- Guttery, D.S., Holder, A.A., and Tewari, R. (2012). Sexual development in *Plasmodium*: lessons from functional analyses. *PLoS Pathog* 8, e1002404.
- Guttery, D.S., Roques, M., Holder, A.A., and Tewari, R. (2015). Commit and Transmit: Molecular Players in *Plasmodium* Sexual Development and Zygote Differentiation. *Trends Parasitol* 31, 676-685.
- Hamilton, A.J., and Baulcombe, D.C. (1999). A species of small antisense RNA in posttranscriptional gene silencing in plants. *Science* 286, 950-952.
- Han, J., Luby-Phelps, K., Das, B., Shu, X., Xia, Y., Mosteller, R.D., Krishna, U.M., Falck, J.R., White, M.A., and Broek, D. (1998). Role of substrates and products of PI 3-kinase in regulating activation of Rac-related guanosine triphosphatases by Vav. *Science* 279, 558-560.
- Hanahan, D. (1983). Studies on transformation of *Escherichia coli* with plasmids. *J Mol Biol* 166, 557-580.
- Harashima, T., Anderson, S., Yates, J.R., 3rd, and Heitman, J. (2006). The kelch proteins Gpb1 and Gpb2 inhibit Ras activity via association with the yeast RasGAP neurofibromin homologs Ira1 and Ira2. *Mol Cell* 22, 819-830.
- Harashima, T., and Heitman, J. (2002). The Galpha protein Gpa2 controls yeast differentiation by interacting with kelch repeat proteins that mimic Gbeta subunits. *Mol Cell* 10, 163-173.
- Haruki, H., Nishikawa, J., and Laemmli, U.K. (2008). The anchor-away technique: rapid, conditional establishment of yeast mutant phenotypes. *Mol Cell* 31, 925-932.
- Heiber, A., Kruse, F., Pick, C., Gruring, C., Flemming, S., Oberli, A., Schoeler, H., Retzlaff, S., Mesen-Ramirez, P., Hiss, J.A., *et al.* (2013). Identification of new PNEPs indicates a substantial non-PEXEL exportome and underpins common features in *Plasmodium falciparum* protein export. *PLoS Pathog* 9, e1003546.

- Helms, M.J., Ambit, A., Appleton, P., Tetley, L., Coombs, G.H., and Mottram, J.C. (2006). Bloodstream form *Trypanosoma brucei* depend upon multiple metacaspases associated with RAB11-positive endosomes. *J Cell Sci* *119*, 1105-1117.
- Henriques, G., van Schalkwyk, D.A., Burrow, R., Warhurst, D.C., Thompson, E., Baker, D.A., Fidock, D.A., Hallett, R., Flueck, C., and Sutherland, C.J. (2015). The Mu subunit of *Plasmodium falciparum* clathrin-associated adaptor protein 2 modulates in vitro parasite response to artemisinin and quinine. *Antimicrob Agents Chemother* *59*, 2540-2547.
- Hiller, N.L., Bhattacharjee, S., van Ooij, C., Liolios, K., Harrison, T., Lopez-Estrano, C., and Haldar, K. (2004). A host-targeting signal in virulence proteins reveals a secretome in malarial infection. *Science* *306*, 1934-1937.
- Howes, R.E., Battle, K.E., Mendis, K.N., Smith, D.L., Cibulskis, R.E., Baird, J.K., and Hay, S.I. (2016). Global Epidemiology of *Plasmodium vivax*. *Am J Trop Med Hyg* *95*, 15-34.
- Howes, R.E., Patil, A.P., Piel, F.B., Nyangiri, O.A., Kabaria, C.W., Gething, P.W., Zimmerman, P.A., Barnadas, C., Beall, C.M., Gebremedhin, A., *et al.* (2011). The global distribution of the Duffy blood group. *Nat Commun* *2*, 266.
- Huang, F., Khvorova, A., Marshall, W., and Sorkin, A. (2004). Analysis of clathrin-mediated endocytosis of epidermal growth factor receptor by RNA interference. *J Biol Chem* *279*, 16657-16661.
- Huh, W.K., Falvo, J.V., Gerke, L.C., Carroll, A.S., Howson, R.W., Weissman, J.S., and O'Shea, E.K. (2003). Global analysis of protein localization in budding yeast. *Nature* *425*, 686-691.
- Hunsicker, A., Steber, M., Mayer, G., Meitert, J., Klotzsche, M., Blind, M., Hillen, W., Berens, C., and Suess, B. (2009). An RNA aptamer that induces transcription. *Chem Biol* *16*, 173-180.
- Hunt, P., Afonso, A., Creasey, A., Culleton, R., Sidhu, A.B., Logan, J., Valderramos, S.G., McNae, I., Cheesman, S., do Rosario, V., *et al.* (2007). Gene encoding a deubiquitinating enzyme is mutated in artesunate- and chloroquine-resistant rodent malaria parasites. *Mol Microbiol* *65*, 27-40.
- Hunt, P., Martinelli, A., Modrzynska, K., Borges, S., Creasey, A., Rodrigues, L., Beraldi, D., Loewe, L., Fawcett, R., Kumar, S., *et al.* (2010). Experimental evolution, genetic analysis and genome re-sequencing reveal the mutation conferring artemisinin resistance in an isogenic lineage of malaria parasites. *BMC Genomics* *11*, 499.
- Huttlin, E.L., Ting, L., Bruckner, R.J., Gebreab, F., Gygi, M.P., Szpyt, J., Tam, S., Zarraga, G., Colby, G., Baltier, K., *et al.* (2015). The BioPlex Network: A Systematic Exploration of the Human Interactome. *Cell* *162*, 425-440.
- Inoue, T., Heo, W.D., Grimley, J.S., Wandless, T.J., and Meyer, T. (2005). An inducible translocation strategy to rapidly activate and inhibit small GTPase signaling pathways. *Nat Methods* *2*, 415-418.
- Inoue, T., and Meyer, T. (2008). Synthetic activation of endogenous PI3K and Rac identifies an AND-gate switch for cell polarization and migration. *PLoS One* *3*, e3068.
- Itoh, K., Wakabayashi, N., Katoh, Y., Ishii, T., Igarashi, K., Engel, J.D., and Yamamoto, M. (1999). Keap1 represses nuclear activation of antioxidant responsive elements by Nrf2 through binding to the amino-terminal Neh2 domain. *Genes Dev* *13*, 76-86.
- Iwamoto, M., Bjorklund, T., Lundberg, C., Kirik, D., and Wandless, T.J. (2010). A general chemical method to regulate protein stability in the mammalian central nervous system. *Chem Biol* *17*, 981-988.
- Jones, M.L., Das, S., Belda, H., Collins, C.R., Blackman, M.J., and Treeck, M. (2016). A versatile strategy for rapid conditional genome engineering using loxP sites in a small synthetic intron in *Plasmodium falciparum*. *Sci Rep* *6*, 21800.
- Josling, G.A., and Llinas, M. (2015). Sexual development in *Plasmodium* parasites: knowing when it's time to commit. *Nat Rev Microbiol* *13*, 573-587.

- Jullien, N., Goddard, I., Selmi-Ruby, S., Fina, J.L., Cremer, H., and Herman, J.P. (2007). Conditional transgenesis using Dimerizable Cre (DiCre). *PLoS One* 2, e1355.
- Jullien, N., Sampieri, F., Enjalbert, A., and Herman, J.P. (2003). Regulation of Cre recombinase by ligand-induced complementation of inactive fragments. *Nucleic Acids Res* 31, e131.
- Kafsack, B.F., Rovira-Graells, N., Clark, T.G., Bancells, C., Crowley, V.M., Campino, S.G., Williams, A.E., Drought, L.G., Kwiatkowski, D.P., Baker, D.A., *et al.* (2014). A transcriptional switch underlies commitment to sexual development in malaria parasites. *Nature* 507, 248-252.
- Kalderon, D., Roberts, B.L., Richardson, W.D., and Smith, A.E. (1984). A short amino acid sequence able to specify nuclear location. *Cell* 39, 499-509.
- Kang, M.I., Kobayashi, A., Wakabayashi, N., Kim, S.G., and Yamamoto, M. (2004). Scaffolding of Keap1 to the actin cytoskeleton controls the function of Nrf2 as key regulator of cytoprotective phase 2 genes. *Proc Natl Acad Sci U S A* 101, 2046-2051.
- Kantele, A., and Jokiranta, T.S. (2011). Review of cases with the emerging fifth human malaria parasite, *Plasmodium knowlesi*. *Clin Infect Dis* 52, 1356-1362.
- Kappe, S., Bruderer, T., Gantt, S., Fujioka, H., Nussenzweig, V., and Menard, R. (1999). Conservation of a gliding motility and cell invasion machinery in Apicomplexan parasites. *J Cell Biol* 147, 937-944.
- Kaushansky, A., Douglass, A.N., Arang, N., Vigdorovich, V., Dambrauskas, N., Kain, H.S., Austin, L.S., Sather, D.N., and Kappe, S.H. (2015). Malaria parasites target the hepatocyte receptor EphA2 for successful host infection. *Science* 350, 1089-1092.
- Keeley, A., and Soldati, D. (2004). The glideosome: a molecular machine powering motility and host-cell invasion by Apicomplexa. *Trends Cell Biol* 14, 528-532.
- Khan, S.M., Janse, C.J., Kappe, S.H., and Mikolajczak, S.A. (2012). Genetic engineering of attenuated malaria parasites for vaccination. *Curr Opin Biotechnol* 23, 908-916.
- Khater, E.I., Sinden, R.E., and Dessens, J.T. (2004). A malaria membrane skeletal protein is essential for normal morphogenesis, motility, and infectivity of sporozoites. *J Cell Biol* 167, 425-432.
- Kim, D.I., Birendra, K.C., Zhu, W., Motamedchaboki, K., Doye, V., and Roux, K.J. (2014). Probing nuclear pore complex architecture with proximity-dependent biotinylation. *Proc Natl Acad Sci U S A* 111, E2453-2461.
- Kim, D.I., Jensen, S.C., Noble, K.A., Kc, B., Roux, K.H., Motamedchaboki, K., and Roux, K.J. (2016). An improved smaller biotin ligase for BioID proximity labeling. *Mol Biol Cell* 27, 1188-1196.
- Kirkman, L.A., Lawrence, E.A., and Deitsch, K.W. (2014). Malaria parasites utilize both homologous recombination and alternative end joining pathways to maintain genome integrity. *Nucleic Acids Res* 42, 370-379.
- Klayman, D.L., Lin, A.J., Acton, N., Scovill, J.P., Hoch, J.M., Milhous, W.K., Theoharides, A.D., and Dobek, A.S. (1984). Isolation of artemisinin (qinghaosu) from *Artemisia annua* growing in the United States. *J Nat Prod* 47, 715-717.
- Klemm, J.D., Beals, C.R., and Crabtree, G.R. (1997). Rapid targeting of nuclear proteins to the cytoplasm. *Curr Biol* 7, 638-644.
- Kohler, S., Delwiche, C.F., Denny, P.W., Tilney, L.G., Webster, P., Wilson, R.J., Palmer, J.D., and Roos, D.S. (1997). A plastid of probable green algal origin in Apicomplexan parasites. *Science* 275, 1485-1489.
- Komatsu, T., Kukelyansky, I., McCaffery, J.M., Ueno, T., Varela, L.C., and Inoue, T. (2010). Organelle-specific, rapid induction of molecular activities and membrane tethering. *Nat Methods* 7, 206-208.

- Kono, M., Herrmann, S., Loughran, N.B., Cabrera, A., Engelberg, K., Lehmann, C., Sinha, D., Prinz, B., Ruch, U., Heussler, V., *et al.* (2012). Evolution and architecture of the inner membrane complex in asexual and sexual stages of the malaria parasite. *Mol Biol Evol* *29*, 2113-2132.
- Kreidenweiss, A., Hopkins, A.V., and Mordmuller, B. (2013). 2A and the auxin-based degron system facilitate control of protein levels in *Plasmodium falciparum*. *PLoS One* *8*, e78661.
- Kreusch, A., Pfaffinger, P.J., Stevens, C.F., and Choe, S. (1998). Crystal structure of the tetramerization domain of the Shaker potassium channel. *Nature* *392*, 945-948.
- Krotoski, W.A., Collins, W.E., Bray, R.S., Garnham, P.C., Cogswell, F.B., Gwadz, R.W., Killick-Kendrick, R., Wolf, R., Sinden, R., Koontz, L.C., *et al.* (1982). Demonstration of hypnozoites in sporozoite-transmitted *Plasmodium vivax* infection. *Am J Trop Med Hyg* *31*, 1291-1293.
- Kulzer, S., Gehde, N., and Przyborski, J.M. (2009). Return to sender: use of *Plasmodium* ER retrieval sequences to study protein transport in the infected erythrocyte and predict putative ER protein families. *Parasitol Res* *104*, 1535-1541.
- LaCount, D.J., Vignali, M., Chettier, R., Phansalkar, A., Bell, R., Hesselberth, J.R., Schoenfeld, L.W., Ota, I., Sahasrabudhe, S., Kurschner, C., *et al.* (2005). A protein interaction network of the malaria parasite *Plasmodium falciparum*. *Nature* *438*, 103-107.
- Ladda, R., Aikawa, M., and Sprinz, H. (1969). Penetration of erythrocytes by merozoites of mammalian and avian malarial parasites. *J Parasitol* *55*, 633-644.
- Laemmli, U.K. (1970). Cleavage of structural proteins during the assembly of the head of bacteriophage T4. *Nature* *227*, 680-685.
- Lambert, J.P., Tucholska, M., Go, C., Knight, J.D., and Gingras, A.C. (2015). Proximity biotinylation and affinity purification are complementary approaches for the interactome mapping of chromatin-associated protein complexes. *J Proteomics* *118*, 81-94.
- Lanzer, M., Wickert, H., Krohne, G., Vincensini, L., and Braun Breton, C. (2006). Maurer's clefts: a novel multi-functional organelle in the cytoplasm of *Plasmodium falciparum*-infected erythrocytes. *Int J Parasitol* *36*, 23-36.
- Lauer, S.A., Rathod, P.K., Ghori, N., and Haldar, K. (1997). A membrane network for nutrient import in red cells infected with the malaria parasite. *Science* *276*, 1122-1125.
- Laveran (1880).
- Laverriere, M., Cazzulo, J.J., and Alvarez, V.E. (2012). Antagonic activities of *Trypanosoma cruzi* metacaspases affect the balance between cell proliferation, death and differentiation. *Cell Death Differ* *19*, 1358-1369.
- Lazarus, M.D., Schneider, T.G., and Taraschi, T.F. (2008). A new model for hemoglobin ingestion and transport by the human malaria parasite *Plasmodium falciparum*. *J Cell Sci* *121*, 1937-1949.
- Le Roch, K.G., Zhou, Y., Blair, P.L., Grainger, M., Moch, J.K., Haynes, J.D., De La Vega, P., Holder, A.A., Batalov, S., Carucci, D.J., *et al.* (2003). Discovery of gene function by expression profiling of the malaria parasite life cycle. *Science* *301*, 1503-1508.
- Lee, R.E., Brunette, S., Puente, L.G., and Megeney, L.A. (2010). Metacaspase Yca1 is required for clearance of insoluble protein aggregates. *Proc Natl Acad Sci U S A* *107*, 13348-13353.
- Leech, J.H., Barnwell, J.W., Aikawa, M., Miller, L.H., and Howard, R.J. (1984). *Plasmodium falciparum* malaria: association of knobs on the surface of infected erythrocytes with a histidine-rich protein and the erythrocyte skeleton. *J Cell Biol* *98*, 1256-1264.
- Lennartz, F., Adams, Y., Bengtsson, A., Olsen, R.W., Turner, L., Ndam, N.T., Ecklu-Mensah, G., Moussiliou, A., Ofori, M.F., Gamain, B., *et al.* (2017). Structure-Guided Identification of a Family of Dual Receptor-Binding PfEMP1 that Is Associated with Cerebral Malaria. *Cell Host Microbe* *21*, 403-414.

- Lewit-Bentley, A., and Rety, S. (2000). EF-hand calcium-binding proteins. *Curr Opin Struct Biol* *10*, 637-643.
- Liang, F.S., Ho, W.Q., and Crabtree, G.R. (2011). Engineering the ABA plant stress pathway for regulation of induced proximity. *Sci Signal* *4*, rs2.
- Liang, J., Choi, J., and Clardy, J. (1999). Refined structure of the FKBP12-rapamycin-FRB ternary complex at 2.2 Å resolution. *Acta Crystallogr D Biol Crystallogr* *55*, 736-744.
- Liu, P., Calderon, A., Konstantinidis, G., Hou, J., Voss, S., Chen, X., Li, F., Banerjee, S., Hoffmann, J.E., Theiss, C., *et al.* (2014). A bioorthogonal small-molecule-switch system for controlling protein function in live cells. *Angew Chem Int Ed Engl* *53*, 10049-10055.
- Livingstone, F. (1984). The Duffy blood groups, vivax malaria, and malaria selection in human populations: a review. *Hum Biol*, 413-425.
- Lu, F., Culleton, R., Zhang, M., Ramaprasad, A., von Seidlein, L., Zhou, H., Zhu, G., Tang, J., Liu, Y., Wang, W., *et al.* (2017). Emergence of Indigenous Artemisinin-Resistant *Plasmodium falciparum* in Africa. *N Engl J Med* *376*, 991-993.
- Lyko, B., Hammershaimb, E.A., Nguitrugool, W., Wellems, T.E., and Desai, S.A. (2012). A high-throughput method to detect *Plasmodium falciparum* clones in limiting dilution microplates. *Malar J* *11*, 124.
- Maier, A.G., Braks, J.A., Waters, A.P., and Cowman, A.F. (2006). Negative selection using yeast cytosine deaminase/uracil phosphoribosyl transferase in *Plasmodium falciparum* for targeted gene deletion by double crossover recombination. *Mol Biochem Parasitol* *150*, 118-121.
- Malleret, B., Claser, C., Ong, A.S., Suwanarusk, R., Sriprawat, K., Howland, S.W., Russell, B., Nosten, F., and Renia, L. (2011). A rapid and robust tri-color flow cytometry assay for monitoring malaria parasite development. *Sci Rep* *1*, 118.
- Mamoun, C.B., Gluzman, I.Y., Goyard, S., Beverley, S.M., and Goldberg, D.E. (1999a). A set of independent selectable markers for transfection of the human malaria parasite *Plasmodium falciparum*. *Proc Natl Acad Sci U S A* *96*, 8716-8720.
- Mamoun, C.B., Truong, R., Gluzman, I., Akopyants, N.S., Oksman, A., and Goldberg, D.E. (1999b). Transfer of genes into *Plasmodium falciparum* by polyamidoamine dendrimers. *Mol Biochem Parasitol* *103*, 117-121.
- Mantel, P.Y., Hoang, A.N., Goldowitz, I., Potashnikova, D., Hamza, B., Vorobjev, I., Ghiran, I., Toner, M., Irimia, D., Ivanov, A.R., *et al.* (2013). Malaria-infected erythrocyte-derived microvesicles mediate cellular communication within the parasite population and with the host immune system. *Cell Host Microbe* *13*, 521-534.
- Marchler-Bauer, A., Bo, Y., Han, L., He, J., Lanczycki, C.J., Lu, S., Chitsaz, F., Derbyshire, M.K., Geer, R.C., Gonzales, N.R., *et al.* (2017). CDD/SPARCLE: functional classification of proteins via subfamily domain architectures. *Nucleic Acids Res* *45*, D200-D203.
- Marti, M., Good, R.T., Rug, M., Knuepfer, E., and Cowman, A.F. (2004). Targeting malaria virulence and remodeling proteins to the host erythrocyte. *Science* *306*, 1930-1933.
- Matthews, K., Kalanon, M., Chisholm, S.A., Sturm, A., Goodman, C.D., Dixon, M.W., Sanders, P.R., Nebl, T., Fraser, F., Haase, S., *et al.* (2013). The *Plasmodium* translocon of exported proteins (PTEX) component thioredoxin-2 is important for maintaining normal blood-stage growth. *Mol Microbiol* *89*, 1167-1186.
- Mbengue, A., Bhattacharjee, S., Pandharkar, T., Liu, H., Estiu, G., Stahelin, R.V., Rizk, S.S., Njimoh, D.L., Ryan, Y., Chotivanich, K., *et al.* (2015a). A molecular mechanism of artemisinin resistance in *Plasmodium falciparum* malaria. *Nature* *520*, 683-687.
- Mbengue, A., Vialla, E., Berry, L., Fall, G., Audiger, N., Demetere-Verceil, E., Boteller, D., and Braun-Breton, C. (2015b). New Export Pathway in *Plasmodium falciparum*-Infected Erythrocytes: Role of the Parasite Group II Chaperonin, PfTRiC. *Traffic* *16*, 461-475.

- McHugh, E., Batinovic, S., Hanssen, E., McMillan, P.J., Kenny, S., Griffin, M.D., Crawford, S., Trenholme, K.R., Gardiner, D.L., Dixon, M.W., *et al.* (2015). A repeat sequence domain of the ring-exported protein-1 of *Plasmodium falciparum* controls export machinery architecture and virulence protein trafficking. *Mol Microbiol* *98*, 1101-1114.
- McNamara, C.W., Lee, M.C., Lim, C.S., Lim, S.H., Roland, J., Nagle, A., Simon, O., Yeung, B.K., Chatterjee, A.K., McCormack, S.L., *et al.* (2013). Targeting *Plasmodium* PI(4)K to eliminate malaria. *Nature* *504*, 248-253.
- Meissner, M., Krejany, E., Gilson, P.R., de Koning-Ward, T.F., Soldati, D., and Crabb, B.S. (2005). Tetracycline analogue-regulated transgene expression in *Plasmodium falciparum* blood stages using *Toxoplasma gondii* transactivators. *Proc Natl Acad Sci U S A* *102*, 2980-2985.
- Melnick, A., Ahmad, K.F., Arai, S., Polinger, A., Ball, H., Borden, K.L., Carlile, G.W., Prive, G.G., and Licht, J.D. (2000). In-depth mutational analysis of the promyelocytic leukemia zinc finger BTB/POZ domain reveals motifs and residues required for biological and transcriptional functions. *Mol Cell Biol* *20*, 6550-6567.
- Menard, D., Barnadas, C., Bouchier, C., Henry-Hallidin, C., Gray, L.R., Ratsimbao, A., Thonier, V., Carod, J.F., Domarle, O., Colin, Y., *et al.* (2010). *Plasmodium vivax* clinical malaria is commonly observed in Duffy-negative Malagasy people. *Proc Natl Acad Sci U S A* *107*, 5967-5971.
- Miao, M., Wang, Z., Yang, Z., Yuan, L., Parker, D.M., Putaporntip, C., Jongwutiwes, S., Xangsayarath, P., Pongvongsa, T., Moji, H., *et al.* (2013). Genetic diversity and lack of artemisinin selection signature on the *Plasmodium falciparum* ATP6 in the Greater Mekong Subregion. *PLoS One* *8*, e59192.
- Minor, D.L., Lin, Y.F., Mobley, B.C., Avelar, A., Jan, Y.N., Jan, L.Y., and Berger, J.M. (2000). The polar T1 interface is linked to conformational changes that open the voltage-gated potassium channel. *Cell* *102*, 657-670.
- Miotto, O., Almagro-Garcia, J., Manske, M., Macinnis, B., Campino, S., Rockett, K.A., Amaratunga, C., Lim, P., Suon, S., Sreng, S., *et al.* (2013). Multiple populations of artemisinin-resistant *Plasmodium falciparum* in Cambodia. *Nat Genet* *45*, 648-655.
- Miyamoto, T., DeRose, R., Suarez, A., Ueno, T., Chen, M., Sun, T.P., Wolfgang, M.J., Mukherjee, C., Meyers, D.J., and Inoue, T. (2012). Rapid and orthogonal logic gating with a gibberellin-induced dimerization system. *Nat Chem Biol* *8*, 465-470.
- Mizuno, E., Kobayashi, K., Yamamoto, A., Kitamura, N., and Komada, M. (2006). A deubiquitinating enzyme UBPY regulates the level of protein ubiquitination on endosomes. *Traffic* *7*, 1017-1031.
- Modrzynska, K., Pfander, C., Chappell, L., Yu, L., Suarez, C., Dundas, K., Gomes, A.R., Goulding, D., Rayner, J.C., Choudhary, J., *et al.* (2017). A Knockout Screen of ApiAP2 Genes Reveals Networks of Interacting Transcriptional Regulators Controlling the *Plasmodium* Life Cycle. *Cell Host Microbe* *21*, 11-22.
- Mok, S., Ashley, E.A., Ferreira, P.E., Zhu, L., Lin, Z., Yeo, T., Chotivanich, K., Imwong, M., Pukrittayakamee, S., Dhorda, M., *et al.* (2015). Drug resistance. Population transcriptomics of human malaria parasites reveals the mechanism of artemisinin resistance. *Science* *347*, 431-435.
- Mony, B.M., Mehta, M., Jarori, G.K., and Sharma, S. (2009). Plant-like phosphofructokinase from *Plasmodium falciparum* belongs to a novel class of ATP-dependent enzymes. *Int J Parasitol* *39*, 1441-1453.
- Moon, R.W., Hall, J., Rangkuti, F., Ho, Y.S., Almond, N., Mitchell, G.H., Pain, A., Holder, A.A., and Blackman, M.J. (2013). Adaptation of the genetically tractable malaria pathogen *Plasmodium knowlesi* to continuous culture in human erythrocytes. *Proc Natl Acad Sci U S A* *110*, 531-536.
- Mootz, H.D., and Muir, T.W. (2002). Protein splicing triggered by a small molecule. *J Am Chem Soc* *124*, 9044-9045.
- Mordmuller, B., Surat, G., Lagler, H., Chakravarty, S., Ishizuka, A.S., Lalremruata, A., Gmeiner, M., Campo, J.J., Esen, M., Ruben, A.J., *et al.* (2017). Sterile protection against human malaria by chemoattenuated PfSPZ vaccine. *Nature* *542*, 445-449.

- Moreno, A., and Joyner, C. (2015). Malaria vaccine clinical trials: what's on the horizon. *Curr Opin Immunol* 35, 98-106.
- Mukherjee, A., Bopp, S., Magistrado, P., Wong, W., Daniels, R., Demas, A., Schaffner, S., Amaratunga, C., Lim, P., Dhorda, M., *et al.* (2017). Artemisinin resistance without pfkelch13 mutations in *Plasmodium falciparum* isolates from Cambodia. *Malar J* 16, 195.
- Muller, I.B., and Hyde, J.E. (2010). Antimalarial drugs: modes of action and mechanisms of parasite resistance. *Future Microbiol* 5, 1857-1873.
- Munro, S., and Pelham, H.R. (1987). A C-terminal signal prevents secretion of luminal ER proteins. *Cell* 48, 899-907.
- Muralidharan, V., Oksman, A., Iwamoto, M., Wandless, T.J., and Goldberg, D.E. (2011). Asparagine repeat function in a *Plasmodium falciparum* protein assessed via a regulatable fluorescent affinity tag. *Proc Natl Acad Sci U S A* 108, 4411-4416.
- Muralidharan, V., Oksman, A., Pal, P., Lindquist, S., and Goldberg, D.E. (2012). *Plasmodium falciparum* heat shock protein 110 stabilizes the asparagine repeat-rich parasite proteome during malarial fevers. *Nat Commun* 3, 1310.
- Murzin, A.G. (1992). Structural principles for the propeller assembly of beta-sheets: the preference for seven-fold symmetry. *Proteins* 14, 191-201.
- Nagao, E., Kaneko, O., and Dvorak, J.A. (2000). *Plasmodium falciparum*-infected erythrocytes: qualitative and quantitative analyses of parasite-induced knobs by atomic force microscopy. *J Struct Biol* 130, 34-44.
- Naslavsky, N., Rahajeng, J., Chenavas, S., Sorgen, P.L., and Caplan, S. (2007). EHD1 and Eps15 interact with phosphatidylinositols via their Eps15 homology domains. *J Biol Chem* 282, 16612-16622.
- Niles, J.C., Derisi, J.L., and Marletta, M.A. (2009). Inhibiting *Plasmodium falciparum* growth and heme detoxification pathway using heme-binding DNA aptamers. *Proc Natl Acad Sci U S A* 106, 13266-13271.
- Nishimura, N., Hitomi, K., Arvai, A.S., Rambo, R.P., Hitomi, C., Cutler, S.R., Schroeder, J.I., and Getzoff, E.D. (2009). Structural mechanism of abscisic acid binding and signaling by dimeric PYR1. *Science* 326, 1373-1379.
- Nobelprize.org (2015). Youyou Tu - Facts.
- Noedl, H., Se, Y., Schaefer, K., Smith, B.L., Socheat, D., Fukuda, M.M., and Artemisinin Resistance in Cambodia 1 Study, C. (2008). Evidence of artemisinin-resistant malaria in western Cambodia. *N Engl J Med* 359, 2619-2620.
- Nussenzweig, R.S., Vanderberg, J., Most, H., and Orton, C. (1967). Protective immunity produced by the injection of x-irradiated sporozoites of *plasmodium berghei*. *Nature* 216, 160-162.
- Nussenzweig, R.S., Vanderberg, J.P., Most, H., and Orton, C. (1969). Specificity of protective immunity produced by x-irradiated *Plasmodium berghei* sporozoites. *Nature* 222, 488-489.
- O'Donnell, R.A., Saul, A., Cowman, A.F., and Crabb, B.S. (2000). Functional conservation of the malaria vaccine antigen MSP-119 across distantly related *Plasmodium* species. *Nat Med* 6, 91-95.
- O'Neill, M.T., Phuong, T., Healer, J., Richard, D., and Cowman, A.F. (2011). Gene deletion from *Plasmodium falciparum* using FLP and Cre recombinases: implications for applied site-specific recombination. *Int J Parasitol* 41, 117-123.
- Oakley, M.S., Gerald, N., McCutchan, T.F., Aravind, L., and Kumar, S. (2011). Clinical and molecular aspects of malaria fever. *Trends Parasitol* 27, 442-449.
- Ogutu, B.R., Apollo, O.J., McKinney, D., Okoth, W., Siangla, J., Dubovsky, F., Tucker, K., Waitumbi, J.N., Diggs, C., Wittes, J., *et al.* (2009). Blood stage malaria vaccine eliciting high antigen-specific antibody concentrations confers no protection to young children in Western Kenya. *PLoS One* 4, e4708.

- Olotu, A., Fegan, G., Wambua, J., Nyangweso, G., Leach, A., Lievens, M., Kaslow, D.C., Njuguna, P., Marsh, K., and Bejon, P. (2016). Seven-Year Efficacy of RTS,S/AS01 Malaria Vaccine among Young African Children. *N Engl J Med* *374*, 2519-2529.
- Patury, S., Geda, P., Dobry, C.J., Kumar, A., and Gestwicki, J.E. (2009). Conditional nuclear import and export of yeast proteins using a chemical inducer of dimerization. *Cell Biochem Biophys* *53*, 127-134.
- Payne, D. (1987). Spread of chloroquine resistance in *Plasmodium falciparum*. *Parasitol Today* *3*, 241-246.
- Perez-Torrado, R., Yamada, D., and Defossez, P.A. (2006). Born to bind: the BTB protein-protein interaction domain. *Bioessays* *28*, 1194-1202.
- Philip, N., and Waters, A.P. (2015). Conditional Degradation of *Plasmodium* Calcineurin Reveals Functions in Parasite Colonization of both Host and Vector. *Cell Host Microbe* *18*, 122-131.
- Pino, P., Sebastian, S., Kim, E.A., Bush, E., Brochet, M., Volkmann, K., Kozłowski, E., Llinas, M., Billker, O., and Soldati-Favre, D. (2012). A tetracycline-repressible transactivator system to study essential genes in malaria parasites. *Cell Host Microbe* *12*, 824-834.
- Pinzon-Ortiz, C., Friedman, J., Esko, J., and Sinnis, P. (2001). The binding of the circumsporozoite protein to cell surface heparan sulfate proteoglycans is required for *plasmodium* sporozoite attachment to target cells. *J Biol Chem* *276*, 26784-26791.
- Plasmodb.org.
- Ponting, C.P. (1996). Novel domains in NADPH oxidase subunits, sorting nexins, and PtdIns 3-kinases: binding partners of SH3 domains? *Protein Sci* *5*, 2353-2357.
- Pratt, M.R., Schwartz, E.C., and Muir, T.W. (2007). Small-molecule-mediated rescue of protein function by an inducible proteolytic shunt. *Proc Natl Acad Sci U S A* *104*, 11209-11214.
- Prommana, P., Uthaiyibull, C., Wongsombat, C., Kamchonwongpaisan, S., Yuthavong, Y., Knuepfer, E., Holder, A.A., and Shaw, P.J. (2013). Inducible knockdown of *Plasmodium* gene expression using the glmS ribozyme. *PLoS One* *8*, e73783.
- Prudencio, M., Rodriguez, A., and Mota, M.M. (2006). The silent path to thousands of merozoites: the *Plasmodium* liver stage. *Nat Rev Microbiol* *4*, 849-856.
- Przyborski, J.M., Wickert, H., Krohne, G., and Lanzer, M. (2003). Maurer's clefts--a novel secretory organelle? *Mol Biochem Parasitol* *132*, 17-26.
- Putyrski, M., and Schultz, C. (2012). Protein translocation as a tool: The current rapamycin story. *FEBS Lett* *586*, 2097-2105.
- Rahimi, B.A., Thakkinian, A., White, N.J., Sirivichayakul, C., Dondorp, A.M., and Chokejindachai, W. (2014). Severe vivax malaria: a systematic review and meta-analysis of clinical studies since 1900. *Malar J* *13*, 481.
- Ralph, S.A., van Dooren, G.G., Waller, R.F., Crawford, M.J., Fraunholz, M.J., Foth, B.J., Tonkin, C.J., Roos, D.S., and McFadden, G.I. (2004). Tropical infectious diseases: metabolic maps and functions of the *Plasmodium falciparum* apicoplast. *Nat Rev Microbiol* *2*, 203-216.
- Reddy, K.S., Amlabu, E., Pandey, A.K., Mitra, P., Chauhan, V.S., and Gaur, D. (2015). Multiprotein complex between the GPI-anchored CyRPA with PfRH5 and PfRipr is crucial for *Plasmodium falciparum* erythrocyte invasion. *Proc Natl Acad Sci U S A* *112*, 1179-1184.
- Regev-Rudzki, N., Wilson, D.W., Carvalho, T.G., Sisquella, X., Coleman, B.M., Rug, M., Bursac, D., Angrisano, F., Gee, M., Hill, A.F., *et al.* (2013). Cell-cell communication between malaria-infected red blood cells via exosome-like vesicles. *Cell* *153*, 1120-1133.

- Reichard, N. (2015). A screen to characterize unknown proteins in the human malaria parasite *Plasmodium falciparum*.
- Reiss, B., Sprengel, R., and Schaller, H. (1984). Protein fusions with the kanamycin resistance gene from transposon Tn5. *EMBO J* 3, 3317-3322.
- Richie, D.L., Miley, M.D., Bhabhra, R., Robson, G.D., Rhodes, J.C., and Askew, D.S. (2007). The *Aspergillus fumigatus* metacaspases CasA and CasB facilitate growth under conditions of endoplasmic reticulum stress. *Mol Microbiol* 63, 591-604.
- Robinson, M.S., Sahlender, D.A., and Foster, S.D. (2010). Rapid inactivation of proteins by rapamycin-induced rerouting to mitochondria. *Dev Cell* 18, 324-331.
- Robson, K.J., Frevert, U., Reckmann, I., Cowan, G., Beier, J., Scragg, I.G., Takehara, K., Bishop, D.H., Pradel, G., Sinden, R., *et al.* (1995). Thrombospondin-related adhesive protein (TRAP) of *Plasmodium falciparum*: expression during sporozoite ontogeny and binding to human hepatocytes. *EMBO J* 14, 3883-3894.
- Roux, K.J., Kim, D.I., Raida, M., and Burke, B. (2012). A promiscuous biotin ligase fusion protein identifies proximal and interacting proteins in mammalian cells. *J Cell Biol* 196, 801-810.
- Rug, M., Cyrklaff, M., Mikkonen, A., Lemgruber, L., Kuelzer, S., Sanchez, C.P., Thompson, J., Hanssen, E., O'Neill, M., Langer, C., *et al.* (2014). Export of virulence proteins by malaria-infected erythrocytes involves remodeling of host actin cytoskeleton. *Blood* 124, 3459-3468.
- Rutledge, G.G., Bohme, U., Sanders, M., Reid, A.J., Cotton, J.A., Maiga-Ascofare, O., Djimde, A.A., Apinjoh, T.O., Amenga-Etego, L., Manske, M., *et al.* (2017). *Plasmodium malariae* and *P. ovale* genomes provide insights into malaria parasite evolution. *Nature* 542, 101-104.
- Sachs, J., and Malaney, P. (2002). The economic and social burden of malaria. *Nature* 415, 680-685.
- Sagara, I., Dicko, A., Ellis, R.D., Fay, M.P., Diawara, S.I., Assadou, M.H., Sissoko, M.S., Kone, M., Diallo, A.I., Saye, R., *et al.* (2009). A randomized controlled phase 2 trial of the blood stage AMA1-C1/Alhydrogel malaria vaccine in children in Mali. *Vaccine* 27, 3090-3098.
- Salama, N.R., Yeung, T., and Schekman, R.W. (1993). The Sec13p complex and reconstitution of vesicle budding from the ER with purified cytosolic proteins. *EMBO J* 12, 4073-4082.
- Sauer, B. (1987). Functional expression of the cre-lox site-specific recombination system in the yeast *Saccharomyces cerevisiae*. *Mol Cell Biol* 7, 2087-2096.
- Schmid, E.M., Ford, M.G., Burtey, A., Praefcke, G.J., Peak-Chew, S.Y., Mills, I.G., Benmerah, A., and McMahon, H.T. (2006). Role of the AP2 beta-appendage hub in recruiting partners for clathrin-coated vesicle assembly. *PLoS Biol* 4, e262.
- Schmidt, S. (2017). Identification of essential parasite-specific genes in the human malaria parasite *Plasmodium falciparum*.
- Schofield, L., Hewitt, M.C., Evans, K., Siomos, M.A., and Seeberger, P.H. (2002). Synthetic GPI as a candidate anti-toxic vaccine in a model of malaria. *Nature* 418, 785-789.
- Schwartz, E.C., Saez, L., Young, M.W., and Muir, T.W. (2007). Post-translational enzyme activation in an animal via optimized conditional protein splicing. *Nat Chem Biol* 3, 50-54.
- Seder, R.A., Chang, L.J., Enama, M.E., Zephir, K.L., Sarwar, U.N., Gordon, I.J., Holman, L.A., James, E.R., Billingsley, P.F., Gunasekera, A., *et al.* (2013). Protection against malaria by intravenous immunization with a nonreplicating sporozoite vaccine. *Science* 341, 1359-1365.
- Seeber, F., and Soldati-Favre, D. (2010). Metabolic pathways in the apicoplast of apicomplexa. *Int Rev Cell Mol Biol* 281, 161-228.

- Seydel, K.B., Kampondeni, S.D., Valim, C., Potchen, M.J., Milner, D.A., Muwalo, F.W., Birbeck, G.L., Bradley, W.G., Fox, L.L., Glover, S.J., *et al.* (2015). Brain swelling and death in children with cerebral malaria. *N Engl J Med* 372, 1126-1137.
- Shortt, H.E., Garnham, P.C.C., Covell, G., and Shute, P.G. (1948). The Pre-Erythrocytic Stage of Human Malaria, *Plasmodium Vivax*. *Brit Med J* 1, 547-547.
- Shrestha, A., and Megeney, L.A. (2012). The non-death role of metacaspase proteases. *Front Oncol* 2, 78.
- Sidik, S.M., Huet, D., Ganesan, S.M., Huynh, M.H., Wang, T., Nasamu, A.S., Thiru, P., Saeij, J.P., Carruthers, V.B., Niles, J.C., *et al.* (2016). A Genome-wide CRISPR Screen in *Toxoplasma* Identifies Essential Apicomplexan Genes. *Cell* 166, 1423-1435 e1412.
- Silvie, O., Rubinstein, E., Franetich, J.F., Prenant, M., Belnoue, E., Renia, L., Hannoun, L., Eling, W., Levy, S., Boucheix, C., *et al.* (2003). Hepatocyte CD81 is required for *Plasmodium falciparum* and *Plasmodium yoelii* sporozoite infectivity. *Nat Med* 9, 93-96.
- Sinden, R.E. (1974). Excystation by sporozoites of malaria parasites. *Nature* 252, 314.
- Sinden, R.E. (2015). The cell biology of malaria infection of mosquito: advances and opportunities. *Cell Microbiol* 17, 451-466.
- Singer, M., Marshall, J., Heiss, K., Mair, G.R., Grimm, D., Mueller, A.K., and Frischknecht, F. (2015). Zinc finger nuclease-based double-strand breaks attenuate malaria parasites and reveal rare microhomology-mediated end joining. *Genome Biol* 16, 249.
- Singh, B., and Daneshvar, C. (2013). Human infections and detection of *Plasmodium knowlesi*. *Clin Microbiol Rev* 26, 165-184.
- Singh, B., Kim Sung, L., Matusop, A., Radhakrishnan, A., Shamsul, S.S., Cox-Singh, J., Thomas, A., and Conway, D.J. (2004). A large focus of naturally acquired *Plasmodium knowlesi* infections in human beings. *Lancet* 363, 1017-1024.
- Sinha, A., Hughes, K.R., Modrzynska, K.K., Otto, T.D., Pfander, C., Dickens, N.J., Religa, A.A., Bushell, E., Graham, A.L., Cameron, R., *et al.* (2014). A cascade of DNA-binding proteins for sexual commitment and development in *Plasmodium*. *Nature* 507, 253-257.
- Sinka, M.E., Bangs, M.J., Manguin, S., Chareonviriyaphap, T., Patil, A.P., Temperley, W.H., Gething, P.W., Elyazar, I.R., Kabaria, C.W., Harbach, R.E., *et al.* (2011). The dominant *Anopheles* vectors of human malaria in the Asia-Pacific region: occurrence data, distribution maps and bionomic precis. *Parasit Vectors* 4, 89.
- Sinka, M.E., Rubio-Palis, Y., Manguin, S., Patil, A.P., Temperley, W.H., Gething, P.W., Van Boeckel, T., Kabaria, C.W., Harbach, R.E., and Hay, S.I. (2010). The dominant *Anopheles* vectors of human malaria in the Americas: occurrence data, distribution maps and bionomic precis. *Parasit Vectors* 3, 72.
- Sleebs, B.E., Lopaticki, S., Marapana, D.S., O'Neill, M.T., Rajasekaran, P., Gazdik, M., Gunther, S., Whitehead, L.W., Lowes, K.N., Barford, L., *et al.* (2014). Inhibition of Plasmeprin V activity demonstrates its essential role in protein export, PfEMP1 display, and survival of malaria parasites. *PLoS Biol* 12, e1001897.
- Smith, A.M., Heisler, L.E., Mellor, J., Kaper, F., Thompson, M.J., Chee, M., Roth, F.P., Giaever, G., and Nislow, C. (2009). Quantitative phenotyping via deep barcode sequencing. *Genome Res* 19, 1836-1842.
- Smith, T.G., Lourenco, P., Carter, R., Walliker, D., and Ranford-Cartwright, L.C. (2000). Commitment to sexual differentiation in the human malaria parasite, *Plasmodium falciparum*. *Parasitology* 121 (Pt 2), 127-133.
- Snow, R.W., Guerra, C.A., Noor, A.M., Myint, H.Y., and Hay, S.I. (2005). The global distribution of clinical episodes of *Plasmodium falciparum* malaria. *Nature* 434, 214-217.
- Soldati, D. (1999). The apicoplast as a potential therapeutic target in and other apicomplexan parasites. *Parasitol Today* 15, 5-7.

- Soltysik-Espanola, M., Rogers, R.A., Jiang, S., Kim, T.A., Gaedigk, R., White, R.A., Avraham, H., and Avraham, S. (1999). Characterization of Mayven, a novel actin-binding protein predominantly expressed in brain. *Mol Biol Cell* *10*, 2361-2375.
- Spain, B.H., Koo, D., Ramakrishnan, M., Dzudzor, B., and Colicelli, J. (1995). Truncated forms of a novel yeast protein suppress the lethality of a G protein alpha subunit deficiency by interacting with the beta subunit. *J Biol Chem* *270*, 25435-25444.
- Spielmann, T., and Gilberger, T.W. (2010). Protein export in malaria parasites: do multiple export motifs add up to multiple export pathways? *Trends Parasitol* *26*, 6-10.
- Spielmann, T., Hawthorne, P.L., Dixon, M.W., Hannemann, M., Klotz, K., Kemp, D.J., Klonis, N., Tilley, L., Trenholme, K.R., and Gardiner, D.L. (2006). A cluster of ring stage-specific genes linked to a locus implicated in cytoadherence in *Plasmodium falciparum* codes for PEXEL-negative and PEXEL-positive proteins exported into the host cell. *Mol Biol Cell* *17*, 3613-3624.
- Spillman, N.J., Beck, J.R., Ganesan, S.M., Niles, J.C., and Goldberg, D.E. (2017). The chaperonin TRiC forms an oligomeric complex in the malaria parasite cytosol. *Cell Microbiol*.
- Srinivasan, P., Beatty, W.L., Diouf, A., Herrera, R., Ambroggio, X., Moch, J.K., Tyler, J.S., Narum, D.L., Pierce, S.K., Boothroyd, J.C., *et al.* (2011). Binding of *Plasmodium* merozoite proteins RON2 and AMA1 triggers commitment to invasion. *Proc Natl Acad Sci U S A* *108*, 13275-13280.
- Stenmark, H. (2009). Rab GTPases as coordinators of vesicle traffic. *Nat Rev Mol Cell Biol* *10*, 513-525.
- Straimer, J., Gnadig, N.F., Witkowski, B., Amaratunga, C., Duru, V., Ramadani, A.P., Dacheux, M., Khim, N., Zhang, L., Lam, S., *et al.* (2015). Drug resistance. K13-propeller mutations confer artemisinin resistance in *Plasmodium falciparum* clinical isolates. *Science* *347*, 428-431.
- Straimer, J., Lee, M.C., Lee, A.H., Zeitler, B., Williams, A.E., Pearl, J.R., Zhang, L., Rebar, E.J., Gregory, P.D., Llinas, M., *et al.* (2012). Site-specific genome editing in *Plasmodium falciparum* using engineered zinc-finger nucleases. *Nat Methods* *9*, 993-998.
- Struck, N.S., Herrmann, S., Schmuck-Barkmann, I., de Souza Dias, S., Haase, S., Cabrera, A.L., Treeck, M., Bruns, C., Langer, C., Cowman, A.F., *et al.* (2008). Spatial dissection of the cis- and trans-Golgi compartments in the malaria parasite *Plasmodium falciparum*. *Mol Microbiol* *67*, 1320-1330.
- Sturm, A., Amino, R., van de Sand, C., Regen, T., Retzlaff, S., Rennenberg, A., Krueger, A., Pollok, J.M., Menard, R., and Heussler, V.T. (2006). Manipulation of host hepatocytes by the malaria parasite for delivery into liver sinusoids. *Science* *313*, 1287-1290.
- Suh, B.C., Inoue, T., Meyer, T., and Hille, B. (2006). Rapid chemically induced changes of PtdIns(4,5)P₂ gate KCNQ ion channels. *Science* *314*, 1454-1457.
- Sullivan, D.J. (2002). Theories on malarial pigment formation and quinoline action. *Int J Parasitol* *32*, 1645-1653.
- Sullivan, D.J., Jr., Gluzman, I.Y., and Goldberg, D.E. (1996). *Plasmodium* hemozoin formation mediated by histidine-rich proteins. *Science* *271*, 219-222.
- Sultan, A.A., Thathy, V., Frevert, U., Robson, K.J., Crisanti, A., Nussenzweig, V., Nussenzweig, R.S., and Menard, R. (1997). TRAP is necessary for gliding motility and infectivity of *Plasmodium* sporozoites. *Cell* *90*, 511-522.
- Sutherland, C.J., Tanomsing, N., Nolder, D., Oguike, M., Jennison, C., Pukrittayakamee, S., Dolecek, C., Hien, T.T., do Rosario, V.E., Arez, A.P., *et al.* (2010). Two nonrecombining sympatric forms of the human malaria parasite *Plasmodium ovale* occur globally. *J Infect Dis* *201*, 1544-1550.

- Szymczak, A.L., Workman, C.J., Wang, Y., Vignali, K.M., Dilioglou, S., Vanin, E.F., and Vignali, D.A. (2004). Correction of multi-gene deficiency in vivo using a single 'self-cleaving' 2A peptide-based retroviral vector. *Nat Biotechnol* 22, 589-594.
- Tawk, L., Chicanne, G., Dubremetz, J.F., Richard, V., Payrastre, B., Vial, H.J., Roy, C., and Wengelnik, K. (2010). Phosphatidylinositol 3-phosphate, an essential lipid in Plasmodium, localizes to the food vacuole membrane and the apicoplast. *Eukaryot Cell* 9, 1519-1530.
- Teckchandani, A., Mulkearns, E.E., Randolph, T.W., Toida, N., and Cooper, J.A. (2012). The clathrin adaptor Dab2 recruits EH domain scaffold proteins to regulate integrin beta1 endocytosis. *Mol Biol Cell* 23, 2905-2916.
- Tilley, L., Straimer, J., Gnadig, N.F., Ralph, S.A., and Fidock, D.A. (2016). Artemisinin Action and Resistance in Plasmodium falciparum. *Trends Parasitol* 32, 682-696.
- Tonkin, C.J., van Dooren, G.G., Spurck, T.P., Struck, N.S., Good, R.T., Handman, E., Cowman, A.F., and McFadden, G.I. (2004). Localization of organellar proteins in Plasmodium falciparum using a novel set of transfection vectors and a new immunofluorescence fixation method. *Mol Biochem Parasitol* 137, 13-21.
- Tonkin, M.L., Roques, M., Lamarque, M.H., Pugniere, M., Douguet, D., Crawford, J., Lebrun, M., and Boulanger, M.J. (2011). Host cell invasion by apicomplexan parasites: insights from the co-structure of AMA1 with a RON2 peptide. *Science* 333, 463-467.
- Toth, D.J., Toth, J.T., Gulyas, G., Balla, A., Balla, T., Hunyady, L., and Varnai, P. (2012). Acute depletion of plasma membrane phosphatidylinositol 4,5-bisphosphate impairs specific steps in endocytosis of the G-protein-coupled receptor. *J Cell Sci* 125, 2185-2197.
- Trager, W., and Jensen, J.B. (1976). Human malaria parasites in continuous culture. *Science* 193, 673-675.
- Trampuz, A., Jereb, M., Muzlovic, I., and Prabhu, R.M. (2003). Clinical review: Severe malaria. *Crit Care* 7, 315-323.
- Tsai, S.Q., Zheng, Z., Nguyen, N.T., Liebers, M., Topkar, V.V., Thapar, V., Wyvekens, N., Khayter, C., Iafrate, A.J., Le, L.P., *et al.* (2015). GUIDE-seq enables genome-wide profiling of off-target cleavage by CRISPR-Cas nucleases. *Nat Biotechnol* 33, 187-197.
- Tsiatsiani, L., Van Breusegem, F., Gallois, P., Zavalov, A., Lam, E., and Bozhkov, P.V. (2011). Metacaspases. *Cell Death Differ* 18, 1279-1288.
- Tu, Y. (2011). The discovery of artemisinin (qinghaosu) and gifts from Chinese medicine. *Nat Med* 17, 1217-1220.
- Tu, Y.Y., Ni, M.Y., Zhong, Y.R., Li, L.N., Cui, S.L., Zhang, M.Q., Wang, X.Z., and Liang, X.T. (1981). [Studies on the constituents of Artemisia annua L. (author's transl)]. *Yao Xue Xue Bao* 16, 366-370.
- van Bergen En Henegouwen, P.M. (2009). Eps15: a multifunctional adaptor protein regulating intracellular trafficking. *Cell Commun Signal* 7, 24.
- van Delft, S., Govers, R., Strous, G.J., Verkleij, A.J., and van Bergen en Henegouwen, P.M. (1997). Epidermal growth factor induces ubiquitination of Eps15. *J Biol Chem* 272, 14013-14016.
- van Dijk, M.R., Douradinha, B., Franke-Fayard, B., Heussler, V., van Dooren, M.W., van Schaijk, B., van Gemert, G.J., Sauerwein, R.W., Mota, M.M., Waters, A.P., *et al.* (2005). Genetically attenuated, P36p-deficient malarial sporozoites induce protective immunity and apoptosis of infected liver cells. *Proc Natl Acad Sci U S A* 102, 12194-12199.
- van Dooren, G.G., and Striepen, B. (2013). The algal past and parasite present of the apicoplast. *Annu Rev Microbiol* 67, 271-289.

- van Schaijk, B.C., Ploemen, I.H., Annoura, T., Vos, M.W., Foquet, L., van Gemert, G.J., Chevalley-Maurel, S., van de Vegte-Bolmer, M., Sajid, M., Franetich, J.F., *et al.* (2014). A genetically attenuated malaria vaccine candidate based on *P. falciparum* b9/slarp gene-deficient sporozoites. *Elife* 3.
- Vander Jagt, D.L., Hunsaker, L.A., and Campos, N.M. (1986). Characterization of a hemoglobin-degrading, low molecular weight protease from *Plasmodium falciparum*. *Mol Biochem Parasitol* 18, 389-400.
- Varnai, P., Thyagarajan, B., Rohacs, T., and Balla, T. (2006). Rapidly inducible changes in phosphatidylinositol 4,5-bisphosphate levels influence multiple regulatory functions of the lipid in intact living cells. *J Cell Biol* 175, 377-382.
- Varnai, P., Toth, B., Toth, D.J., Hunyady, L., and Balla, T. (2007). Visualization and manipulation of plasma membrane-endoplasmic reticulum contact sites indicates the presence of additional molecular components within the STIM1-Orai1 Complex. *J Biol Chem* 282, 29678-29690.
- Veres, A., Gosis, B.S., Ding, Q., Collins, R., Ragavendran, A., Brand, H., Erdin, S., Cowan, C.A., Talkowski, M.E., and Musunuru, K. (2014). Low incidence of off-target mutations in individual CRISPR-Cas9 and TALEN targeted human stem cell clones detected by whole-genome sequencing. *Cell Stem Cell* 15, 27-30.
- Volz, J.C., Yap, A., Sisquella, X., Thompson, J.K., Lim, N.T., Whitehead, L.W., Chen, L., Lampe, M., Tham, W.H., Wilson, D., *et al.* (2016). Essential Role of the PfRh5/PfRipr/CyRPA Complex during *Plasmodium falciparum* Invasion of Erythrocytes. *Cell Host Microbe* 20, 60-71.
- Wagner, J.C., Platt, R.J., Goldfless, S.J., Zhang, F., and Niles, J.C. (2014). Efficient CRISPR-Cas9-mediated genome editing in *Plasmodium falciparum*. *Nat Methods* 11, 915-918.
- Waller, R.F., Keeling, P.J., Donald, R.G., Striepen, B., Handman, E., Lang-Unnasch, N., Cowman, A.F., Besra, G.S., Roos, D.S., and McFadden, G.I. (1998). Nuclear-encoded proteins target to the plastid in *Toxoplasma gondii* and *Plasmodium falciparum*. *Proc Natl Acad Sci U S A* 95, 12352-12357.
- Waller, R.F., Reed, M.B., Cowman, A.F., and McFadden, G.I. (2000). Protein trafficking to the plastid of *Plasmodium falciparum* is via the secretory pathway. *EMBO J* 19, 1794-1802.
- Walliker, D., Quakyi, I.A., Wellems, T.E., McCutchan, T.F., Szarfman, A., London, W.T., Corcoran, L.M., Burkot, T.R., and Carter, R. (1987). Genetic analysis of the human malaria parasite *Plasmodium falciparum*. *Science* 236, 1661-1666.
- Wanaguru, M., Liu, W., Hahn, B.H., Rayner, J.C., and Wright, G.J. (2013). RH5-Basigin interaction plays a major role in the host tropism of *Plasmodium falciparum*. *Proc Natl Acad Sci U S A* 110, 20735-20740.
- Wang, P., Wang, Q., Sims, P.F., and Hyde, J.E. (2002). Rapid positive selection of stable integrants following transfection of *Plasmodium falciparum*. *Mol Biochem Parasitol* 123, 1-10.
- Wassmer, S.C., Taylor, T.E., Rathod, P.K., Mishra, S.K., Mohanty, S., Arevalo-Herrera, M., Duraisingh, M.T., and Smith, J.D. (2015). Investigating the Pathogenesis of Severe Malaria: A Multidisciplinary and Cross-Geographical Approach. *Am J Trop Med Hyg* 93, 42-56.
- Watermeyer, J.M., Hale, V.L., Hackett, F., Clare, D.K., Cutts, E.E., Vakonakis, I., Fleck, R.A., Blackman, M.J., and Saibil, H.R. (2016). A spiral scaffold underlies cytoadherent knobs in *Plasmodium falciparum*-infected erythrocytes. *Blood* 127, 343-351.
- Webster, W.A., and McFadden, G.I. (2014). From the genome to the phenome: tools to understand the basic biology of *Plasmodium falciparum*. *J Eukaryot Microbiol* 61, 655-671.
- Weiss, G.E., Crabb, B.S., and Gilson, P.R. (2016). Overlaying Molecular and Temporal Aspects of Malaria Parasite Invasion. *Trends Parasitol* 32, 284-295.
- Weiss, G.E., Gilson, P.R., Taechalertrapisarn, T., Tham, W.H., de Jong, N.W., Harvey, K.L., Fowkes, F.J., Barlow, P.N., Rayner, J.C., Wright, G.J., *et al.* (2015). Revealing the sequence and resulting cellular morphology

- of receptor-ligand interactions during *Plasmodium falciparum* invasion of erythrocytes. *PLoS Pathog* *11*, e1004670.
- Wellems, T.E., and Plowe, C.V. (2001). Chloroquine-resistant malaria. *J Infect Dis* *184*, 770-776.
- White, L.J., Flegg, J.A., Phyto, A.P., Wiladpai-ngern, J.H., Bethell, D., Plowe, C., Anderson, T., Nkhoma, S., Nair, S., Tripura, R., *et al.* (2015). Defining the in vivo phenotype of artemisinin-resistant *falciparum* malaria: a modelling approach. *PLoS Med* *12*, e1001823.
- White, N.J. (2011). Determinants of relapse periodicity in *Plasmodium vivax* malaria. *Malar J* *10*, 297.
- WHO (2017). Status report on artemisinin and ACT resistance
- Witkowski, B., Amaratunga, C., Khim, N., Sreng, S., Chim, P., Kim, S., Lim, P., Mao, S., Sopha, C., Sam, B., *et al.* (2013). Novel phenotypic assays for the detection of artemisinin-resistant *Plasmodium falciparum* malaria in Cambodia: in-vitro and ex-vivo drug-response studies. *Lancet Infect Dis* *13*, 1043-1049.
- Woelk, T., Oldrini, B., Maspero, E., Confalonieri, S., Cavallaro, E., Di Fiore, P.P., and Polo, S. (2006). Molecular mechanisms of coupled monoubiquitination. *Nat Cell Biol* *8*, 1246-1254.
- Wong, W., Bai, X.C., Sleebs, B.E., Triglia, T., Brown, A., Thompson, J.K., Jackson, K.E., Hanssen, E., Marapana, D.S., Fernandez, I.S., *et al.* (2017). Mefloquine targets the *Plasmodium falciparum* 80S ribosome to inhibit protein synthesis. *Nat Microbiol* *2*, 17031.
- Woodrow, C.J., and White, N.J. (2017). The clinical impact of artemisinin resistance in Southeast Asia and the potential for future spread. *FEMS Microbiol Rev* *41*, 34-48.
- Wu, Y., Kirkman, L.A., and Wellems, T.E. (1996). Transformation of *Plasmodium falciparum* malaria parasites by homologous integration of plasmids that confer resistance to pyrimethamine. *Proc Natl Acad Sci U S A* *93*, 1130-1134.
- Wu, Y., Sifri, C.D., Lei, H.H., Su, X.Z., and Wellems, T.E. (1995). Transfection of *Plasmodium falciparum* within human red blood cells. *Proc Natl Acad Sci U S A* *92*, 973-977.
- Xu, T., Johnson, C.A., Gestwicki, J.E., and Kumar, A. (2010). Conditionally controlling nuclear trafficking in yeast by chemical-induced protein dimerization. *Nat Protoc* *5*, 1831-1843.
- Yamada, K., Ono, M., Perkins, N.D., Rocha, S., and Lamond, A.I. (2013). Identification and functional characterization of FMN2, a regulator of the cyclin-dependent kinase inhibitor p21. *Mol Cell* *49*, 922-933.
- Yap, A., Azevedo, M.F., Gilson, P.R., Weiss, G.E., O'Neill, M.T., Wilson, D.W., Crabb, B.S., and Cowman, A.F. (2014). Conditional expression of apical membrane antigen 1 in *Plasmodium falciparum* shows it is required for erythrocyte invasion by merozoites. *Cell Microbiol* *16*, 642-656.
- Yeh, E., and DeRisi, J.L. (2011). Chemical rescue of malaria parasites lacking an apicoplast defines organelle function in blood-stage *Plasmodium falciparum*. *PLoS Biol* *9*, e1001138.
- Zetsche, B., Volz, S.E., and Zhang, F. (2015). A split-Cas9 architecture for inducible genome editing and transcription modulation. *Nat Biotechnol* *33*, 139-142.
- Zhu, X.D., and Sadowski, P.D. (1995). Cleavage-dependent ligation by the FLP recombinase. Characterization of a mutant FLP protein with an alteration in a catalytic amino acid. *J Biol Chem* *270*, 23044-23054.
- Ziegelbauer, J., Shan, B., Yager, D., Larabell, C., Hoffmann, B., and Tjian, R. (2001). Transcription factor MIZ-1 is regulated via microtubule association. *Mol Cell* *8*, 339-349.
- Zoncu, R., Perera, R.M., Sebastian, R., Nakatsu, F., Chen, H., Balla, T., Ayala, G., Toomre, D., and De Camilli, P.V. (2007). Loss of endocytic clathrin-coated pits upon acute depletion of phosphatidylinositol 4,5-bisphosphate. *Proc Natl Acad Sci U S A* *104*, 3793-3798.

Appendix A. Oligonucleotides

Primers	Sequence
XhoI-NLS_Mlul_L1_fwd	GAGActcgagATGGCACAAAAAAGAAAAGTTacgctGATCCAACAAG AAGTGCAAATAGTGGAGC
L1_NheI_FRB_fwd	AGTGCAAATAGTGGAGCAGGAGCAGGAGCAATATTAAGTAGAgcta gcATGGCTTCTAGAATCCTCTGGCATG
FRB_SpeI_L2_KpnI_rev	GAGAGGTACCTAATGTTGCAACTGGTGCATAATCTGGATTATCATATGGATA ACTTGTACTAGTCTTTGAGATTCTGCGGAACACATG
Mul1-NLS-NLS-L1_fw	cagaacgcgtCCGAAGAAGAAGCGCAAGGTGCCTAAGAAAAAGCGAAAGGTGg atccaacaagaagtgcaaatagtggag
L-2xfkbp-L-nhei_fwd	cagcgctagcTCAGGATTGAGATCAAGATCTGCTGC
L_2xfkbp_L-avrii-rev	cagccctaggTCTACCTGCACCTCCAGCACCAGCAG
AvrII_linkerL3_FKBP_fwd	GAGAcctaggAGTGGATTAAGAAGTAGAAGTGCAGCAGCAGGAGCAGGAGG AGCAGCAAGAGCAGCAGGAGTGCAGGTGAAAACCATCTCCC
FKBP_linkerL4_KpnI_rev	TCTCGTACCTCTTCTGCTCCTCTGCTCCTGCTGCTGCTCCTTGTCTCCAG TTTTAGAAGCTCCACATC
FRB*-2A-AvrIIrv	tcctctaggactgattggctctgattttctctacatctccacatgtaataaactcctctctctctcc ataactagtcttgagattcgtcgg
Mito-Xholfw	cttctcgcgcaaaatgaaaagttttataacaagaataaaacagc
NotI-PFD0095c_F	GCACGCGGCCGCTAGCATTGCTGAAGAGAAATGGCAAGAATG
AvrII-PFD0095c_R	CGCGCCTAGGACCTGAACCTGAACCTTGTCTATCATTCAAAGTTGACATATTA TTTCC
XmaI-PFD0095c_R	CGCGCCCGGGACCTGAACCTGAACCTTGTCTATCATTCAAAGTTGACATATTA TTTCC
NotI-Rex1_F	GCACGCGGCCGCTAGGATGAATATTTACAATTAAGATC
AvrII-Rex1_R	CGCGCCTAGGACCTGAACCTGAACCTTAAATACAGAACTTTCTAGTAATG
XmaI-Rex1_R	CGCGCCCGGGACCTGAACCTGAACCTTAAATACAGAACTTTCTAGTAATG
mDHF ^{recod} Xmalfw	CTCGCCCGGGATGGTAAGCCTTTGAATTGTATAGTTGC
mDHF ^{recod} KpnIrv	TAATGGTACCGTCTTTTTTTCGTAACCTCGAACTATATTTTATTCC
2A_fw_AvrII-Nhe	GTCTCTAGGGCTAGCGGAGAAGGAAGAGGAAGTTTATTAAC
BSD_rv_XhoI	TCCTCTCGAGTTAGCCCTCCACACATAACCAGAGGGCAGC
Sall_T2A_Neo_fw	gtagGTCGACGGAGAAGGAAGAGGAAGTTTATTAACATGTGGAGATGTAGAA GAAAATCCAGGACCAATGATTGAACAAGATGGATTGCACGC
Neo_Stop_XhoI_rev	ggttCTCGAGTTAGAAGAACTCGTCAAGAAGGCGATAGAAGGCG
GFP-2xFKBP_fw	CTGGGATTACACATGGCATGGATGAGCTTACAAAGTCGACGCCAGGGGAG CAGCCGACAGGAGCAGGGGGGCGAGGAAGGCGTGGTGTTCAGGTCGAGAC
GFP-2xFKBP_rv	CTCCACATGTTAATAAACTTCTCTTCTTCTCCGTCGACAGTTTCCAGTTTCAA AAGTTCC
BglII_Hsp86_promoter_fw	GcatAGATCTATAATTATTAATAGGTACTTTTTTTTTTATATATGGG
Hsp86_promoter_Xho_rv	gcatctcgagTTTATTCGAAATGTGGGAAG
Lyn-PM-targeting_fw	agctctcgagATGGGATGTATAAAATCAAAGGGAAAGACAGCGCGGGAGCAG ATCCACCAGAcgctgatccaacaagaag
mCherry_88as	GGCCGTTACGGAGCCCTCC
BGIII_NMD3_Promoter_fw	gctaAGATCTtattattattacatGTTGAAATATAAATTTCAAAAAAATGATC
NMD3_Promoter_Xho_rv	cgactctcgagTTATCTTTAAATGATATACG
DHODH_backbone_fw	TAATAATAAATACCTAATAGAAATATATCAGGATCCATGACAGCCAGTTTAAAC TACCAAG

DHODH_backbone_rv	TTTTATAATATTTTAAATCTATTATTAATAAGCTTTTAAATGCTGTTCAACTTC CCACGGAAC
GFP 85 rv	ACCTTCACCCTCTCCACTGAC
pArl sense 55	ggaattgtgagcggataacaatttcacacagg
PF3D7_1220900_NotI_fw	gcatgcggccgcTAAGTATTAATCAAAAGGTAGAAG
PF3D7_1220900_AvrII_rv	cgatcctaggAGCTGTACGGTATCTTAGTCTTG
PF3D7_1220900_int_check_5_fw	GATGGGAAAATTTGAAAAATC
PF3D7_1220900_int_check_3_rv	ACATATGTATATATGTATATTTGC
GD_PF3D7_1220900_NotI_fw	cgatgcggccgcTAAATATACTTGAAATAAAAAAAAAAG
GD_PF3D7_1220900_MluI_rv	cgatacgcgtCTTATTTTAAATACGAACG
GD_PF3D7_1220900_int_check_5_fw	GAAGAAAAAATGACAGGGTC
GD_PF3D7_1220900_int_check_3_rv	TCTACCCATTGTGGAGATTC
PF3D7_1337800_NotI_fw	gcatgcggccgcTAATATATTTTATTATGTGGATATCCACCATTTAATGG
PF3D7_1337800_AvrII_rv	cgatcctaggTTCTTTAACTCCCGTCATCATCTTATAAAATTCATC
PF3D7_1337800_int_check_5_fw	GACACCTTATTATATAGCACC
PF3D7_1337800_int_check_3_rv	GTTTGATTTAAAAAATTTTTCG
GD_PF3D7_1337800_NotI_fw	gcatgcggccgcTAAATAGATACAAGTTAGGCAAAGGATC
GD_PF3D7_1337800_MluI_rv	cgatacgcgtATCTACATATAAAATATTTTCTGG
GD_PF3D7_1337800_int_check_5_fw	AAAGGTAGATGTAGTGTTAG
GD_PF3D7_1337800_int_check_3_rv	ATTTGTATAGGAGAATCTTCTG
PF3D7_1244600_NotI_fwd	cgatgcggccgcTAACAATATTCAAATGAAGAACC
PF3D7_1244600_AvrII_rev	cgatcctaggATTAAGTTGAATTATTTTCATTCATTC
PF3D7_1244600_int_check_5_fw	AAGAAAGAAGATGAAAGC
PF3D7_1244600_int_check_3_rv	GTTTGATTTTTCCATTTTC
PF3D7_1352800_NotI_fwd	cagcgcggccgcagatgataaaattatagttatcattatc
PF3D7_1352800_AvrII_rev	ctgccctaggagatgttattgctttatattattaataaatatc
PF3D7_1352800_int_check_5_fw	cgtaataaagtacataatcttatatcc
PF3D7_1352800_int_check_3_rv	gataatattaatagtctatgtaatatcc
mcherry-gibson-fwd	gattatgcAccagttgcaacattaggtaccatggtgagcaagggcgaggaggat
mcherry-gibson-rev	CCTTCTCCcctagGctgtacagctcgtc
DiCre-XhoI-fwd	gagcctcgagacaaaatggcaccacaaagaaaaagagaaaag
DiCre-XmaI-rev	attaccgggtaatttaattacacatgctgccaac
DiCre_Part2_fw	TTGTTTTTTTTAATTTCTTACATATAActcgagcaaaaatggcaccacaaagaaaaagag
DiCre_T2A_ca_rv	TGGACCTGGATTTTCTCAACATCACCACAAGTCAACAAAGAACCTCTACCTTC ACCatctccatcttctaataatcttac
DiCre_T2a_ca_1xNLS_fw	CTTGTGGTGATGTTGAAGAAAATCCAGGTCCAACCGGTatggcaccacaaaaaaaaa aagaaaag
1xNLS_T2a_DiCre_rv	Tggtcctggatcttctcatatctccatgttaataaaactcctctccttctccctgtacagctcgtcc atgccgc

T2A_DiCre_fw	Gtggagatgtagaagaaaatccaggaccaatggctcctaagaaaaaaagaaaggtaagtag
DiCre_Part1_rv	aaacgaacattaagctgcatatccctcgaCCCGGGttaatttaatttacaccatgctg
PF3D7_0525000_Notl_fw	cgatgcggccgcTAATTTTCTACAAAGAACCTTCCACACCTATGAGAATGTCAAG C
PF3D7_0525000_Avrll_rv	cgatcctaggATAATCAAAAATTTCCACCTTCTGGGCC
PF3D7_0525000_int_check_5_fw	GAAATATGAATATTCTTATG
PF3D7_0525000_int_check_3_rv	ATATTTTTTTTTTTTTTTTTATATTTTC
GD_PF3D7_0525000_Notl_fw	agctatttagtgacactatagaatactcgcggcgctaaTGAAGAATGGAAGTAATAACC AATC
GD_PF3D7_0525000_Mlul_rv	CTCCAGCACCAGCAGCAGCACCTCTAGCacgcgtAGGCCTTAATTCACATACAG AATG
GD_PF3D7_0525000_int_check_5_fw	CCCACGACGTAATCAAATGATG
GD_PF3D7_0525000_int_check_3_rv	GAGCAGTTTTATATAAATCTCCTG
PF3D7_0526800_Notl_fw	gcatgcggccgcTAAGGCAAGGAATATGAATATTGTAATGAAAAAGATGACCG
PF3D7_0526800_Avrll_rv	cgatcctaggGACGTATCGTCTTGATGATCTGCTTCTTGG
PF3D7_0526800_int_check_5_fw	CTTGAAGGACACACATATGAAG
PF3D7_0526800_int_check_3_rv	CATAAAAATAGGTATTGTTTTG
GD_PF3D7_0526800_Notl_fw	cgatgcggccgcTAAGAAGATAAACATAAGGAAGAAG
GD_PF3D7_0526800_Mlul_rv	cgatacgcgtTAATGGTTGAAAATTTAGATACC
GD_PF3D7_0526800_int_check_5_fw	cgatgcggccgcTAAGAAGATAAACATAAGGAAGAAG
GD_PF3D7_0526800_int_check_3_rv	TTTCCAATATTGTCAATAG
PF3D7_0720600_Notl_fw	gcatgcggccgcTAACTTATCTGGTCGTTATAAGGCAG
PF3D7_0720600_Avrll_rv	ccatcctaggTAAATAAATTTTTTTATTTTCTTATATATTTATGTGCAATTTTCATC TCCaAGcGTGTTTACTACCTTTTCTAG
PF3D7_0720600_int_check_5_fw	GAAAAGCTTAAAAAGAAACCTC
PF3D7_0720600_int_check_3_rv	ATTTTATGATTTTATTATTTTTTG
GD_PF3D7_0720600_Notl_fw	gcatgcggccgcTAAgtagGATAGAAAATAAGGGAAG
GD_PF3D7_0720600_Mlul_rv	cgatacgcgtATAAGGAATATCATAACTTTTTTC
GD_PF3D7_0720600_int_check_5_fw	cgatgcggccgcTAAGACAACCTGCACTAgtacg
GD_PF3D7_0720600_int_check_3_rv	CATCCTTGTTGGTAAAATTG
PF3D7_0807600_Notl_fw	gcatgcggccgcTAAAGGGGTGGTTATAGTATGAGAAATGATCAACG
PF3D7_0807600_Avrll_rv	cgatcctaggCATTGAAGAATCGTCATTATTGTA AAAATTGC
PF3D7_0807600_int_check_5_fw	GTATCTGCATCGCACGCAAAC
PF3D7_0807600_int_check_3_rv	AGATATGTTATTTATTTCTTCG
GD_PF3D7_0807600_Notl_fw	gcatgcggccgcTAAgtagGCCTGAGTTTTAATATTAACG
GD_PF3D7_0807600_Mlul_rv	cgatacgcgtTCTTCGTTTTCTTCATAGTATTC
GD_PF3D7_0807600_int_check_5_fw	Cttatacgttcatcccttctc

5_fw	
GD_PF3D7_0807600_int_check_3_rv	cgatacgcgtAATGGCATCATCATATAAATG
PF3D7_1317400_NotI_fw	gcatcgccgcTAACAGAAAAGAAGTTTAATTAATGATGAAAAAATGG
PF3D7_1317400_AvrII_rv	cgatcctaggTGTTTTGTAATTAATTTTTTTTTTTGTAC
PF3D7_1317400_int_check_5_fw	GTCGTAAATTCAGACGATAC
PF3D7_1317400_int_check_3_rv	ATATAACGTTTTGTTTTCAAG
GD_PF3D7_1317400_NotI_fw	gcatcgccgcTAACAGAAAAGAAGTTTAATTAATGATGAAAAAATGG
GD_PF3D7_1317400_MluI_rv	cgatacgcgtATTAGATGAATCTAAACTATG
GD_PF3D7_1317400_int_check_5_fw	CAATGGAATGTGTTTGTTC
GD_PF3D7_1317400_int_check_3_rv	TTTTTAGATTTAACTAAC
PF3D7_1445700_NotI_fw	gcatcgccgcTAAAATATGGATAGAAGAACTATAACCC
PF3D7_1445700_AvrII_rv	cgatcctaggTTTACTTGTTAAAGATGGAAAAGCTCTTG
PF3D7_1445700_int_check_5_fw	GTAACGCTTCGACCAATATTC
PF3D7_1445700_int_check_3_rv	TTTTTTTTATGAATTCATATC
GD_PF3D7_1445700_NotI_fw	gcatcgccgcTAAGATAGATATAAATATCCAGTGACCAG
GD_PF3D7_1445700_MluI_rv	cgatacgcgtGTATTTTCTACCTGCCTTACTAC
GD_PF3D7_1445700_int_check_5_fw	TATAACAAGAGAGTGAATGTTT
GD_PF3D7_1445700_int_check_3_rv	GATCATAATCTATGGTTACTG
PF3D7_1451200_NotI_fw	gcatcgccgcTAAAAGAAGAGGAAGATAATGAAAAC
PF3D7_1451200_AvrII_rv	cgatcctaggATTTTCATTTTCATTATATCCAAATG
PF3D7_1451200_int_check_5_fw	ATTATAATTTAGAAAAAGGAG
PF3D7_1451200_int_check_3_rv	TTTATTTATTTATTCATTTTC
GD_PF3D7_1451200_NotI_fw	gcatcgccgcTAAATAAGAATTATGTATCTGAAAC
GD_PF3D7_1451200_MluI_rv	cgatacgcgtAGACACCTCATTTTTTAGCTC
GD_PF3D7_1451200_int_check_5_fw	AAGAAAAAGAAAATATTATAG
GD_PF3D7_1451200_int_check_3_rv	ATATTCATTTTTGATAAAATC
PF3D7_1463000_NotI_fw	gcatcgccgcTAAGGTATATGTTGTTTAACGGTTGCTTCAAG
PF3D7_1463000_AvrII_rv	cgatcctaggTGTTTTATGTTTTGTTTCATAATATGCTTC
PF3D7_1463000_int_check_5_fw	GTAATAGTAAATTTTTAAATG
PF3D7_1463000_int_check_3_rv	ATTTTCTTCTTTAATTTTTG
GD_PF3D7_1463000_NotI_fw	cgatcgccgcTAAGCGTAAAATAATTACGAATACCAG
GD_PF3D7_1463000_MluI_rv	cgatacgcgtCACAGGTGAATAATTTTTTCG
GD_PF3D7_1463000_int_check_5_fw	GAAAAATGGAGAAGGTTATTAC
GD_PF3D7_1463000_int_check_3_rv	TTCATTATTTGATTTAATTC

3_rv	
PF3D7_0202400_NotI_fwd	cgatgcgccgcTAAAATATACAAGATCGACATGATCC
PF3D7_0202400_AvrII_rev	cgatcctaggTAATGCTTTGTTTGCATTTGATTG
PF3D7_0202400_int_check_5_fw	GTATATAATAATTCTCC
PF3D7_0202400_int_check_3_rv	GATAATTTTGTATAATTTTG
GD_PF3D7_0202400_NotI_fw	atttagtgacactatagaataactcgcgccgcTAATATTATATTAATATATATCGGTG
GD_PF3D7_0202400_MluI_rv	CTCCAGCACCAGCAGCAGCACCTCTAGCacgcgtTTGTTTTTGGACACAATTCTC TG
GD_PF3D7_0202400_int_check_5_fw	TAATAAGAAGAGAATGTTAAAG
GD_PF3D7_0202400_int_check_3_rv	ATAACTACGAGGAAATTGATTG
PF3D7_0205100_NotI_fwd	cgatgcgccgcTAAAATGATCATATGAAGGAAGTTAC
PF3D7_0205100_AvrII_rev	cgatcctaggTTGCTCATCTATATTATCC
PF3D7_0205100_int_check_5_fw	GAAACGAAAAATGCGGAAG
PF3D7_0205100_int_check_3_rv	ATAAAGTACACATAAATG
GD_PF3D7_0205100_NotI_fwd	cgatgcgccgcTAATCTAATATGTCGACTATTTTAA
GD_PF3D7_0205100_MluI_rev	cgatacgcgtGTGAATAACATATCTATCCTC
GD_PF3D7_0205100_int_check_5_fw	gtgcgtatttaattgtg
GD_PF3D7_0205100_int_check_3_rv	CTAAATATGGAGTTTG
PF3D7_0205600_NotI_fwd	cgatgcgccgcTAATGCAGCAAATTATTTAAGTATAC
PF3D7_0205600_AvrII_rev	cgatcctaggGTTGGGCTCAGTATGTTGTTG
PF3D7_0205600_int_check_5_fw	CAATCAGAAATATATG
PF3D7_0205600_int_check_3_rv	CTTCATAATATACATATGG
GD_PF3D7_0205600_NotI_fwd	cgatgcgccgcTAAGATAATAAAGACCATTTTCATG
GD_PF3D7_0205600_MluI_rv	cgatacgcgtCCAAGCTAATGTATTCATAGG
GD_PF3D7_0205600_int_check_5_fw	GTATATATGAAGATATC
GD_PF3D7_0205600_int_check_3_rv	GTATGAGTATAATTAAG
PF3D7_0209700_NotI_fwd	cgatgcgccgcTAAGAAGAACCATCTTATAAAG
PF3D7_0209700_AvrII_rev	cgatcctaggATTAAACGTATAACTCAAACG
PF3D7_0209700_int_check_5_fw	GGGAAAACATCGACAG
PF3D7_0209700_int_check_3_rv	CACACAATACCAAATG
GD_PF3D7_0209700_NotI_fwd	cgatgcgccgcTAAACTGAAAAGGAGTTAGAGAATGG
GD_PF3D7_0209700_MluI_rv	cgatacgcgtTGTAGCTAAGCATTTCCAACAG
GD_PF3D7_0209700_int_check_5_fw	CATAACCACTCGGGTATG
GD_PF3D7_0209700_int_check_3_rv	CAGGATGGACAATTATC

3_rv	
PF3D7_0210200_NotI_fwd	cgatgcggccgcTAAAAGAATACCACATATACGATAAC
PF3D7_0210200_AvrII_rev	cgatcctaggCAATAAAAGGATTTTCTTGACATC
PF3D7_0210200_int_check_5_fw	GAACATATTCATATGG
PF3D7_0210200_int_check_3_rv	CGATTATATAATCACAATTGC
GD_PF3D7_0210200_NotI_fwd	cgatgcggccgcTAAGAAACAATATTATGTAAAG
GD_PF3D7_0210200_MluI_rv	cgatacgcgtGTTTTTATTAGCTAGTAAACA
GD_PF3D7_0210200_int_check_5_fw	GAATAATTTATTACATGG
GD_PF3D7_0210200_int_check_3_rv	GCATCAATAAATAACTGG
PF3D7_0211700_NotI_fwd	cgatgcggccgcTAACAATATGGAACCTTTATTTGATATC
PF3D7_0211700_AvrII_rev	cgatcctaggAAAAAAAAAACTGGTGTGATCCTCC
PF3D7_0211700_int_check_5_fw	CAATAAATAATCCAAGAGC
PF3D7_0211700_int_check_3_rv	ATCCCTCTTGCTATAG
GD_PF3D7_0211700_NotI_fwd	cgatgcggccgcTAAAAGAATATTGACATGAAAC
GD_PF3D7_0211700_MluI_rv	cgatacgcgtATCATTGGATATATTTGTACG
GD_PF3D7_0211700_int_check_5_fw	GTTGATATGTTATTTTCAAAGG
GD_PF3D7_0211700_int_check_3_rv	TTATAGTTGTATGTTTGTGG
PF3D7_0210900_NotI_fwd	cgatgcggccgcTAAAGAAATTTTCATAATGGAAGAG
PF3D7_0210900_AvrII_rev	cgatcctaggATTTTTCTTTGTTGTTGCATTATTTAATG
PF3D7_0210900_int_check_5_fw	GAAAGAAAAAATGAGAAAAT
PF3D7_0210900_int_check_3_rv	TTCCAGTTGACGTTATCTG
GD_PF3D7_0210900_NotI_fwd	aagctatttagtgacactatagaataactcgggccgctaataataaGATTACTTATCATGCCCCCTCGAC
GD_PF3D7_0210900_MluI_rv	CTCCAGCACCAGCAGCAGCACCTCTAGCacgcgtAATTAATCTATTATTATAATATG
GD_PF3D7_0210900_int_check_5_fw	GAAAGAAAAAATGAGAAAAT
GD_PF3D7_0210900_int_check_3_rv	TTCCAGTTGACGTTATCTG
PF3D7_0213700_NotI_fwd	cgatgcggccgcTAACATGTTAATAACATAAGTACG
PF3D7_0213700_AvrII_rev	cgatcctaggTTTCATTTCTCCTTTAACG
PF3D7_0213700_int_check_5_fw	GTTCCATTATTAAGAGG
PF3D7_0213700_int_check_3_rv	GTAGATATATAATATTTTC
GD_PF3D7_0213700_NotI_fwd	cgatgcggccgcTAACTAAGTAGCCCTTCAACAAATC
GD_PF3D7_0213700_MluI_rv	cgatacgcgtTGGAGAGTACTTATAAAAGCACG

GD_PF3D7_0213700_int_check_5_fw	GTTCCCATTATTAAGAGG
GD_PF3D7_0213700_int_check_3_rv	GTAGATATATAATATTTTC
PF3D7_0213900_NotI_fwd	cgatgcggccgcTAAACCATTTAGAAGATGATGAATC
PF3D7_0213900_AvrII_rev	cgatcctaggATAAAAATTGTTTTGAAAAAAAAGC
PF3D7_0213900_int_check_5_fw	GATATTTCCATAAATATG
PF3D7_0213900_int_check_3_rv	ATATATGTGAGGAAAAG
GD_PF3D7_0213900_NotI_fwd	cgatgcggccgcTAACATATCATCTGTAATAATTCTCC
GD_PF3D7_0213900_MluI_rev	cgatacgcgtGGTTTCTTTCTTTCATTTG
GD_PF3D7_0213900_int_check_5_fw	TGATGATAATATAAACAATAACC
GD_PF3D7_0213900_int_check_3_rv	CACTTGTTTTTATCATGATAATG
PF3D7_0218200_NotI_fwd	cgatgcggccgcTAATAAATTAAGTCATCTCATGCAG
PF3D7_0218200_AvrII_rev	cgatcctaggTAACGAGGGAAAGTCAATATC
PF3D7_0218200_int_check_5_fw	CACATATATCAAAAAATG
PF3D7_0218200_int_check_3_rv	CAATATAATGTTATGTG
GD_PF3D7_0218200_NotI_fwd	cgatgcggccgcTAAGACAATATAAATAAAAAATCAAGAG
GD_PF3D7_0218200_MluI_rv	cgatacgcgtGTTATTAATATATGCATACTGG
GD_PF3D7_0218200_int_check_5_fw	GGTATTAATGAATCTGG
GD_PF3D7_0218200_int_check_3_rv	GAATTATTATGATATATATG
PF3D7_1343700_NotI_fw	gcatgcggccgcTAAAGATGCAGCAAATCTTATAAATG
PF3D7_1343700_Pme_rv	gcatgttaaaccATCAATCATAGTTTCAGTAGC
Kelch_codon_adjust_fw	CTGCTGCTGGTGCTGGAGGTGCAGGTAGAcctaggATGGAGGGTGAGAAGGT TAAGACTAAAG
Kelch_codon_adjust_rv	tataaataagaaaaacgaacattaagctgccatctcctcgagTCAaataacttcgtataatgtatgc tatacgaagttataggcctTCAAATGTTAGCAATCAATACTG
PF3D7_1343700_int_check_5_fw	TTATGAATACCAACAAAAAAGAG
PF3D7_1343700_int_check_3_rv	GTTTCAAAAATAGCTCCACCAAC
Kelch_C580Y_fw	TAGCTCCATTAACACTCCAAGGTCTAGTGCAATGTATGTAGCATTGACAAC AAGATATAC
Kelch_C580Y_rv	CATTGCACTAGACCTTGGAGTG
Kelch_351-726_rv	taaataagaaaaacgaacattaagctgccatctcctcgagTCAaataacttcgtataatgtatgc atacgaagttataccggtTCAAATGTTAGCAATCAATACTG
Kelch_351-726_fw	GAGGTGCTGCTGCTGGTGCTGGAGGTGCAGGTAGAcctaggATGATAGACATA AACGTAGGAG
GD_PF3D7_1343700_NotI_fw	cgatgcggccgcTAAGTCTAAAGATAATATAGG

GD_PF3D7_1343700_Mlul_rv	cgatacgcgtTCTTTCCATTTCTAGTTCTTTC
GD_PF3D7_1343700_int_check_5_fw	gcatcgggccgcTAAGATTCGAACTTTGATAGTAAAAAAG
GD_PF3D7_1343700_int_check_3_rv	CAATATCTAATTTCTTTCTTTC
nTerm-DHODH_fw_(1)	ataacttcgtatagcatacattatacgaagttatCCGGAGAAGGAAGAGGAAGTTTATTA ACATGTGGAGATGTAGAAGAAAATCCAGGACCAATGACAGCCAGTTTAACTA CC
nTerm-DHODH_fw_(2)	GAGCAGAAGTTAATATCAGAAGAGGATTTGGGTGAACAAAACTCATAAGC GAAGAAGATTTAataacttcgtatagcatacattatac
nTerm-DHODH_fw_(3)	GATAAAAAAAAAATTGTTGATGCAAATATTGCTACTGAACTATGATTGATGG TTTAAACGAGCAGAAGTTAATATCAGAAGAG
nTerm-DHODH_rv	tccagtgaagttcttctcttactcatgctagcTGGACCTGGATTTTCTCAACATCACC ACAAGTCAACAAAGAACCTCTACCTTACCAATGCTGTTCAACTTCCCACG
nT6-DHODH-2x2FKBP_fw	TGACTTGTGGTGATGTTGAAGAAAATCCAGGTCCAgctagcCGTGGTGTTCAG GTCGAGAC
nT6-DHODH-2x2FKBP_rv	acaactccagtgaagttcttctcttactcatgctagcCCTTCTGCCCCCTGCTCCTG CGGCTGCTCCCTGGCAGTTTCCAGTTTCAAAGTTTCGAC
KBI.1 TGD fw	ttagtgacactatagaataactcgggccgctaaGAACAATTCAGGCAATAATTCAAC
KBI.1 TGD rv	CAGCACCAGCAGCAGCACCTCTAGCacgcgtTATGTCAGACAAATCCTTCATAT TTG
KBI.1 fw	tagtgacactatagaataactcgggccgctaaTATGAAAACTGAAAGATAGTAAAC
KBI.1 rv	AGCAGCAGATCTTGATCTCAATCCTGAcctaggCTCGTTCATAAAAAATTTTCAAC TG
KBI.2 TGD fw	ttagtgacactatagaataactcgggccgctaaGGTTAGCGACACAAAATCCGAGG
KBI.2 TGD rv	TCCAGCACCAGCAGCAGCACCTCTAGCacgcgtTGTATTACATTGATCATTITTT TC
KBI.2 fw	ttagtgacactatagaataactcgggccgctaaAAATTATTAAGTAAACACATTCATAG
KBI.2 rv	AGCAGCAGATCTTGATCTCAATCCTGAcctaggTCTAACTACAGTTTTTAACAAA TAATC
KBI.3 TGD fw	atttagtgacactatagaataactcgggccgctaaGACAAACGCTGGAACACTGATTTA AG
KBI.3 TGD rv	CAGCACCAGCAGCAGCACCTCTAGCacgcgtTATGGTTGTAATTAATTGCTTATT TTC
KBI.3 fw	ttagtgacactatagaataactcgggccgctaaTTATTCAGCTGATGATCTTTTAC
KBI.3 rv	AGCAGCAGATCTTGATCTCAATCCTGAcctaggTGAATGTTTTGATATAAGTACT TTAAATTC
KBI.4 TGD fw	atttagtgacactatagaataactcgggccgctaaGAACACATATCCCCTTTATATAG
KBI.4 TGD rv	TCCAGCACCAGCAGCAGCACCTCTAGCacgcgtTCGTTTCTATCATTTTCACTTTc
KBI.4 fw	ttagtgacactatagaataactcgggccgctaaCGTAATAATACAAAAGAACAAG
KBI.4 rv	AGCAGCAGATCTTGATCTCAATCCTGAcctaggGGAACACATTTAATATTCAA ATC

KBI.5 TGD fw	atntaggtgacctatagaataactcgcggccgctaaGGCTATATGTAAAGGCAAATATAAA AATG
KBI.5 TGD rv	CCAGCACCAGCAGCAGCACCTCTAGCacgcgtAGGTATGGAAATTTATTTTTT C
KBI.5 fw	atntaggtgacctatagaataactcgcggccgctaaagAATGCAAGACATGTTAAGAAG
KBI.5 rv	GCAGCAGCAGATCTTGATCTCAATCCTGAcctaggCGTCTCATGTTCTTGTCAT TCAG
KBI.6 TGD fw	atntaggtgacctatagaataactcgcggccgctaaGAAAAATAACCTTGGAAGCAC
KBI.6 TGD rv	TCCAGCACCAGCAGCAGCACCTCTAGCacgcgtATTATGTTTTTCTTTTTCTGT TTTG
KBI.6 fw	atntaggtgacctatagaataactcgcggccgctaaTAAAATATATATGAATATTTACG
KBI.6 rv	AGCAGCAGATCTTGATCTCAATCCTGAcctaggTAATATTTGCTTAAACAAATTA ATAG
KBI.7 TGD fw	atntaggtgacctatagaataactcgcggccgctaaGGAAAAAAAAAAAAAAAAAATAG TTTC
KBI.7 TGD rv	TCCAGCACCAGCAGCAGCACCTCTAGCacgcgtTGACTGGTCATAATTTTTTATA TAG
KBI.7 fw	ttaggtgacctatagaataactcgcggccgctaaATTGATTGTGGTGATAATCAAATTG
KBI.7 rv	AGCAGCAGATCTTGATCTCAATCCTGAcctaggTTTTTGTATAAAAAAGAGACC AC
KBI.8 TGD fw	tatttaggtgacctatagaataactcgcggccgctaaGTCTCATATAAATTATAATGTCG
KBI.8 TGD rv	TCCAGCACCAGCAGCAGCACCTCTAGCacgcgtATCATATGTATCATTATTTTTTC C
KBI.8 fw	gctatttaggtgacctatagaataactcgcggccgctaaTTATAATTGGTCCTTTAGCTCAA AC
KBI.8 rv	AGCAGCAGATCTTGATCTCAATCCTGAcctaggAAAGTACAAATCTGGAGATAT GG
KBI.1 TGD int check 5 fw	AAAAAGAAAAATATGACTAATG
KBI.1 TGD int check 3 rv	GTTATTATTATTATTATTATTATTG
KBI.1 int check 5 fw	TGTGAGTGATGATCACAATATAG
KBI.1 int check 3 rv	ACACTTCATAAACATTTTTGCC
KBI.2 TGD int check 5 fw	AATCATAAATTTTTTGATATTTTC
KBI.2 TGD int check 3 rv	TTGCATTCTTTAACAATAGGAAG
KBI.2 int check 5 fw	AAAAAATGAAGATCATTTAAG
KBI.2 int check 3 rv	TCACATTATATAAAAAATATACATAC
KBI.3 TGD int check 5 fw	TTTTTTTTGTTATTATAAATTG
KBI.3 TGD int check 3 rv	tttattttttttttgctatacC
KBI.3 int check 5 fw	Cattttgttcgaaacgatcattc
KBI.3 int check 3 rv	AATATATATATGTTTTCTTTTTG
KBI.4 TGD int check 5 fw	AATTAATAAATAAATGAATAG
KBI.4 TGD int check 3 rv	AGCATCTGCTTTTTCTGTATAG
KBI.4 int check 5 fw	Tatgttcattttatttttag

KBI.4 int check 3 rv	AATTTAATAAAGAACAAATATC
KBI.5 TGD int check 5 fw	TTGTTCATAATATTATTATTATC
KBI.5 TGD int check 3 rv	ATGATAAAGAATCATTTGCCTTTTG
KBI.5 int check 5 fw	Catatgcttaatttcctttgtc
KBI.5 int check 3 rv	TTAATGACTCTTCTCATGG
KBI.6 TGD int check 5 fw	tttttagAGATTTAATTTAC
KBI.6 TGD int check 3 rv	TCTTTTTTCATGTTTTCTATC
KBI.6 int check 5 fw	TGGAAAATAATCTAACAAATG
KBI.6 int check 3 rv	AATAACTGTTCTTTGTTTTGTC
KBI.7 TGD int check 5 fw	TATTAACAACCTTAGATAC
KBI.7 TGD int check 3 rv	ttttattgttttttacC
KBI.7 int check 5 fw	TTGTGGGTGACGAATTATTGATAG
KBI.7 int check 3 rv	AATATAGAAAATCTAATATTTCG
KBI.8 TGD int check 5 fw	GAAAATAATAATAATTAATAAAAGG
KBI.8 TGD int check 3 rv	ATTGTTTCGCTTTATCCTGATC
KBI.8 int check 5 fw	AAAGTACAATGTCAAAAATGTC
KBI.8 int check 3 rv	TAATTTTTGTTTCGCTATTCTTG
KBI.9 TGD fw	tgacactatagaataactcgcggccgctaaTGTCGTCAGCAACACAATTGGGTATATC
KBI.9 TGD rv	CTCCAGCACCAGCAGCAGCACCTCTAGCacgcgtATGTTTATTATTACTATG TTG
KBI.9 fw	gctatttaggtgacactatagaataactcgcggccgctaaGAGTAATATGAGTAATATGAGT AAC
KBI.9 rv	CAGCAGCAGATCTTGATCTCAATCCTGAcctaggAAATTTTTGTTTGAATCAAA AACAG
KBI.10 TGD fw	gctatttaggtgacactatagaataactcgcggccgctaaGTTTTTTAATTTAAATAAAGATTC C
KBI.10 TGD rv	CTCCAGCACCAGCAGCAGCACCTCTAGCacgcgtATTCCATAAAAAACTTCTTC TTC
KBI.10 fw	gctatttaggtgacactatagaataactcgcggccgctaaGATATTAATAGAAATGCAAATTC TTTTTC
KBI.10 rv	CAGCAGCAGATCTTGATCTCAATCCTGAcctaggCATATTTGAAAAAAGGTAT TCTTG
KBI.11 TGD fw	gctatttaggtgacactatagaataactcgcggccgctaaTGAAAAAATAGAAACGAAAA CAAG
KBI.11 TGD rv	CTCCAGCACCAGCAGCAGCACCTCTAGCacgcgtCTTATCCTCCCAGGTTTTTC TG
KBI.11 fw	gctatttaggtgacactatagaataactcgcggccgctaaTAGAAACAAAAAATGATAATAT ACAAAG
KBI.11 rv	CAGCAGCAGATCTTGATCTCAATCCTGAcctaggATTAATATTTATTTTTCTAA GCTG
KBI.9 TGD int check 5 fw	AGAAATTGTACATAATAAATAAG
KBI.9 TGD int check 3 rv	TGATGGTGATGGTGGTGGTGATG

KBI.9 int check 5 fw	CACCACAAATAATATGAATAAC
KBI.9 int check 3 rv	TATTTCTTTTTTATATTGCTTC
KBI.10 TGD int check 5 fw	AAAATAAAAAAAAAACCGAAATG
KBI.10 TGD int check 3 rv	TATTTAGAACTGAAATATCTTC
KBI.10 int check 5 fw	AAAAGAGAATGATATGATTATG
KBI.10 int check 3 rv	TTTATAAACTTTTTATAATTC
KBI.11 TGD int check 5 fw	AATGCAGTGCAATATAGTATAG
KBI.11 TGD int check 3 rv	TTCTTTATTCATTCTAATAATG
KBI.11 int check 5 fw	TAATATTAATAATGATACAAAAG
KBI.11 int check 3 rv	ATATAAATGAGGACGACTTTTTG
GRASP mCh fw	ATTTATAACGTATATCATTTTTAAAGATAActcgagATGGGAGCAGGACAAACGA AGG
GRASP mCh rv	aatctggattatcatatggataactgtactagtTATGTTCTTTCTTACATCGTGAAC
mCherry für K13-coloc fw	TATTTATAACGTATATCATTTTTAAAGATAActcgagatggtgagcaagggcgaggagga taac
mCherry für K13-coloc rv	ctacttaattgctcctgctcctgctcctgctcctcactattgcaactctgttggatcacgcgtctgtaca gctcgtccatgccgccg
K13 coloc fw	aggagcaggagcaggagcaatattaagtagagctagcATGGAAGGAGAAAAAGTAAAAA C
K13 coloc rv	ACGAACATTAAGCTGCCATATCCCTCGACCCGGGTTATATATTTGCTATTAA ACGGAG
SF3A2 for K13 fw	CGGCCGCTAACGTAACAGACTTAGGAGGAGATCTtaaAGTCTCCTTTTCTTTAT TTTACAGTTG
SF3A2 for K13 rv	ttatcctcctgccttctcaccatctcgagTTACTTTTTAAATTATATTTTATATATTATG
Stev_mScarlett fw1	GATGTATAACCTTAAAATGTTATTGTTACCTTTTAAATAAATACATTAGCATT ACCACATTATGATAATTATCAAATAGCCATATGGTGAGTAAGGGTGAGGCA GTG
Stev_mScarlett fw2	ATTTATAACGTATATCATTTTTAAAGATAActcgagATGAAGATGTATAACCTTAA AATGTTATTG
Stev_mScarlett rv	AACATTAAGCTGCCATATCCCTCGACCCGGGTTATAATTCATCACTCTTGTA GCTCATCCATACCACCTG

Appendix B. Methods for directed gene and protein inactivation in *P. falciparum* ¹

method	advantages	disadvantages	improvements for the method with the systems presented in this study	successful use for essential targets
Targeted gene disruption (TGD)²	- simplicity	- disruptions reducing parasite fitness are not obtained and essential genes can not be targeted - requires passive selection of integration which is slow and may not always be successful - leads to a truncation only	- SLI-TGD increases speed and success rate to obtain parasites with gene disruptions (this study) - SLI might make possible to obtain deletions with a growth disadvantage - with SLI short targeting regions are possible which will reduce the proportion of the gene that is left	- used for many non-essentials targets, for example ² - indispensability of a target can be inferred from failure to obtain integrants, but due to lack of means for selection, the predictive value of this is limited
Thymidine kinase (TK) and cytosine deaminase (CD) selected double crossover^{3,4}	- deletion of entire open reading frame possible	- essential genes can not be targeted - resistance of parasites to negative selectable marker can occur		- used on several occasions for non-essential targets (e.g. 53 non-essential targets in a single study ⁵) - indispensability of a target may be inferred from failure to obtain integrants
TetO regulated transcription^{6,7}	- suitable for essential targets	- requires passive selection of integration which is slow and may not always be successful - lack of promoter information may hamper its use - not so far used for an essential <i>P. falciparum</i> gene	- SLI can increase speed and success rate for integration	- none in <i>P. falciparum</i> so far
ribozyme based mRNA degradation⁸	- permits analysis of essential genes	- requires passive selection of integration which is slow and may not always be successful - regulation levels rarely exceed 90% ⁹ - glucosamine is toxic, requiring exact titration to avoid detrimental effects on the parasite	- SLI can increase speed and success rate for integration	- one essential ¹⁰
Protein destabilisation using ddFKBP¹¹	- permits analysis of essential genes - if regulation is not affected, combination of ddFKBP with GFP can at the same time also localise the native protein	- requires passive selection of integration which is slow and may not always be successful - cost of shield - regulation levels vary and some proteins are not regulated at all - shield, depending on concentration required, may be toxic/affect parasite growth ¹²	- SLI can increase speed and success rate for integration, thereby also reducing the costs for shield	So far close to 10 essential targets were analysed, for example ^{13,14}
Protein destabilisation using <i>E. coli</i> DHFR¹⁵	- permits the analysis of essential chaperones and other targets - stabilising reagent is cheap	- requires passive selection of integration which is slow and may not always be successful - so far shown to work mostly for chaperones	- SLI can increase speed and success rate for integration	- 3 essential targets (2 chaperones, one other) ¹⁵⁻¹⁷
Protein	- similar to ddFKBP	- similar to ddFKBP without	- SLI can increase speed	- no essential targets have

destabilisation using the Auxin system (AID)^{18,19}	<ul style="list-style-type: none"> - lower cost (compared to ddFKBP) - Auxin is applied to reduce protein levels, not requiring addition during the long period to obtain integration 	the cost issue	and success rate for integration	so far been analysed in <i>P. falciparum</i>
Zinc finger nucleases²⁰	<ul style="list-style-type: none"> - ideal to introduce small genomic changes, e.g. point mutations that are not detrimental to parasite growth - rapid compared to passive cycling - leaves no traces other than the desired change 	<ul style="list-style-type: none"> - modifications detrimental to the parasite are not obtained, hampering the analysis of essential genes - expensive/difficult to make - efficiency usually below 100%, requiring cloning of parasites - can have off target effects 		- no essential targets have so far been inactivated
CRISPR/CAS^{21,22}	<ul style="list-style-type: none"> - similar to zinc finger nucleases - can be used to place loxP sites for diCre²³ 	<ul style="list-style-type: none"> - so far not inducible for <i>P. falciparum</i>, precluding the analysis of essential genes - lack of NHEJ in the parasite makes necessary to use helper sequences -> 3 component system - efficiency usually below 100%, requiring cloning of parasites - so far not used for GFP tagging - can have off-target effects 	<ul style="list-style-type: none"> - FKBP/FRB system could be used to render it inducible in <i>P. falciparum</i> - SLI could be used to select parasites with the correct modification and avoid the need for cloning 	- so far only genes not affecting <i>in vitro</i> parasite growth have been targeted in <i>P. falciparum</i> ^{21,22}
diCre²⁴	<ul style="list-style-type: none"> - permits analysis of essential genes - gene excision can be rapid enough to permit analysis in the same cycle 	<ul style="list-style-type: none"> - placing loxP sites to flank entire gene difficult (even in the CRISPR/CAS9 placed loxP sites a truncated gene remained²³) - the simpler alternative of placing loxP sites to remove 3' untranslated region alone may not affect gene expression^{24,25} - efficiency and speed of gene excision varies - protein can remain for some time after removal of the gene 	<ul style="list-style-type: none"> - rapid SLI based integration to place loxP sites (this study) - combinable with KS (this study) 	- 6 essentials ^{23,26,27}
intron diCre²⁸	<ul style="list-style-type: none"> - inducible, making possible to target essential genes (advantage over TGD) 	<ul style="list-style-type: none"> - requires passive selection of integration which is slow and may not always be successful - due to the need to place the intron after the targeting region in the gene, only truncations are achieved (similar to TGD) 	<ul style="list-style-type: none"> - SLI can increase speed and success rate for integration - with SLI short targeting regions are possible which will reduce the proportion of the gene that is left after floxing 	- 1 essential target ²⁸
Morpholino-based RNA targeting^{29,30}	<ul style="list-style-type: none"> - permits targeting of essential genes 	<ul style="list-style-type: none"> - reduction of mRNA levels only moderate 		- 5 essential targets ²⁹⁻³¹ (effect on protein levels was not analysed)
Synthetic post translational regulation^{32,33}	<ul style="list-style-type: none"> - permits targeting of essential genes 	<ul style="list-style-type: none"> - requires passive selection of integration which is slow and may not always be successful 	<ul style="list-style-type: none"> - SLI can increase speed and success rate for integration 	- 1 essential target ³²
SLI-TGD (this	<ul style="list-style-type: none"> - rapid 	<ul style="list-style-type: none"> - disruptions of essential genes 		- 11 non essentials (this

study)	<ul style="list-style-type: none"> - simplicity - robust (demonstrated for many targets) - due to selection may allow gene-disruptions causing a growth disadvantage 	<ul style="list-style-type: none"> can not be obtained - leads to a truncation only 	study)	<ul style="list-style-type: none"> - failure to disrupt indicated indispensability for 8 genes which was confirmed in 4 cases by KS (this study)
KS (this study)	<ul style="list-style-type: none"> -permits analysis of essential genes - combination with GFP permits localisation of target in live cells - visual control of fate of target at all times - fast inactivation - demonstrated to work for many targets (this study: 17 targets) 	<ul style="list-style-type: none"> - some proteins can not be mislocalised - potential for mislocalised protein to have a detrimental effect at site of mislocalisation (no indication for this for all non-essential targets analysed in this study) 		- 8 essentials (this study)

Publications

A genetic system to study *Plasmodium falciparum* protein function

Birnbaum, J., Flemming, S., Reichard, N., Soares A.B., Mesén-Ramírez, P., Jonscher, E., Bergmann, B. & Spielmann, T.

Nature Methods 14, 450-456 (2017), doi:10.1038/nmeth.4223

Danksagung

An erster Stelle möchte ich Dr. Tobias Spielmann dafür danken, dass er mir ermöglichte meine Doktorarbeit in seiner Gruppe durchzuführen. Ich weiß es sehr zu schätzen, dass du dir so viel Zeit für die Betreuung genommen hast und jederzeit ansprechbar warst. Es war eine sehr lehrreiche und interessante Zeit. Mir hat sehr viel Spaß gemacht an einem so motivierenden Projekt zu arbeiten und sich in den letzten dreieinhalb Jahren über allerlei Ideen auszutauschen.

Des Weiteren möchte ich bei Prof. Iris Bruchhaus, PD Dr. Thomas Jacobs und PD Dr. Hartwig Lüthen für Co-Betreuung bedanken. Mein Dank geht an auch Prof. Tim Gilberger für die Übernahme des Dissertationsgutachtens.

Many thanks to Wieteke Hoeijmakers for performing the mass spectrometry experiments. It was a pleasure to get to know you in Wood Hole.

Vielen Dank auch an alle Praktikanten und Masterstudenten die zum Projekt beigetragen haben.

Wer in diesen Zeilen fehlen auf keinen Fall darf sind alle Leute der AG Spielmann und AG Gilberger, welche ich in meiner Zeit miterleben durfte. Ihr habt es allesamt geschafft, dass ich mich immer sehr wohl gefühlt habe und ohne euch wäre die Zeit nicht halb so schön gewesen – es hat riesengroßen Spaß gemacht! Ich denke nicht viele Leute können von ihrem Arbeitsplatz sagen, dass sie mit Freunden zusammen arbeiten :). Ich werde die unvergleichliche Atmosphäre, die Partys und die gemeinsamen Ausflüge in guter Erinnerung behalten und da ich auch noch eine wenig länger im Labor sein werde freue ich mich schon jetzt auf die nächsten gemeinsamen Aktionen!

Nicht zu vergessen sind natürlich auch die Freunde auch außerhalb des Labors, die mir eine so schöne Zeit in Hamburg bereitet haben.

Zu guter Letzt möchte ich mich ganz herzlich bei meiner Familie bedanken. Danke für die Unterstützung und den Rückhalt und dafür, dass ich mich immer auf euch verlassen kann.